



**UNIVERSIDAD NACIONAL AUTÓNOMA DE MÉXICO
POSGRADO EN CIENCIAS BIOLÓGICAS**

FACULTAD DE MEDICINA
BIOLOGÍA EXPERIMENTAL

ANÁLISIS MULTILOCUS DE AISLADOS CLÍNICOS Y DE LA NATURALEZA DE *Histoplasma capsulatum* DE DISTINTAS PROCEDENCIAS GEOGRÁFICAS

TESIS

QUE PARA OPTAR POR EL GRADO DE:

DOCTORA EN CIENCIAS

PRESENTA:

M. EN C. VITE GARÍN TANIA MAYELA

TUTORA PRINCIPAL DE TESIS: DRA. MARIA LUCIA TAYLOR DA CUNHA E MELLO
FACULTAD DE MEDICINA, UNAM
COMITÉ TUTOR: DR. JOAQUÍN CIFUENTES BLANCO
FACULTAD DE MEDICINA, UNAM
DR. DAVID SEBASTIAN GERNANDT
INSTITUTO DE BIOLOGÍA, UNAM

CIUDAD UNIVERSITARIA, CD. MX., JUNIO, 2023



UNAM – Dirección General de Bibliotecas

Tesis Digitales
Restricciones de uso

DERECHOS RESERVADOS ©
PROHIBIDA SU REPRODUCCIÓN TOTAL O PARCIAL

Todo el material contenido en esta tesis está protegido por la Ley Federal del Derecho de Autor (LFDA) de los Estados Unidos Mexicanos (Méjico).

El uso de imágenes, fragmentos de videos, y demás material que sea objeto de protección de los derechos de autor, será exclusivamente para fines educativos e informativos y deberá citar la fuente donde la obtuvo mencionando el autor o autores. Cualquier uso distinto como el lucro, reproducción, edición o modificación, será perseguido y sancionado por el respectivo titular de los Derechos de Autor.



**UNIVERSIDAD NACIONAL AUTÓNOMA DE MÉXICO
POSGRADO EN CIENCIAS BIOLÓGICAS**

FACULTAD DE MEDICINA
BIOLOGÍA EXPERIMENTAL

ANÁLISIS MULTILOCUS DE AISLADOS CLÍNICOS Y DE LA NATURALEZA DE *Histoplasma capsulatum* DE DISTINTAS PROCEDENCIAS GEOGRÁFICAS

TESIS

QUE PARA OPTAR POR EL GRADO DE:

DOCTORA EN CIENCIAS

PRESENTA:

M. EN C. VITE GARÍN TANIA MAYELA

TUTORA PRINCIPAL DE TESIS: DRA. MARIA LUCIA TAYLOR DA CUNHA E MELLO
FACULTAD DE MEDICINA, UNAM

COMITÉ TUTOR: DR. JOAQUÍN CIFUENTES BLANCO
FACULTAD DE MEDICINA, UNAM
DR. DAVID SEBASTIAN GERNANDT
INSTITUTO DE BIOLOGÍA, UNAM

CIUDAD UNIVERSITARIA, CD. MX., JUNIO, 2023

COORDINACIÓN DEL POSGRADO EN CIENCIAS BIOLÓGICAS

FACULTAD DE MEDICINA

OFICIO CPCB/318/2023

ASUNTO: Oficio de Jurado

M. en C. Ivonne Ramírez Wence
Directora General de Administración Escolar, UNAM
P r e s e n t e

Me permito informar a usted qué en la reunión ordinaria del Comité Académico del Posgrado en Ciencias Biológicas, celebrada el día **23 de enero de 2023** se aprobó el siguiente jurado para el examen de grado de **DOCTORA EN CIENCIAS** de la estudiante **VITE GARÍN TANIA MAYELA** con número de cuenta **97159535** con la tesis titulada "**ANÁLISIS MULTILOCUS DE AISLADOS CLÍNICOS Y DE LA NATURALEZA DE *Histoplasma capsulatum* DE DISTINTAS PROCEDENCIAS GEOGRÁFICAS**", realizada bajo la dirección de la **DRA. MARÍA LUCIA TAYLOR DA CUNHA E MELLO**, quedando integrado de la siguiente manera:

Presidente: DRA. MARÍA DEL ROCÍO ALICIA REYES MONTES
Vocal: DRA. MARÍA DEL CARMEN LETICIA CALDERÓN EZQUERRO
Vocal: DR. ARMANDO PÉREZ TORRES
Vocal: DR. ERICK OBED MARTÍNEZ HERRERA
Secretario: DR. DAVID SEBASTIAN GERNANDT

Sin otro particular, me es grato enviarle un cordial saludo.

A T E N T A M E N T E
"POR MI RAZA HABLARÁ EL ESPÍRITU"
Ciudad Universitaria, Cd. Mx., a 29 de marzo de 2023

COORDINADOR DEL PROGRAMA


DR. ADOLFO GERARDO NAVARRO SIGÜENZA



COORDINACIÓN DEL POSGRADO EN CIENCIAS BIOLÓGICAS

Unidad de Posgrado, Edificio D, 1º Piso. Circuito de Posgrados, Ciudad Universitaria
Alcaldía Coyoacán. C. P. 04510 CDMX Tel. (+5255)5623 7002 <http://pcbiol.posgrado.unam.mx/>

AGRADECIMIENTOS INSTITUCIONALES

Al Posgrado en Ciencias Biológicas de la UNAM por permitirme terminar satisfactoriamente en tiempo y forma el Doctorado en Ciencias.

Al Consejo Nacional de Ciencia y Tecnología (CONACYT) por otorgarme la beca con referencia- 324232/231985, durante el período 30 de enero de 2012 hasta el 29 de enero de 2016

A la Dirección General de Personal Académico (DGAPA) a través del Programa de Apoyo a Proyectos de Investigación e Innovación Tecnológica (PAPIIT-IN213515) por el financiamiento de la última etapa de este proyecto durante el período enero de 2015 a diciembre de 2017.

A los miembros del comité Tutorial, Dra. María Lucía Taylor (tutora principal), Dr. David Sebastian Gernandt y Dr. Joaquín Cifuentes, por sus valiosos aportes al proyecto y por el tiempo que dedicaron para analizar y aportar una crítica constructiva a este trabajo.

AGRADECIMIENTOS

A la Dra. María Lucía Taylor, por haberme permitido realizar con ella y su equipo mis estudios de posgrado y por la gran cantidad de conocimientos que me han dejado los años en su equipo de trabajo, pues forma una parte fundamental en mi formación académica y profesional.

A los miembros del jurado de examen Dra. María del Rocío Alicia Reyes Montes, Dra. María del Carmen Leticia Calderon Ezquerro, Dr. Armando Pérez Torres, Dr. Erick Obed Martínez Herrera, por sus importantes observaciones realizadas a este trabajo.

Al M. en C. José Antonio Ramírez Bárcenas quien también ha formado parte importante en mis procesos de aprendizaje a través de su apoyo como Técnico Académico en el equipo de trabajo del Laboratorio de Inmunología de Hongos.

A la M. en C. Gabriela Rodríguez Arellanes por su apoyo a través de sus actividades dentro del Banco de Cepas de *Histoplasma capsulatum* del Laboratorio de Inmunología de Hongos.

A todos mis amigos y compañeros de la Unidad de Micología de la Facultad de Medicina (Jorge, Amelia, Laura, Lisandra) con quienes compartí varios años, muchas gracias por su amistad y apoyo en todo momento.

A mí mamá, mí hijo y mí esposo por su infinita paciencia en el desarrollo de este trabajo.

ÍNDICE

	Pág
ÍNDICE DE TABLAS	
ÍNDICE DE FIGURAS	
RESUMEN	1
ABSTRACT	2
INTRODUCCIÓN	3
• Sistemática de <i>Histoplasma capsulatum</i>	5
• Delimitación de especies de <i>H. capsulatum</i> por métodos de reconstrucción filogenética.	8
• Delimitación de especies de <i>H. capsulatum</i> con base en el estudio de estructura de poblaciones.	11
• Delimitación de especies de <i>H. capsulatum</i> por métodos de coalescencia	12
PLANTEAMIENTO DEL PROBLEMA	13
HIPÓTESIS	13
OBJETIVO GENERAL	14
OBJETIVOS PARTICULARES	14
METODOLOGÍA	14
• Aislados fúngicos	14
• Procedimiento de seguridad	15
• Cultivo de micelio de <i>H. capsulatum</i> y extracción del DNA	15
• Reacción en cadena de la polimerasa (PCR)	16
• Secuenciación	18
• Análisis de BLASTn (Basic Local Alignment Search Tool)	18
• Alineamiento de secuencias	19
• Análisis de congruencia	19
• Reconstrucción filogenética	19
• Análisis de coalescencia	20
• Diversidad nucleotídica	21
• Redes CSTs (Concatenated Sequence-Types)	21
RESULTADOS	22
• Aislados fúngicos	22
• Secuencias	22
• Análisis de BLASTn	23
• Alineamiento de secuencias	23
• Análisis de congruencia	24
• Reconstrucción filogenética	25
• Análisis de coalescencia	27
• Diversidad nucleotídica	28

• Redes CSTs	28
DISCUSIÓN	29
• Características relevantes de los aislados de <i>H. capsulatum</i> estudiados	29
• Marcadores filogenéticos y análisis BLASTn de las secuencias generadas	30
• Congruencia filogenética	31
• Reconstrucción filogenética	32
• Coalescencia	34
• Diversidad nucleotídica	34
• Redes CSTs	35
CONCLUSIONES	36
PERSPECTIVAS INMEDIATAS Y FUTURAS	36
TABLAS	38
FIGURAS	54
REFERENCIAS BIBLIOGRÁFICAS	84
ANEXOS	94
1. Artículo requisito para la obtención del grado	95
2. Otros Artículos, Capítulo de Libro y Memorias Publicadas, Congresos	113
3. Artículo por Enviar	176
4. Alineamientos individuales	177

ÍNDICE DE TABLAS

	Pág.
• Tabla 1. Datos de las cepas y/o aislados seleccionados para el estudio	39
• Tabla 2. Datos migratorios y alimenticios de los murciélagos incluidos en el estudio	41
• Tabla 3. No. de acceso de las secuencias depositadas en diferentes bases de datos	42
• Tabla 4. Datos genéticos de los alineamientos estudiados	51
• Tabla 5. Resultados del análisis Incongruence Length Difference (ILD) usando los marcadores estudiados	52
• Tabla 6. Análisis de diversidad nucleotídica (π)	53

ÍNDICE DE FIGURAS

	Pág.
• Figura 1. Árbol filogenético no enraizado de <i>H. capsulatum</i> generado por una matriz individual de secuencias de arf, utilizando el método de Parsimonia.	55
• Figura 2. Árbol filogenético no enraizado de <i>H. capsulatum</i> generado por una matriz individual de secuencias de arf, utilizando el método de Máxima Verosimilitud.	56
• Figura 3. Árbol filogenético no enraizado de <i>H. capsulatum</i> generado por una matriz individual de secuencias de arf, utilizando el método de Inferencia Bayesiana.	57
• Figura 4. Árbol filogenético no enraizado de <i>H. capsulatum</i> generado por una matriz individual de secuencias de H-anti, utilizando el método de Parsimonia.	58
• Figura 5. Árbol filogenético no enraizado de <i>H. capsulatum</i> generado por una matriz individual de secuencias de H-anti, utilizando el método de Máxima Verosimilitud.	59
• Figura 6. Árbol filogenético no enraizado de <i>H. capsulatum</i> generado por una matriz individual de secuencias de H-anti, utilizando el método de Inferencia Bayesiana.	60
• Figura 7. Árbol filogenético no enraizado de <i>H. capsulatum</i> generado por una matriz individual de secuencias de ole1, utilizando el método de Parsimonia.	61
• Figura 8. Árbol filogenético no enraizado de <i>H. capsulatum</i> generado por una matriz individual de secuencias de ole1, utilizando el método de Máxima Verosimilitud.	62
• Figura 9. Árbol filogenético no enraizado de <i>H. capsulatum</i> generado por una matriz individual de secuencias de ole1, utilizando el método de Inferencia Bayesiana.	63
• Figura 10. Árbol filogenético no enraizado de <i>H. capsulatum</i> generado por una matriz individual de secuencias de tub1, utilizando el método de Parsimonia.	64
• Figura 11. Árbol filogenético no enraizado de <i>H. capsulatum</i> generado por una matriz individual de secuencias de tub1, utilizando el método de Máxima Verosimilitud.	65
• Figura 12. Árbol filogenético no enraizado de <i>H. capsulatum</i> generado por una matriz individual de secuencias de tub1, utilizando el método de Inferencia Bayesiana.	66

- **Figura 13.** Árbol filogenético no enraizado de *H. capsulatum* generado por una matriz individual de secuencias del microsatélite (GA)n, utilizando el método de Parsimonia. 67
- **Figura 14.** Árbol filogenético no enraizado de *H. capsulatum* generado por una matriz individual de secuencias del microsatélite (GA)n, utilizando el método de Máxima Verosimilitud. 68
- **Figura 15.** Árbol filogenético no enraizado de *H. capsulatum* generado por una matriz individual de secuencias del microsatélite (GA)n, utilizando el método de Inferencia Bayesiana. 69
- **Figura 16.** Árbol filogenético no enraizado de *H. capsulatum* generado por una matriz individual de secuencias de la región ITS1-5.8S-ITS2, utilizando el método de Parsimonia. 70
- **Figura 17.** Árbol filogenético no enraizado de *H. capsulatum* generado por una matriz individual de secuencias de la región ITS1-5.8S-ITS2, utilizando el método de Máxima Verosimilitud. 71
- **Figura 18.** Árbol filogenético no enraizado de *H. capsulatum* generado por una matriz individual de secuencias de la región ITS1-5.8S-ITS2, utilizando el método de Inferencia Bayesiana. 72
- **Figura 19.** Árbol filogenético no enraizado de *H. capsulatum* generado por una matriz concatenada, utilizando el método de Parsimonia. 73
- **Figura 20.** Árbol filogenético no enraizado de *H. capsulatum* generado por una matriz concatenada, utilizando el método de Máxima Verosimilitud. 74
- **Figura 21.** Árbol filogenético no enraizado de *H. capsulatum* generado por una matriz concatenada, utilizando el método de Inferencia Bayesiana. 75
- **Figura 22.** Árbol filogenético enraizado de *H. capsulatum* generado por una matriz individual de secuencias de arf, utilizando el método de Inferencia Bayesiana. 76
- **Figura 23.** Árbol filogenético enraizado de *H. capsulatum* generado por una matriz individual de secuencias de ole1, utilizando el método de Inferencia Bayesiana. 77
- **Figura 24.** Árbol filogenético enraizado de *H. capsulatum* generado por una matriz individual de secuencias de tub1, utilizando el método de Inferencia Bayesiana. 78
- **Figura 25.** Árbol filogenético enraizado de *H. capsulatum* generado por una matriz individual de secuencias de la región ITS1-5.8S-ITS2, utilizando el método de Inferencia Bayesiana. 79

- **Figura 26.** Árbol filogenético enraizado de *H. capsulatum* generado por una matriz concatenada, utilizando el método de Inferencia Bayesiana. 80
- **Figura 27.** Árbol de especies de *H. capsulatum* generado por el método de delimitación de especies con base en coalescencia con edades de los clados. 81
- **Figura 28.** Árbol de especies de *H. capsulatum* generado por el método de delimitación de especies con base en coalescencia. 82
- **Figura 29.** Red de dispersión del complejo *H. capsulatum* de acuerdo con los tipos de secuencias concatenadas (CSTs, del inglés concatenated sequence-types). 83

RESUMEN

Histoplasma capsulatum es un complejo de especies crípticas formado por ascomicetos dimórficos que en su fase levaduriforme (parasitaria-virulenta) son patógenos de mamíferos, incluyendo al humano, y causa la micosis sistémica denominada histoplasmosis. Como muchos hongos microscópicos, *H. capsulatum* presenta pocos caracteres morfológicos que sean útiles para su estudio taxonómico, por lo cual las técnicas de biología molecular han resultado de gran importancia para la identificación de la diversidad genética que presenta este hongo. En el presente estudio, se utilizaron seis fragmentos génicos en diferentes análisis multilocus (MLS) de reconstrucción filogenética en forma independiente y concatenada, con la finalidad de aportar nuevos datos a la filogenia de *H. capsulatum*. Se manejaron las secuencias de los fragmentos génicos arf, H-anti, ole1, tub1, microsatélite (GA)n y la región ITS1-5.8S-ITS2 de 119 aislados de *H. capsulatum*, de éstos, las secuencias de 65 aislados fueron obtenidas durante el desarrollo de la tesis y las secuencias de los 54 aislados restantes procedieron de tres bases de datos. Se lograron nuevos hallazgos filogenéticos que apoyan la gran diversidad de *H. capsulatum*, destacando la nueva especie filogenética (NAm 3) integrada por 16 aislados de *H. capsulatum* obtenidos de murciélagos infectados (15 de *Tadarida brasiliensis* y uno de *Mormoops megalophylla*) todos capturados al azar en diferentes regiones de México. Esta especie filogenética está sustentada por los métodos de MLS, coalescencia, diversidad nucleotídica y redes CSTs (del inglés Concatenated Sequence-Types). Interesantemente, un aislado adicional (EH-696P) de *T. brasiliensis* se agrupó con un linaje de Brasil (H153), previamente reportado. Los resultados obtenidos, confirman la filogeografía del complejo *H. capsulatum*, y asimismo, sugieren la existencia de una posible relación huésped-específica, como se ha detectado en la especie filogenética NAm 3 asociada hasta la fecha sólo a murciélagos infectados, particularmente de la especie *T. brasiliensis*.

Palabras clave: *Histoplasma capsulatum*; reconstrucción filogenética; coalescencia; diversidad nucleotídica; nuevo clado.

ABSTRACT

Histoplasma capsulatum is a cryptic species complex formed by dimorphic ascomycetes that in their yeast-like form (parasitic-virulent), are pathogenic to mammals, including humans, and causes a systemic mycosis, histoplasmosis. As many microscopic fungi, *H. capsulatum* has few morphological characteristics useful for its taxonomic study; as a result, therefore, molecular biology techniques have become relevant for the taxonomic identification of the fungus based on its genetic diversity. In the present study, we used six gene fragments in different multilocus sequence typing analyses (MLST) aimed at providing new data on the phylogeny of *H. capsulatum*. We used the sequences of gene fragments arf, H-anti, ole1, tub1, microsatellite (GA)_n, and region ITS1-5.8S-ITS2 of 119 *H. capsulatum* isolates; of these, the sequences of 65 isolates were obtained during the development of this dissertation, and those of the remaining 54 isolates were from three databases. New phylogenetic findings were identified that support the large diversity of *H. capsulatum*, highlighting the new phylogenetic species (NAm 3) composed of 16 isolates of *H. capsulatum* obtained from infected bats (15 from *Tadarida brasiliensis* and one isolate from *Mormoops megalophylla*) all randomly captured in different regions of Mexico. The phylogenetic species NAm 3 is supported by different genetic analyses performed with the processed markers: MLS, coalescence, nucleotide diversity and Concatenated Sequence-Types (CST) networks. Interestingly, another isolate (EH-696P) obtained from *T. brasiliensis* was grouped with a previously reported lineage from Brazil (H153). These findings confirm the phylogeography of the *H. capsulatum* complex, and suggest the existence of a possible host-specific relation, as detected in the phylogenetic species NAm 3, preferentially associated, up to now, only with infected *T. brasiliensis* bats.

Key words: *Histoplasma capsulatum*; phylogenetic reconstruction; coalescence; nucleotide diversity; new clade.

INTRODUCCIÓN

El complejo de especies crípticas *Histoplasma capsulatum* está conformado por hongos dimórficos que presentan una fase micelial (M) infectiva y una fase levaduriforme (L) parasitaria-virulenta. La fase M es saprobio-geofílica y se desarrolla en suelos enriquecidos con guano de murciélagos y aves que contiene altas concentraciones de nutrientes, principalmente nitrógeno y fósforo además de otros oligoelementos y que representan los factores bióticos necesarios para el crecimiento del hongo. Asimismo, los factores abióticos que este hongo requiere para su crecimiento son poca luz que favorece la esporulación, temperaturas óptimas de ambiente y de suelo en el rango 25-30 °C y humedad relativa > 60% (Taylor et al. 1999a; 1999b; 1999c; 2000b; Tewari et al. 1998). En el laboratorio, *H. capsulatum* presenta crecimiento lento en medios de cultivo y desarrolla colonias albinas (A) o pigmentadas (B, del inglés “brown”) (Kwon-Chung y Bennett 1992; Tewari et al. 1998), cuyo color varía de pardo claro a oscuro por la presencia de melanina en las paredes de hifas y conidios (Nosanchuck et al. 2002). Comúnmente, se registran colonias B que conforme se resiembran en medios de cultivo cambian a A (Taylor et al. 1999c) y, ocasionalmente, presentan un pigmento rojo difusible en el medio que no está asociado a las estructuras celulares del hongo y que aun no ha sido caracterizado (Morris et al. 1986). Microscópicamente, las hifas miden de 1.2-1.5 µm de diámetro y forman microconidios y macroconidios. Los microconidios son redondos, piriformes o claviformes de 1-4 x 2-6 µm, sésiles o unidos a conidióforos. Los macroconidios típicos de la especie son redondos o clavados con paredes gruesas, miden de 8-14 µm de diámetro y presentan aspecto tuberculado con proyecciones digitiformes (Tewari et al. 1998). Sin embargo, algunas veces se observan macroconidios atípicos sin proyecciones. Por lo general, los macroconidios se encuentran adheridos a las hifas a través de conidióforos cortos que suelen formar ángulos de aproximadamente 90°.

En México, *H. capsulatum* se encuentra en lugares especiales que pueden ser definidos como sitios de alto riesgo de infección y que se asocian a la forma epidémica de la enfermedad, en particular, ambientes cerrados como cavernas,

cuevas, minas, bocaminas, túneles, puentes, criptas de iglesias y edificios abandonados, donde se acumulan diferentes tipos de guano de murciélagos. *Histoplasma* también se encuentra disperso en los denominados sitios de bajo riesgo de infección asociados a la forma endémica de la enfermedad, en general, ambientes abiertos como patios caseros, bajo el follaje de los árboles en parques y paseos públicos donde se acumula guano de aves y murciélagos (Taylor et al. 2000b).

La fase (L) de *H. capsulatum* es preferencialmente intracelular. Las levaduras se desarrollan dentro de macrófagos, polimorfonucleares, células dendríticas, células epiteliales y endoteliales de huéspedes susceptibles, así como a 37 °C tanto en medios de cultivo complejos o sintéticos adicionados con suplementos, especialmente glucosa y cisteína. Las colonias tienen aspecto cremoso con color variable del beige claro a oscuro, pueden ser adherentes o no al medio y presentan superficie rugosa (colonias R) o lisa (colonias S), esta última asociada a células avirulentas sin α -(1,3)-glucana en la pared celular (Eissenberg et al. 1996). La micromorfología de las levaduras está representada por células ovaladas que varían de 1.3-2 x 2-6 μm de diámetro, uninucleadas y unigemantes con brotes de base estrecha (Tewari et al. 1998). Las levaduras también presentan melanina asociada a la pared celular (Nosanchuck et al. 2002).

Histoplasma capsulatum, es un hongo anamorfo heterotálico que tiene dos tipos haploides de compatibilidad sexual denominados (a/+) y (a/-), representados en el locus MAT1 por los idiomorfos *MAT1-1* y *MAT1-2* respectivamente (Rodríguez-Arellanes et al. 2013). El teleomorfo *Ajellomyces capsulatus* (= *Emmonsia capsulata* Kwon-Chung, 1972), resultante del apareamiento de estos haplotipos, presenta cuerpos fructíferos cerrados denominados cleistotecios que contienen ascas subesféricas evanescentes, donde se forman ascosporas de 1.2-1.5 μm de diámetro (Kwon-Chung y Bennett 1992).

Sistemática de *Histoplasma capsulatum*

La sistemática de *H. capsulatum* ha sido poco clara, y por tal motivo existen diferentes clasificaciones para este hongo, la primera clasificación biológica consideraba al género *Histoplasma* con una sola especie, *H. capsulatum*, y tres variedades taxonómicas: *H. capsulatum* var. *capsulatum* Darling, 1906; *H. capsulatum* var. *duboisii* (Vanbreuseghem, 1957) Ciferri, 1960; y *H. capsulatum* var. *farciminosum* (Rivolta, 1873) Weeks, Padhye, et Ajello, 1985, identificadas por micromorfología, distribución geográfica, asociación con el huésped y formas clínicas de la enfermedad que producen, la cual es actualmente obsoleta. Con el advenimiento de las técnicas moleculares surgieron otras propuestas de clasificaciones con base en marcadores moleculares para la genotipificación del hongo, destacando la de Vincent et al. (1986) que agrupa cepas clínicas en tres clases de acuerdo con patrones de RFLP (Restriction Fragment Length Polymorphism) e hibridación con sondas de DNA mitocondrial y ribosomal (mtDNA y rDNA, respectivamente), posteriormente esta clasificación fue ampliada a 6 clases por otros autores, como Spitzer et al. (1989; 1990) y Keath et al. (1992).

En la base de datos Mycobank (www.mycobank.org), el género *Histoplasma* está conformado por las especies descritas en la siguiente clasificación.

Clasificación de *Histoplasma* reportada en MycoBank

Reino Fungi
Phylum Ascomycota
Subphylum Ascomycotina
Clase Eurotiomycetes
Orden Onygenales
Familia Ajellomycetaceae
Género *Histoplasma*
Especies *Histoplasma capsulatum* sensu stricto
 H. duboisii
 *H. mississippiense**
 *H. ohiense**
 *H. suramericanum**

* Especies propuestas por Sepúlveda et al. (2017), aunque no han sido validadas a la fecha por MycoBank.

Por otro lado, en la base de datos *Index Fungorum* (www.indexfungorum.org) el género *Histoplasma* comprende solo dos especies y enlista todas las sinonimias para el género, como se describe a continuación.

Clasificación de *Histoplasma* reportada en *Index Fungorum*

Reino Fungi

Phylum Ascomycota

Subphylum Ascomycotina

Clase Eurotiomycetes

Orden Onygenales

Familia Ajellomycetaceae

Género *Histoplasma*

Especies *Histoplasma capsulatum*

H. duboisii

Sinonimias de *H. capsulatum* Darling, *Journal of the American Medical Association* 46: 1285 (1906):

Cryptococcus capsulatus (Darling) Castell. & Chalm., *Manual of Tropical Medicine* (London): 1076 (1919)

Turolopsis capsulata (Darling) F.P. Almeida, *Annales Fac. Med. São Paulo* 9: 76 (1933)

Posadasia capsulata (Darling) M. Moore, *Ann. Mo. Bot. Gdn* 21: 348 (1934)

Cryptococcus farciminosus Rivolta en Torino & Speirani, *Dei parassiti vegetali*: 246-252, 525-525 (1873)

Saccharomyces farciminosus (Rivolta) Vuill., *Rev. Gen. Sci. Pures Appl.* 12: 732-751 (1901)

Endomyces farciminosus (Rivolta) Nègre & Bouquet, *Bull. Soc. Path. Exot.* 10: 274 (1917)

Parendomyces farciminosus (Rivolta) Mello & L. G. Fern., *Arq. Hig. Pat. Exot.* 6: 29 (1918)

Grubyella farciminosa (Rivolta) M. Ota, *Annls Parasit. Hum. Comp.* 3: 78 (1952)

Coccidioides farciminosa (Rivolta) Vuill., *Encyclop. Mycol.* 2: 140 (1931)

Turolopsis farciminosa (Darling) F.P. Almeida, *Annales Fac. Med. São Paulo* 9: 76 (1933)

Histoplasma farciminosum (Rivolta) Redaelli & Cif., *Boll. Sez. Ital. Soc. Int. Microbiol.* 6: 378 (1934)

Zymonema farciminosum (Rivolta) C.W. Dodge, *Medical Mycology. Fungous Diseases of Men and Other Mammals* 169 (1935)

Histoplasma capsulatum var. *farciminosum* (Rivolta) R.J. Weeks, A.A. Padhye & Ajello, *Mycologia* 77 (6): 969 (1986)

Saccharomyces equi Marcone, *Atti R. Ist. Incoragg. Napoli* 8-6: 1-19 (1895)

Histoplasma capsulatum var. *capsulatum* Darling, *Journal of the American Medical Association* 46: 1285 (1906)

Cryptococcus tokishigei Vuill. Ex Guég., *Les Champignons parasites de l'homme et des animaux domestiques* : 108 (1907)

Parendomyces tokishigei (Vuill. Ex Guég.) Mello, *Arq. Hig. Pat. Exot.* 6: 295 (1918)

Sinonimias de *H. duboisii* Vanbreus., *Ann. Soc. Bel. Méd. Trop.* 32: 578 (1952):
Histoplasma capsulatum var. *duboisii* (Vanbreus.) Cif., *J. Amer. Med. Assoc.* 2: 342 (1960)

Uno de los principales debates que existen en la Biología moderna es la definición de “especie”. En la actualidad existe una gran plasticidad en el concepto de especie, ya que éste se modifica y se incrementa a la luz de los avances en el conocimiento de los procesos evolutivos de diferentes organismos (Ereshefsky 2010). Los cambios conceptuales se han dado con base en el empleo de unidades taxonómicas operativas que han buscado entender cómo se llevan a cabo procesos biológicos de interés humano. Los hongos, por ejemplo, son seres vivos cuyas relaciones evolutivas aun resultan poco conocidas, a pesar de ser un grupo con alta diversidad biológica y que desempeña funciones de gran importancia en los diferentes aspectos de su ecología (Sánchez-García 2010).

Entre las principales razones por las que existe poca información sobre los procesos evolutivos en hongos, destacan las siguientes: 1) los caracteres macro- y microscópicos de algunas especies no son suficientemente robustos para apoyar la identificación de especies estrechamente relacionadas, sea porque no son suficientemente informativos o bien presentan demasiada variabilidad intraespecífica; 2) la existencia de estadios morfológicos distintos (sexual y asexual) con nombres diferentes dentro de la misma especie; 3) la inadecuada clasificación

de algunos hongos, a los que no se les ha identificado su fase sexual, en las divisiones que conforman el Reino Fungi (Fungi Imperfecti); 4) la dificultad de determinar la posición taxonómica de hongos que no se pueden cultivar en laboratorio (Freallé et al. 2005); y 5) la polémica sobre el concepto de especie que sitúe correctamente a los hongos (Gazis et al. 2011).

Delimitación de especies de *H. capsulatum* por métodos de reconstrucción filogenética.

El reconocimiento de especies en Micología, se hace por lo general utilizando los conceptos y/o criterios de especie biológicos y morfológicos, de acuerdo con lo señalado por Taylor et al. (2000a), siendo que la mayoría de las especies descritas se han identificado con base en caracteres fenotípicos como, tipos de esporas y de micelio, estructuras de reproducción sexual y asexual, crecimiento a diferentes temperaturas, producción de metabolitos secundarios, presencia de pigmentos, etc. Sin embargo, hay hongos, entre los que destacan patógenos de plantas y animales (incluyendo al humano), que no cuentan con caracteres morfológicos bien diferenciables o bien presentan una alta variación intraespecífica, lo que genera una clasificación compleja, controversial e incompleta (Freallé et al. 2005; Gazis et al. 2011).

Una herramienta útil para apoyar los estudios taxonómicos y evolutivos de los hongos en general ha sido el uso de datos moleculares los cuales deben ser corroborados por la comparación de datos obtenidos con diferentes marcadores. En el caso de los hongos, los marcadores génicos más utilizados para inferir relaciones filogenéticas son los genes ribosomales 18S, 5.8S, 28S y las regiones internas espaciadoras (del inglés, Internal Transcribed Spacers-ITS); el factor de elongación (EF1 α); las subunidades de la RNA polimerasa II (RPB1 y RPB2); los genes que codifican para β -tubulina; además de la subunidad 6 de la ATPasa mitocondrial (ATP6) (Hibbet et al. 2007; James et al. 2006; Sánchez-García 2010). Además de los marcadores anteriores, en hongos patógenos de humanos, se han utilizado otros

fragmentos génicos (Denis et al. 2000; Fréalle et al. 2005; 2007; Kasuga et al. 1999; 2003; Taylor et al. 2005; 2012).

En la actualidad, los datos moleculares han contribuido al conocimiento de procesos genéticos evolutivos, especiaciones, y a la distribución geográfica de ejemplares fúngicos en general (De Luna et al. 2005), así como han logrado identificar especies de hongos patógenos, entre los que destacan *Aspergillus flavus*, *Cryptococcus neoformans* e *H. capsulatum*, y que permanecieron como crípticas con base en conceptos morfológicos o biológicos y que se desvelaron a través de los conceptos de especie filogenética, genealógica o especie filogenética por concordancia de genes, cuyas hipótesis se han enriquecido en el transcurso de las últimas dos décadas y que circunscriben a las especies con base en la variación de sus ácidos nucléicos (Freallé et al. 2005; Gazis et al. 2011; Kasuga et al. 1999; 2003; Taylor et al. 2000a; Taylor y Fisher 2003).

Los análisis moleculares han sido fundamentales para el conocimiento de las relaciones filogenéticas del complejo *H. capsulatum*. Entre los que han aportado mayor información a la clasificación de hongos patógenos, se encuentra el análisis multilocus de secuencias o “Multi-Locus Sequence (MLS)”, el cual emplea secuencias de diversos genes con suficiente polimorfismo para diferenciar aislados de la misma especie y es una excelente herramienta molecular para caracterizar la diversidad genética de microorganismos que son considerados complejos de especies crípticas, como es el caso de *H. capsulatum* (Taylor y Fisher 2003). Así, hasta el momento, se han realizado análisis MLS, empleando diversos métodos, tales como UPGMA, neighbor-joining, máxima parsimonia, máxima verosimilitud, inferencia bayesiana, ya sea empleando las secuencias parciales de algunos genes (Balajee et al. 2012; Galo et al. 2013; Kasuga et al. 1999; 2003; Rodrigues et al. 2020; Taylor et al. 2005; Teixeira et al. 2016; Vite-Garín et al. 2014; Vite-Garín et al. 2021), o incluso análisis concordancia bayesiana con genomas completos, por ejemplo, el trabajo de Sepúlveda et al. (2017), quienes, basados en el estudio del genoma completo de 30 aislados provenientes de cuatro áreas donde la histoplasmosis es endémica, proponen al menos cuatro especies taxonómicas: *Histoplasma capsulatum* sensu stricto Darling 1906, *Histoplasma mississippiense*

sp. nov., *Histoplasma ohiense* sp. nov. e *Histoplasma suramericanum* sp. nov. las cuales son genéticamente distintas entre sí y normalmente no se entrecruzan. Sin embargo, esta propuesta desconsidera la existencia de clados filogeográficos como el Australiano y el Holandés previamente descritos por Kasuga et al. (2003), quienes sentaron las bases de la filogenia actual de *H. capsulatum*.

El estudio filogeográfico de Kasuga et al. (2003) incluyó 137 aislados del hongo procedentes de 25 países, siendo la mayoría de ellos de origen clínico. Se analizaron utilizando las secuencias parciales de cuatro genes: factor de ribosilación del ADP (arf), precursor del antígeno H (H-anti), desaturasa delta-9 de ácido graso (ole1) y α-tubulina (tub1). Como resultado, se propuso una clasificación filogenética de la especie, que incluyó los ocho clados (poblaciones genéticas), Norte América clase 1 (NAm 1); Norte América clase 2 (NAm 2); Latinoamérica grupo A (LAm A); Latinoamérica grupo B (LAm B); Australia; Holanda; África y Eurasia, todos con excepción de este último, son considerados especies filogenéticas. Posteriormente, se realizaron análisis utilizando los mismos genes con aislados de distinto origen y/o procedencia, particularmente los de Taylor et al. (2005), quienes sugieren la existencia de un nuevo clado como resultado del estudio de 14 aislados del hongo obtenidos de murciélagos naturalmente infectados capturados en México y con distintos hábitos migratorios (*Artibeus hirsutus*- no migradores y *Leptonycteris nivalis*, *L. curasoae*, *Tadarida brasiliensis*-migradores), y Teixeira et al. (2016), quienes, por medio de un análisis *in silico* de 234 aislados, reportaron 11 especies filogenéticas, entre las que se conservaron Australia, Holanda, África, NAm 1 y NAm 2 y se incrementaron seis nuevas especies crípticas, RJ, BAC1, LAm A1 y LAm A2 (originadas de LAm A), además de LAm B1 y LAm B2 (originadas de LAm B). Debido a lo anterior e incluyendo además las aportaciones hechas a la filogenia del hongo por otros autores como Rodrigues et al. (2020) quienes proponen las especies filogenéticas LAm C, LAm D y LAm E, Taylor et al. (2022) señalan que se pueden considerar alrededor de 14 especies filogenéticas y cuatro linajes independientes distribuidas en el mundo, siendo 11 de ellas procedentes de las Américas y particularizando 9 en Latinoamérica. Almeida-Silva et al. (2021) analizaron datos filogenómicos según Sepúlveda et al. (2017) además de la estructura de población

de aislados clínicos y ambientales de Brasil, clasificados previamente como LAm A, identificando por lo menos dos poblaciones de *H. suramericanum*.

Delimitación de especies de *H. capsulatum* con base en el estudio de estructura de poblaciones.

Distintas estructuras de poblaciones (clonales y recombinantes) de *H. capsulatum* han sido referidas (Carter et al. 1996; 1997; 2001; Kasuga et al. 1999; Taylor et al. 1999b). El análisis de poblaciones genéticas de *H. capsulatum* con marcadores bialélicos y, en particular, los multialélicos (microsatélites) que se caracterizan por tener motivos repetitivos hipervariables y ser altamente polimórficos, fue utilizado para distinguir aislados individuales e identificar poblaciones fúngicas de Estados Unidos de América y de otras procedencias geográficas (Carter et al. 1997; 2001; Taylor et al. 2012). Con base en el análisis de los marcadores microsatélites (GA)_n, (GT)_n y GT(A)_n, Carter et al. (1997; 2001) observaron diferencias en la estructura de población de *H. capsulatum* en un gran número de aislados de Estados Unidos de América y en escasos aislados de Colombia, sugiriendo los autores la separación de ambas poblaciones del hongo en distintas especies de acuerdo con el concepto de especie filogenética.

A partir de nuevos datos obtenidos con los cuatro marcadores antes referidos (arf, H-anti, ole1 y tub1) (Taylor et al. 2005) y de resultados recientes de Taylor et al. (2012) con el microsatélite (GA)_n, el cual está ubicado en el gen *HSP60* que codifica una proteína de choque térmico, se analizaron aislados de *H. capsulatum* recuperados de murciélagos con hábitat cavernícola y los resultados resaltan la separación de un grupo de aislados obtenidos del murciélagos migratorio *T. brasiliensis* constituyéndose en una nuevo clado y/o nueva especie filogenética (Taylor et al. 2005; 2012; Vite-Garín 2011; 2014; 2016).

Recientemente, Sahaza et al. (2019), a través del análisis estadístico de valores de índices de asociación de aislados clínicos de humanos de *H. capsulatum*, reportaron la existencia de una estructura poblacional clonal en Argentina y

confirmaron una estructura poblacional recombinante para aislados de Colombia y México.

Delimitación de especies de *H. capsulatum* por métodos de coalescencia

Los análisis MLS han sido ampliamente utilizados para la delimitación de especies en estudios realizados con diversos tipos de organismos, incluyendo animales, plantas y hongos macro y microscópicos. Sin embargo, se han detectado algunas desventajas con el uso de éste tipo de análisis, entre ellas, y quizá una de las más importantes, es que en ocasiones se pueden obtener árboles con topologías que presentan altos valores de soporte pero que son incorrectas, pues los análisis MLS por métodos de reconstrucción filogenética pueden ser sensibles a diversos factores por ejemplo los parámetros seleccionados, el uso de genes parálogos como marcadores, o genes que están involucrados en eventos tales como hibridación, transferencia horizontal, introgresión, sorteo incompleto de linajes y coalescencia profunda (Carstens y Dewey 2010; Fujita et al. 2012; Heled y Drummond 2010; Liu et al. 2009; Maddison 1998).

Para resolver este problema se han propuesto diversos métodos basados en la teoría de la coalescencia (Degnan y Rosenberg 2009; Liu et al. 2009), la cual es un modelo matemático retrospectivo que se basa en la genealogía de genes, y que permite describir como se unen los linajes hacia atrás en el tiempo hasta encontrar el ancestro común más reciente (Degnan y Salter 2005). Actualmente, se han propuesto diversos métodos basados en la teoría de la coalescencia que, además del reconocimiento de las relaciones filogenéticas entre especies, permite identificar linajes evolutivos independientes, y que no caen bajo ningún tipo de concepto de especie.

En el caso de hongos microscópicos, este tipo de métodos se ha utilizado como herramienta para delimitar especies y establecer relaciones filogenéticas entre los géneros *Penicillium*, *Debaryomyces* y *Alternaria*, entre otros. Con respecto a *H. capsulatum* la aplicación de métodos de coalescencia para delimitar especies es novedosa y, de acuerdo con Vite-Garín et al. (2016) los resultados muestran

diferencias importantes en las relaciones filogenéticas entre clados y/o especies filogenéticas, cuando se comparan los árboles de especie con las genealogías multilocus, lo cual, de acuerdo con los autores, puede deberse a procesos de recombinación, que ya han sido reportados con anterioridad para el complejo *H. capsulatum* (Kasuga et al. 1999).

La delimitación de especies de hongos de importancia médica como *H. capsulatum* es necesaria para el conocimiento de su diversidad biológica, patrones geográficos y respuesta a cambios ambientales, los cuales son factores indispensables para el conocimiento de la epidemiología del patógeno (Estrada-Bárcenas et al. 2014).

Con el propósito de contribuir al estudio de la diversidad genética de *H. capsulatum* que permita aportar mayor información a su filogenia, para el presente trabajo se seleccionaron varios marcadores ya estudiados en *H. capsulatum* para realizar análisis multilocus amplio que permita arrojar datos substanciales para distinguir diferencias genéticas dentro del complejo *H. capsulatum*.

PLANTEAMIENTO DEL PROBLEMA

Con base en los antecedentes filogenéticos del complejo *H. capsulatum*, el análisis MLS utilizando un mayor número de loci altamente polimórficos y de aislados de *H. capsulatum* permitiría aportar más información a la gran diversidad genética del hongo, al generar nuevos datos para inferir una filogenia más robusta y contribuir al conocimiento evolutivo del patógeno, así como apoyar la epidemiología de la enfermedad asociada. Los marcadores propuestos para este estudio son: los fragmentos de los genes arf, H-anti, ole1, tub1, el microsatélite (GA)n (HSP-TC), y la región ITS1-5.8S-ITS2 del rDNA.

HIPÓTESIS

El estudio multilocus con marcadores moleculares muy informativos de aislados de *H. capsulatum* obtenidos de diferentes huéspedes, fuentes y procedencias

geográficas, permitirá generar mayor información sobre la diversidad genética del complejo *H. capsulatum* la cual podrá discriminar nuevos grupos genéticos que contribuirán a una filogenia más robusta de este patógeno.

OBJETIVO GENERAL

Contribuir al mayor conocimiento de la diversidad genética y de la filogenia del complejo *H. capsulatum* por medio de varios marcadores moleculares altamente polimórficos, utilizando aislados de diferentes huéspedes, fuentes y procedencias geográficas.

OBJETIVOS PARTICULARES

- 1) Aportar nuevos conocimientos a la diversidad genética de *H. capsulatum*, a través de varios análisis más robustos de los aislados asociados a diferentes ambientes y procedencias geográficas.
- 2) Actualizar la información de las especies filogenéticas del hongo, asociadas a su ambiente y distribución geográfica.
- 3) Buscar nuevas especies filogenéticas del hongo.
- 4) Identificar la estructura de población de los aislados de *H. capsulatum* estudiados.

METODOLOGÍA

Aislados fúngicos

Se utilizaron 65 aislados de *H. capsulatum* (Tabla 1), obtenidos de: murciélagos naturalmente infectados y capturados al azar en México y Brasil; guano de murciélagos y de aves procedentes de México y Guatemala; así como, aislados clínicos de pacientes con histoplasmosis procedentes de México, Guatemala, Colombia y Brasil. Además, se utilizaron tres cepas del American Type Culture Collection (ATCC) consideradas como referencia, dos de Estados Unidos de

América, G-217B (ATCC-26032) y Downs (ATCC-38904) y G-186B (ATCC-26030) de Panamá. Todos los aislados y cepas del estudio están depositadas en el Banco de Cepas de *Histoplasma capsulatum* del Laboratorio de Inmunología de Hongos del Departamento de Microbiología y Parasitología, de la Facultad de Medicina, UNAM (www.histoplas-mex.unam.mx), la cual está registrada en el “World Data Centre for Microorganisms” como LIH-UNAM WDCM817.

Procedimientos de bioseguridad

Debido a que *H. capsulatum* es clasificado como un patógeno de riesgo biológico nivel 3, su manejo se realizó en una área restringida de la Unidad de Micología del Departamento de Microbiología y Parasitología de la Facultad de Medicina, UNAM. Esta área fue adaptada para funcionar bajo condiciones adecuadas de bioseguridad de tipo BCL2 Plus y cuenta con un gabinete de bioseguridad para patógenos fúngicos nivel 3. Asimismo, cercano a esta área se adaptaron espacios específicos para los diferentes procedimientos de Biología Molecular. El acceso a cualquiera de los espacios de trabajo de riesgo biológico y molecular está limitado al personal de la Unidad de Micología y bajo un reglamento específico. Los desechos de todo el material biológico y molecular se manejan de acuerdo con lo establecido por la Comisión de Manejo de Residuos Biológicos y Químicos de la Facultad de Medicina, UNAM.

Cultivo de micelio de *H. capsulatum* y extracción del DNA

Los aislados de *H. capsulatum* fueron cultivados en medio GYE-líquido (glucosa 2% y extracto de levadura 1%), entre 26-28 °C con agitación constante, hasta alcanzar un buen rendimiento de biomasa micelial. La biomasa se cosechó por filtración, se lavó con TE (Tris-HCl 10mM, EDTA 1 mM a pH 8.0), se secó con papel filtro estéril y se almacenó a -20 °C. La extracción del DNA se realizó a partir de 5 a 7 g de la biomasa de micelio agregando suficiente amortiguador de lisis (50 mM Tris-HCl a pH 7.1, 50 mM EDTA a pH 8.0, 3% SDS, 1% β-mercaptoetanol). Se trituró el micelio

con un homogeneizador ULTRA-TURRAX T8 (IKA® Works Wilmington, NC, EUA), durante tres pulsos de 1 mim cada uno. El homogeneizado se distribuyó en tubos Eppendorf (Brinkmann Instruments Inc., Westbury, NY, EUA) de 1.5 mL y se centrifugó a 14000 rpm a 4 °C-15 min. Se trataron 0.5 mL del sobrenadante con 5 µL de RNasa, se agitó en vórtex y se incubó a 37 °C-2 h. Enseguida, se agregaron 10 µL de proteinasa K (200 µg/mL), se agitó en vórtex y se incubó a 60 °C-1 h. Se adicionó un volumen de fenol-cloroformo-alcohol isoamílico mezclando por inversión hasta homogeneizar. Se centrifugó a 14000 rpm-15 min, se recuperó la fase acuosa y se repitió el procedimiento anterior. A la fase acuosa recuperada se le añadió acetato de sodio 3 M (1/40 v/v) y dos volúmenes de etanol absoluto frío, agitando suavemente para precipitar el DNA. Se centrifugó a 14000 rpm-2 min. Una vez descartado el sobrenadante, el precipitado se lavó con etanol al 70%, se centrifugó a 14000 rpm-1 min, se decantó y se dejó evaporar el etanol. Finalmente, el DNA obtenido se resuspendió en 100 µL de agua Milli-Q, se cuantificó y se almacenó a –20 °C hasta su uso.

Reacción en cadena de la polimerasa (PCR)

La PCR para cada uno de los marcadores moleculares de *H. capsulatum* seleccionados se realizó siguiendo protocolos previamente establecidos y probados:

Para **arf, H-anti, ole1 y tub1** (Kasuga et al. 2003; modificado por Taylor et al. 2005). Los oligonucleótidos utilizados para estos genes fueron: arf1 (5'-AGAATATGGGGCAAAAGGA-3') y arf2 (5'-CGCAATTCTCATCTCGTTGAG-3'); H-anti3 (5'-CGCAGTCACCTCCATACTATC-3') y H-anti4 (5'-GCGCCGACATTAACCC-3'); ole3 (5'-TTTAAACGAAGCCCCCACGG-3') y ole4 (5'-CACCAACCTCCAACAGCAGCA-3'); y tub1 (5'-GGTGGCCAAATCGCAAACTC-3') y tub2 (5'-GGCAGCTTCCGTTCTCAGT-3'). La PCR de estos marcadores se llevó a cabo con las siguientes condiciones: 20 ng de DNA genómico en una mezcla de reacción de 25 µL conteniendo 0.2 µM de los oligonucleótidos (sentido + antisentido) del marcador a ser amplificado; 1 U de *Taq*-DNA polimerasa (Applied

Biosystems Inc. Foster City, CA, EUA); 1 X del amortiguador comercial B10X de la *Taq*; 2.5 mM MgCl₂ y 200 µM de cada dNTP (Applied Biosystems). La amplificación se llevó a cabo en un termociclador MAXYGENE Thermal Cycler (Axygen Scientific, Inc., Union City, CA, EUA) con el siguiente programa de ciclado: un ciclo inicial a 94 °C-5 min; seguido de 32 ciclos de 94 °C-15 s, 65 °C-30 s, 72 °C-1 min; y un ciclo final de extensión a 72 °C-5 min. La PCR se desarrolló en un gradiente de temperatura de “annealing”, iniciando a 65 °C, con reducción paulatina de 0.7 °C por ciclo, durante los primeros 12 ciclos. Al llegar a los 56 °C, la temperatura se mantuvo constante durante los 20 ciclos restantes.

Para **(GA)n (HSP-TC)** (Carter et al. 1997; 2001; Taylor et al. 2012). Los oligonucleótidos utilizados para este microsatélite fueron: HSP-TC/L (5' GAAGCCCTGGAGGTAGACGA-3') y HSP-TC/U (5' GACCACGAGTGGTTCCCGAA-3'). La PCR se llevó a cabo con las siguientes condiciones: 20 ng de DNA genómico en una mezcla de reacción de 25 µL conteniendo 0.2 µM de los oligonucleótidos (sentido + antisentido) del marcador; 1 U de *Taq*-DNA polimerasa (Applied Biosystems); 1 X del amortiguador comercial B10X de la *Taq*; 2.0 mM MgCl₂ y 200 µM de cada dNTP (Applied Biosystems). La amplificación se realizó en un termociclador MAXYGENE Thermal Cycler (Axygen) con el siguiente programa de ciclado: un ciclo inicial a 94 °C-5 min; seguido de 30 ciclos de 94 °C-1 min, 60 °C-1 min y un ciclo final de extensión a 72 °C-5 min.

Para **ITS1-5.8S-ITS2** (modificado de Muñiz et al. 2010). Los oligonucleótidos son: ITS4 (5'-TCCTCCGCTTATTGATATGC-3') e ITS5 (5'-GGAAGTAAAAGTCGTAACAAGG-3'). La PCR se llevó a cabo con las siguientes condiciones: 25 ng de DNA genómico en una mezcla de reacción de 25 µL conteniendo 0.2 µM de los oligonucleótidos (sentido + antisentido) del marcador; 1 U de *Taq*-DNA polimerasa (Applied Biosystems); 1 X del amortiguador comercial B10X de la *Taq*; 1.5 mM MgCl₂ y 200 µM de cada dNTP (Applied Biosystems). La amplificación se realizó en el mismo termociclador y con el mismo programa de ciclado que se utilizó para los marcadores arf, H-anti, ole1 y tub1.

Secuenciación

Los productos amplificados (amplicones) de cada marcador se resolvieron por electroforesis (120 V-50 min) en gel de agarosa al 1.5% preparado en amortiguador TBE 0.5 X, pH 8.0 (Tris-Base 45 mM, ácido bórico 45 mM, EDTA 1 mM) con GelRed (Biotium, Inc., Hayward, CA, EUA) a 10 000 X (2 µL/mL). Se mezclaron 2 µL de cada amplicón con 2 µL de solución indicadora de carga 10 X (azul de bromofenol 0.25%, xilen-cianol 25% y Ficoll-400 25%) y se aplicaron en cada carril del gel, reservando el carril extremo para la aplicación del marcador de tamaño molecular (100-pb DNA Ladder). El gel se visualizó en un Transiluminador UV MultiDoc-It Digital Imaging System (UVP Inc., Upland, CA, EUA) y la imagen fue fotodocumentada en archivos digitales formato JPEG. Los amplicones fueron secuenciados en el High-Throughput Genomics Center (University of Washington, Seattle, WA, EUA). La secuenciación se realizó para ambas hebras (sentido y anti-sentido) del DNA, generando una secuencia consenso para cada marcador, de cada aislado. La mayoría de las secuencias obtenidas con los marcadores arf, H-anti, ole1 y tub1 fueron depositadas en GenBank (<http://www.ncbi.nlm.nih.gov/Sequin/index.html>). Las secuencias de la región ITS1-5.8S-ITS2 fueron depositadas en la base de datos del grupo de trabajo “DNA Barcoding of Human and Animal Pathogenic Fungi” de la “International Society for Human and Animal Mycology” (ISHAM) (<http://www.isham.org/>; <http://its.mycologylab.org>).

Análisis de BLASTn (Basic Local Alignment Search Tool)

El análisis de BLASTn se realizó según Altschul et al. (1990), utilizando sólo las secuencias obtenidas en este estudio para los seis marcadores moleculares y considerando como referencia los genes completos de la cepa G-217B (ATCC-26032) reportados en GenBank para arf, H-anti, ole1, tub1 y (GA)n (HSP-TC) (números de acceso: L25117.1, U20346.1, X85962.1, M28358.1 y L11390.2, respectivamente) y de la cepa Downs (ATCC-38904) para la región ITS1-5.8S-ITS2 (número de acceso AF322378.1).

Alineamiento de secuencias

Se alinearon las secuencias de cada gen y se construyeron alineamientos concatenados con MESQUITE ver. 2.75 (Maddison y Maddison 2014) utilizando: 1) secuencias generadas para este trabajo, las cuales se editaron manualmente por medio de Chromas Lite ver. 2.1.1 (<http://technelysium.com.au/>); 2) secuencias obtenidas de TreeBase y GenBank. Para las matrices concatenadas se tomaron en cuenta todos los aislados que tenían al menos tres secuencias de los distintos marcadores y las secuencias faltantes se consideraron como datos perdidos.

Análisis de congruencia

La congruencia entre las genealogías de los genes incluídos en este estudio fue evaluada por medio de la prueba Incongruence Length Difference (ILD) desarrollada por Farris et al. (1994) e implementada en PAUP* ver. 4.0a136 como Partition Homogeneity Test (Swofford 2003). Para cada prueba, los caracteres no informativos fueron excluidos y la partición actual fue comparada con 1000 particiones seleccionadas al azar. Según la hipótesis nula, para detectar heterogeneidad entre los conjuntos de datos, se utilizó el porcentaje de casos (“instances”) en que la suma de las longitudes de los árboles de cada partición al azar es mayor que la de la partición actual del conjunto de datos analizados.

Reconstrucción filogenética

La reconstrucción filogenética se realizó para cada una de las matrices individuales y concatenadas (análisis MLS) obtenidas, por medio de los siguientes métodos: 1- Análisis de parsimonia, con TNT ver. 1.1 (Goloboff et al. 2008) a partir de un árbol inicial generado al azar y 1000 iteraciones (Nixon 1999), donde los caracteres se consideraron desordenados y con pesos iguales. 2- Análisis probabilísticos por medio de máxima verosimilitud (ML) e inferencia Bayesiana (IB). El análisis de ML fue realizado en RAxMLGUI ver. 1.31 (Silvestro y Michalak 2012), utilizando como

modelo de sustitución el “General Time Reversible (GTR)” con distribución Gamma. El análisis de IB se llevó a cabo en MrBayes ver. 3.2 (Ronquist et al. 2012) con cuatro cadenas y un total de 100,000,000 de generaciones y muestreo de árboles cada 10,000 generaciones. La convergencia de las cadenas y los valores de tamaños efectivos de muestra (ESS) fueron corroborados con Tracer ver. 1.6 (<http://beast.bio.ed.ac.uk/Tracer>). Los modelos de sustitución utilizados para cada partición fueron seleccionados con base en el resultado del análisis “Bayesian information criteria” realizado por medio de jModeltest ver. 2.1.4 (Posada 2008), a saber: K80 para H-anti; K80+G con cuatro categorías para arf y tub1; K80+I para ole1; TrN+G para (GA)n y HKY para la región ITS1-5.8S-ITS2.

Los valores de bootstrap (bt) para parsimonia y ML se obtuvieron por medio de una búsqueda heurística de 1000 réplicas con el método “Tree-Bisection-Reconnection” (TBR). Para IB, se seleccionó un “maximum clade credibility tree” con un límite de probabilidad posterior de 0.95, utilizando TreeAnnotator ver. 1.8.2 implementado en *BEAST (Drummond et al. 2012; Heled y Drummond 2010). Se generaron árboles no enraizados para todos los análisis de reconstrucción filogenética. Asimismo, de modo alterno, se realizaron análisis de IB para generar árboles enraizados individuales sólo con arf, ole1, tub1 e ITS1-5.8S-ITS2, utilizando como grupo externo las secuencias del hongo *Blastomyces dermatitidis* disponibles en GenBank, considerando que de los seis marcadores estudiados, sólo éstos tienen secuencias depositadas para *B. dermatitidis* en las bases de datos. Se generaron también árboles concatenados enraizados, incluyendo H-anti y (GA)n como datos faltantes.

En las figuras, las cepas de *H. capsulatum* reportadas por Kasuga et al. (2003) como H81, H82 y H83 aparecen con su nombre original de G-184B, G-186A y G-186B, respectivamente.

Análisis de coalescencia

Se realizó un análisis de coalescencia por medio de *BEAST implementado en BEAST ver. 1.8.2 (Drummond et al. 2012; Heled y Drummond 2010). Se generó un

archivo XML con los alineamientos de algunos de los loci estudiados por medio de BEAUti ver. 1.8.2. Se utilizó K80 como modelo de sustitución para arf, H-anti, ole1 y tub1, y se consideró distribución Gamma para arf y tub1 y sitios invariables para ole1; para (GA)n se utilizó el modelo TrN y distribución Gamma. Para todas las particiones, se emplearon frecuencias de bases empíricas. Debido a que *BEAST utiliza IB para generar el árbol de especies, los parámetros incluidos en este análisis fueron los mismos que se describieron para la reconstrucción filogenética con IB. Se comparó el resultado obtenido con reloj molecular estricto y relajado, asimismo se aplicaron las pruebas de “stepping-stone” y “marginal likelihoods” por medio de Mr.Bayes ver. 3.2 (Ronquist et al. 2012). Las tasas de mutación consideradas para estos cinco genes fueron las siguientes: arf- 0.86×10^{-9} , H-anti- 1.17×10^{-9} , ole1- 0.87×10^{-9} , tub1- 1.63×10^{-9} (Kasuga et al. 2003), (GA)n (HSP-TC)- 2.39×10^{-9} (Taylor et al. 2012).

Diversidad nucleotídica

Se estimó la diversidad nucleotídica (π) intra e inter-específica de las secuencias de *H. capsulatum* utilizadas con el programa para Windows DnaSP ver. 5.10 (Librado y Rozas 2009), a partir de las matrices concatenadas tomando en consideración los grupos generados por los análisis de IB.

Redes CSTs (Concatenated Sequence-Types)

Se realizó un análisis de CSTs, con la matriz concatenada de los genes arf, H-anti, ole1 y tub1 y se generó una red no enraizada construida con el algoritmo median-joining (Bandelt et al. 1999), a través del software Network ver. 4.613 (www.fluxus-engineering.com).

RESULTADOS

Aislados fúngicos

Según las características del tipo de huésped, fuente de aislamiento y procedencia geográfica de los aislados seleccionados, 15 se obtuvieron a partir de muestras clínicas de pacientes con histoplasmosis de México, Guatemala, y Colombia, dos de guano de aves de Guatemala y 48 de distintas especies de murciélagos capturados en México y Brasil, incluyendo *Mormoops megalophylla*, *Artibeus hirsutus*, *Leptonycteris nivalis*, *L. curasoae*, *Tadarida brasiliensis*, *Desmodus rotundus*, *Molossus molossus* y *M. rufus* (Tabla 1), los cuales presentan diferentes hábitos migratorios y alimenticios (Tabla 2). El hongo fue aislado de diferentes órganos internos de murciélagos y el mayor número de aislamientos corresponde a murciélagos migratorios-insectívoros (Tablas 1 y 2).

Secuencias

En este estudio se incluyeron en total 544 secuencias procedentes de los seis marcadores utilizados (Tabla 3 y 4), distribuidas en diferentes análisis. De éstas, 171 se obtuvieron durante el curso del presente estudio: 31 para arf, 34 para H-anti, 30 para ole1, 30 para tub1, 10 para (GA)n y 36 para la región ITS1-5.8S-ITS2 y las 373 secuencias restantes derivaron de las bases de datos GenBank, TreeBase y BOLD Systems. Algunas secuencias del GenBank y del TreeBase fueron depositadas previamente para la publicación de dos trabajos asociados al desarrollo de la tesis (Vite-Garín et al. 2014; Vite-Garín et al. 2017) (ver Anexo 1). Asimismo, se depositaron secuencias de la región ITS1-5.8S-ITS2 en el BOLD Systems, para la publicación de un artículo (Estrada-Bárcenas et al. 2014) donde Vite-Garín participó como coautora (ver Anexo 1).

Análisis de BLASTn

Se realizó un análisis de BLASTn de las 171 secuencias obtenidas para este trabajo, el cual reveló una similitud entre 95 y 99% con respecto a la mayoría de las secuencias de *H. capsulatum* reportadas en las bases de datos y de 94% de similitud para las secuencias de aislados del hongo procedentes de gatos infectados originarios de Texas (Balajee et al. 2012).

Alineamiento de secuencias

Se construyeron matrices individuales para cada uno de los genes estudiados (Anexo 2) y se determinaron los sitios de inicio y término de cada fragmento génico con respecto a las secuencias completas de cepas de referencia depositadas en el GenBank para arf, H-anti, ole1, tub1 y (GA)n de la cepa G-217B; mientras que para la región ITS1-5.8S-ITS2 se comparó con la secuencia de la cepa Downs. Los datos de cada fragmento génico estudiado representados en cada matriz se muestran en la tabla 4, donde se refieren los números totales de secuencias analizadas, el tamaño del fragmento obtenido (que correspondió en su totalidad al fragmento esperado de cada gen), sitios de inicio y término de cada fragmento génico, los sitios variables e informativos, así como las mutaciones únicas, los indels y los números de transiciones y transversiones. En relación con los marcadores moleculares individuales la región ITS1-5.8S-ITS2 fue la que presentó un mayor número de pares de bases (625 nt) seguida de arf (458 nt), mientras que el fragmento más corto correspondió al microsatélite (GA)n (240 nt). Con respecto a los sitios de inicio y término de cada marcador comparado con las secuencias de los genes completos de la cepa de referencia G-217B, se determinó lo siguiente: arf presentó un total de 5 exones y 4 intrones; H-anti 6 exones y 5 intrones; ole1 con 2 exones y 1 intrón; tub1 presentó 6 exones y 5 intrones; y finalmente el microsatélite (GA)n se encuentra incluido en el exón 3 del gen *HSP60*. La región ITS1-5.8S-ITS2, que es en sí un intrón, fue analizada completa incluyendo 33 nt del gen 18S y 35 nt del gen 28S (Tabla 4). Entre los marcadores, los que presentaron mayor número de sitios

variables fueron tub1 y H-anti, mientras que el microsatélite (GA)n y la región ITS1-5.8S-ITS2 fueron menos variables. En consecuencia, los marcadores con más y menos sitios informativos correspondieron a tub1 y H-anti, así como el microsatélite (GA)n y la región ITS1-5.8S-ITS2, respectivamente (Tabla 4). Las mutaciones únicas fueron más frecuentes en la región ITS1-5.8S-ITS2 (36 nt), mientras que las menos frecuentes fueron en el microsatélite (GA)n (19 nt) y en tub1 (15 nt).

Se generó una matriz concatenada con un tamaño molecular de 2404 nt, utilizando las secuencias de los seis marcadores estudiados en 119 aislados (113 de arf, 119 de H-anti, 109 de ole1, 116 tub1, 51 de (GA)n y 36 de la región ITS1-5.8S-ITS2) (Tabla 4). Los datos de las secuencias reportadas en TreeBase, GenBank y BOLD Systems se describen en la tabla 3.

Análisis de congruencia

La prueba de ILD encontró que no hay heterogeneidad entre las genealogías. La suma de las longitudes del árbol generado con la partición original no fue significativamente menor que la suma de las longitudes en los árboles de cualquiera de las 1000 particiones determinadas al azar para el conjunto de datos estudiados (Tabla 5). Asimismo, el análisis visual de los árboles individuales, reveló los mismos grupos en cada árbol, a saber: los clados previamente descritos por Kasuga et al. (2003); la agrupación de los aislados del hongo obtenidos de gatos infectados dentro del clado NAm 1, según lo descrito previamente por Balajee et al (2012); el clado asociado a murciélagos *T. brasiliensis*; y la agrupación del aislado EH-696P obtenido de *T. brasiliensis* con el aislado clínico H153, procedente de Brasil (linaje H153/EH-696P). Sin embargo, se detectaron incongruencias en relación con la ubicación de algunos clados en los árboles generados con los diferentes marcadores (Figuras 1-18).

Reconstrucción filogenética

Se construyeron, por los métodos de parsimonia, ML e IB, árboles de las matrices individuales de cada marcador y de la matriz concatenada de seis marcadores (arf, H-anti, ole1, tub1, (GA)n y la región ITS1-5.8S-ITS2). En general, los análisis de los marcadores individuales y concatenados generaron árboles no enraizados (Figuras 1-21) y enraizados (Figuras 22-26) con topologías similares. A continuación, se describen las topologías de cada árbol.

Árboles individuales- En los análisis de los árboles de arf, H-anti, ole1 y tub1 se recuperaron todos los clados previamente descritos para el complejo *H. capsulatum*, mientras que, con los dos marcadores restantes, sólo se identificaron los clados LAm A y NAm 1 para la región ITS1-5.8S-ITS2, así como LAm A y NAm 2 para el microsatélite (GA)n. En todos los árboles individuales, se formó un único clado, el cual se denominó NAm 3, conteniendo un aislado procedente de *M. megalophylla* y 15 aislados de *H. capsulatum* obtenidos de murciélagos de la especie *T. brasiliensis*. Un aislado adicional (EH-696P) también procedente de *T. brasiliensis* se agrupó con el aislado H153, previamente descrito como linaje para Brasil (ahora considerado linaje H153/EH-696P) (Figuras 1-18). Los aislados 154-04 y 190-03, recuperados de las especies de murciélagos *Molossus molossus* y *M. rufus*, respectivamente, ambos capturados en São Paulo, Brasil, se agruparon en el clado LAm B (Figuras 1-18), mientras que el aislado clínico 1980 de Colombia se incluyó en el clado NAm 2 en la mayoría de los árboles generados (Figuras 1-6; 10-18). Finalmente, los aislados de *H. capsulatum* obtenidos de otras especies de murciélagos (*Leptonycteris nivalis*, *L. curasoae*, *Artibeus hirsutus* y *Desmodus rotundus*), así como los aislados clínicos restantes, se concentraron en el clado LAm A.

Los análisis individuales de cada marcador se describen a continuación. En **arf**, el clado formado con aislados obtenidos de *T. brasiliensis* compartió un nodo con los clados Holanda, Australia, África, LAm B, NAm 1, NAm 2 y todos los linajes, mientras que el clado LAm A se formó de manera independiente (Figuras 1-3). En **H-anti**, se observaron tres grupos: uno conteniendo tres subgrupos (NAm 3 y NAm

2, NAm 1 y H167 (aislado clínico de Argentina), linaje H153/EH-696P y Holanda; el segundo grupo se formó con los clados África, LAm B y Australia, además de los linajes H140/H185 de Perú, H66 y H69 de Colombia y Panamá que incluye los aislados G-184B, G-186A, G186B; el tercer grupo se generó con los clados LAm A y Eurasia (Figuras 4-6). **En ole1**, la topología resultante fue muy similar a la de arf. Los clados Holanda, Australia, África, LAm B, NAm 1, NAm 2, NAm 3 y la mayoría de los linajes, comparten un sólo nodo, mientras que el clado LAm A se formó de manera independiente, aunque cercano a éste se ubicó el linaje H140/H185 (Figuras 7-9). **En tub1**, también se observó un nodo a partir del cual se generaron los subgrupos Australia, Holanda y el linaje H153/EH-696P; NAm 3 y NAm 2; el clado NAm 1 y los linajes H167 y Panamá. Los clados LAm B, África y el linaje H140/H185 compartieron otro nodo y, finalmente, los clados LAm A y Eurasia se formaron de modo independiente (Figuras 10-12). **En (GA)n**, se recuperaron los subgrupos Ib y Ic descritos previamente por Taylor et al. (2012). Asimismo, se observó que NAm 3 compartió un nodo con las ramas formadas por las secuencias del clado NAm 2 (cepa G-217B y el aislado 1980) y la cepa G-186B (Linaje de Panamá), además de los aislados de Brasil 154-04 y 190-03 (ambos agrupados en LAm B con los otros marcadores) y el aislado EH-696P (Linaje H153/EH-696P) (Figuras 13-15). Finalmente, **en ITS1-5.8S-ITS2**, se confirmaron los clados LAm A y NAm 3 y, de manera independiente, se formaron dos ramas, una con la secuencia de la cepa Downs (NAm 1) y otra con las secuencias del aislado EH-696P (linaje H153/EH-696P) y de la cepa G-186B (linaje de Panamá) (Figuras 16-18).

En los análisis independientes de cada marcador, destaca que algunos clados, linajes y el aislado EH-376 (obtenido de un murciélagos de la especie *Artibeus hirsutus*), cambiaron de ubicación en los árboles de genes, dependiendo del marcador con el cual fue generado (Figuras 1-18). Los árboles enraizados utilizando como grupo externo las secuencias de *B. dermatitidis* para arf, ole1 e ITS1-5.8S-ITS2 (Figuras 22-25), revelaron la misma distribución de los clados y linajes para la mayoría de los marcadores analizados en los árboles no enraizados (Figuras 3; 9; 12), mientras que en el árbol generado para tub1 los aislados de los diferentes clados y linajes se distribuyeron de forma aleatoria. Sin embargo, en

todos los árboles enraizados destacan que la raíz del árbol se ubicó en diferentes clados, según el marcador analizado (ver Figuras 22-25).

Árboles concatenados- En los árboles generados por análisis MLS se discriminaron dos grandes grupos: uno donde se incluyeron los clados LAm A con la mayoría de los aislados estudiados y Eurasia, los cuales se originaron de un mismo nodo; el otro también compartió un mismo nodo, donde derivaron los clados África, Holanda, Australia, NAm 1, NAm 2, LAm B y la mayoría de los linajes descritos por Kasuga et al (2003), destacando el clado NAm 3 y el linaje H153/EH-696P que incluyeron los aislados del hongo obtenidos de *T. brasiliensis* (Figuras 19-21).

Se generó un árbol concatenado enraizado con *B. dermatitidis* (grupo externo) incluyendo los seis marcadores, considerando H-anti y (GA)n como datos faltantes, sin embargo, el arbol resultante mostró valores poco confiables tanto de tamaño efectivo de muestra (ESS) como de probabilidad posterior, lo cual fue atribuído a la ausencia de aproximadamente la mitad de los datos del alineamiento para el grupo externo. Asimismo, se generó otro árbol enraizado considerando los marcadores arf, ole1, tub1 e ITS (Figura 26), el cual mostró una topología similar a su correspondiente MLS sin enraizar (Figura 21). Asimismo, como en los árboles individuales enraizados (Figuras 22-25), en el concatenado la rama del grupo externo fue más larga que las ramas internas (ver Figura 26).

Análisis de coalescencia

Se generó un árbol de especies utilizando arf, H-anti, ole1, tub1 y (GA)n, el cual se comparó con los árboles filogenéticos. Para este análisis se asumió un reloj molecular estricto con base en los resultados de los métodos “stepping-stone” y “marginal likelihoods” aplicados a la matriz concatenada por medio de Mr.Bayes ver. 3.2. Las tasas de mutación consideradas para estos cinco genes fueron mencionadas en material y métodos. mientras que las edades absolutas de los clados calculadas a través de BEAUTi ver. 1.8.2. se muestran en la figura 27.

A diferencia de los árboles filogenéticos, el clado NAm 3 se comportó como grupo hermano de LAm A. Asimismo, el aislado EH-696P se apartó del resto de los clados formados, corroborándolo como en los demás análisis su comportamiento como un linaje independiente (Figura 28).

Diversidad nucleotídica

De acuerdo con los análisis de diversidad intra-específica (Tabla 6), los grupos que presentaron la mayor diversidad fueron NAm 3 ($\pi= 0.00788$) y LAm A ($\pi= 0.00704$), mientras que los grupos con menor diversidad intra-específica fueron Australia, Holanda y LAm B ($\pi= 0.00026$, $\pi= 0.00066$ y $\pi= 0.00082$, respectivamente).

Con respecto a los análisis de diversidad inter-específica (Tabla 6), el grupo que presentó la mayor diversidad fue el linaje H167 con respecto a los linajes de Colombia H66 ($\pi= 0.02881$) y H69 ($\pi= 0.02808$), mientras que el menor valor de π se presentó entre Holanda vs. Eurasia ($\pi= 0.00066$) y entre Australia vs. LAm B ($\pi= 0.00110$).

Redes CSTs

Por medio del análisis de CSTs de la matriz concatenada de 119 secuencias de arf, H-anti, ole1 y tub 1 obtenidas de 103 aislados de *H. capsulatum*, se encontraron 58 CSTs (Figura 29). Con esta red se confirmó que el clado LAm A fue el más diverso (24 CSTs), seguido de NAm 3 (9 CSTs), NAm 2 (3 CSTs), Eurasia (3 CSTs), LAm B (3 CSTs) y África (3 CSTs). Los clados menos diversos fueron NAm 1 (2 CSTs), Holanda (2 CSTs) y Australia (2 CSTs). De los 58 CSTs encontrados, siete fueron asociados con los seis linajes descritos en la figura 29.

De acuerdo con las distancias genéticas entre las CSTs, los clados LAm A y NAm 1 fueron los más distantes entre sí, Eurasia emergió de LAm A y NAm 3 compartió ancestros comunes con NAm 2, mientras que África, Holanda y Australia fueron genéticamente cercanos (Figura 29). Esta última asociación también se

observó en los árboles filogenéticos no enraizados, representados en las figuras 1-21.

DISCUSIÓN

Características relevantes de los aislados de *H. capsulatum* estudiados

Este trabajo destaca por reunir el mayor número de aislados del complejo *H. capsulatum* obtenidos de murciélagos naturalmente infectados reportados en la literatura científica hasta la fecha. El uso de este tipo de aislados de *H. capsulatum* ha sido privilegiado por el grupo de investigación asociado al Laboratorio de Inmunología de Hongos de la Facultad de Medicina de la UNAM. En los últimos años, junto con colaboradores internacionales, se han generado publicaciones que consecutivamente van perfilando informaciones sobre el complejo *H. capsulatum* (Kasuga et al. 2003; Teixeira et al. 2016; Taylor et al. 2005; Vite-Garín et al. 2014; Vite-Garín et al. 2021), con énfasis en aquellos aislados obtenidos del murciélago guanero *T. brasiliensis*, los cuales han revelado características muy peculiares.

La obtención de aislados de *H. capsulatum* no es un evento común incluso cuando proceden de muestras clínicas y más raro aún resulta su aislamiento de reservorios y dispersores naturales como es el murciélago. De los 119 aislados del hongo utilizados en los análisis, 48 procedieron de murciélagos infectados capturados al azar principalmente en las zonas Centro y Sur-Sureste de México, los cuales tienen diversos hábitos migratorios y alimenticios (Tablas 1 y 2). Estos aislados confieren relevancia a este estudio, ya que los análisis genéticos a partir de muestras ambientales enriquecen la información asociada a la diversidad genética de este patógeno, así como, aportan información sobre eventos de dispersión natural del hongo y permiten reconstruir una posible historia evolutiva de su distribución geográfica, considerando que al ser obtenidos de animales infectados podrían arrojar información más fidedigna sobre la coevolución de este patógeno con su hospedero natural como ha sido demostrado para otros patógenos de murciélagos (Akbar et al., 2012), tomando en cuenta tanto el papel de los

murciélagos no migratorios (que se mueven en zonas cercanas a su hábitat) y los migratorios (que son fieles a sus rutas migratorias). En contraste, los aislados clínicos de *H. capsulatum*, que son los más utilizados en investigación, presentan inconvenientes para definir su área de procedencia, debido a la migración errática de los humanos, la cual sesga la información filogeográfica del hongo.

Marcadores filogenéticos y análisis BLASTn de las secuencias generadas

Los seis marcadores empleados en esta tesis se seleccionaron tomando como referencia su utilidad para discriminar grupos o genotipificar aislados de *H. capsulatum*. La mayoría de los trabajos de reconstrucción filogenética de este hongo, publicados a la fecha, fueron realizados sólo con marcadores individuales o abordando análisis de matrices construidas a partir de 3 o 4 marcadores concatenados. En un esfuerzo por dar más robustez a los hallazgos filogenéticos, se incrementó el número de muestras obtenidas de la naturaleza, particularmente de murciélagos naturalmente infectados, el número de marcadores moleculares utilizados y se realizaron análisis más informativos no comúnmente aplicados en este hongo. Además, se incluyeron secuencias procedentes de otros trabajos asociados a la presente tesis (Estrada-Bárcenas et al. 2014; Rodríguez-Arellanes et al. 2013; Damasceno et al. 2019a; 2019b; Vite-Garín et al. 2014) y de colaboraciones del Laboratorio de Inmunología de Hongos con otros grupos de investigación (Kasuga et al. 1999; 2003; Teixeira et al. 2016; Taylor et al. 2005; 2012). Para determinar sus porcentajes de similitud, las secuencias obtenidas se compararon por medio de BLASTn con secuencias previamente reportadas en diferentes bases de datos. Los valores obtenidos mostraron que las secuencias analizadas presentaron alta similitud con la mayoría de las secuencias depositadas en las bases de datos, por lo que se descarta cualquier posibilidad de que no correspondan al modelo fúngico de estudio.

Congruencia filogenética

Los marcadores seleccionados se analizaron de manera independiente y concatenada. El uso de MLS como herramienta para proponer filogenias moleculares de organismos aporta información útil, siendo que en el caso del complejo *H. capsulatum* ha sido relevante para entender las relaciones filogenéticas de diferentes cepas y o aislados del hongo (Kasuga et al. 1999, 2003; Taylor et al. 2005; Balajee et al. 2012; Vite-Garín et al. 2014; Teixeira et al. 2016). Sin embargo, existe una inconveniencia con el empleo de los análisis MLS, ya que procesos como el sorteo incompleto de linajes, la hibridación, la introgresión y la recombinación pueden resultar en incongruencia filogenética entre marcadores moleculares no ligados. Ésta, se puede incrementar según se añadan más marcadores al análisis. En el pasado, Kasuga et al. (1999) reportaron incongruencias entre los árboles de genes de *H. capsulatum* generados con los cuatro fragmentos génicos arf, H-anti, ole1 y tub1, las cuales no tuvieron efecto en la filogenia realizada por MLS; en consecuencia, estos autores explicaron que la incongruencia encontrada se derivó de procesos de recombinación. En esta tesis, para identificar posibles incongruencias se realizaron dos pruebas. La primera, consistió en un análisis visual de los árboles individuales obtenidos, el cual mostró incongruencia entre sus topologías, donde algunos clados y linajes presentaron diferentes posiciones según el marcador analizado, siendo que en todos los casos fue posible reconocer los clados y linajes previamente reportados por Kasuga et al. (2003), a saber: LAm A, LAm B, NAm 1, NAm 2, Holanda, África, Australia, Eurasia, la mayoría de los linajes únicos, y el clado asociado a murciélagos denominado BAC1 por Texeira et al. (2017) y ahora considerado como la especie filogenética NAm 3 por Vite-Garín et al. (2021). La segunda prueba, denominada ILD, no detectó incongruencias, lo cual posiblemente se debió a los bajos valores de soporte de las ramas de los árboles, según lo referido por Farris et al. (1994). Además, según estos autores, la medición de la incongruencia, sea por observación de los datos o por la aplicación de índices, es intuitiva y arbitraria puesto que no hay criterios que indiquen que tan grande debe ser un índice para demostrarla (Farris et al. 1994). Asimismo, Hipp et al. (2004)

señalaron que las pruebas de incongruencia no siempre son conclusivas, ya que al concatenar genes no se pueden demostrar errores en la filogenia. En consecuencia, las distintas posiciones de algunos clados y linajes, derivadas de la prueba visual que contradice los resultados de la prueba ILD, no deben ser consideradas como críticas para establecer las relaciones filogenéticas de las secuencias de los aislados del complejo *H. capsulatum* estudiados.

Reconstrucción filogenética

Los análisis filogenéticos individuales y concatenados revelaron que el clado LAm A (Kasuga et al. 2003) fue el mejor representado y el que muestra la mayor diversidad genética, lo cual coincide con lo reportado previamente y que es claramente señalado por Taylor et al. (2022) quienes mencionan que en Latinoamérica coexisten por lo menos 9 especies filogenéticas, a saber: Nam 3, LAm A1, LAm A2, LAm B1, LAm B2, RJ, LAm C, LAm D, LAm E y algunos linajes. Sin embargo, en la presente tesis, no se pudo corroborar la separación de LAm B en varias poblaciones, debido a que esta especie está conformado sólo por aislados de Suramérica y carecemos de aislados fúngicos de esta región, aunque los resultados de los análisis MLS y CSTs sugieren que los dos únicos aislados de Brasil (154/04 y 190/03) podrían corresponder a distintas poblaciones dentro de LAm B, por lo que se considera aquí, que para clarificar las relaciones filogenéticas de estos aislados sería necesario realizar nuevos análisis incluyendo mayor número de aislados provenientes de Suramérica, privilegiando los aislados obtenidos de animales naturalmente infectados.

La presencia de dos clados monofiléticos, LAm B1 y LAm B2 reportados por Teixeira et al. (2016) dentro del clado LAm B previamente descrito por Kasuga et al. (2003) para Suramérica, apoya la hipótesis de que LAm B ha pasado por un proceso de especiación reciente como refiere Teixeira et al. (2016), el cual está asociado a la expansión de poblaciones representadas en un único grupo. Una característica de los árboles generados con secuencias de *H. capsulatum* es que comúnmente presentan bajos valores de bt y pp, lo cual coincide con lo observado en organismos

que se diversifican rápidamente en períodos de tiempo evolutivo cortos (JW Taylor, comunicación personal).

Como se refirió en resultados, los árboles individuales de arf, H-anti, ole1 y tub1 mostraron los mismos clados y linajes descritos por Kasuga et al. (2003), aunque es necesario destacar que algunos aislados tienden a distribuirse de manera aleatoria en los árboles para tub1, posiblemente por la alta tasa de mutación que presenta este gen con respecto al resto de los marcadores estudiados, lo cual indicaría que este gen, al menos para *H. capsulatum*, se mantiene en constante cambio. Aún así, la topología del árbol individual permite diferenciar de manera general los principales clados. Se realizaron los análisis correspondientes a cada uno de los marcadores estudiados pero debido a la ausencia de secuencias en los bancos de datos para aislados del hongo, provenientes de Australia, Holanda, África, Eurasia y algunos linajes únicos, en los análisis para la región ITS1-5.8S-ITS2 y el microsatélite (GA)n sólo se formaron los clados LAm A y NAm 1 así como LAm A y NAm 2, respectivamente.

En estudios previos, el aislado EH-696P de *H. capsulatum* obtenido de *T. brasiliensis* se ubicaba separado del resto de los demás aislados fúngicos en diferentes análisis filogenéticos, tanto individuales como concatenados (Vite-Garín 2011; Vite-Garín et al. 2014). Los resultados actuales lo agrupan con el aislado clínico H153 de Brasil, reportado por Kasuga et al. (2003), formando el linaje H153/EH-696P. Tal hallazgo es interesante porque sugiere la gran dispersión del hongo asociado al desplazamiento de su huésped y dispersor natural, el murciélagos migratorio *T. brasiliensis*, que ha sido asociado a migraciones de grandes distancias continentales (Wilkins 1989; McCracken et al. 1994). Por otro lado, los aislados EH-672B y EH-672H referidos como un posible linaje independiente en Vite-Garín et al. (2021), se incluyeron en el clado NAm 3 tanto en los análisis individuales como concatenados, posiblemente debido al aumento en el número de secuencias analizadas de aislados fúngicos de los murciélagos *T. brasiliensis* infectados (Figuras 1-18).

Sorprendentemente, el aislado clínico 1980 de un paciente nativo de Colombia, que refirió nunca haber salido de su país, se incluyó en el clado NAm 2

en los análisis realizados con la mayoría de los marcadores (Figuras 1-6; 10-18), constituyendo el primer reporte del clado NAm 2 en Sudamérica. Los clados de Norteamérica NAm 1 y NAm 2 coexisten en la misma área geográfica (Kasuga et al. 2003) y, según Teixeira et al. (2016), son consideradas poblaciones monofiléticas y no se ha detectado flujo génico entre ellas.

Coalescencia

El árbol de especies (Figura 28) generado a través del análisis de coalescencia, mostró algunas incongruencias con respecto a la topología del resto de los análisis realizados, al asociar la especie NAm 3 con LAm A y Eurasia, sin embargo, estas diferencias pudieran estar dadas por la disminución de la variación genética en la matriz estudiada, pues esta se construyó sólo con cinco de los seis genes estudiados debido a que no se pudo calcular la tasa de mutación para la región ITS1-5.8S-ITS2 (sexto marcador). Sin embargo, el aislado EH-696P de un murciélago *T. brasiliensis* capturado en México mostró un comportamiento similar al observado en los árboles generados mediante análisis de reconstrucción filogenética, pues coincidentemente, este análisis sugiere que EH-696P junto con el aislado clínico de Brasil H153 conforman un linaje independiente tal como fue reportado previamente (Kasuga et al. 2003; Vite-Garín et al. 2021).

Diversidad nucleotídica

Los análisis de diversidad nucleotídica muestran la alta diversidad genética que existe entre las diferentes especies de *Histoplasma*, pero también resaltan la alta diversidad que existe entre aislados de una misma especie, destacando los valores de π de NAm 3 ($\pi= 0.00788$) y LAm A ($\pi=0.00704$). En análisis de coalescencia realizados para cada gen individual de las secuencias que conforman el clado LAm A, establecido por Kasuga et al. (2003), se observó que este grupo está conformado por al menos 16 especies (datos no presentados), lo cual resulta congruente con el valor de π , y fue corroborado en 2016 por Teixeira et al., quien dividió el clado en

varios clados nuevos. Esta gran diversidad sugiere que lo que reconocemos como LAm A es un grupo que está aún pasando por un proceso de especiación. Con respecto a NAm 3, es necesario reunir un mayor número de secuencias para observar si en los análisis para obtener valores de π intraespecífica, lo cual podrá sugerir si se trata también de un solo clado o de varios.

De acuerdo con los valores de diversidad intra-específica para los clados Australia ($\pi= 0.00026$) y LAm B ($\pi= 0.0082$), en estos dos clados la diversidad es menor, lo cual sugiere que existe menor flujo genético entre individuos, asociado a las rutas migratorias de los murciélagos, y en el caso de Australia a que es un continente aislado lo cual podría limitar el flujo génico entre cepas distintas del hongo.

Redes CSTs

Las redes CSTs fueron generadas para investigar la diversidad y la relación entre todos los aislados de *H. capsulatum* estudiados. Con base en el número de CSTs encontrados en cada clado, el más diverso fue nuevamente LAm A seguido de LAm B, del nuevo clado NAm 3 y de NAm 2, independientemente del número de aislados analizados en cada clado. Los aislados de *H. capsulatum* del clado NAm 3 comparten una alta similitud entre sus CSTs y en sus análisis por reconstrucción filogenética. Así, es factible considerar el clado NAm 3 como una especie filogenética, con base en el concepto de especie filogenética y de acuerdo con el concepto de concordancia genealógica (Freallé et al. 2005; Gazis et al. 2011; Taylor et al. 2000a).

Finalmente, los análisis obtenidos para el microsatélite (GA)n y para la región ITS1-5.8S-ITS2, junto con los resultados de los cuatro marcadores (arf, H-anti, ole1 y tub1), mostraron que la diversidad genética del complejo de especies *Histoplasma capsulatum* se asocia a su distribución geográfica y, asimismo, que algunas especies del complejo *H. capsulatum* pudieran presentar una relación huésped-específica, conocida como estenoxenismo, como se ha detectado en las especies

filogenéticas del hongo obtenidas de murciélagos *T. brasiliensis* naturalmente infectados.

CONCLUSIONES

Actualmente, las filogenetica de las relaciones entre las especies del complejo *H. capsulatum*, se encuentran en constante cambio debido al análisis de nuevos aislados y el apoyo de técnicas moleculares y genómicas novedosas y más informativas. Por medio de aportaciones recientes, ha quedado de manifiesto la gran diversidad genética de *H. capsulatum*, particularmente en Latinoamérica.

En esta tesis, destaca la formación de un clado previamente sugerido por Taylor et al. (2005), Vite-Garín et al. (2014) y Texeira et al. (2016), que ha sido considerado por Vite-Garín et al. (2021) como una nueva especie filogenética referida aquí como NAm 3. Oportunamente, esta especie deberá ser nombrada siguiendo las reglas de nomenclatura biológica. Esta especie filogenética está sustentada por la mayoría de los aislados fúngicos de *T. brasiliensis* conteniendo también los aislados EH-672B/EH-672H que se clasificaron previamente como linaje independiente en Vite-Garín et al. (2021) y que en este estudio se asociaron con NAm 3 después de los análisis realizados, posiblemente por la inclusión de otros genes en el análisis que estén aportando mayor información acerca de la diversidad de estos aislados. Asimismo, los resultados obtenidos dieron mayor robustez al linaje H153 con la incorporación del aislado de *T. brasiliensis* EH-696P y además revelaron por primera vez la presencia de un aislado NAm 2 en Colombia.

PERSPECTIVAS INMEDIATAS Y FUTURAS

Cada día surgen nuevos métodos para trabajar con datos moleculares, o los ya existentes son optimizados. Es por esto que para microorganismos como *Histoplasma*, que presentan poca variabilidad fenotípica, es indispensable que además de los análisis moleculares clásicos, se exploren nuevas herramientas que permitan inferir relaciones filogenéticas más confiables, conocer la dinámica poblacional en forma más precisa y que además permitan conocer con mayor

detalle la genética del complejo *H. capsulatum*, además de la necesidad de obtener un mayor número de aislados de distintas fuentes, particularmente aquellos provenientes de la naturaleza, ya que estos reflejan mejor la distribución natural del hongo en el mundo.

TABLAS

Tabla 1. Datos de las cepas y/o aislados seleccionados para el estudio

Cepa y/o aislado (especie filogenética)*	Huésped	Fuente	Procedencia
EH-315 (linaje)	<i>Mormoops megalophylla</i>	Intestino	GR, MX
EH-372 (LAm A)	<i>Artibeus hirsutus</i>	Intestino	MS, MX
EH-373 (LAm A)	<i>A. hirsutus</i>	Pulmón	MS, MX
EH-374 (LAm A)	<i>A. hirsutus</i>	Bazo	MS, MX
EH-375	<i>A. hirsutus</i>	Pulmón	MS, MX
EH-376 (LAm A)	<i>A. hirsutus</i>	Pulmón	MS, MX
EH-377 (LAm A)	<i>A. hirsutus</i>	Pulmón	MS, MX
EH-378 (LAm A)	<i>A. hirsutus</i>	Pulmón	MS, MX
EH-383H	<i>Leptonycteris nivalis</i>	Hígado	MS, MX
EH-383I	<i>L. nivalis</i>	Intestino	MS, MX
EH-383P (LAm A)	<i>L. nivalis</i>	Pulmón	MS, MX
EH-384H	<i>Tadarida brasiliensis</i>	Hígado	OC, MX
EH-384I	<i>T. brasiliensis</i>	Intestino	OC, MX
EH-384P	<i>T. brasiliensis</i>	Pulmón	OC, MX
EH-391 (LAm A)	<i>L. nivalis</i>	Hígado	MS, MX
EH-393 (LAm A)	<i>L. nivalis</i>	Bazo	MS, MX
EH-394B (LAm A)	<i>L. curasoae</i>	Bazo	MS, MX
EH-394H (LAm A)	<i>L. curasoae</i>	Hígado	MS, MX
EH-394P (LAm A)	<i>L. curasoae</i>	Pulmón	MS, MX
EH-395B (LAm A)	<i>L. curasoae</i>	Bazo	OC, MX
EH-395P (LAm A)	<i>L. curasoae</i>	Pulmón	OC, MX
EH-398P (LAm A)	<i>L. curasoae</i>	Pulmón	OC, MX
EH-408H (LAm A)	<i>L. nivalis</i>	Hígado	PL, MX
EH-408P (LAm A)	<i>L. nivalis</i>	Pulmón	PL, MX
EH-436	<i>A. hirsutus</i>	Pulmón	MS, MX
EH-437	<i>Desmodus rotundus</i>	Pulmón	MS, MX
EH-449B	<i>L. nivalis</i>	Bazo	MS, MX
EH-449I	<i>L. nivalis</i>	Intestino	MS, MX
EH-449P (LAm A)	<i>L. nivalis</i>	Pulmón	MS, MX
EH-450H	<i>L. curasoae</i>	Hígado	OC, MX
EH-521	<i>A. hirsutus</i>	Pulmón	MS, MX
EH-522	<i>A. hirsutus</i>	Pulmón	MS, MX
EH-626B	<i>L. curasoae</i>	Bazo	MS, MX
EH-655I	<i>T. brasiliensis</i>	Intestino	CS, MX
EH-655P	<i>T. brasiliensis</i>	Pulmón	CS, MX
EH-658H	<i>T. brasiliensis</i>	Hígado	CS, MX
EH-658P	<i>T. brasiliensis</i>	Pulmón	CS, MX
EH-659P	<i>T. brasiliensis</i>	Pulmón	CS, MX
EH-670B	<i>T. brasiliensis</i>	Bazo	CS, MX
EH-670H	<i>T. brasiliensis</i>	Hígado	CS, MX
EH-671B	<i>T. brasiliensis</i>	Bazo	MN, MX
EH-671H	<i>T. brasiliensis</i>	Hígado	MN, MX
EH-671P	<i>T. brasiliensis</i>	Pulmón	MN, MX
EH-672B	<i>T. brasiliensis</i>	Bazo	HG, MX
EH-672H	<i>T. brasiliensis</i>	Hígado	HG, MX
EH-696P	<i>T. brasiliensis</i>	Pulmón	NL, MX
154/04	<i>Molossus molossus</i>	ND	SP, BR
190/03	<i>M. rufus</i>	ND	SP, BR
CEPA 2 (LAm A)	Zanate	Guano	GT, GT
L-100-91 (LAm A)	Zanate	Guano	GT, GT
CEPA 3 (LAm A)	Humano	Peritoneo	GT, GT

EH-46	Humano	Hígado	GR, MX
EH-53	Humano	Sangre	HG, MX
EH-317	Humano	Sangre	MS, MX
AP	Humano	LCR**	CO
GeM	Humano	ND	CO
WCh	Humano	Sangre	CO
1980	Humano	ND	CO
H.1.02.W (LAm A)	Humano	ND	GT, GT
H.1.04.91 (LAm A)	Humano	ND	GT, GT
H.1.11.94 (LAm A)	Humano	Espreso	GT, GT
H.1.12.96 (LAm A)	Humano	ND	GT, GT
Downs (NAm 1)***	Humano	Vagina	IL, EUA
G-186B (linaje)***	Humano	ND	PA
G-271B (NAm 2)***	Humano	ND	LA, EUA

Abreviaturas: Brasil (BR) - SP: São Paulo; Colombia (CO); Estados Unidos de América (EUA) - Illinois (IL); LA: Louisiana; Guatemala (GT); México (MX) - CS: Chiapas; GR: Guerrero; HG: Hidalgo; MN: Michoacán; MS: Morelos; NL: Nuevo León; OC: Oaxaca; PL: Puebla; Panamá (PA).

*Cepas de distintas especies filogenéticas clasificadas por Kasuga et al. (2003).

** LCR= Líquido cefalorraquídeo.

*** Cepas de referencia de *H. capsulatum* comúnmente utilizadas.

Tabla 2. Datos migratorios y alimenticios de los murciélagos incluidos en el estudio

Especie	Hábito		No. de individuos (Procedencia)
	Migratorio	Alimenticio	
<i>Mormoops megalophylla</i>	Migratorio	Insectívoro	1 (GR)
<i>Artibeus hirsutus</i>	Residente	Frugívoro	10 (MS)
<i>Leptonycteris nivalis</i>	Migratorio	Polinívoro-nectarívoro	8 (MS), 2 (PL)
<i>L. curasaoae</i>	Migratorio	Polinívoro-nectarívoro	4 (MS), 4 (OC)
<i>Tadarida brasiliensis</i>	Migratorio	Insectívoro	7 (CS), 2 (HG), 3 (MN), 1 (NL), 3 (OC)
<i>Desmodus rotundus</i>	Residente	Hematófago	1 (MS)
<i>Molossus molossus</i>	Migratorio	Insectívoro	1 (SP, BR)
<i>M. rufus</i>	Migratorio	Insectívoro	1(SP, BR)

Abreviaturas: BR: Brasil; CS: Chiapas; CDMX: Ciudad de México; GR: Guerrero; HG: Hidalgo; MN: Michoacán; MS: Morelos; NL: Nuevo León; OC: Oaxaca; PL: Puebla; SP: São Paulo.

Tabla 3: No. de acceso de las secuencias depositadas en diferentes bases de datos

Aislado		Marcador molecular				
	arf	H-anti	ole1	tub1	(GA)n	ITS1-5.8S-ITS2
EH-315	TreeBase	TreeBase	TreeBase	TreeBase	No depositada	BOLD Systems
	S1063	S1063	S1063	S1063		HIST002-13
EH-372	GenBank	GenBank	GenBank	GenBank	GenBank	Sin secuencia
	AF495595	AF495596	AF49559	AF49559		GQ223269
EH-373	GenBank	GenBank	GenBank	GenBank	GenBank	BOLD Systems
	AF495599	AF495600	AF495601	AF495602	GQ223270	HIST004-13
EH-374	GenBank	GenBank	GenBank	GenBank	GenBank	BOLD Systems
	AF495603	AF495604	AF495605	AF495606	GQ223271	HIST020-13
EH-375	GenBank	GenBank	GenBank	GenBank	GenBank	BOLD Systems
	AF495607	AF495608	AF495609	AF495610	GQ184595	HIST005-13
EH-376	GenBank	GenBank	GenBank	GenBank	GenBank	BOLD Systems
	AF495611	AF495612	AF495613	AF495614	GQ223272	HIST021-13
EH-377	GenBank	GenBank	GenBank	GenBank	GenBank	No depositada
	AF495615	AF495616	AF495617	AF495618	GQ223273	
EH-378	TreeBase S1063	TreeBase S1063	TreeBase S1063	TreeBase S1063	GenBank	BOLD Systems
					GQ219669	HIST022-13
EH-383H	No depositada	No depositada	No depositada	No depositada	GenBank	BOLD Systems
					GQ219672	HIST023-13
EH-383I	GenBank	GenBank	GenBank	GenBank	GenBank	Sin secuencia
	AF495619	AF495620	AF495621	AF495621		GQ219670
EH-383P	GenBank	GenBank	GenBank	GenBank	GenBank	Sin secuencia
	AF495623	AF495624	AF495625	AF495625		GQ219671
EH-384H	Sin secuencia	No depositada	No depositada	Sin secuencia	GenBank	No depositada
						GQ180984

EH-384I	GenBank AF495627	GenBanK AF495628	GenBank AF495629	GenBank AF495629	GenBank GQ180983	Sin secuencia
EH-384P	GenBank AF495631	GenBank AF495632	GenBank AF495633	GenBank AF495633	GenBank GQ180982	Sin secuencia
EH-391	TreeBase S1063	TreeBase S1063	TreeBase S1063	GenBank GQ223274	GenBank GQ223274	BOLD Systems HIST006-13
EH-393	GenBank AF495635	GenBank AF495636	GenBank AF495637	GenBank AF495638	GenBank GQ219673	BOLD Systems HIST007-13
EH-394B	Sin secuencia	No depositada	No depositada	No depositada	GenBank GQ225774	No depositada
EH-394H	No depositada	No depositada	No depositada	No depositada	GenBank GQ225773	Sin secuencia
EH-394P	GenBank AF495640	GenBank AF495639	GenBank AF495641	GenBank AF495642	GenBank GQ225775	BOLD Systems HIST008-13
EH-395B	No depositada	No depositada	No depositada	Sin secuencia	GenBank GQ225776	Sin secuencia
EH-395P	No depositada	No depositada	No depositada	Sin secuencia	GenBank GQ254644	Sin secuencia
EH-398P	No depositada	BOLD Systems HIST009-13				
EH-408H	GenBank AF495644	GenBank AF495643	GenBank AF495645	GenBank AF495646	GenBank GQ223265	Sin secuencia
EH-408P	GenBank AF495647	GenBank AF495648	GenBank AF495649	GenBank AF495650	GenBank GQ223264	Sin secuencia
EH-436	No depositada	No depositada	No depositada	No depositada	GenBank GQ223266	Sin secuencia
EH-437	No depositada	No depositada	No depositada	No depositada	GenBank GQ223276	No depositada

EH-449B	GenBank KT601373	GenBank KT601437	GenBank KT601410	GenBank KT601455	GenBank GQ223280	Sin secuencia
EH-449I	No depositada	No depositada	No depositada	No depositada	GenBank GQ223277	No depositada
EH-449P	No depositada	No depositada	No depositada	No depositada	Sin secuencia	No depositada
EH-450H	Sin secuencia	No depositada	No depositada	Sin secuencia	GenBank GQ223278	Sin secuencia
EH-521	Sin secuencia	No depositada	No depositada	No depositada	Sin secuencia	BOLD Systems HIST026-13
EH-522	Sin secuencia	No depositada	No depositada	No depositada	GenBank GQ223279	BOLD Systems HIST027-13
EH-626B	No depositada	No depositada	No depositada	No depositada	GenBank GQ223267	BOLD Systems HIST028-13
EH-655I	No depositada	Sin secuencia	No depositada	No depositada	GenBank GQ180986	No depositada
EH-655P	GenBank KT601374	GenBank KT601438	GenBank KT601411	GenBank KT601458	GenBank GQ180985	BOLD Systems HIST012-13
EH-658H	GenBank KT601375	GenBank KT601439	GenBank KT601412	GenBank KT601459	GenBank GQ0180987	BOLD Systems HIST013-13
EH-658P	No depositada	No depositada	No depositada	No depositada	GenBank GQ254643	Sin secuencia
EH-659P	Sin secuencia	No depositada	Sin secuencia	Sin secuencia	Sin secuencia	No depositada
EH-670B	GenBank KT601376	GenBank KT601440	GenBank KT601414	GenBank KT601460	GenBank GQ180988	No depositada
EH-670H	GenBank KT601377	GenBank KT601441	GenBank KT601415	GenBank KT601461	GenBank GQ180989	BOLD Systems HIST015-13
EH-671B	No depositada	No depositada	Sin secuencia	No depositada	No depositada	No depositada
EH-671H	No depositada	No depositada	Sin secuencia	No depositada	No depositada	Sin secuencia

EH-671P	No depositada	BOLD Systems HIST016-13				
EH-672B	GenBank KT601378	GenBank KT601442	GenBank KT601413	GenBank KT601456	No depositada	BOLD Systems HIST017-13
EH-672H	GenBank KT601379	GenBank KT601443	GenBank KT601416	GenBank KT601457	No depositada	BOLD Systems HIST029-13
EH-696P	GenBank KT601380	GenBank KT601444	GenBank KT601417	GenBank KT601462	No depositada	BOLD Systems HIST018-13
154-04	No depositada	No depositada	No depositada	No depositada	GenBank FJ977617	Sin secuencia
190-03	No depositada	No depositada	No depositada	No depositada	GenBank FJ977617	Sin secuencia
CEPA 2	TreeBase S1063	TreeBase S1063	TreeBase S1063	TreeBase S1063	Sin secuencia	Sin secuencia
L-100-91	TreeBase S1063	TreeBase S1063	TreeBase S1063	TreeBase S1063	Sin secuencia	Sin secuencia
CEPA 3	TreeBase S1063	TreeBase S1063	TreeBase S1063	TreeBase S1063	Sin secuencia	Sin secuencia
EH-46	TreeBase S1063	TreeBase S1063	TreeBase S1063	TreeBase S1063	No depositada	BOLD Systems HIST019-13
EH-53	TreeBase S1063	TreeBase S1063	TreeBase S1063	TreeBase S1063	GenBank GQ223268	BOLD Systems HIST001-13
EH-317	GenBank AF495541	GenBank AF495542	GenBank AF495543	GenBank AF495544	No depositada	BOLD Systems HIST003-13
AP	GenBank KT601352	GenBank KT601427	GenBank KT601389	GenBank KT601471	Sin secuencia	Sin secuencia
GeM	GenBank KT601354	GenBank KT601445	GenBank KT601391	GenBank KT601473	Sin secuencia	Sin secuencia

WCh	GenBank KT601362	GenBank KT601454	GenBank KT601399	GenBank KT601481	Sin secuencia	Sin secuencia
1980	No depositada	No depositada	Sin secuencia	No depositada	No depositada	Sin secuencia
H.1.02.W	TreeBase S1063	TreeBase S1063	TreeBase S1063	TreeBase S1063	Sin secuencia	Sin secuencia
H.1.04.91	TreeBase S1063	TreeBase S1063	TreeBase S1063	TreeBase S1063	Sin secuencia	Sin secuencia
H.1.11.94	TreeBase S1063	TreeBase S1063	TreeBase S1063	TreeBase S1063	Sin secuencia	Sin secuencia
H.1.12.96	TreeBase S1063	TreeBase S1063	TreeBase S1063	TreeBase S1063	Sin secuencia	Sin secuencia
Downs	TreeBase S1063	TreeBase S1063	TreeBase S1063	TreeBase S1063	Sin secuencia	No depositada
G-186B	TreeBase S1063	TreeBase S1063	TreeBase S1063	TreeBase S1063	No depositada	No depositada
G-217B	GenBank L25117.1	GenBank U20346.1	GenBank X85962.1	GenBank M28358.1	GenBank L11390.2	Sin secuencia
CA-1	GenBank JX033954.1	GenBank JX033955.1	Sin secuencia	GenBank JX033956.1	Sin secuencia	Sin secuencia
CA-2	GenBank JX033960.1	GenBank JX033961.1	Sin secuencia	GenBank JX033962.1	Sin secuencia	Sin secuencia
CO-1	GenBank JX033948.1	GenBank JX033949.1	Sin secuencia	GenBank JX033950.1	Sin secuencia	Sin secuencia
CO-2	GenBank JX033951.1	GenBank JX033952.1	Sin secuencia	GenBank JX033953.1	Sin secuencia	Sin secuencia
CO-3	GenBank JX033957.1	GenBank JX033958.1	Sin secuencia	GenBank JX033959.1	Sin secuencia	Sin secuencia
TX-1	GenBank	GenBank	Sin secuencia	GenBank	Sin secuencia	Sin secuencia

	JX033963.1	JX033964.1	JX033965.1			
G-184B	TreeBase	TreeBase	TreeBase	TreeBase	Sin secuencia	Sin secuencia
	S1063	S1063	S1063	S1063		
G-186A	TreeBase	TreeBase	TreeBase	TreeBase	Sin secuencia	Sin secuencia
	S1063	S1063	S1063	S1063		
H11	TreeBase	TreeBase	TreeBase	TreeBase	Sin secuencia	Sin secuencia
	S1063	S1063	S1063	S1063		
H60	TreeBase	TreeBase	TreeBase	TreeBase	Sin secuencia	Sin secuencia
	S1063	S1063	S1063	S1063		
H61	TreeBase	TreeBase	TreeBase	TreeBase	Sin secuencia	Sin secuencia
	S1063	S1063	S1063	S1063		
H62	TreeBase	TreeBase	TreeBase	TreeBase	Sin secuencia	Sin secuencia
	S1063	S1063	S1063	S1063		
H63	TreeBase	TreeBase	TreeBase	TreeBase	Sin secuencia	Sin secuencia
	S1063	S1063	S1063	S1063		
H66	TreeBase	TreeBase	TreeBase	TreeBase	Sin secuencia	Sin secuencia
	S1063	S1063	S1063	S1063		
H67	TreeBase	TreeBase	TreeBase	TreeBase	Sin secuencia	Sin secuencia
	S1063	S1063	S1063	S1063		
H69	TreeBase	TreeBase	TreeBase	TreeBase	Sin secuencia	Sin secuencia
	S1063	S1063	S1063	S1063		
H77	TreeBase	TreeBase	TreeBase	TreeBase	Sin secuencia	Sin secuencia
	S1063	S1063	S1063	S1063		
H79	TreeBase	TreeBase	TreeBase	TreeBase	Sin secuencia	Sin secuencia
	S1063	S1063	S1063	S1063		
H87	TreeBase	TreeBase	TreeBase	TreeBase	Sin secuencia	Sin secuencia
	S1063	S1063	S1063	S1063		
H97	TreeBase	TreeBase	TreeBase	TreeBase	Sin secuencia	Sin secuencia

	S1063	S1063	S1063	S1063		
H126	TreeBase	TreeBase	TreeBase	TreeBase	Sin secuencia	Sin secuencia
	S1063	S1063	S1063	S1063		
H127	TreeBase	TreeBase	TreeBase	TreeBase	Sin secuencia	Sin secuencia
	S1063	S1063	S1063	S1063		
H137	TreeBase	TreeBase	TreeBase	TreeBase	Sin secuencia	Sin secuencia
	S1063	S1063	S1063	S1063		
H139	TreeBase	TreeBase	TreeBase	TreeBase	Sin secuencia	Sin secuencia
	S1063	S1063	S1063	S1063		
H140	TreeBase	TreeBase	TreeBase	TreeBase	Sin secuencia	Sin secuencia
	S1063	S1063	S1063	S1063		
H144	TreeBase	TreeBase	TreeBase	TreeBase	Sin secuencia	Sin secuencia
	S1063	S1063	S1063	S1063		
H146	TreeBase	TreeBase	TreeBase	TreeBase	Sin secuencia	Sin secuencia
	S1063	S1063	S1063	S1063		
H147	TreeBase	TreeBase	TreeBase	TreeBase	Sin secuencia	Sin secuencia
	S1063	S1063	S1063	S1063		
H148	TreeBase	TreeBase	TreeBase	TreeBase	Sin secuencia	Sin secuencia
	S1063	S1063	S1063	S1063		
H149	TreeBase	TreeBase	TreeBase	TreeBase	Sin secuencia	Sin secuencia
	S1063	S1063	S1063	S1063		
H150	TreeBase	TreeBase	TreeBase	TreeBase	Sin secuencia	Sin secuencia
	S1063	S1063	S1063	S1063		
H151	TreeBase	TreeBase	TreeBase	TreeBase	Sin secuencia	Sin secuencia
	S1063	S1063	S1063	S1063		
H152	TreeBase	TreeBase	TreeBase	TreeBase	Sin secuencia	Sin secuencia
	S1063	S1063	S1063	S1063		
H153	TreeBase	TreeBase	TreeBase	TreeBase	Sin secuencia	Sin secuencia

	S1063	S1063	S1063	S1063		
H155	TreeBase	TreeBase	TreeBase	TreeBase	Sin secuencia	Sin secuencia
	S1063	S1063	S1063	S1063		
H157	TreeBase	TreeBase	TreeBase	TreeBase	Sin secuencia	Sin secuencia
	S1063	S1063	S1063	S1063		
H158	TreeBase	TreeBase	TreeBase	TreeBase	Sin secuencia	Sin secuencia
	S1063	S1063	S1063	S1063		
H159	TreeBase	TreeBase	TreeBase	TreeBase	Sin secuencia	Sin secuencia
	S1063	S1063	S1063	S1063		
H160	TreeBase	TreeBase	TreeBase	TreeBase	Sin secuencia	Sin secuencia
	S1063	S1063	S1063	S1063		
H161	TreeBase	TreeBase	TreeBase	TreeBase	Sin secuencia	Sin secuencia
	S1063	S1063	S1063	S1063		
H162	TreeBase	TreeBase	TreeBase	TreeBase	Sin secuencia	Sin secuencia
	S1063	S1063	S1063	S1063		
H163	TreeBase	TreeBase	TreeBase	TreeBase	Sin secuencia	Sin secuencia
	S1063	S1063	S1063	S1063		
H164	TreeBase	TreeBase	TreeBase	TreeBase	Sin secuencia	Sin secuencia
	S1063	S1063	S1063	S1063		
H165	TreeBase	TreeBase	TreeBase	TreeBase	Sin secuencia	Sin secuencia
	S1063	S1063	S1063	S1063		
H166	TreeBase	TreeBase	TreeBase	TreeBase	Sin secuencia	Sin secuencia
	S1063	S1063	S1063	S1063		
H167	TreeBase	TreeBase	TreeBase	TreeBase	Sin secuencia	Sin secuencia
	S1063	S1063	S1063	S1063		
H176	TreeBase	TreeBase	TreeBase	TreeBase	Sin secuencia	Sin secuencia
	S1063	S1063	S1063	S1063		
H178	TreeBase	TreeBase	TreeBase	TreeBase	Sin secuencia	Sin secuencia

	S1063	S1063	S1063	S1063		
H179	TreeBase	TreeBase	TreeBase	TreeBase	Sin secuencia	Sin secuencia
	S1063	S1063	S1063	S1063		
H185	TreeBase	TreeBase	TreeBase	TreeBase	Sin secuencia	Sin secuencia
	S1063	S1063	S1063	S1063		
H187	TreeBase	TreeBase	TreeBase	TreeBase	Sin secuencia	Sin secuencia
	S1063	S1063	S1063	S1063		
H189	TreeBase	TreeBase	TreeBase	TreeBase	Sin secuencia	Sin secuencia
	S1063	S1063	S1063	S1063		
H192	TreeBase	TreeBase	TreeBase	TreeBase	Sin secuencia	Sin secuencia
	S1063	S1063	S1063	S1063		
H194	TreeBase	TreeBase	TreeBase	TreeBase	Sin secuencia	Sin secuencia
	S1063	S1063	S1063	S1063		

Tabla 4. Datos genéticos de los alineamientos estudiados

Gen	Número de secuencias	Tamaño del fragmento (nt)	Sitios				Mutaciones únicas	Indels	Número de Transiciones	Número de Transversiones
			Inicio (nt)	Término (nt)	Variables (nt)	Informativos (nt)				
arf	112	458	415	872	65	41	22	10	25	25
H-anti	119	394	394	786	82	63	15	6	32	19
ole1	109	415	37	451	66	46	19	9	38	13
tub1	114	274	590	863	87	72	13	82	50	25
(GA)n	49	239	1971	2209	30	21	6	20	15	6
ITS1-5.8S-ITS2	37	624	33(18S)*	35(28S)*	55	18	37	31	37	25

Los datos referidos en la tabla se generaron para cada secuencia obtenida, comparándolas con las secuencias completas de las cepas de referencia G-217B [para arf, H-anti, ole1, tub1 y (GA)n] y Downs (para ITS1-5.8S-ITS2) depositadas en GenBank.

*El fragmento de la región ITS1-5.8S-ITS2 incluyó los últimos 33 nt del gen 18S y los primeros 35 nt del gen 28S como sitios de inicio y término, respectivamente.

Tabla 5: Resultados del análisis Incongruence Length Difference (ILD) usando los marcadores estudiados

Partición	Suma de las longitudes de los árboles		Valor <i>P</i>
	Partición original	Rango de Réplicas	
arf vs. H-anti	121	136	
arf vs. ole1	114	153-154	0.002000
arf vs. tub1	152	173-174	0.002000
arf vs. (GA)n	67	71	0.002000
arf vs. ITS1-5.8S-ITS2	73	84-89	0.002000
H-anti vs. ole1	131	174-176	0.002000
H-anti vs. tub1	169	189-190	0.002000
H-anti vs. (GA)n	84	85	0.002000
H-anti vs. ITS1-5.8S-ITS2	90	99-101	0.002000
ole1 vs. tub1	162	196-199	0.002000
ole1 vs. (GA)n	77	74-82	0.0026000
ole1 vs. ITS1-5.8S-ITS2	83	89-99	0.002000
tub1 vs. (GA)n	115	112-119	0.208000
tub1 vs. ITS1-5.8S-ITS2	121	123-132	0.002000
(GA)n vs. ITS1-5.8S-ITS2	36	37-40	0.006000
6 genes	319	448-452	0.0100000

Tabla 6: Análisis de diversidad nucleotídica (π)

	África	Australia	EH-672B/ EH-672H	Eurasia	G-184B G-186A G-186B	Holanda	H66	H69	H140 H185	H153/ EH-696P	H167	LAm A	LAm B	NAm 1	NAm 2	NAm 3	
África																	
Australia	0.01628																
EH-672B/	0.01295	0.01222															
EH-672H																	
Eurasia	0.01277	0.01456	0.00787														
G-184B	0.01397	0.01412	0.01435	0.01305													
G-186A																	
G-186B																	
Holanda	0.01787	0.01192	0.01923	0.00066	0.02094												
H66	0.00899	0.00762	0.00833	0.00675	0.01196	0.01989											
H69	0.01241	0.00981	0.01323	0.00894	0.01331	0.02340	0.01454										
H140	0.01516	0.01328	0.01611	0.01159	0.01176	0.02244	0.01235	0.01277									
H185																	
H153/ EH-696P	0.01769	0.01535	0.01687	0.01334	0.01802	0.02373	0.01808	0.02158	0.02072								
H167	0.01506	0.01110	0.01963	0.01124	0.01563	0.02562	0.02881	0.02808	0.01738	0.02420							
LAm A	0.00784	0.00853	0.00583	0.00581	0.00679	0.00595	0.00508	0.00508	0.00583	0.00638	0.00527						
LAm B	0.01364	0.00110	0.00655	0.01277	0.01002	0.01244	0.00387	0.00491	0.00727	0.01132	0.00738	0.00883					
NAm 1	0.02513	0.02603	0.01613	0.02693	0.01783	0.02188	0.01152	0.01124	0.01432	0.01977	0.00710	0.01443	0.01982				
NAm 2	0.01873	0.02118	0.01013	0.01901	0.01439	0.01900	0.00851	0.01031	0.01304	0.01674	0.01075	0.01033	0.01449	0.02674			
NAm 3	0.00851	0.01103	0.00128	0.01209	0.00664	0.00572	0.00372	0.00372	0.00568	0.00662	0.00405	0.01155	0.01016	0.01587	0.0937		
π intra																	
específica	0.00356	0.00026	0.00385	0.00143	0.00409	0.00066	*NA	*NA	0.00150	0.00396	*NA	0.00704	0.00082	0.00480	0.00158	0.00788	

Para determinar los valores de diversidad nucleotídica intra e inter específica se utilizó el software DnaSP ver. 5.10 (ver Materiales y Métodos).

*NA= No aplica. El valor de π no puede ser calculado en una sola secuencia.

FIGURAS

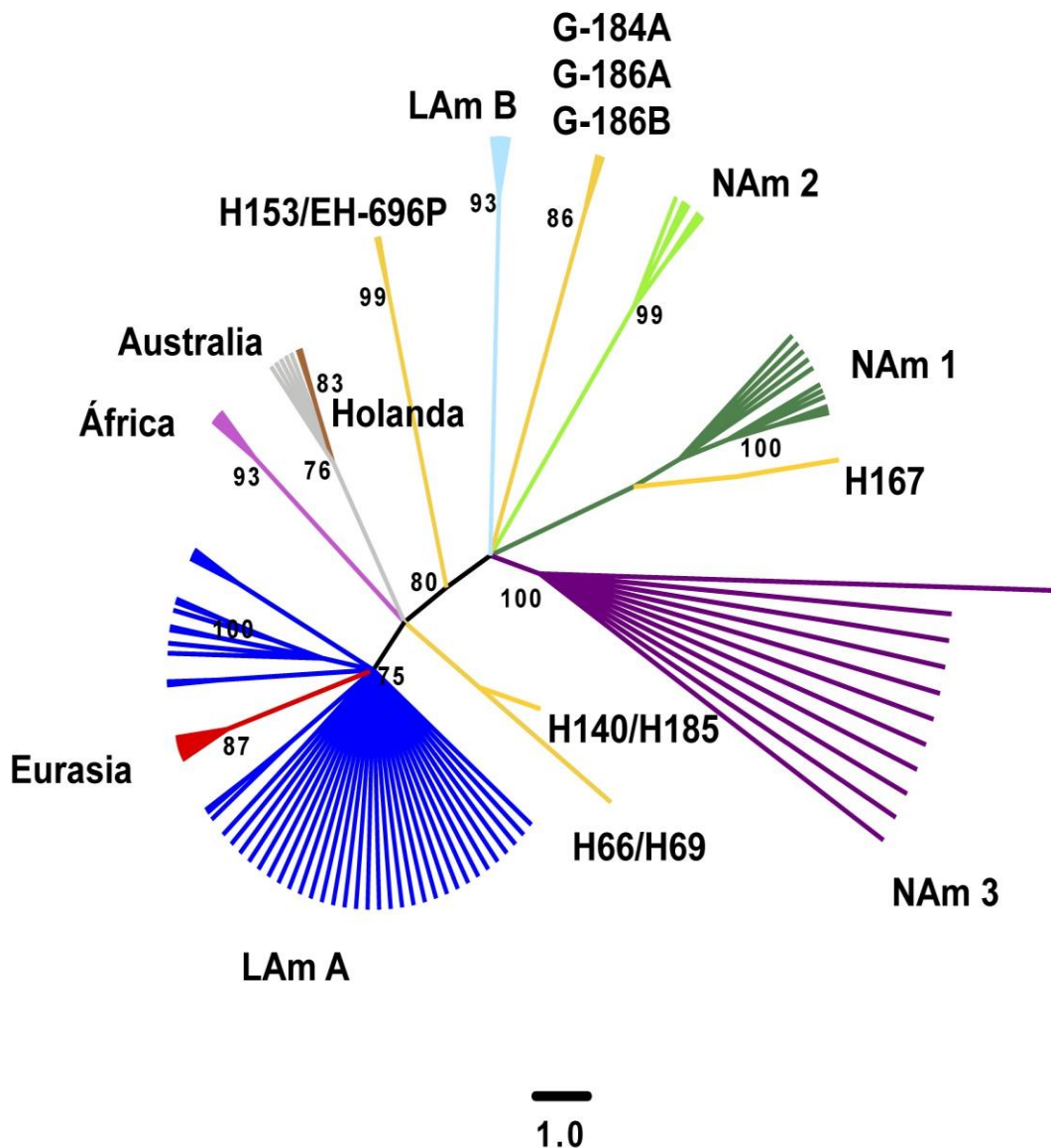


Fig.1. Árbol filogenético no enraizado de *H. capsulatum* generado por una matriz individual de secuencias de arf, utilizando el método de parsimonia. Se obtuvo el árbol de consenso estricto a partir del análisis de 112 secuencias, considerando valores de bt $\geq 70\%$, los cuales se indican en los nodos correspondientes.

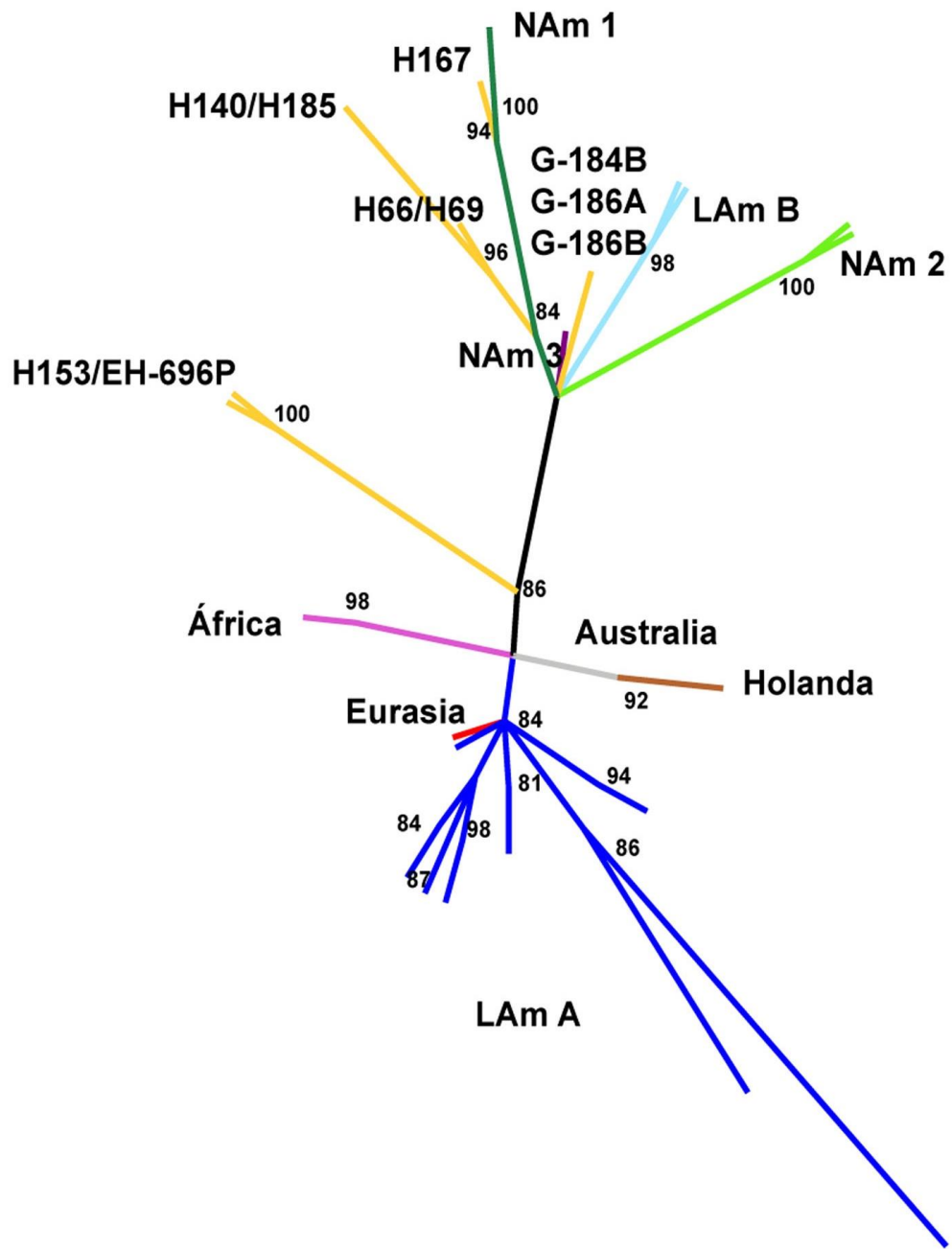


Fig.2. Árbol filogenético no enraizado de *H. capsulatum* generado por una matriz individual de secuencias de arf, utilizando el método de máxima verosimilitud. Se obtuvo el árbol a partir del análisis de 112 secuencias, considerando valores de bt $\geq 70\%$, los cuales se indican en los nodos correspondientes.

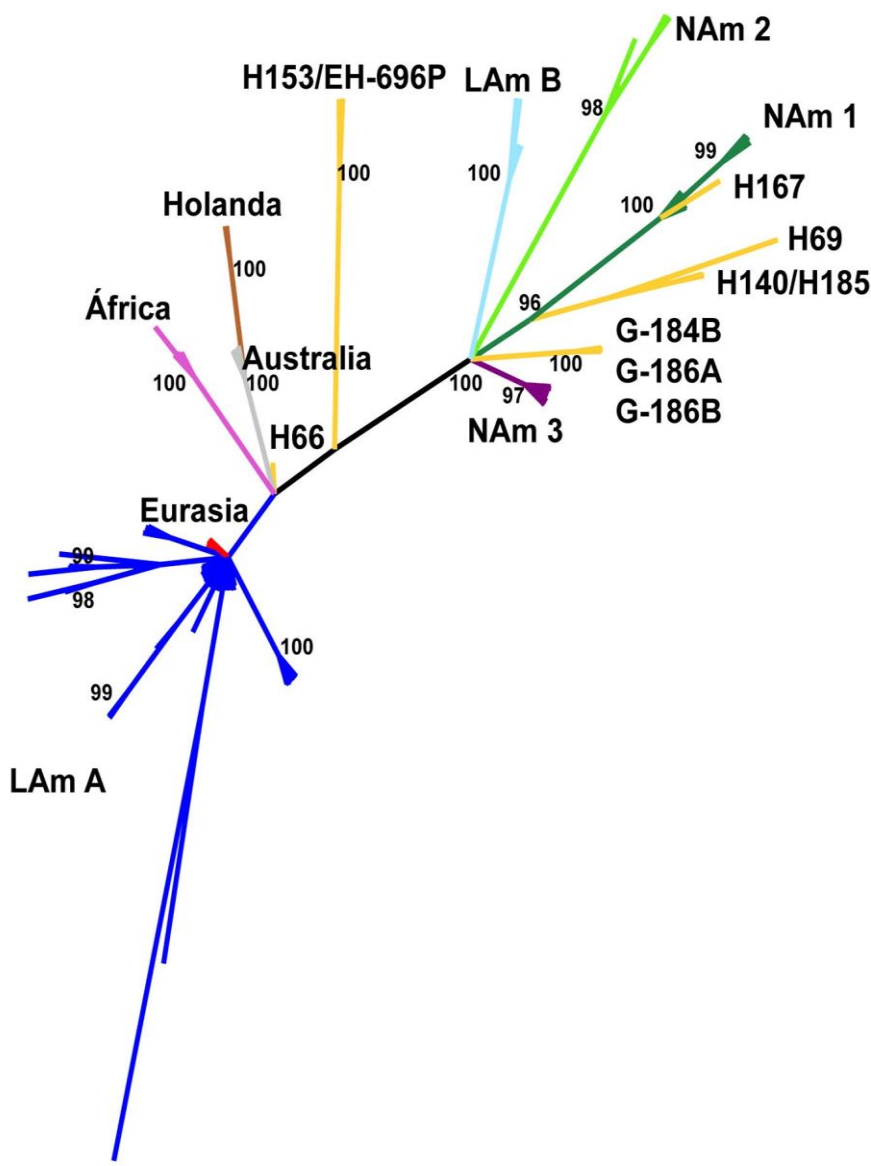


Fig.3. Árbol filogenético no enraizado de *H. capsulatum* generado por una matriz individual de secuencias de arf, utilizando el método de inferencia bayesiana. Se obtuvo el árbol de “Maximum-clade credibility” a partir del análisis de 112 secuencias, considerando valores de pp $\geq 95\%$, los cuales se indican en los nodos correspondientes.

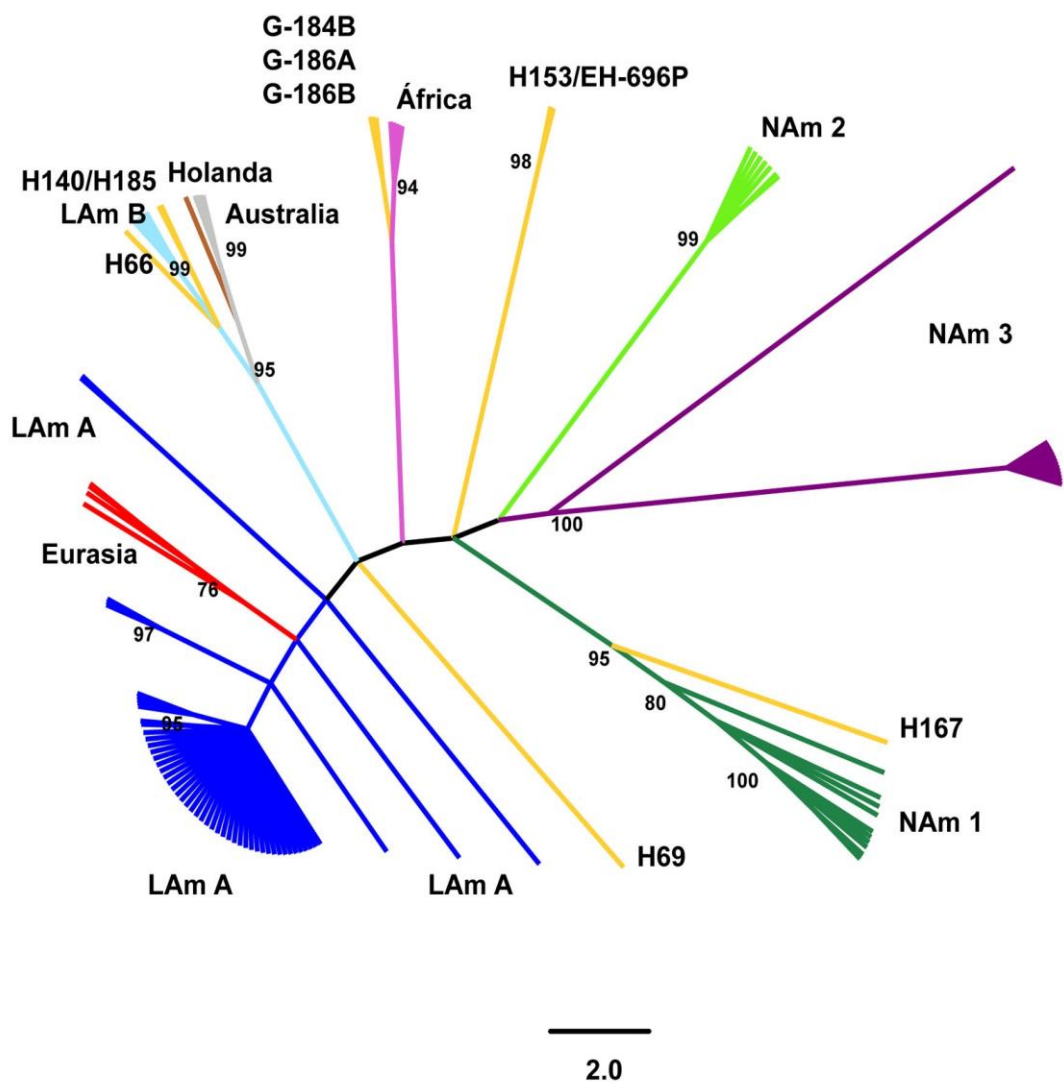


Fig.4. Árbol filogenético no enraizado de *H. capsulatum* generado por una matriz individual de secuencias de H-anti, utilizando el método de parsimonia. Se obtuvo el árbol de consenso estricto a partir del análisis de 119 secuencias, considerando valores de bt $\geq 70\%$, los cuales se indican en los nodos correspondientes.

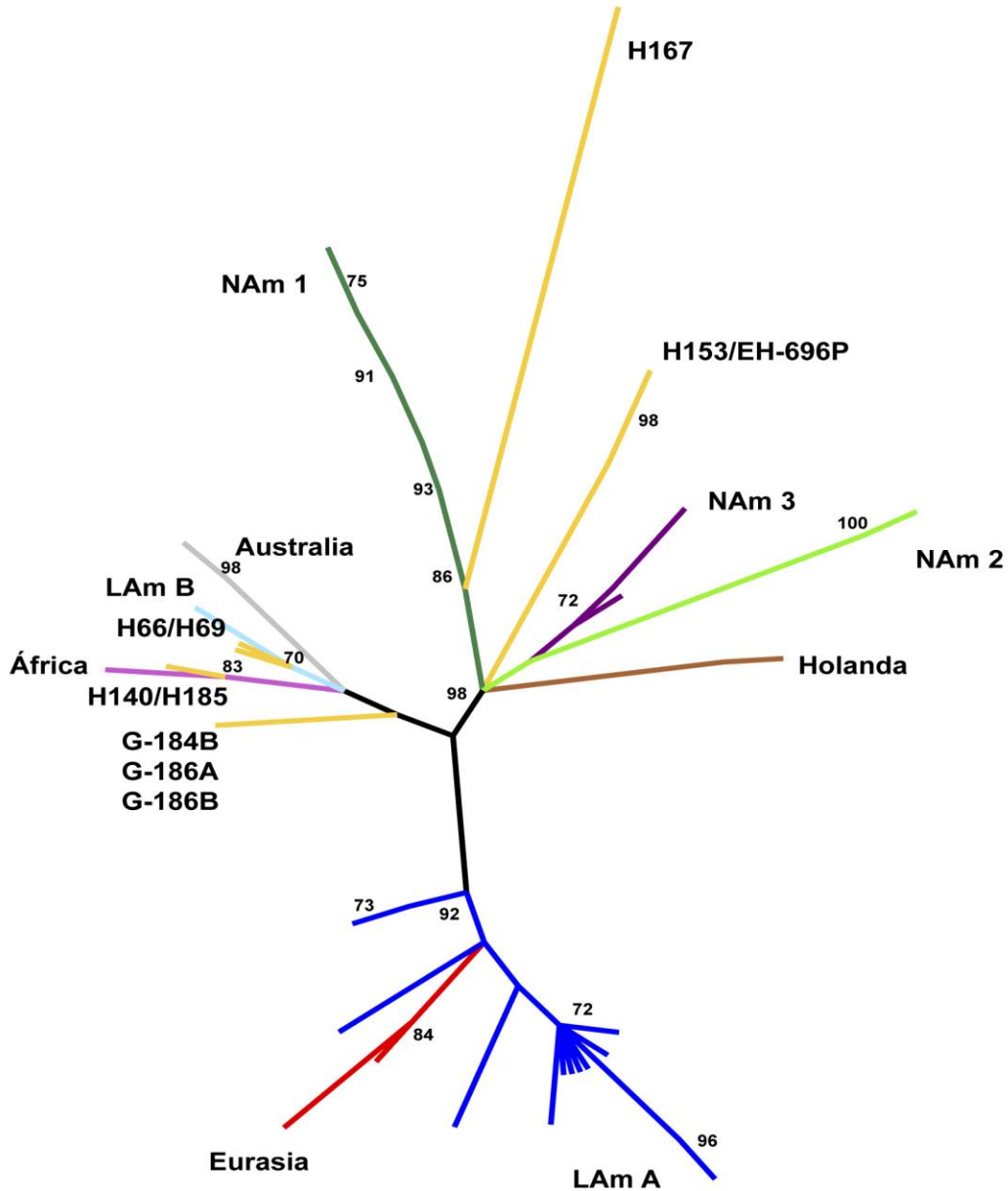


Fig.5. Árbol filogenético no enraizado de *H. capsulatum* generado por una matriz individual de secuencias de H-anti, utilizando el método de máxima verosimilitud. Se obtuvo el árbol a partir del análisis de 119 secuencias, considerando valores de bt $\geq 70\%$, los cuales se indican en los nodos correspondientes.

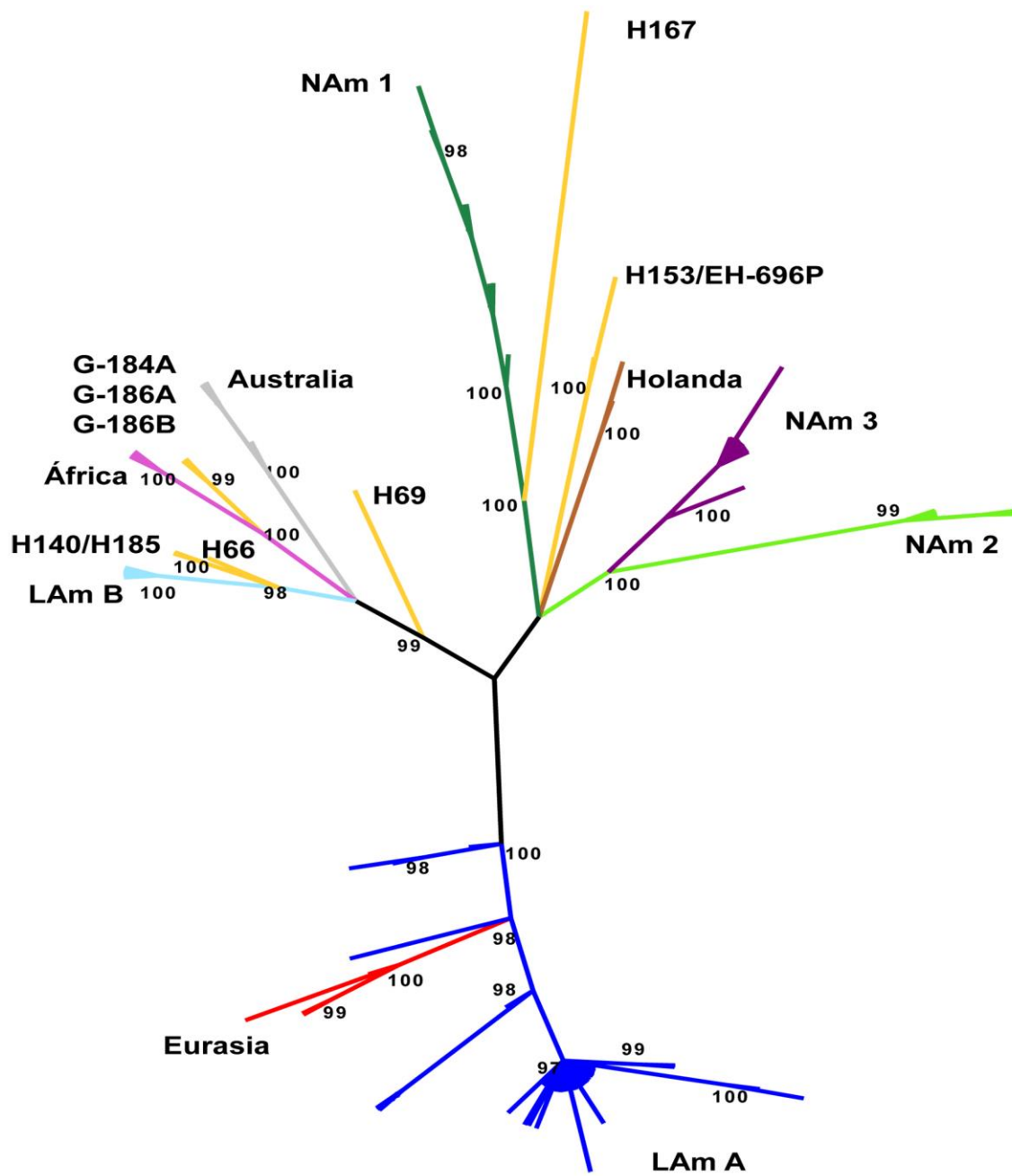


Fig.6. Árbol filogenético no enraizado de *H. capsulatum* generado por una matriz individual de secuencias de H-anti, utilizando el método de inferencia bayesiana. Se obtuvo el árbol de “Maximum-clade credibility” a partir del análisis de 119 secuencias, considerando valores de pp $\geq 95\%$, los cuales se indican en los nodos correspondientes.

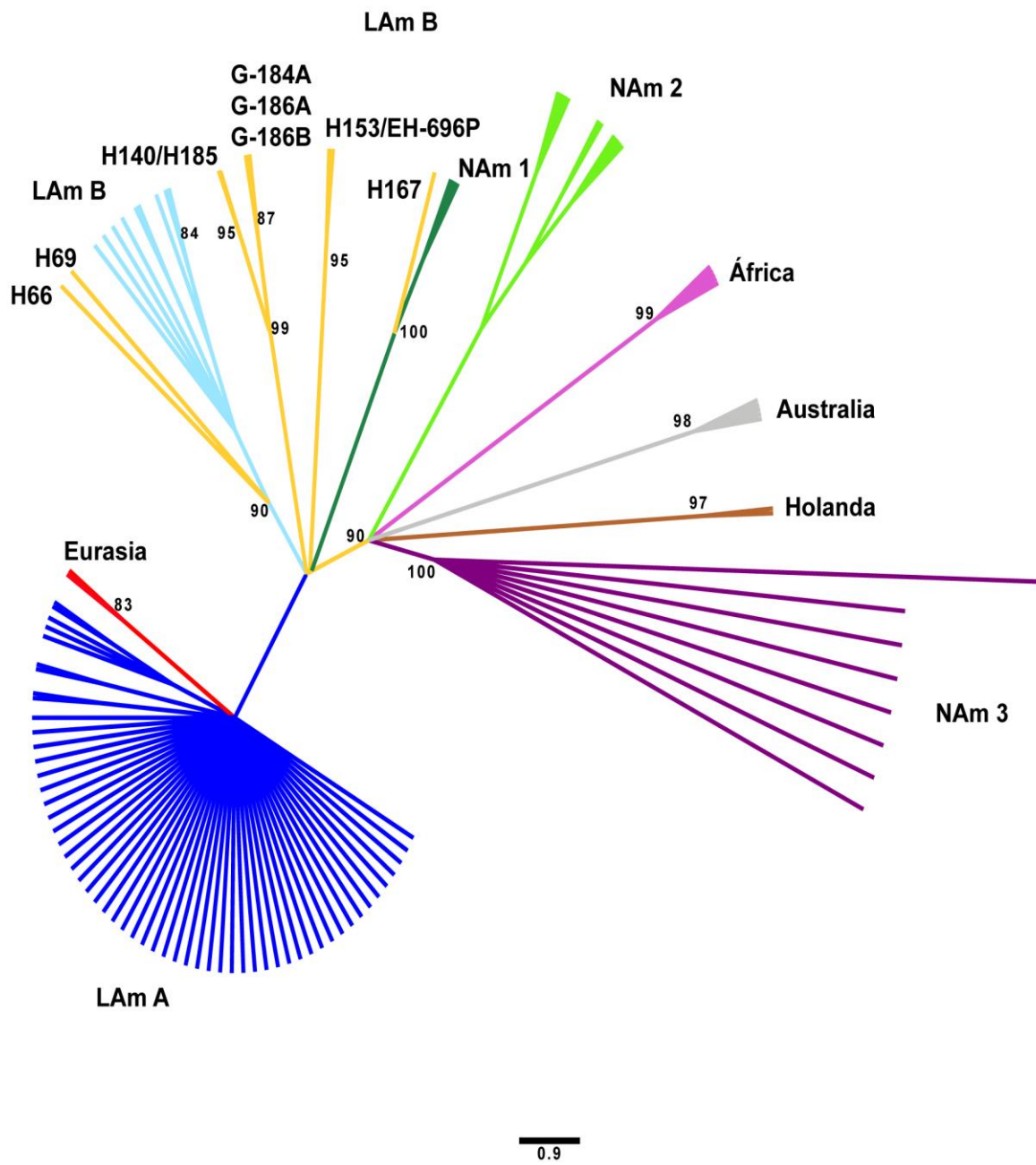


Fig.7. Árbol filogenético no enraizado de *H. capsulatum* generado por una matriz individual de secuencias de *ole1*, utilizando el método de parsimonia. Se obtuvo el árbol de consenso estricto a partir del análisis de 109 secuencias, considerando valores de bt $\geq 70\%$, los cuales se indican en los nodos correspondientes.

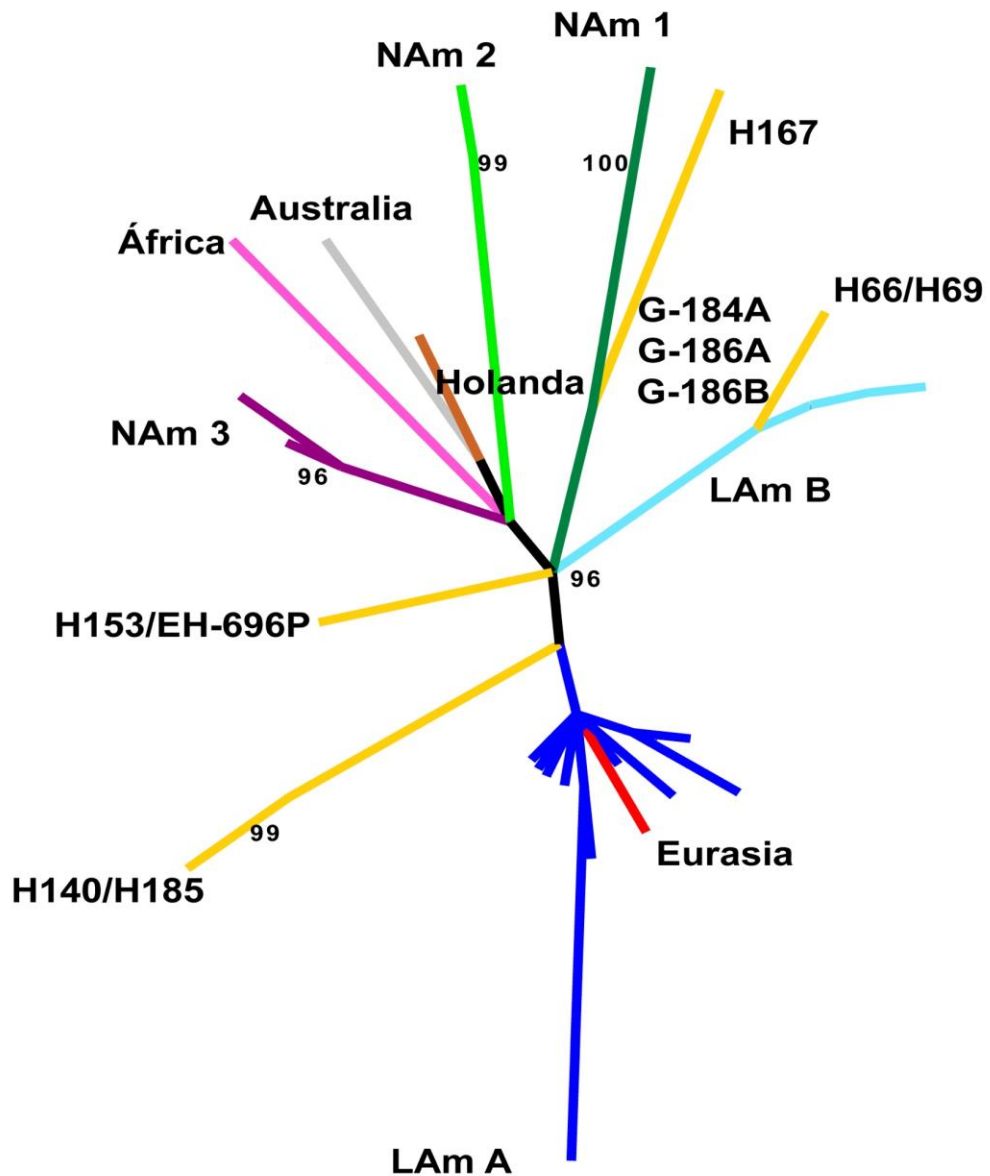


Fig.8. Árbol filogenético no enraizado de *H. capsulatum* generado por una matriz individual de secuencias de *ole1*, utilizando el método de máxima verosimilitud. Se obtuvo el árbol a partir del análisis de 109 secuencias, considerando valores de *bt* $\geq 70\%$, los cuales se indican en los nodos correspondientes.

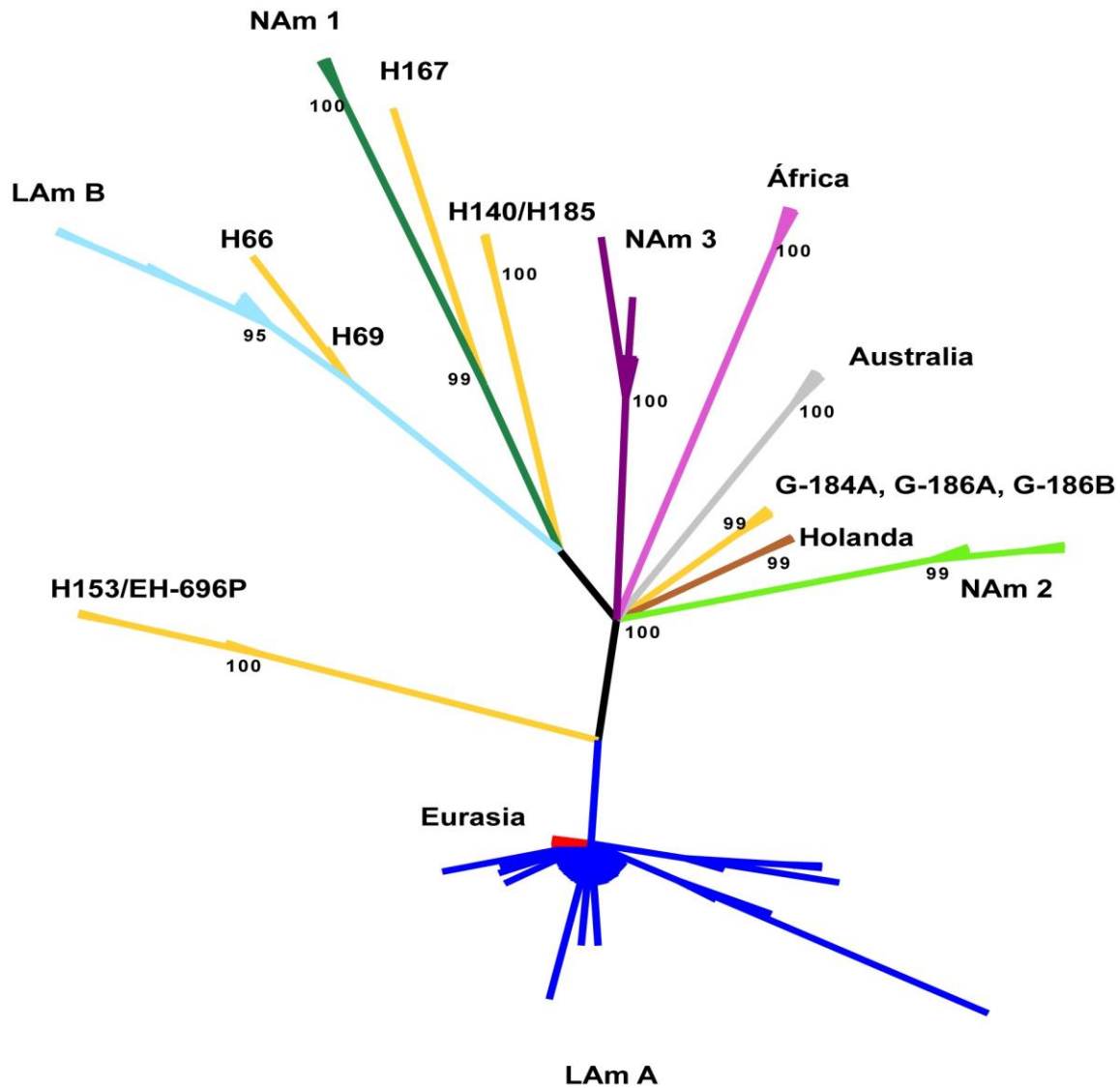


Fig.9. Árbol filogenético no enraizado de *H. capsulatum* generado por una matriz individual de secuencias de *ole1*, utilizando el método de inferencia bayesiana. Se obtuvo el árbol de “Maximum-clade credibility” a partir del análisis de 109 secuencias, considerando valores de pp $\geq 95\%$, los cuales se indican en los nodos correspondientes.

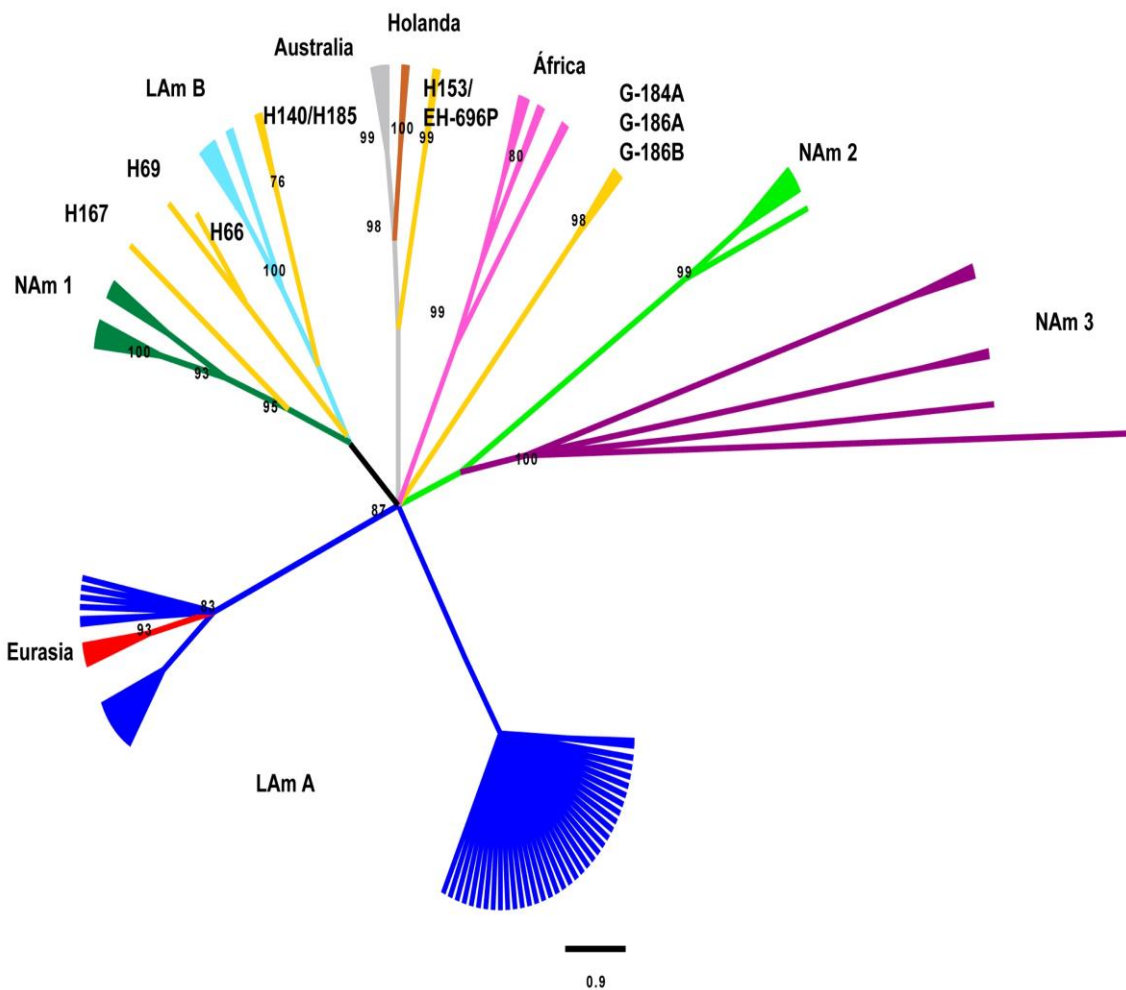


Fig.10. Árbol filogenético no enraizado de *H. capsulatum* generado por una matriz individual de secuencias de tub1, utilizando el método de parsimonia. Se obtuvo el árbol de consenso estricto a partir del análisis de 114 secuencias, considerando valores de bt $\geq 70\%$, los cuales se indican en los nodos correspondientes.

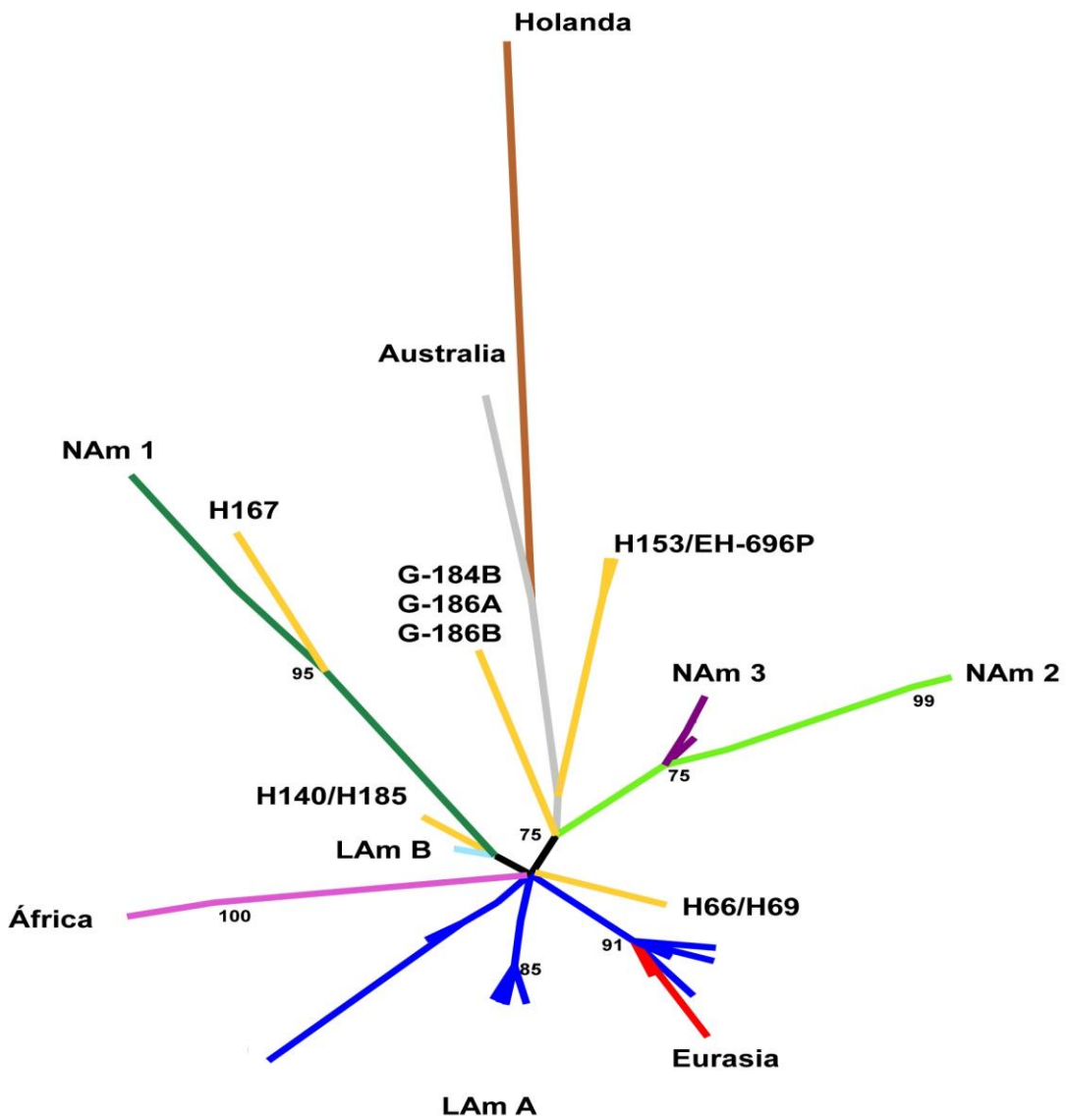


Fig.11. Árbol filogenético no enraizado de *H. capsulatum* generado por una matriz individual de secuencias de tub1, utilizando el método de máxima verosimilitud. Se obtuvo el árbol a partir del análisis de 114 secuencias, considerando valores de bt $\geq 70\%$, los cuales se indican en los nodos correspondientes.

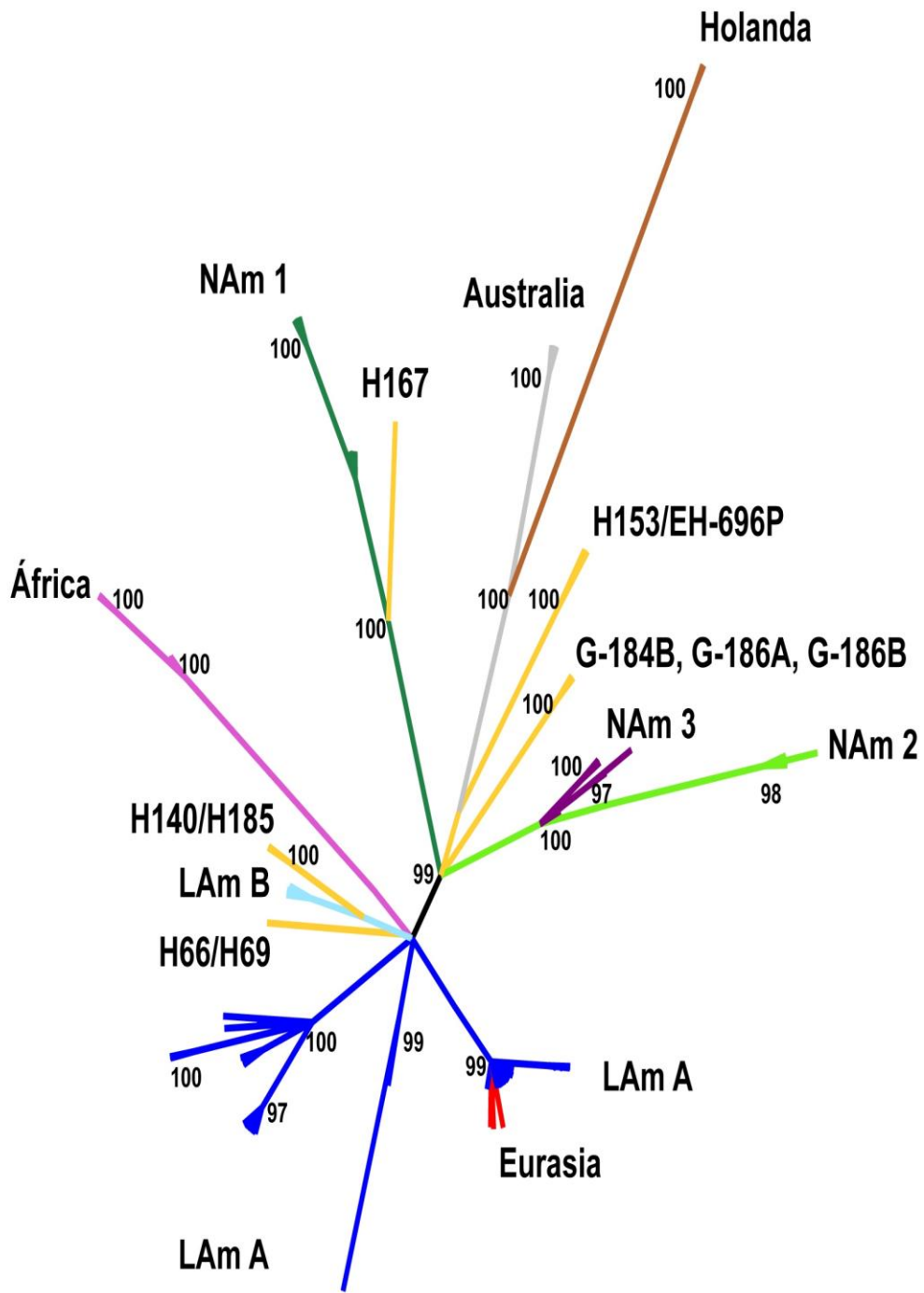


Fig.12. Árbol filogenético no enraizado de *H. capsulatum* generado por una matriz individual de secuencias de tub1, utilizando el método de inferencia bayesiana. Se obtuvo el árbol de “Maximum-clade credibility” a partir del análisis de 114 secuencias, considerando valores de pp $\geq 95\%$, los cuales se indican en los nodos correspondientes.

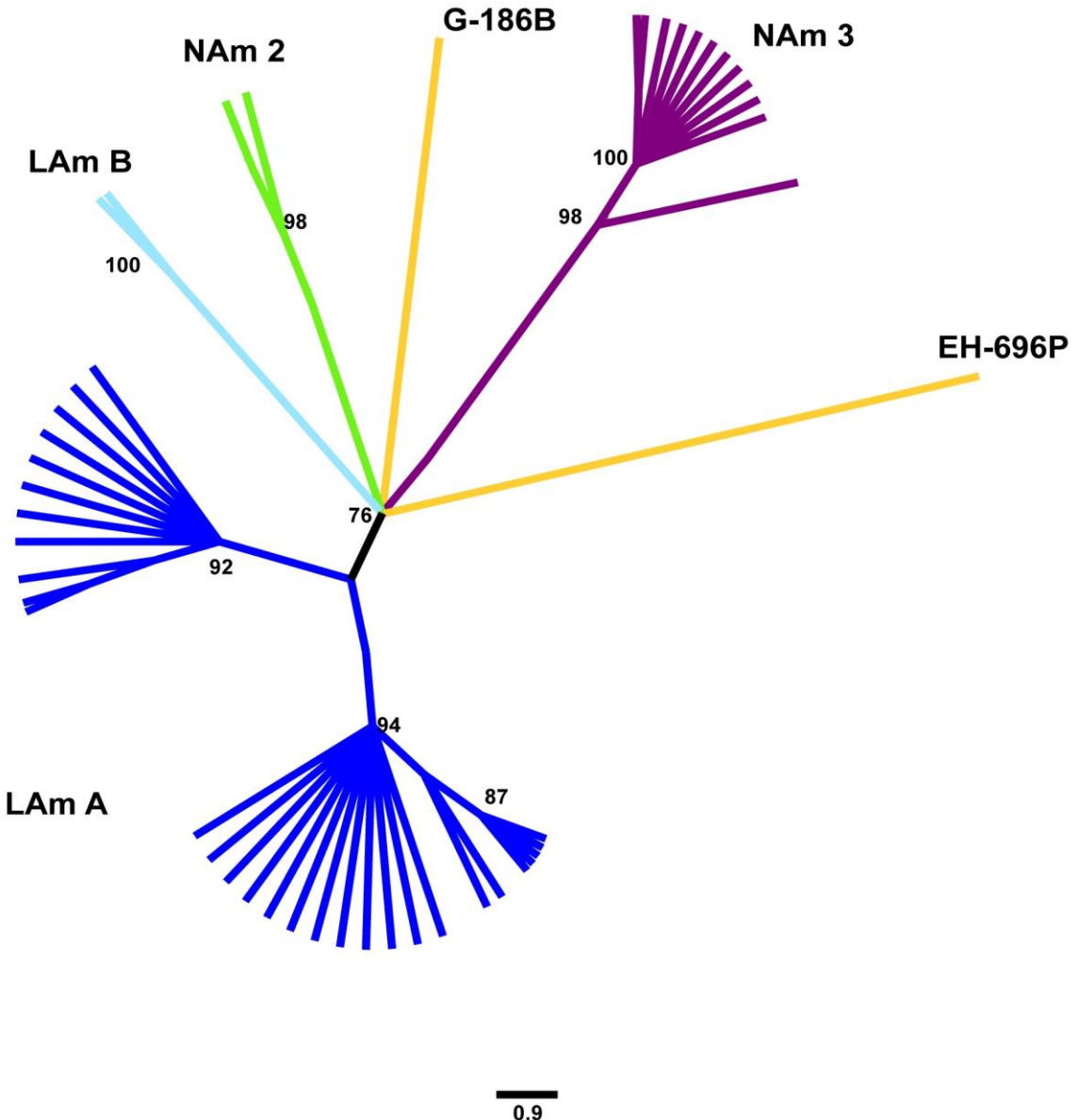


Fig.13. Árbol filogenético no enraizado de *H. capsulatum* generado por una matriz individual de secuencias del microsatélite (GA)_n, utilizando el método de parsimonia. Se obtuvo el árbol de consenso estricto a partir del análisis de 49 secuencias, considerando valores de bt ≥70%, los cuales se indican en los nodos correspondientes.

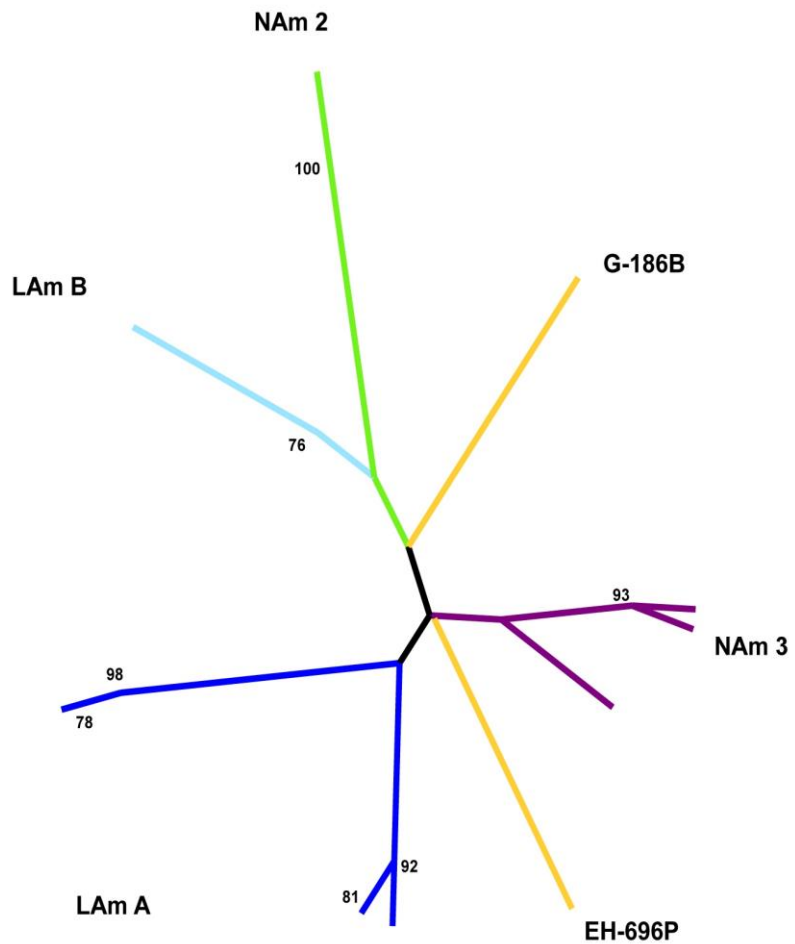


Fig.14. Árbol filogenético no enraizado de *H. capsulatum* generado por una matriz individual de secuencias del microsatélite (GA)_n, utilizando el método de máxima verosimilitud. Se obtuvo el árbol a partir del análisis de 49 secuencias, considerando valores de bt ≥70%, los cuales se indican en los nodos correspondientes.

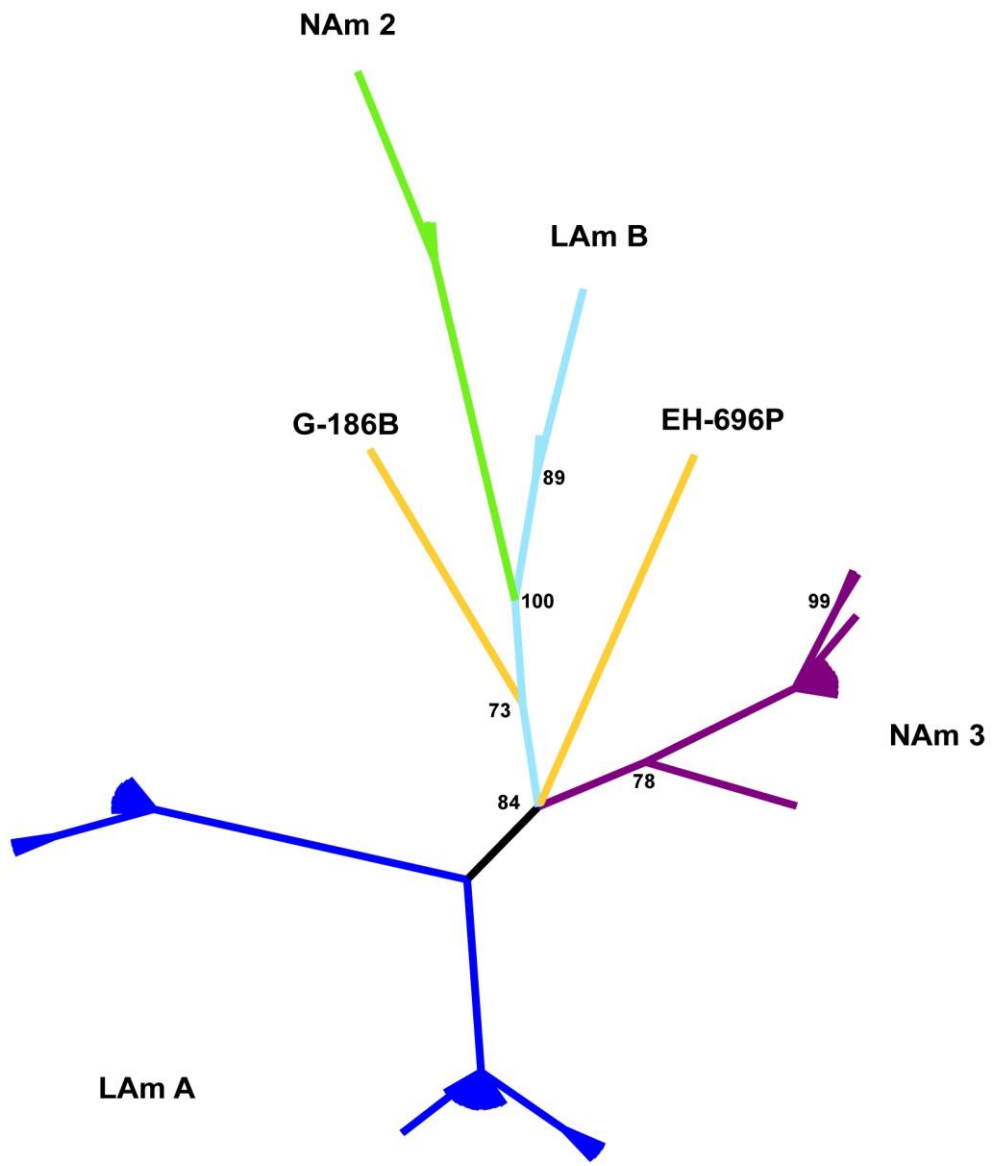


Fig.15. Árbol filogenético no enraizado de *H. capsulatum* generado por una matriz individual de secuencias del microsatélite (GA)_n, utilizando el método de inferencia bayesiana. Se obtuvo el árbol de “Maximum-clade credibility” a partir del análisis de 49 secuencias, considerando valores de pp ≥95%, los cuales se indican en los nodos correspondientes.

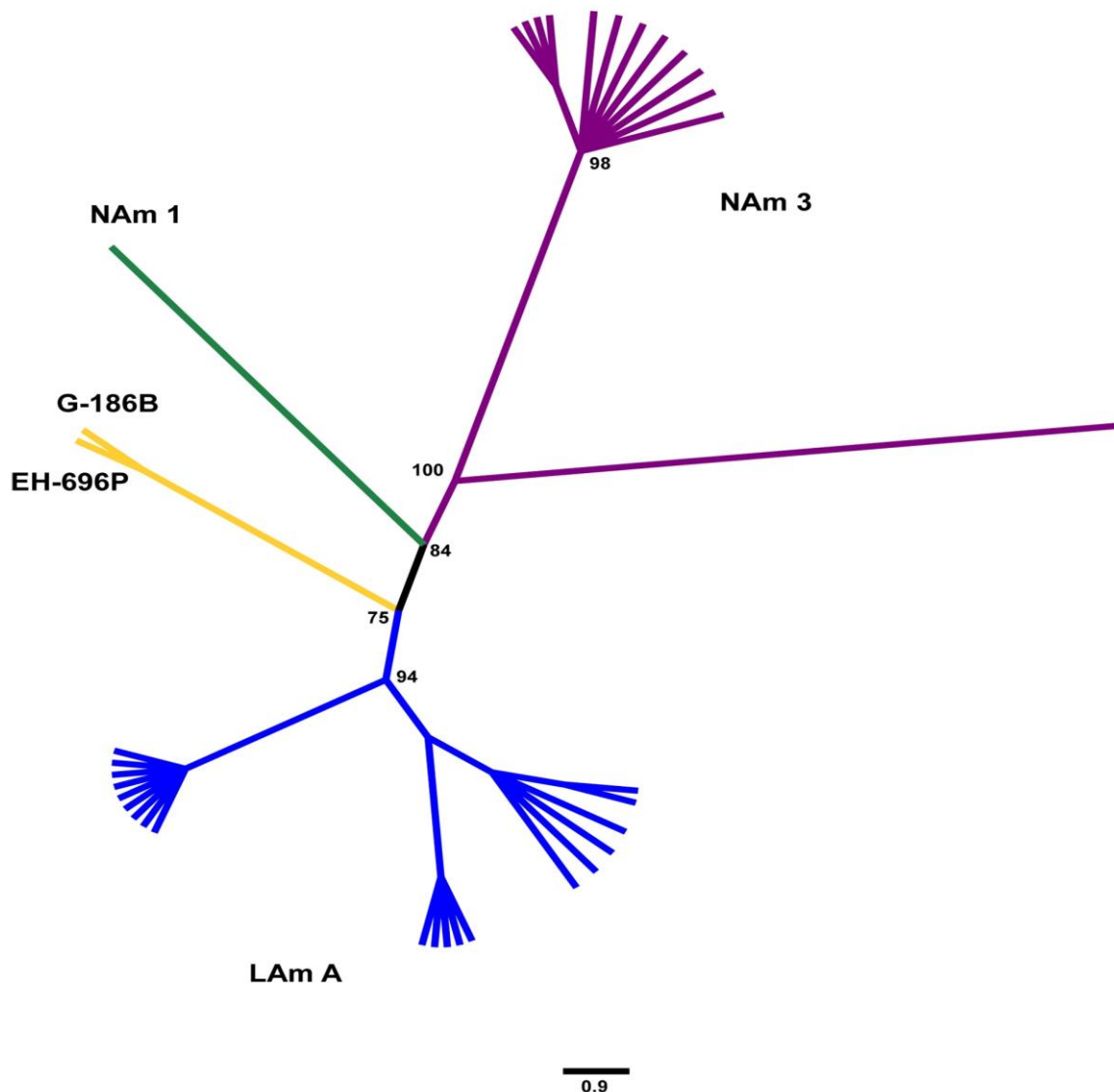


Fig.16. Árbol filogenético no enraizado de *H. capsulatum* generado por una matriz individual de secuencias de la región ITS1-5.8S-ITS2, utilizando el método de parsimonia. Se obtuvo el árbol de consenso estricto a partir del análisis de 36 secuencias, considerando valores de bt $\geq 70\%$, los cuales se indican en los nodos correspondientes.

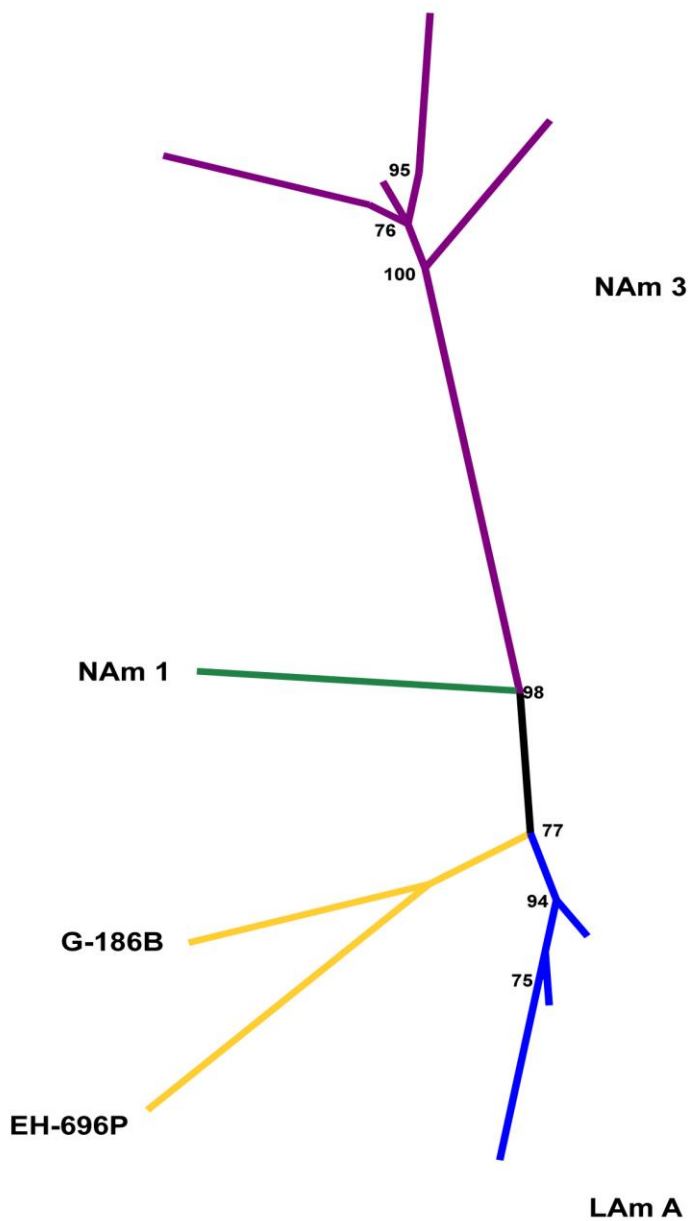


Fig.17. Árbol filogenético no enraizado de *H. capsulatum* generado por una matriz individual de secuencias de la región ITS1-5.8S-ITS2, utilizando el método de máxima verosimilitud. Se obtuvo el árbol a partir del análisis de 36 secuencias, considerando valores de $bt \geq 70\%$, los cuales se indican en los nodos correspondientes.

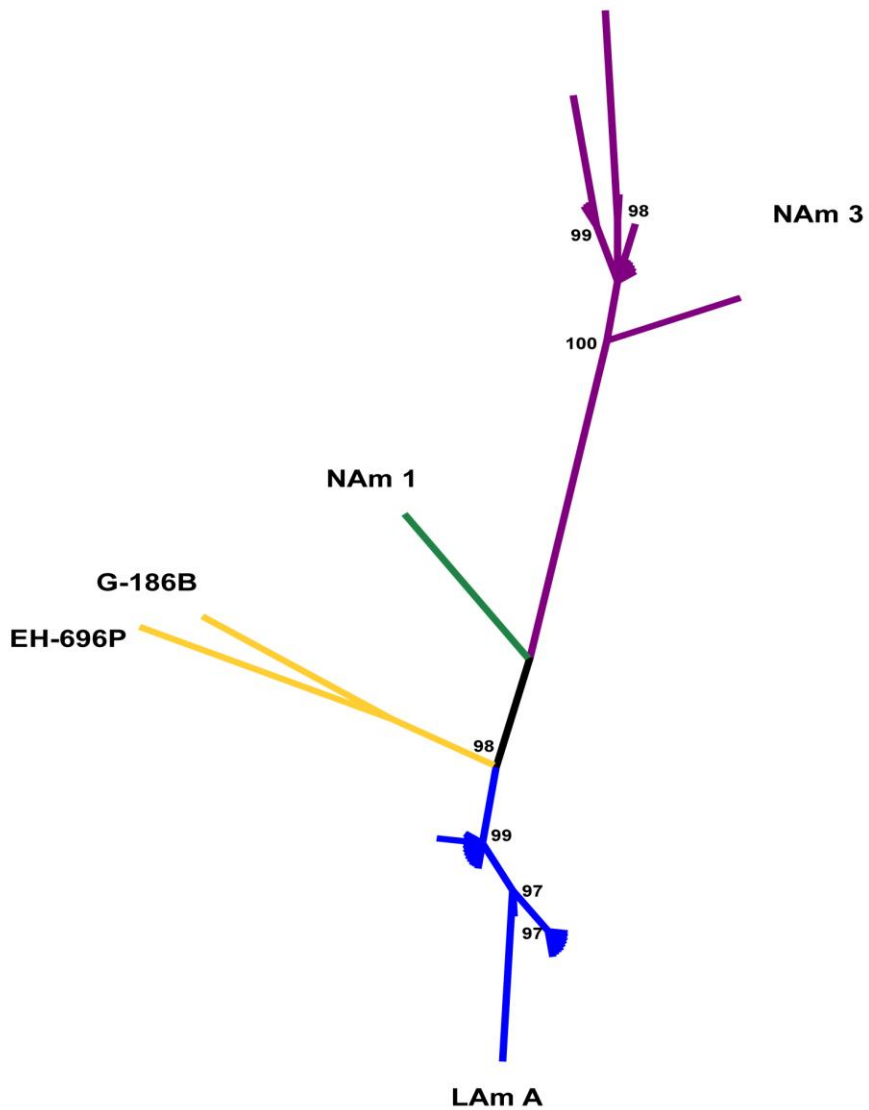


Fig.18. Árbol filogenético no enraizado de *H. capsulatum* generado por una matriz individual de secuencias de la región ITS1-5.8S-ITS2, utilizando el método de inferencia bayesiana. Se obtuvo el árbol de “Maximum-clade credibility” a partir del análisis de 36 secuencias, considerando valores de $pp \geq 95\%$, los cuales se indican en los nodos correspondientes.

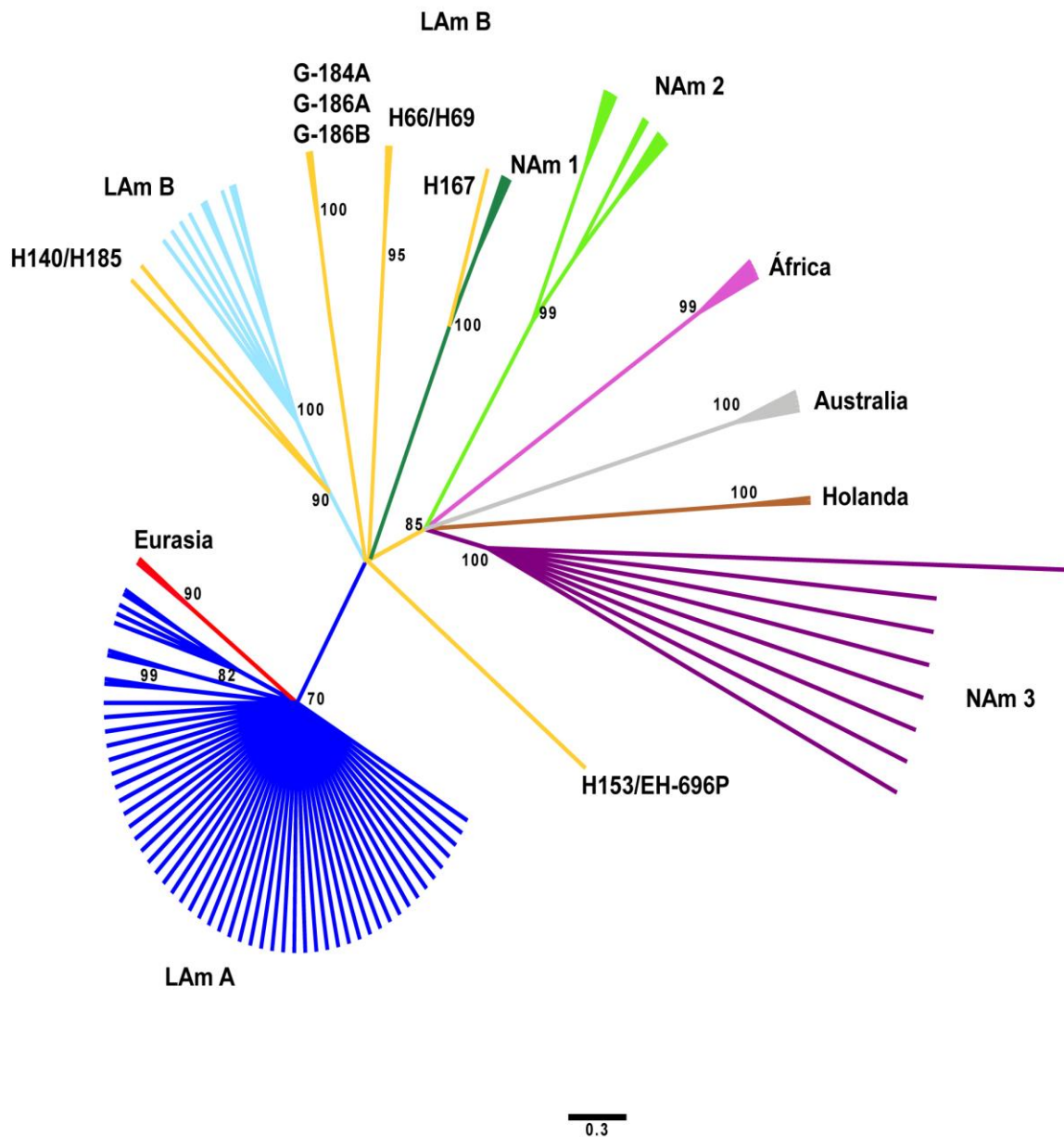


Fig.19. Árbol filogenético no enraizado de *H. capsulatum* generado por una matriz concatenada, utilizando el método de parsimonia. Se obtuvo el árbol de consenso estricto a través del análisis de una matriz concatenada construida con las secuencias de seis fragmentos génicos (arf, H-anti, ole1, tub1, (GA)n e ITS1-5.8S-ITS2) de 119 aislados de *H. capsulatum*. Se consideraron valores de bt $\geq 70\%$, los cuales se indican en los nodos correspondientes.

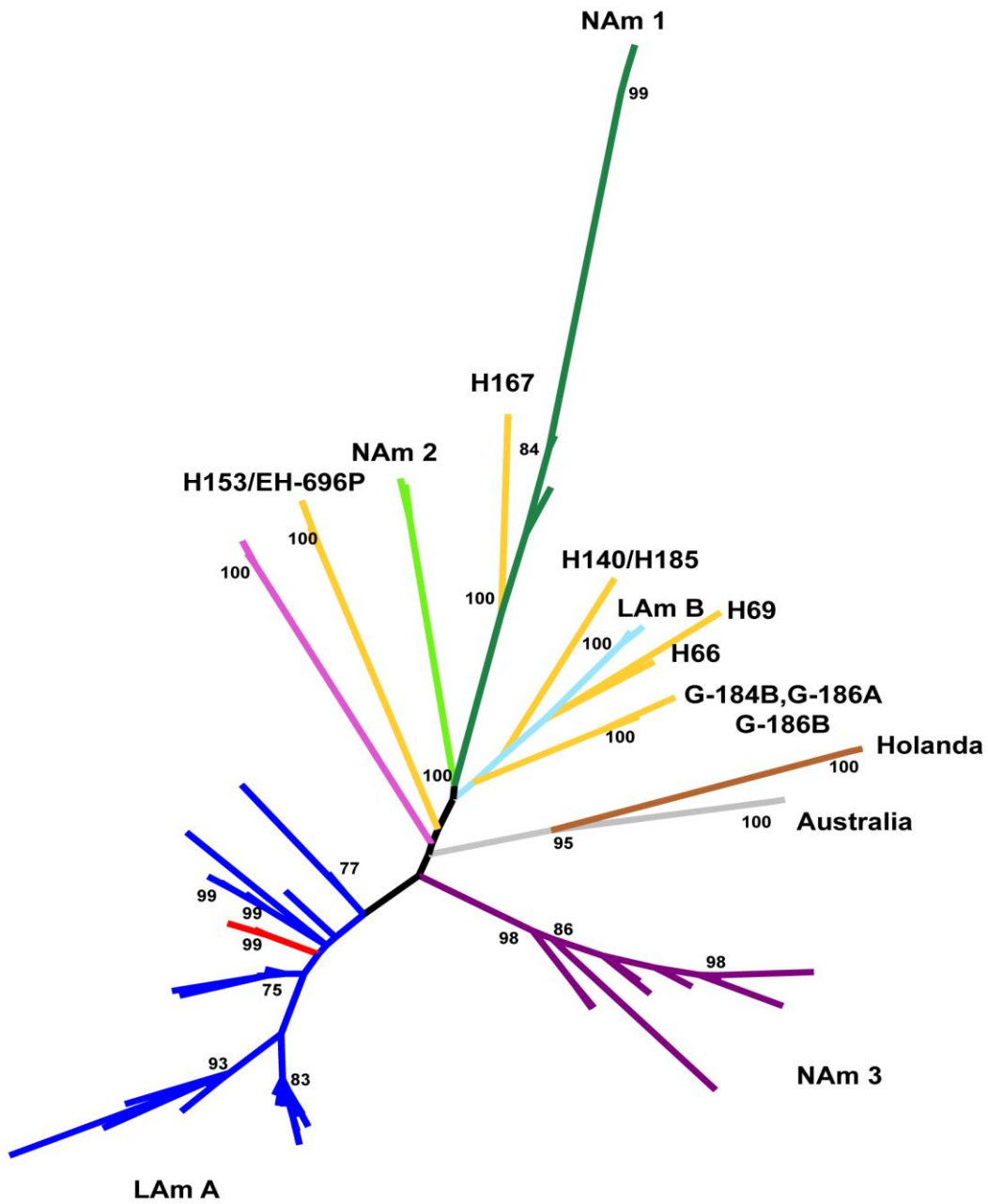


Fig.20. Árbol filogenético no enraizado de *H. capsulatum* generado por una matriz concatenada, utilizando el método de máxima verosimilitud. El árbol fue obtenido a través del análisis de una matriz concatenada construida con las secuencias de seis fragmentos génicos (arf, H-anti, ole1, tub1, (GA)_n e ITS1-5.8S-ITS2) de 119 aislados de *H. capsulatum*. Se consideraron valores de bt ≥70%, los cuales se indican en los nodos correspondientes.

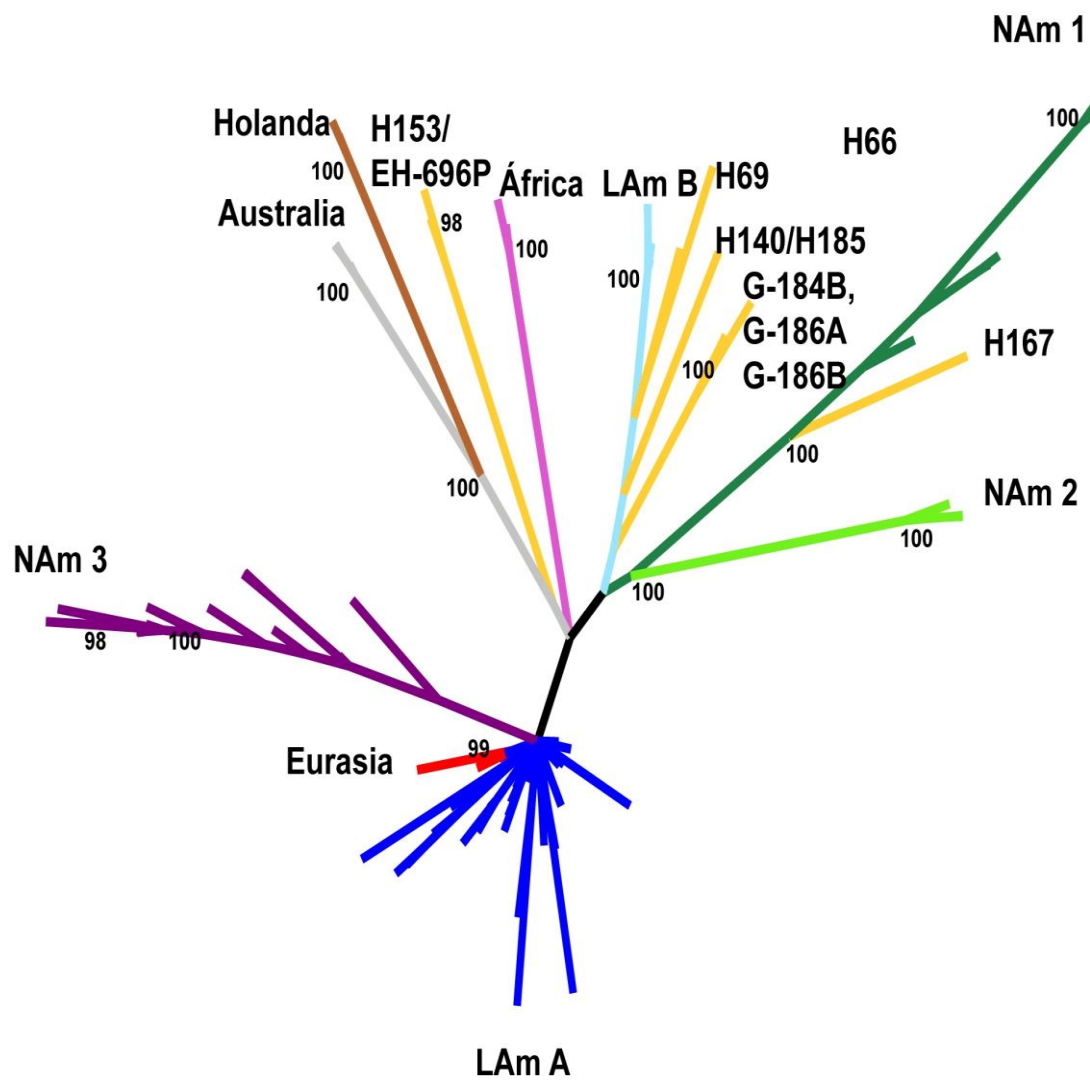


Fig.21. Árbol filogenético no enraizado de *H. capsulatum* generado por una matriz concatenada, utilizando el método de inferencia bayesiana. Se obtuvo el árbol de “Maximum-clade credibility” a través del análisis de una matriz concatenada construida con las secuencias de seis fragmentos génicos (arf, H-anti, ole1, tub1, (GA)n e ITS1-5.8S-ITS2) de 119 aislados de *H. capsulatum*. Se consideraron valores de pp ≥95%, los cuales se indican en los nodos correspondientes.

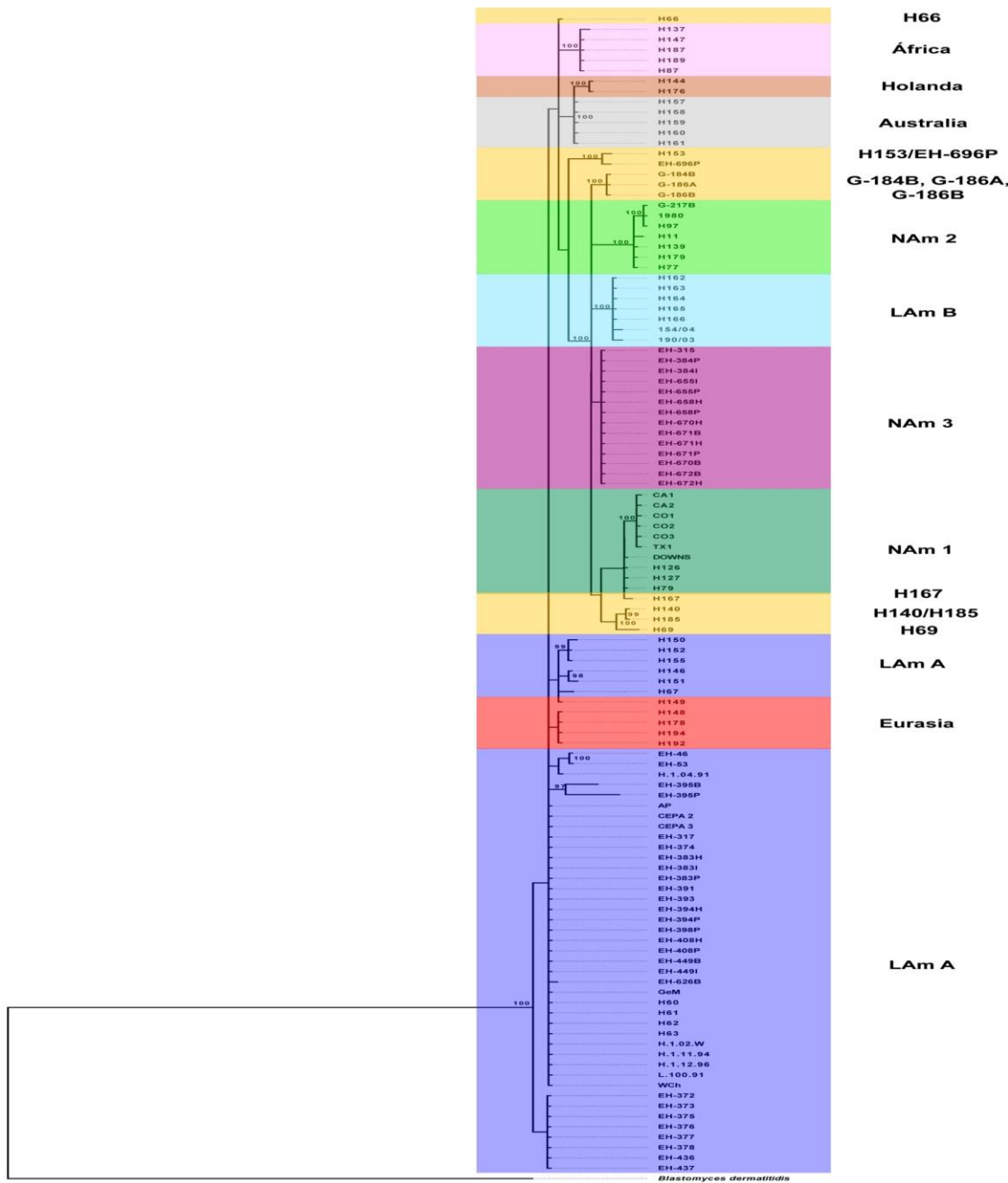


Fig.22. Árbol filogenético enraizado de *H. capsulatum* generado por una matriz individual de secuencias de arf, utilizando el método de inferencia bayesiana. Se obtuvo el árbol de “Maximum-clade credibility” a partir del análisis de 112 secuencias de *H. capsulatum* utilizando *B. dermatitidis* como grupo externo. Se consideraron los valores de pp $\geq 95\%$, los cuales se indican en los nodos correspondientes.

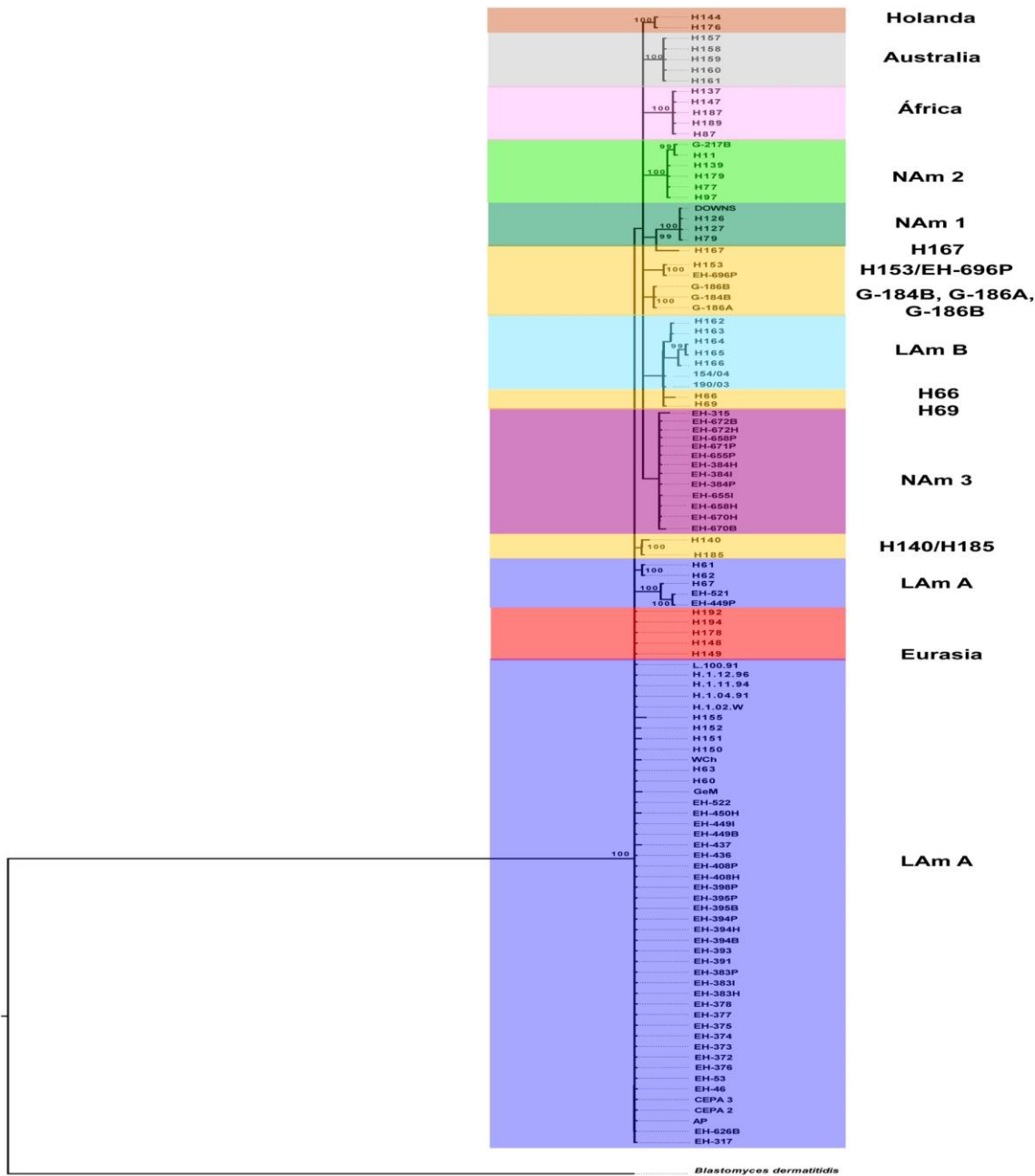


Fig.23. Árbol filogenético enraizado de *H. capsulatum* generado por una matriz individual de secuencias de ole1, utilizando el método de inferencia bayesiana. Se obtuvo el árbol de “Maximum-clade credibility” a partir del análisis de 109 secuencias de *H. capsulatum*, utilizando *B. dermatitidis* como grupo externo. Se consideraron los valores de pp $\geq 95\%$, los cuales se indican en los nodos correspondientes.

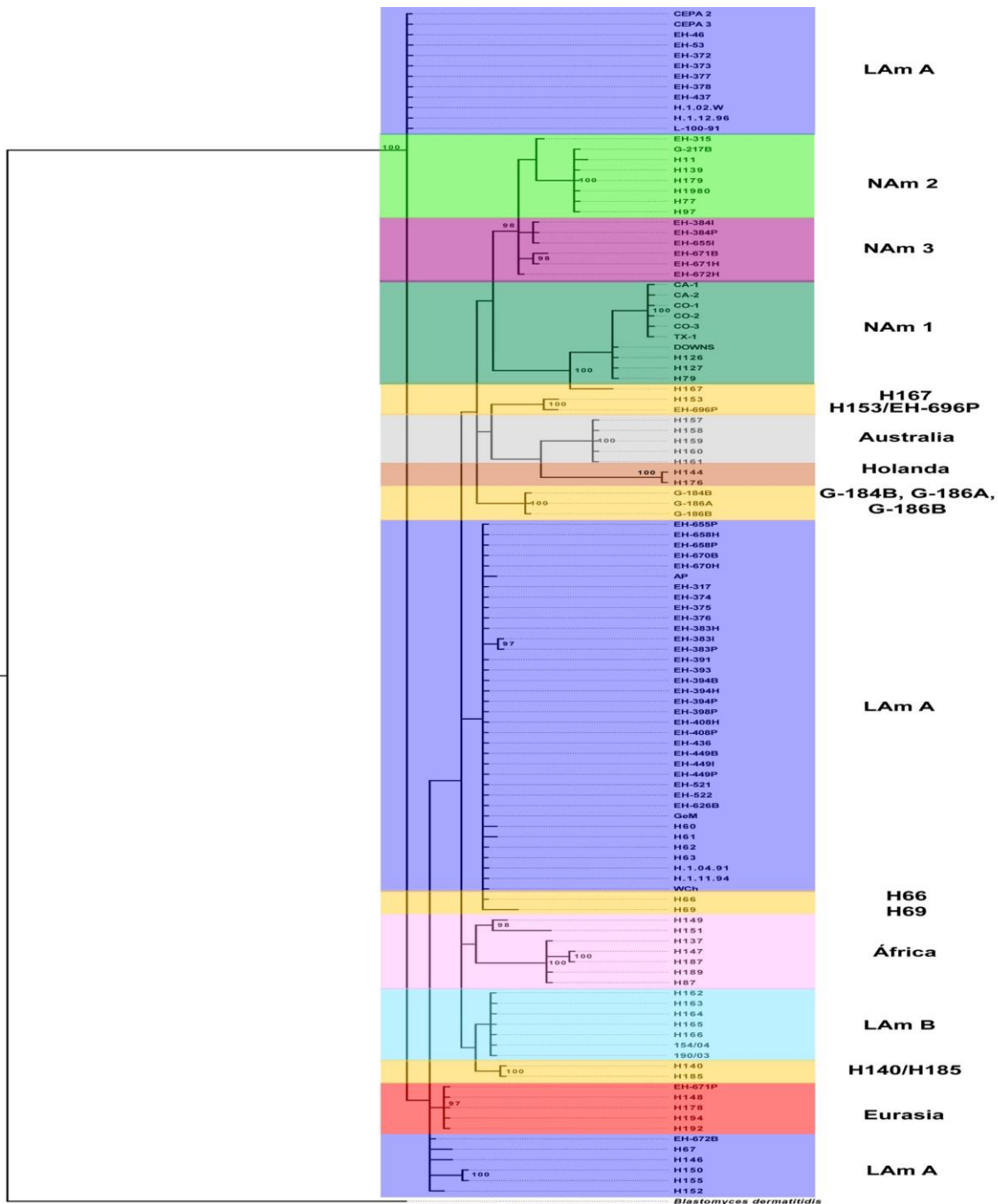


Fig.24. Árbol filogenético enraizado de *H. capsulatum* generado por una matriz individual de secuencias de tub1, utilizando el método de inferencia bayesiana. Se obtuvo el árbol de “Maximum-clade credibility” a partir del análisis de 114 secuencias de *H. capsulatum*, utilizando *B. dermatitidis* como grupo externo. Se consideraron los valores de pp $\geq 95\%$, los cuales se indican en los nodos correspondientes.

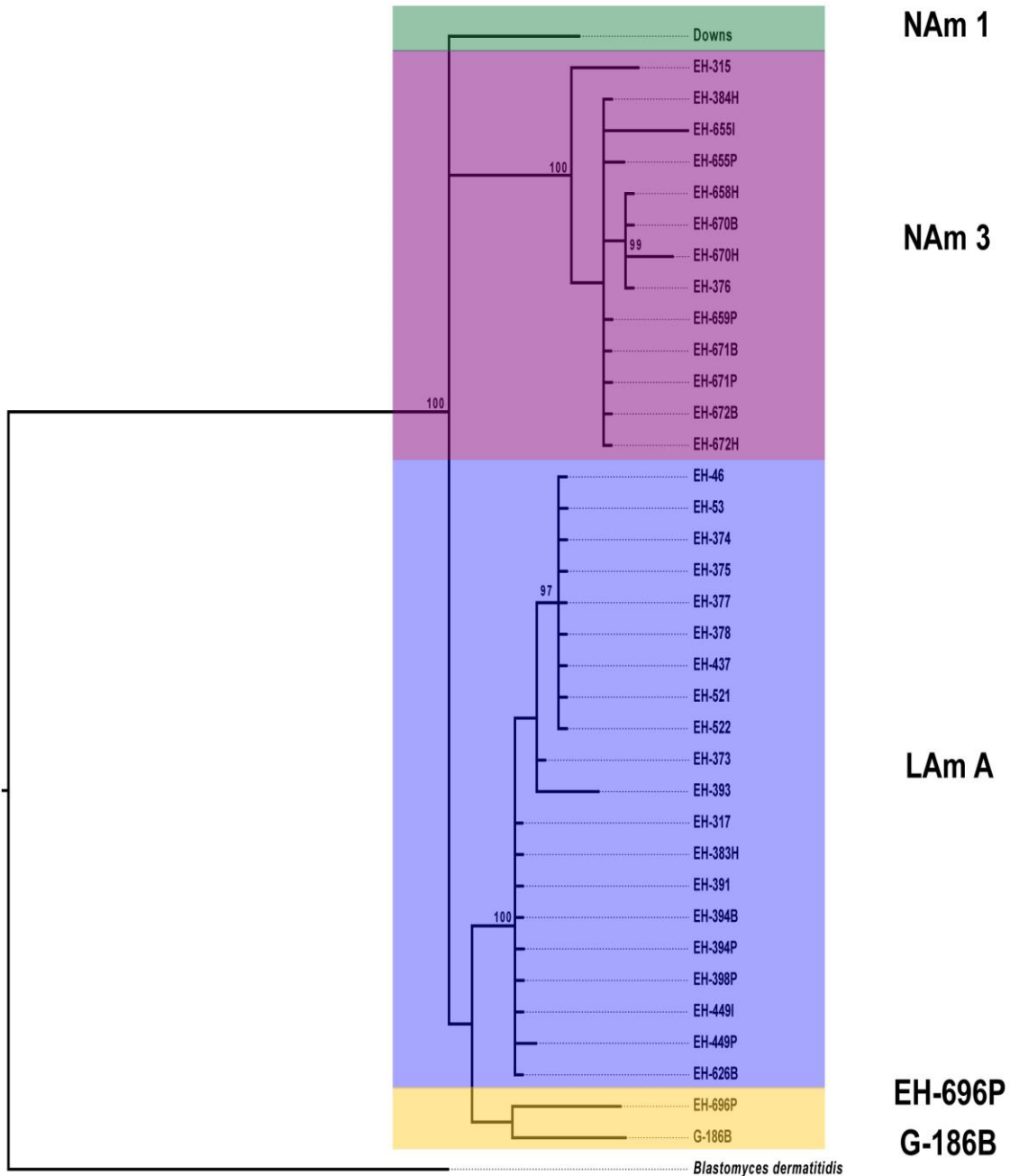


Fig.25. Árbol filogenético enraizado de *H. capsulatum* generado por una matriz individual de secuencias de la región ITS1-5.8S-ITS2, utilizando el método de inferencia bayesiana. Se obtuvo el árbol de “Maximum-clade credibility” a partir del análisis de 36 secuencias de *H. capsulatum*, utilizando *B. dermatitidis* como grupo externo. Se consideraron los valores de pp $\geq 95\%$, los cuales se indican en los nodos correspondientes.

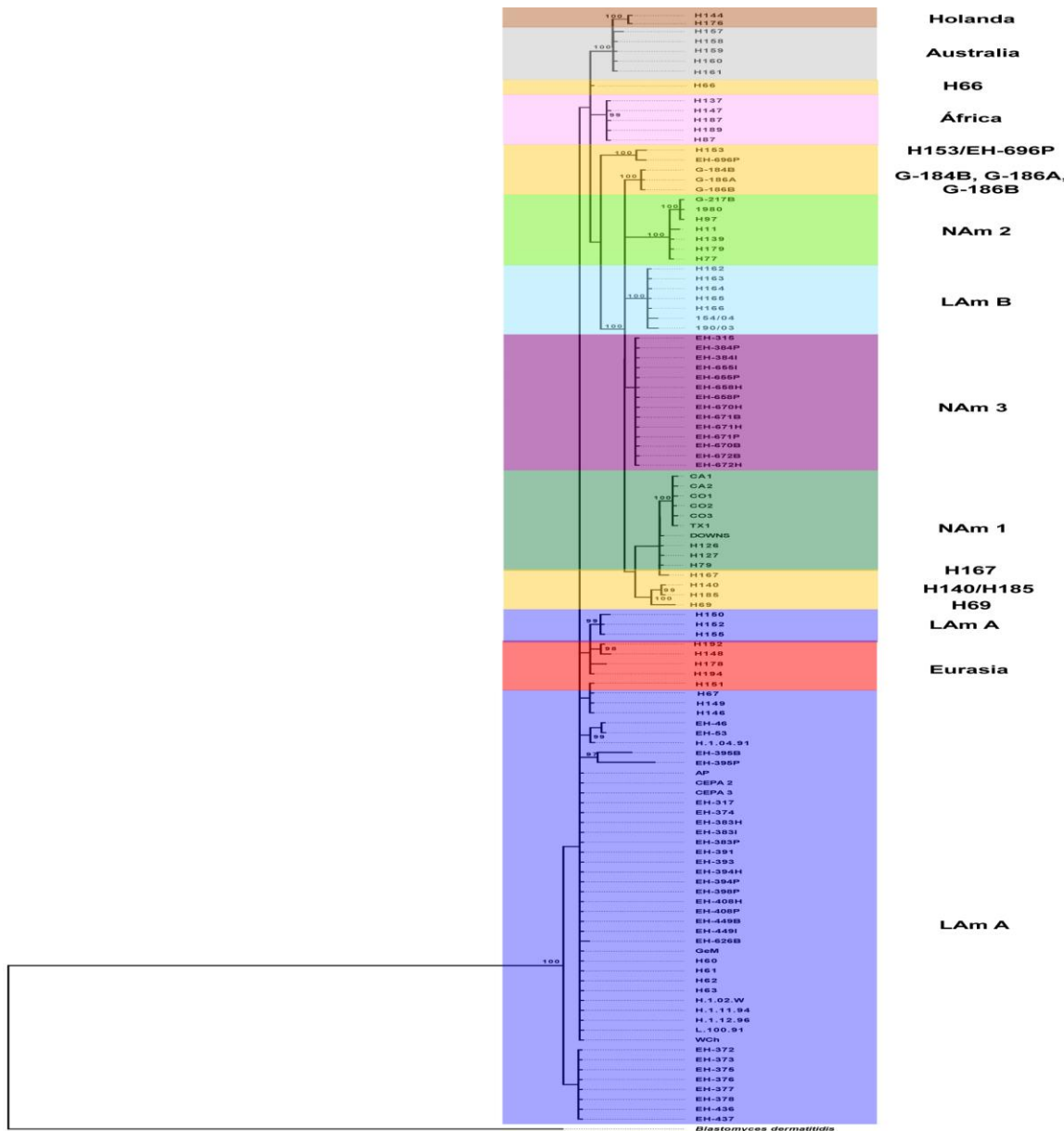


Fig.26. Árbol filogenético enraizado de *H. capsulatum* generado por una matriz concatenada, utilizando el método de inferencia bayesiana. Se obtuvo el árbol de “Maximum-clade credibility” a través del análisis de una matriz concatenada construida con las secuencias de cuatro fragmentos génicos (arf, ole1, tub1, e ITS1-5.8S-ITS2) de 119 aislados de *H. capsulatum*, utilizando *B. dermatitidis* como grupo externo. Se consideraron los valores de pp ≥95%, los cuales se indican en los nodos correspondientes.

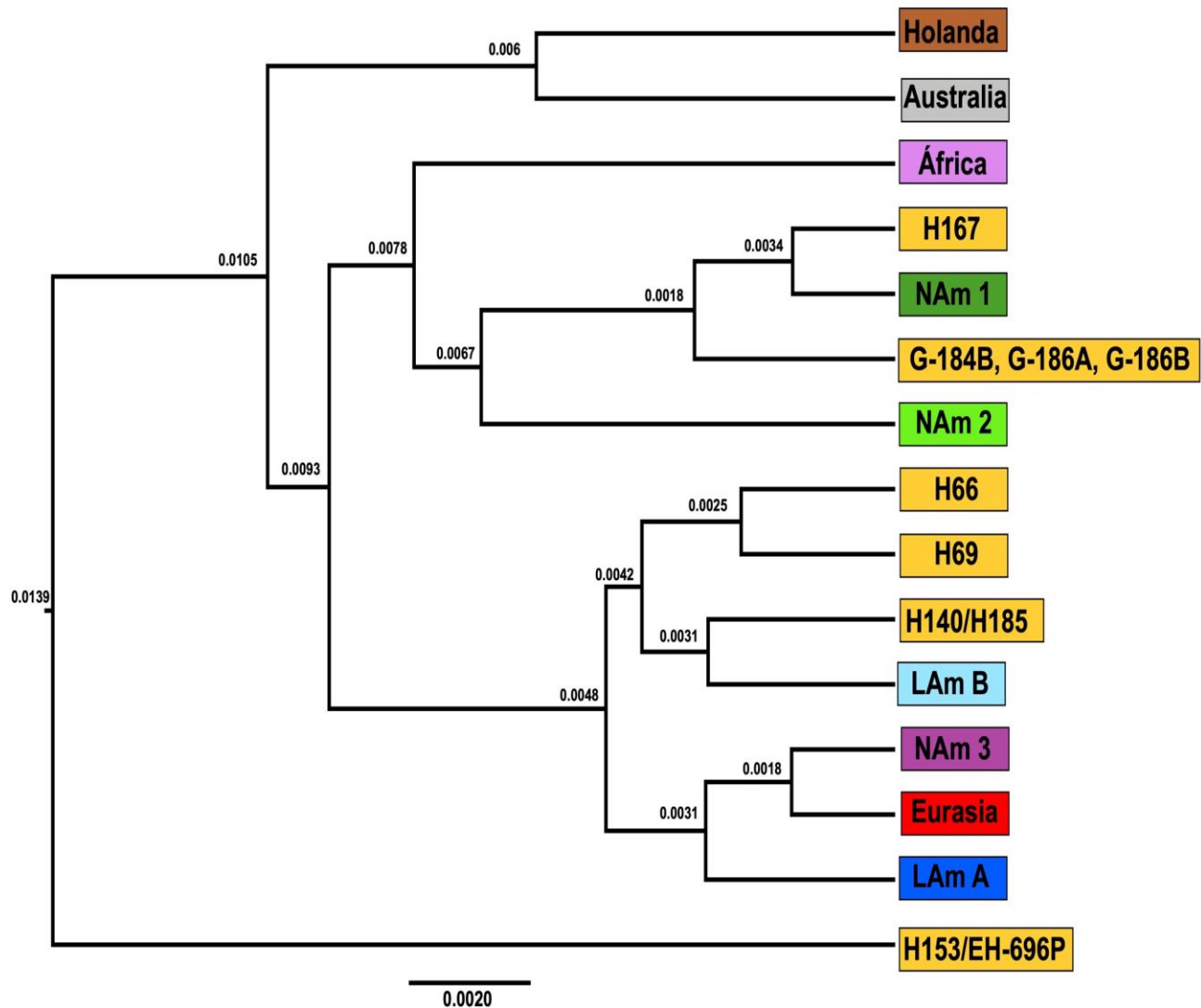


Fig.27. Árbol de especies de *H. capsulatum* generado por el método de delimitación de especies con base en coalección. Se obtuvo el árbol de “Maximum-clade credibility” a través del análisis de una matriz concatenada construida con las secuencias de cinco fragmentos génicos (arf, H-anti, ole1, tub1 y (GA)n) de 119 aislados de *H. capsulatum*. Se consideró un reloj molecular estricto y valores de pp $\geq 95\%$. En cada nodo se muestran las edades de los clados, estimadas mediante BEAUti 1.8.2.

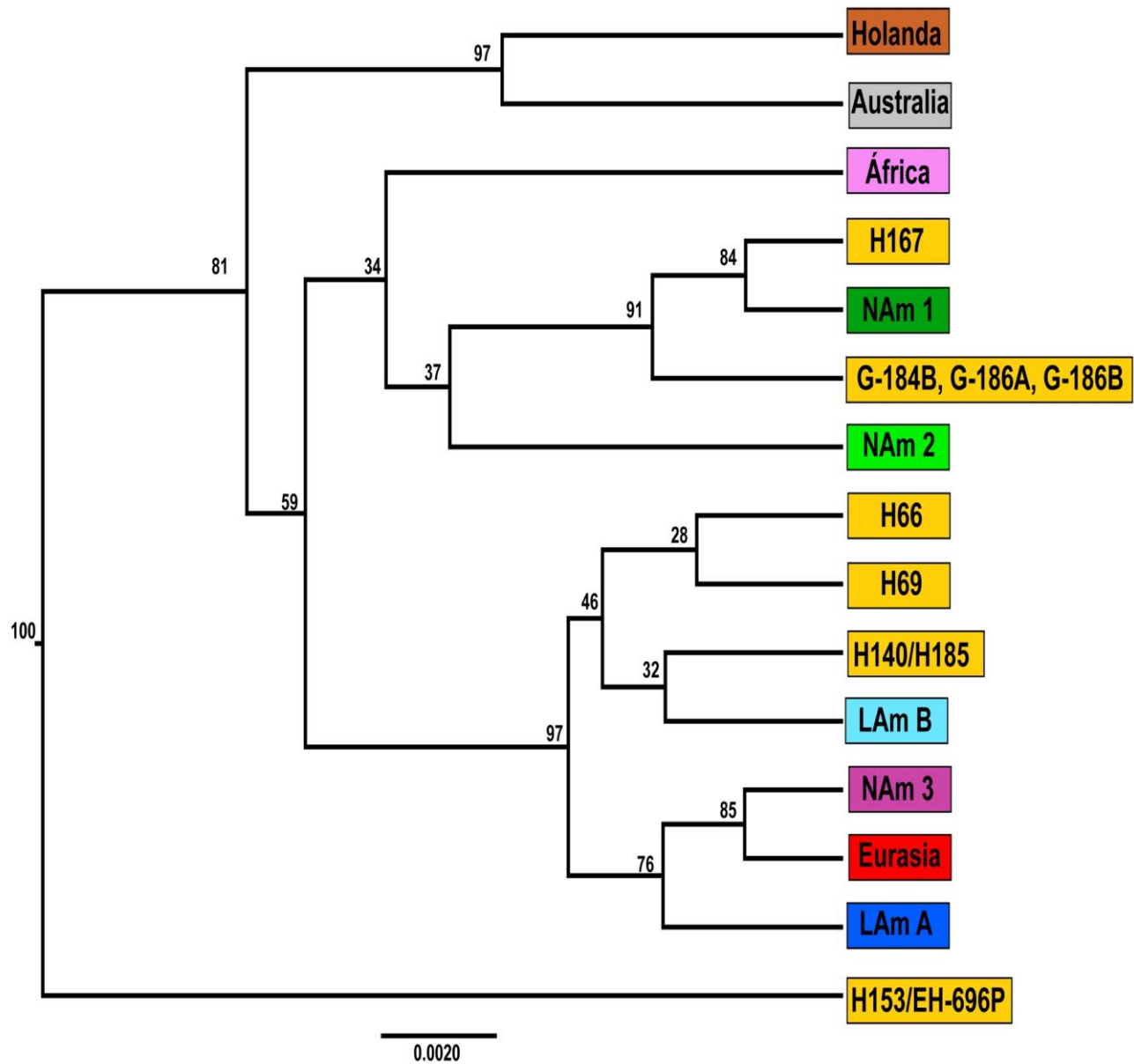


Fig.28. Árbol de especies de *H. capsulatum* generado por el método de delimitación de especies con base en coalescencia. Se obtuvo el árbol de “Maximum-clade credibility” a través del análisis de una matriz concatenada construida con las secuencias de cinco fragmentos génicos (arf, H-anti, ole1, tub1 y (GA)n) de 119 aislados de *H. capsulatum*. Se consideró un reloj molecular estricto y valores de pp ≥95%, los cuales se indican en los nodos correspondientes.

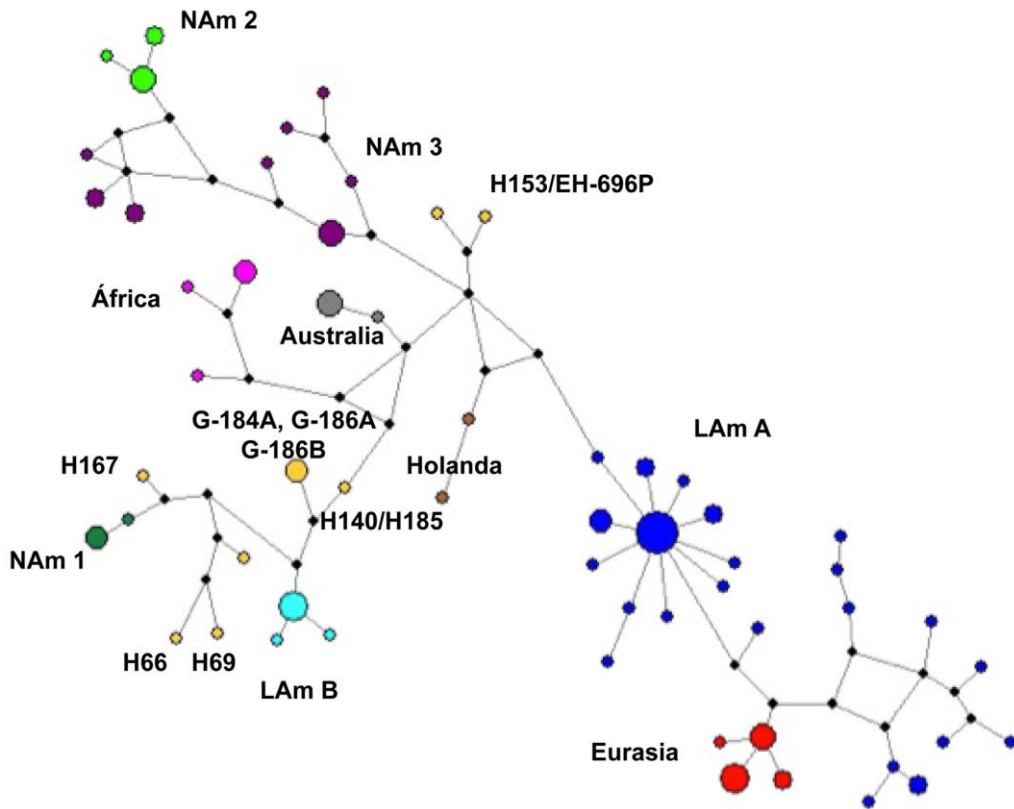


Fig.29. Red de dispersión del complejo *H. capsulatum* de acuerdo con los tipos de secuencias concatenadas (CSTs, del inglés concatenated sequence-types) de 119 aislados estudiados. Un total de 58 CSTs fueron generados a partir de 1538-nt alineados y analizados por el método “median-joining network”, utilizando los cuatro fragmentos génicos concatenados arf, H-anti, ole1 y tub1. La longitud de las ramas en la red es proporcional al número de substituciones y el tamaño relativo de los círculos es proporcional con la frecuencia de las CSTs. Cada nodo (circulo negro) indica una CST hipotética perdida. Los colores de cada CST corresponden a los diferentes clados y linajes descritos.

REFERENCIAS BIBLIOGRÁFICAS

- Akbar, H., Pinçon, C., Aliouat-Denis, C.M., Derouiche, S., Taylor, M.L., Pottier, M., Carreto-Binaghi, L.E., Gonzalez-Gonzalez, A.E., Courpon, A., Barriel, V., Guillot, J., Chabé, M., Suarez-Alvarez, R.O., Aliouat, E.M., Dei-Cas, E., Demanche, C. 2012. Characterizing *Pneumocystis* in the lungs of bats: understanding *Pneumocystis* evolution and the spread of *Pneumocystis* organisms in mammal populations. *Appl. Environ. Microbiol.* 78(22):8122-8136. <https://doi.org/10.1128/AEM.01791-12>
- Almeida-Silva, F., Teixeira, M.M., Matute, D.R., Faria Ferreira, M., Barker, B.M., Almeida-Paes, R., Guimarães, A.J., Zancopé-Oliveira, R.M. 2021. Genomic diversity analysis reveals a strong population structure in *Histoplasma capsulatum* LAmA (*Histoplasma suramericanum*). *J. Fungi* 7:865. <https://doi.org/10.3390/jof7100865>
- Altschul, S.F., Gish, W., Miller, W., Myers, E.W., Lipman, D.J., 1990. Basic local alignment search tool. *J. Mol. Biol.* 215, 403-410. [https://doi.org/10.1016/S0022-2836\(05\)80360-2](https://doi.org/10.1016/S0022-2836(05)80360-2)
- Balajee, S.A., Hurst, S.F., Chang, L.S., Miles, M., Beeler, W., Hale, C., Kasuga, T., Benedict, K., Chiller, T., Lindsley, M.D., 2012. Multilocus sequence typing of *Histoplasma capsulatum* in formalin-fixed paraffin-embedded tissues from cats living in non-endemic regions reveals a new phylogenetic clade. *Med. Mycol.* 50, 91-98. <https://doi.org/10.3109/13693786.2012.733430>
- Bandelt, H.J., Forster, P., Röhl, A., 1999. Median-joining networks for inferring intraspecific phylogenies. *Mol. Biol. Evol.* 16, 37-48. <https://doi.org/10.1093/oxfordjournals.molbev.a026036>
- Carstens, B.C., Dewey, T.A. 2010. Species delimitation using a combined coalescent and information-theoretic approach: an example from North American *Myotis* bats. *Syst. Biol.* 59, 400–414. <https://doi.org/10.1093/sysbio/syq024>
- Carter, D.A., Burt, A., Taylor, J.W., Koenig, G.L., Dechairo, B.M., White, T.J., 1997. A set of electrophoretic molecular markers for strain typing and population

genetic studies of *Histoplasma capsulatum*. Electrophoresis 18, 1047-1053.

<https://doi.org/10.1002/elps.1150180703>

Carter, D.A., Burt, A., Taylor, J.W., Koenig, G.L., White, T.J., 1996. Clinical isolates of *Histoplasma capsulatum* from Indianapolis, Indiana, have a recombining population structure. J. Clin. Microbiol. 34, 2577-2584.

<https://doi.org/10.1128/jcm.34.10.2577-2584.1996>

Carter, D.A., Taylor, J.W., Dechairo, B., Burt, A., Koenig, G.L., White, T.J., 2001. Amplified single-nucleotide polymorphisms and a (GA)_n microsatellite marker reveal genetic differentiation between populations of *Histoplasma capsulatum* from the Americas. Fungal Genet. Biol. 34, 37-48.

<https://doi.org/10.1006/fgb.2001.1283>

Damasceno, L.S., Vite-Garín, T., Ramírez, J.A., Rodríguez-Arellanes, G., Abreu De Almeida, M., Muniz, Mdm., Lima De Mesquita, J.R., Silva Leitão T.M.J., Taylor, M.L. y Zancopé-Oliveira, R.M. (2019a). Mixed infection by *Histoplasma capsulatum* isolates with different mating types in Brazilian AIDS-patients. Rev. Inst. Med. Trop. São Paulo 61:e8. <https://doi.org/10.1590/S1678-9946201961008>

Damasceno, L.S., Teixeira, M.D.M., Barker, B.M., Almeida, M.A., Muniz, Mdm., Pizzini, C.V., Lima Mesquita, J.R, Rodríguez-Arellanes, G., Ramírez, J.A., Vite-Garín, T., Silva Leitão, T.M.J., Taylor, M.L., Almeida-Paes, R. y Zancopé-Oliveira, R.M. (2019b). Novel clinical and dual infection by *Histoplasma capsulatum* genotypes in HIV patients from northeastern, Brazil. Sci. Rep. 9:11789, <https://doi.org/10.1038/s41598-019-48111-6>.

Degnan, J.H., Rosenberg, N.A., 2009. Gene tree discordance, phylogenetic inference and the multispecies coalescent. Trends Ecol. Evol. 6, 332-340. <https://doi.org/10.1016/j.tree.2009.01.009>

Degnan, J.H., Salter, L.A., 2005. Gene tree distributions under the coalescent process. Evolution 59, 24-37. <https://doi.org/10.1111/j.0014-3820.2005.tb00891.x>

- De Luna, E., Guerrero, J.A., Chew-Taracena, T., 2005. Sistemática biológica: avances y direcciones en la teoría y los métodos de la reconstrucción filogenética. *Hidrobiológica* 15, 351-370.
- Denis, C.M., Mazars, E., Guyot, K., Odberg-Ferragut, C., Viscogliosi, E., Dei-Cas, E., Wakefield, A.E., 2000. Genetic divergence at the SODA locus of six different formae speciales of *Pneumocystis carinii*. *Med. Mycol.* 38, 289–300. <https://doi.org/10.1080/mmy.38.4.289.300>
- Drummond, A.J., Suchard, M.A., Xie, D., Rambaut, A., 2012. Bayesian phylogenetics with BEAUti and the BEAST 1.7. *Mol. Biol. Evol.* 29, 1969-1973. <https://doi.org/10.1093/molbev/mss075>
- Eissenberg LG, Poirier S, Goldman WE. 1996. Phenotypic variation and persistence of *Histoplasma capsulatum* yeasts in host cells. *Infect. Immun.* 64, 5310-5314. <https://doi.org/10.1128/iai.64.12.5310-5314.1996>
- Ereshefsky, M., 2010. Darwin's solutions to the species problem. *Synthese* 175, 405-425. <https://doi.org/10.1007/s11229-009-9538-4>
- Estrada-Bárcenas, D.A., Vite-Garín, T., Navarro-Barranco, H., De La Torre Arciniega, R., Pérez-Mejía, A., Rodríguez-Arellanes, G., Ramírez, J.A., Sahaza, J.H., Taylor, M.L., Toriello, C., 2014. Genetic diversity of *Histoplasma* and *Sporothrix* complexes based on sequences of their ITS1-5.8S-ITS2 regions from the Bold System. *Rev. Iberoam. Micol.* 31, 11-15. <https://doi.org/10.1016/j.riam.20131.10.003>
- Farris, J.S., Källersjö, M., Kluge, A.G., Bult, C., 1994. Testing significance of incongruence. *Cladistics* 10, 315-319. <https://doi.org/10.1111/j.1096-0031.1994.tb00181.x>
- Fréalle, E., Noël, C., Viscogliosi, E., Camus, D., Dei-Cas, E., Delhaes, L., 2005. Manganese superoxide dismutase in pathogenic fungi: An issue with pathophysiological and phylogenetic involvements. *FEMS Immunol. Med. Microbiol.* 45, 411-422. <https://doi.org/10.1016/j.femsim.2005.06.003>
- Fréalle, E., Rodrigue, M., Gantois, N., Aliouat, C.M., Delaporte, E., Camus, D., Dei-Cas, E., Kauffmann-Lacroix, C., Guillot, J., Delhaes, L., 2007. Phylogenetic analysis of *Trichophyton mentagrophytes* human and animal isolates based on

- MnSOD and ITS sequence comparison. *Microbiology* 153, 3466–3477. <https://doi.org/10.1099/mic.0.2006/004929-0>
- Fujita, M.K., Leache, L.A., Burbrink, F.T., McGuire, J.A., Moritz, C., 2012. Coalescent-based species delimitation in an integrative taxonomy. *Tree* 27, 480-488. <https://doi.org/10.1016/j.tree.2012.04.012>
- Galo, C., Sanchez, A.L., Fontecha, G.A., 2013. Genetic diversity of *Histoplasma capsulatum* isolates from Honduras. *Science Journal of Microbiology*. 2013: 2013; <https://doi.org/10.7237/sjmb/288>.
- Gazis, R., Rehner, S., Chaverri, P., 2011. Species delimitation in fungal endophyte diversity studies and its implications in ecological and biogeographic inferences. *Mol. Ecol.* 20: 3001-3013. <https://doi.org/10.1111/j.1365-294X.2011.05110.x>
- Goloboff, P.A., Farris, J.S., Nixon, K.C., 2008. TNT, a free program for phylogenetic analysis. *Cladistics* 24, 774-786. <https://doi.org/10.1111/j.1096-0031.2008.00217.x>
- Heled, J., Drummond, A.J., 2010. Bayesian inference of species trees from multilocus data. *Mol. Biol. Evol.* 27, 570-580. <https://doi.org/10.1093/molbev/msp274>
- Hibbett, D.S., Binder, M., Bischoff, J.F., Blackwell, M., Cannon, P.F., Eriksson, O.E., Huhndorf, S., James, T., Kirk, P.M., Lücking, R., Thorsten Lumbsch, H., Lutzoni, F., Matheny, P.B., McLaughlin, D.J., Powell, M.J., Redhead, S., Schoch, C.L., Spatafora, J.W., Stalpers, J.A., Vilgalys, R., Aime, M.C., Aptroot, A., Bauer, R., Begerow, D., Benny, G.L., Castlebury, L.A., Crous, P.W., Dai, Y.C., Gams, W., Geiser, D.M., Griffith, G.W., Gueidan, C., Hawksworth, D.L., Hestmark, G., Hosaka, K., Humber, R.A., Hyde, K.D., Ironside, J.E., Köljalg, U., Kurtzman, C.P., Larsson, K.H., Lichtwardt, R., Longcore, J., Miadlikowska, J., Miller, A., Moncalvo, J.M., Mozley-Standridge, S., Oberwinkler, F., Parmasto, E., Reeb, V., Rogers, J.D., Roux, C., Ryvarden, L., Sampaio, J.P., Schüssler, A., Sugiyama, J., Thorn, R.G., Tibell, L., Untereiner, W.A., Walker, C., Wang, Z., Weir, A., Weiss, M., White, M.M., Winka, K., Yao, Y.J., Zhang,

- N., 2007. A higher-level phylogenetic classification of the fungi. Myc. Res. 111, 509-547. <https://doi.org/10.1016/j.mycres.2007.03.004>
- Hipp, A.L., Hall, J.C., Sytsma KJ., 2004. Congruence versus phylogenetic accuracy: revisiting the incongruence length difference test. Syst. Biol. 53, 81–89. <http://dx.doi.org/10.1080/10635150490264752>.
- James, T.Y., Kauff, F., Schoch, C.L., Matheny, P.B., Hofstetter, V., Cox, C.J., Celio, G., Gueidan, C., Fraker, E., Miadlikowska, J., Lumbsch, H.T., Rauhut, A., Reeb, V., Arnold, A.E., Amtoft, A., Stajich, J.E., Hosaka, K., Sung, G.H., Johnsonm, D., O'Rourke, B., Crockett, M., Binder, M., Curtis, J.M., Slot, J.C., Wang, Z., Wilson, A.W., Schüssler, A., Longcore, J.E., O'Donnell, K., Mozley-Standridge, S., Porter, D., Letcher, P.M., Powell, M.J., Taylor, J.W., White, M.M., Griffith, G.W., Davies, D.R., Humber, R.A., Morton, J.B., Sugiyama, J., Rossman, A.Y., Rogers, J.D., Pfister, D.H., Hewitt, D., Hansen, K., Hambleton, S., Shoemaker, R.A., Kohlmeyer, J., Volkmann-Kohlmeyer, B., Spotts, R.A., Serdani, M., Crous, P.W., Hughes, K.W., Matsuura, K., Langer, E., Langer, G., Untereiner, W.A., Lücking, R., Büdel, B., Geiser, D.M., Aptroot, A., Diederich, P., Schmitt, I., Schultz, M., Yahr, R., Hibbett, D.S., Lutzoni, F., McLaughlin, D.J., Spatafora, J.W., Vilgalys, R., 2006. Reconstructing the early evolution of fungi using a six-gene phylogeny. Nature 443, 818-822. <https://doi.org/10.1038/nature05110>
- Kasuga, T., Taylor, J.W., White, T.J., 1999. Phylogenetic relationships of varieties and geographical groups of the human pathogenic fungus *Histoplasma capsulatum* Darling. J. Clin. Microbiol. 37, 653-663. <https://doi.org/10.1128/jcm.37.3.653-663.1999>
- Kasuga, T., White, T.J., Koenig, G., McEwen, J., Restrepo, A., Castañeda, E., Da Silva Lacaz, C., Heins-Vaccari, E.M., De Freitas, R.S., Zancopé-Oliveira, R.M., Qin, Z., Negroni, R., Carter, D.A., Mikami, Y., Tamura, M., Taylor, M.L., Miller, G.F., Poonwan, N., Taylor, J.W., 2003. Phylogeography of the fungal pathogen *Histoplasma capsulatum*. Mol. Ecol. 12, 3383-3401. <https://doi.org/10.1046/j.1365-294x.2003.01995.x>.

- Keath, E.J., Kobayashi, G.S., Medoff, G., 1992. Typing of *Histoplasma capsulatum* by restriction fragment length polymorphisms in a nuclear gene. J. Clin. Microbiol. 30, 2104-2107. <https://doi.org/10.1128/jcm.30.8.2104-2107.1992>
- Kwon-Chung, K.J., Bennett, J.E., 1992. Histoplasmosis. En: *Medical Mycology*. Lea and Febiger, Philadelphia, pp. 305-341.
- Librado, P., Rozas, J., 2009. DnaSP v5: a software for comprehensive analysis of DNA polymorphism data. Bioinformatics 25, 1451-1452. <https://doi.org/10.1093/bioinformatics/btp187>
- Liu, L., Yu, L., Kubatko, L., Pearl, D.K., Edwards, S.V., 2009. Coalescent methods for estimating phylogenetic trees. Mol. Phyl. Evol. 53, 320-328. <https://doi.org/10.1016/j.ympev.2009.05.033>
- Maddison, W.P., 1998. Gene trees in species trees. Syst. Biol. 46: 523-536. <https://doi.org/10.1093/sysbio/46.3.523>
- Maddison, W.P., Maddison, D.R., 2014. Mesquite: a modular system for evolutionary analysis Version 3.01. <http://mesquiteproject.org>.
- McCracken, G.F., McCracken, M.K., Vawter, A.T. 1994. Genetic structure in migratory populations of the bat *Tadarida brasiliensis mexicana*. J Mammal 75: 500–514. <https://doi.org/10.1111/j.1365-294X.2005.02552.x>
- Morris, P.R., Terreni, A.A., DiSalvo, F., 1986. Red-pigmented *Histoplasma capsulatum*-an unusual variant. J. Med. Vet. Mycol. 24, 231-233. <https://doi.org/10.1080/02681218680000331>
- Muniz, M. de M., Morais, P.M.S., Meyer, W., Nosanchuk, J.D., Zancopé-Oliveira, R.M., 2010. Comparison of different DNA-based methods for molecular typing of *Histoplasma capsulatum*. Appl. Environ. Microbiol. 76, 4438-4447. <https://doi.org/10.1128/AEM.02004-09>
- Nixon, K.C., 1999. The parsimony ratchet, a new method for rapid parsimony analysis. Cladistics 15, 407–414. <https://doi.org/10.1111/j.1096-0031.1999.tb00277.x>
- Nosanchuk, J.D., Gomez, B.L., Youngchim, S., Diez, S., Aisen, P., Zancopé-Oliveira, R.M., Restrepo, A., Casadevall, A., Hamilton, A.J., 2002. *Histoplasma capsulatum* synthesizes melanin-like pigments *in vitro* and during mammalian

- infection. Infect. Immun. 70, 5124-5131. <https://doi.org/10.1128/IAI.70.9.5124-5131.2002>
- Posada, D., 2008. JModelTest: phylogenetic model averaging. Mol. Biol. Evol. 25, 1253-1256. <https://doi.org/10.1093/molbev/msn083>
- Rodríguez-Arellanes, G., Nascimento de Sousa, C., de Medeiros-Muniz, M., Ramírez, J.A., Pizzini, CV., de Abreu-Almeida, M., Evangelista de Oliveira, M.M., Fusco-Almeida, A.M., Vite-Garín, T., Pitangui, N.S., Estrada-Bárcenas, D.A., González-González, A.E., Mendes-Giannini, M.J.S., Zancopé-Oliveira, R.M., Taylor, M.L. 2013. Frequency and genetic diversity of the *MAT1* locus of *Histoplasma capsulatum* isolates in Mexico and Brazil. Eukaryot. Cell 12, 1033-1038. <https://doi.org/10.1128/EC.00012-13>
- Rodrigues, A.M., Beale, M.A., Hagen., F., Fisher, M.C., Terra, P.P.D., de Hoog, S., Brilhante, R.S.N., de Aguiar Cordeiro, R., de Souza Collares, Maia Castelo-Branco, D., Rocha, M.F.G., Sidrim, J.J.C., de Camargo, Z.P. 2020. The global epidemiology of emerging *Histoplasma* species in recent years. Stud Mycol 97: 100095.001. <https://doi.org/10.1016/j.simyco.2020.02.001>.
- Ronquist, F., Teslenko, M., Van Der Mark, P., Ayres, D.L., Darling, A., Hohnä, S., Larget, B., Liu, L., Suchard, M.A., Huelsenbeck, J.P., 2012. MrBayes 3.2: Efficient bayesian phylogenetic inference and model selection across a large model space. Syst. Biol. 61, 539-542. <https://doi.org/10.1093/sysbio/sys029>
- Sánchez-García, M., 2010. Estudio sistemático del género Melanoleuca (Fungi: Agaricales). Tesis de Maestría. Posgrado en Ciencias Biológicas, UNAM. México, D.F.
- Sepúlveda VE, Márquez R, Turissini DA, Goldman WE, Matute DR, 2017. Genome sequences reveal cryptic speciation in the human pathogen *Histoplasma capsulatum*. Mbio 8: e01339-17. <https://doi.org/10.1128/mBio.01339-17>
- Silvestro, D., Michalak, I., 2012. RAxMLGUI: a graphical front-end for RAxML. Org. Divers. Evol. 12, 335–337. <https://doi.org/10.3389/fevo.2022.933632>
- Spitzer, E.D., Keath, E.J., Travis, S.J., Painter, A.A., Kobayashi, G.S., Medoff, G., 1990. Temperature-sensitive variants of *Histoplasma capsulatum* isolated from

- patients with acquired immunodeficiency syndrome. J. Infect. Dis. 162, 258-261. <https://doi.org/10.1016/j.bjid.2019.12.007>
- Spitzer, E.D., Lasker, B.A., Travis, S.J., Kobayashi, G.S., Medoff, G., 1989. Use of mitochondrial and ribosomal DNA polymorphisms to classify clinical and soil isolates of *Histoplasma capsulatum*. Infect. Immun. 57, 1409-1412. <https://doi.org/10.1128/iai.57.5.1409-1412.1989>
- Swofford, D.L., 2003. PAUP*. Phylogenetic Analysis Using Parsimony (*and other methods). Version 4. <http://paup.csit.fsu.edu/downl.html>
- Taylor, M.L., Chávez-Tapia, C.B., Rojas-Martínez, A., Reyes-Montes, M.R., Bobadilla del Valle, M., Zúñiga, G., 2005. Geographical distribution of genetic polymorphism of the pathogen *Histoplasma capsulatum* isolated from infected bats, captured in a central zone of Mexico. FEMS Immunol. Med. Microbiol. 45, 451-458. <https://doi.org/10.1016/j.femsim.2005.05.019>
- Taylor, M.L., Chávez-Tapia, C.B., Vargas-Yáñez, R., Rodríguez-Arellanes, G., Peña-Sandoval, G.R., Toriello, C., Pérez, A., Reyes-Montes, M.R., 1999a. Environmental conditions favoring bat infection with *Histoplasma capsulatum* in Mexican shelters. Am. J. Trop. Med. Hyg. 61, 914-919. <https://doi.org/10.4269/ajtmh.1999.61.914>
- Taylor, J.W., Fisher, M.C., 2003. Fungal multilocus sequence typing: it's not just for bacteria. Curr. Opin. Microbiol. 4, 351-356. [https://doi.org/10.1016/s1369-5274\(03\)00088-2](https://doi.org/10.1016/s1369-5274(03)00088-2)
- Taylor, J.W., Geiser, D.M., Burt, A., Koufopanou, V., 1999b. The evolutionary biology and population genetics underlying fungal strain typing. Clin. Microbiol. Rev. 12, 126-146. <https://doi.org/10.1128/CMR.12.1.126>
- Taylor, M.L., Hernández-García, L., Estrada-Bárcenas, D.A., Salas-Lizana, R., Zancopé-Oliveira, R.M., García de la Cruz, S., Galvão-Dias, M.A., Curiel-Quesada, E., Canteros, C.E., Bojórquez-Torres, G., Bogard-Fuentes, C.A., Zamora-Tehozol, E., 2012. Genetic diversity of microsatellite (GA)_n and their flanking regions of *Histoplasma capsulatum* isolated from bats captured in three Latin-American countries. Fung. Biol. 116, 308-317. <https://doi.org/10.1016/j.funbio.2011.12.004>

- Taylor, J.W., Jacobson, D.J., Kroken, S., Kasuga, T., Geiser, D.M., Hibbett, D.S., Fisher, M.C., 2000a. Phylogenetic species recognition and species concepts in fungi. *Fungal Genet. Biol.* 31, 21-32. <https://doi.org/10.1006/fgb.2000.1228>
- Taylor, M.L., Reyes-Montes, M.R., Chávez-Tapia, C.B., Curiel-Quesada, E., Duarte-Escalante, E., Rodríguez-Arellanes, G., Peña-Sandoval, G.R., Valenzuela-Tovar, F., 2000b. Ecology and molecular epidemiology findings of *Histoplasma capsulatum*, in Mexico. En: Mojan RM, Benedik M (eds.). *Research Advances in Microbiology*, vol. I. Global Research Network, Kerala, pp. 29-35.
- Taylor, M.L., Reyes-Montes, M.R.; Estrada-Bárcenas, D.A.; Zancopé-Oliveira, R.M.; Rodríguez-Arellanes. G. And Ramírez, J.A., 2022. Considerations about the geographic distribution of the *Histoplasma* species. *Appl. Environ. Microbiol.* 88(7):E0201021 <https://doi.org/10.1128/Aem.02010-21>
- Taylor, M.L., Rodríguez-Arellanes, G., Duarte-Escalante, E., 1999c. Catálogo de Cepas de “*Histoplasma capsulatum*”. Universidad Nacional Autónoma de México, México DF.
- Teixeira M.M., Patané J.S.L., Taylor M.L., Gómez B.L., Theodoro R.C., de Hoog S., Engelthaler D.M., Zancopé-Oliveira R.M., Felipe M.S.S., Barker B.M., 2016. Worldwide phylogenetic distributions and population dynamics of the genus *Histoplasma*. PLoS Negl. Trop. Dis. <https://doi.org/10.1371/journal.pntd.0004732>
- Tewari, R., Wheat, L.J., Ajello, L., 1998. Agents of histoplasmosis. En: Ajello L, Hay RJ (eds.). *Topley & Wilson's Microbiology and Microbial Infections. Medical Mycology*, vol. 4. Arnold and Oxford University Press, Inc., New York, pp. 373-407.
- Vincent, R.D., Goewert, R., Goldman, W.E., Kobayashi, G.S., Lambowitz, A.M., Medoff, G., 1986. Classification of *Histoplasma capsulatum* isolates by restriction fragment polymorphisms. *J. Bacteriol.* 165, 813-818. <https://doi.org/10.1128/jb.165.3.813-818.1986>
- Vite-Garín, T., 2011. Aportación a la filogeografía de *Histoplasma capsulatum*: análisis filogenético de aislados de murciélagos y humanos, procedentes de

Latinoamérica. Tesis Maestría. Posgrado en Ciencias Biológicas, UNAM.
México, D.F.

Vite-Garín, T., Estrada-Bárcenas, D.A., Gernandt, D.S., Reyes-Montes, M.R.,
Sahaza, J.H., Canteros, C.E., Ramírez, J.A., Rodríguez-Arellanes, G., Serra-
Damasceno, L., Zancopé-Oliveira, R.M., Taylor, J.W. and Taylor, M.L. 2021.
Histoplasma capsulatum isolated from *Tadarida brasiliensis* bats captured in
Mexico form a sister group to North American class 2 clade. *J. Fungi* 7(07):529-
545. <https://doi.org/10.3390/jof7070529>.

Vite-Garín, T., Estrada-Bárcenas, D.A., Cifuentes, J., Taylor, M.L., 2014. The
importance of molecular analyses for understanding the genetic diversity of
Histoplasma capsulatum: An overview. *Rev. Iberoam. Micol.* 31, 11-15.
<http://dx.doi.org/10.1016/j.riam.2013.09.013>

Wilkins, K.T., 1989. *Tadarida brasiliensis*. *Mammalian Species* 331, 1-10.
<https://doi.org/10.2307/3504148>

ANEXOS

1. ARTÍCULO REQUISITO PARA LA OBTENCIÓN DEL GRADO

Vite-Garín, T., Estrada-Bárcenas, D.A., Gernandt, D.S., Reyes-Montes, M.R., Sahaza, J.H., Canteros, C.E., Ramírez, J.A., Rodríguez-Arellanes, G., Serra-Damasceno, L., Zancopé-Oliveira, R.M., Taylor, J.W. and Taylor, M.L. 2021. *Histoplasma capsulatum* isolated from *Tadarida brasiliensis* bats captured in Mexico form a sister group to North American class 2 clade. *J. Fungi* 7(07):529-545.
<https://doi.org/10.3390/jof7070529>.

Article

***Histoplasma capsulatum* Isolated from *Tadarida brasiliensis* Bats Captured in Mexico Form a Sister Group to North American Class 2 Clade**

Tania Vite-Garín ¹, Daniel A. Estrada-Bárcenas ², David S. Gernandt ³, María del Rocío Reyes-Montes ¹ , Jorge H. Sahaza ¹, Cristina E. Canteros ⁴, José A. Ramírez ¹ , Gabriela Rodríguez-Arellanes ¹, Lisandra Serra-Damasceno ⁵, Rosely M. Zancopé-Oliveira ⁶, John W. Taylor ⁷ and María Lucia Taylor ^{1,*}

¹ Unidad de Micología, Departamento de Microbiología y Parasitología, Facultad de Medicina, Universidad Nacional Autónoma de México (UNAM), Ciudad de México 04510, Mexico; tania.vite.garin@gmail.com (T.V.-G.); remoa@unam.mx (M.d.R.R.-M.); jhsahaza@hotmail.com (J.H.S.); jarb@unam.mx (J.A.R.); batgaby@unam.mx (G.R.-A.)

² Colección Nacional de Cepas Micróbianas y Cultivos Celulares, Centro de Investigación y de Estudios Avanzados, Instituto Politécnico Nacional (CINVESTAV, IPN), Ciudad de México 07360, Mexico; destrada@cinvestav.mx

³ Departamento de Botánica, Instituto de Biología, Universidad Nacional Autónoma de México (UNAM), Ciudad de México 04510, Mexico; dsgernandt@ib.unam.mx

⁴ Departamento de Micología, Instituto Nacional de Enfermedades Infecciosas (INEI), Administración Nacional de Laboratorios e Institutos de Salud (ANLIS) "Dr. Carlos G. Malbrán", Buenos Aires 1281, Argentina; cecanteros@gmail.com

⁵ Centro de Ciências da Saúde, Departamento de Saúde Comunitária, Universidade Federal do Ceará, Fortaleza 60455-610, Brazil; lisainfecto@gmail.com

⁶ Laboratório de Micologia, Setor Imunodiagnóstico, Instituto Nacional de Infectologia Evandro Chagas, Fundação Oswaldo Cruz (FIOCRUZ), Rio de Janeiro 21040-360, Brazil; rosely.zancope@ini.fiocruz.br

⁷ Department of Plant and Microbial Biology, University of California, Berkeley, CA 94720, USA; jtaylor@berkeley.edu

* Correspondence: emello@unam.mx



Citation: Vite-Garín, T.; Estrada-Bárcenas, D.A.; Gernandt, D.S.; Reyes-Montes, M.d.R.; Sahaza, J.H.; Canteros, C.E.; Ramírez, J.A.; Rodríguez-Arellanes, G.; Serra-Damasceno, L.; Zancopé-Oliveira, R.M.; et al. *Histoplasma capsulatum* Isolated from *Tadarida brasiliensis* Bats Captured in Mexico Form a Sister Group to North American Class 2 Clade. *J. Fungi* **2021**, *7*, 529. <https://doi.org/10.3390/jof7070529>

Academic Editor: Gudrun Wibbelt

Received: 16 April 2021

Accepted: 11 June 2021

Published: 30 June 2021

Publisher's Note: MDPI stays neutral with regard to jurisdictional claims in published maps and institutional affiliations.



Copyright: © 2021 by the authors. Licensee MDPI, Basel, Switzerland. This article is an open access article distributed under the terms and conditions of the Creative Commons Attribution (CC BY) license (<https://creativecommons.org/licenses/by/4.0/>).

Abstract: *Histoplasma capsulatum* is a dimorphic fungus associated with respiratory and systemic infections in mammalian hosts that have inhaled infective mycelial propagules. A phylogenetic reconstruction of this pathogen, using partial sequences of *arf*, *H-anti*, *ole1*, and *tub1* protein-coding genes, proposed that *H. capsulatum* has at least 11 phylogenetic species, highlighting a clade (BAC1) comprising three *H. capsulatum* isolates from infected bats captured in Mexico. Here, relationships for each individual locus and the concatenated coding regions of these genes were inferred using parsimony, maximum likelihood, and Bayesian inference methods. Coalescent-based analyses, a concatenated sequence-types (CSTs) network, and nucleotide diversities were also evaluated. The results suggest that six *H. capsulatum* isolates from the migratory bat *Tadarida brasiliensis* together with one isolate from a *Mormoops megalophylla* bat support a NAm 3 clade, replacing the formerly reported BAC1 clade. In addition, three *H. capsulatum* isolates from *T. brasiliensis* were classified as lineages. The concatenated sequence analyses and the CSTs network validate these findings, suggesting that NAm 3 is related to the North American class 2 clade and that both clades could share a recent common ancestor. Our results provide original information on the geographic distribution, genetic diversity, and host specificity of *H. capsulatum*.

Keywords: *Histoplasma capsulatum*; bat host; NAm 3 clade; new lineage; phylogenetic reconstruction; concatenated sequence-types network

1. Introduction

Histoplasma capsulatum is a pathogenic ascomycete that infects humans and other mammals. This fungus is distributed worldwide and is usually found in bird and bat

droppings. Its saprobe and infective mycelial morphotype grow in environmental conditions that favor the production of aerosolized mycelial propagules, mainly microconidia and hyphal fragments that are inhaled by susceptible hosts, initiating respiratory and systemic infections.

Bats are able to develop natural and experimental histoplasmosis infections [1–6]. Infected bats could act as reservoirs and dispersers of *H. capsulatum* in favorable environments, playing a possible role in the incorporation of the fungus in new ecological niches [7–9].

Over the last three decades, *H. capsulatum* has been the subject of several genotyping studies that have engaged its DNA polymorphism using molecular tools such as restriction fragment length polymorphism and random amplified polymorphic DNA methods [10–16], analyses of individual and concatenated genes [17–26] and whole genomes [27,28], which have contributed to the knowledge of the genetic diversity and phylogeny of this pathogen. Currently, *H. capsulatum* consists of various groups of isolates that differ genetically and correlate with particular geographic distributions, which are considered as a complex of cryptic species [20,26]. Phylogenetic analyses using molecular markers have been a useful tool for species recognition and for studying the evolutionary genetics of microbial pathogens in the fields of the host–parasite relationship, epidemiology, and medicine [29,30].

In general, fungal species recognition is based on biological or morphological species concepts; however, the description of several cryptic species among micromycetes have been proposed by exploring different methods and concepts to delimit species, such as the phylogenetic species concept and its derivatives [29]. In regard to the *H. capsulatum* species delimitation, the genealogical concordance phylogenetic species recognition (GCPSR) concept, mentioned by Taylor et al. [29], is one of the most validated concepts because it allows the analysis of micromycetes with certain characteristics, highlighting the lack of morphological characters, the absence of sexual spores, and the heterothallic species.

Kasuga et al. [20] studied the phylogenetic relationships of 137 *H. capsulatum* isolates from 25 countries and interpreted the results by applying the GCPSR concept. They used multilocus sequence typing (MLST) analyses of partial DNA sequences of four protein-coding genes: ADP ribosylation factor (*arf*), H-antigen precursor (*H-anti*), delta-9 fatty acid desaturase (*ole1*), and alpha-tubulin (*tub1*). Based on the analyses of these isolates with different geographical origins and sources, they identified eight *H. capsulatum* clades corresponding to genetically distinct geographical populations: North American class 1 (NAm 1), North American class 2 (NAm 2), Latin American group A (LAm A), Latin American group B (LAm B), Australian, Netherlands, Eurasian, and African. Seven of these clades (NAm 1, NAm 2, LAm A, LAm B, Australian, Netherlands, and African) were recognized as phylogenetic species belonging to the *H. capsulatum* complex. These authors also proposed the existence of seven lone lineages, which delimit an isolate or a small group of isolates that have a single multilocus genotype. Taylor et al. [21], using the same molecular markers, suggested the existence of a particular clade of *H. capsulatum* isolates, which contained one isolate from a *Mormoops megalophylla* bat (Chiroptera: Mormoopidae) and two isolates recovered from different tissues of the free-tailed bat, *Tadarida brasiliensis* (Chiroptera: Molossidae), all captured in Mexico. Later, Vite-Garin et al. [25], in their overview of the genetic diversity of *H. capsulatum*, referred to this clade when more *H. capsulatum* isolates were analyzed from *T. brasiliensis* bats.

Based on criteria involving MLST and population structure analyses, after examining the sequences of 234 isolates deposited in different databases, Teixeira et al. [26] proposed that *H. capsulatum* has at least 11 cryptic phylogenetic species, six of which are always concordant (RJ, LAm A1, LAm A2, LAm B1, LAm B2, and BAC1) and reported as new phylogenetic species. According to Teixeira et al. [26], the population structure of the highly diverse LAm A clade has three phylogenetic species (RJ, LAm A1, and LAm A2); besides, although the LAm B phylogenetic species showed low variation compared to other clades [17,20], its analysis suggests the presence of two monophyletic clades (LAm B1 and LAm B2) within LAm B.

Recent information about *H. capsulatum* genetic diversity is based on a precise approach reported by Sepúlveda et al. [27], using whole-genome resequencing data and the phylogenetic analyses of *Histoplasma* isolates from endemic areas of histoplasmosis, mainly from the United States of America (USA). Sepúlveda et al. [27] studied 30 isolates from five phylogeographical clusters (Panama lineage-H81, NAm 1, NAm 2, LAm A, and African) and considering their results, renamed four of them: *H. capsulatum sensu stricto* Darling 1906 (comprising three isolates from the Panama lineage-H81), *H. mississippiense* sp. nov. (comprising 10 isolates from the NAm 1 clade); *H. ohense* sp. nov. (comprising 11 isolates from the NAm 2 clade); and *H. suramericanum* sp. nov. (comprising four isolates from Colombia, previously classified as the LAm A clade). The African phylogenetic species remains without a taxonomic modification in the *H. capsulatum* complex.

The aim of this study was to contribute to the phylogenetic understanding of the *H. capsulatum* complex, by incorporating an important number of isolates from bats, the main wild host of this fungus. We analyzed the sequences of 176 isolates, 30 of which were isolated from wild bats. The *H. capsulatum* phylogeny, based on the GCPGR criterion, was reconstructed using individual locus and concatenated analyses of four protein-coding genes. To do this, we used parsimony, maximum likelihood, and Bayesian inference methods, as well as the coalescence-based methods. A concatenated sequence-types network and nucleotide diversity were also generated. Overall, these analyses provide robust support for the existence of a species-level clade containing seven *H. capsulatum* isolates from bats.

2. Materials and Methods

2.1. New *Histoplasma capsulatum* Isolates Studied

The sequences of 42 isolates were analyzed for the first time. These isolates are deposited in the *H. capsulatum* Culture Collection of the Fungal Immunology Laboratory (<http://www.wfcc.info/ccinfo/index.php?strain/display/817/fungi/>), Department of Microbiology and Parasitology, School of Medicine-UNAM, where they are maintained. This collection is registered in the database of the World Data Centre for Microorganisms as LIH-UNAM WDCM817. The data on bats and clinical *H. capsulatum* isolates used in this study are accessible in the culture collection catalogue, partially published by Rodríguez-Arellanes et al. [31] and in a website (<https://www.facmed.unam.mx/histoplas-mex/>).

For the isolation of *H. capsulatum* from randomly captured bats, only those species not in danger of extinction were processed, and they were used solely for research purposes. In all cases, national regulations for bat species protection, capture, and processing were strictly complied with, and we adhered to ethical recommendations and to the guidelines published by Gannon, Sikes, and the Animal Care and Use Committee of the American Society of Mammalogists [32]. Bats were processed for fungal isolation in accordance with the Ethics Committee of the School of Medicine, UNAM, following the recommendations of the Animal Care and Use Committee of the UNAM and the Mexican Official Guide (NOM 062-ZOO-1999).

Clinical isolates from Mexico were obtained from different hospitals in the country. Clinical isolates from Argentina and Colombia were donations to our collection by the INEI-ANLIS-“Dr. Carlos G. Malbrán” and the Corporación para Investigaciones Biológicas institutions, respectively. All clinical isolates were obtained as part of standard care procedures for fungal diagnosis, in hospital microbiology laboratories.

This study was approved by the School of Medicine Research and Ethics Committee (Ref. No. 017/2014).

2.2. *Histoplasma capsulatum* Sequences

Sequences of four individual loci from a total of 176 isolates were analyzed, considering the 42 new isolates here processed (details in Table 1) together with 134 isolates previously reported by Kasuga et al. [20]. Of the 134 isolates studied by Kasuga et al. [20], 17 of them derived from infected bats captured in Mexico. Incomplete sequences of three

isolates (EH-325, EH-383, and H190) were omitted from the total 137 isolates studied by Kasuga et al. [20]. Four sequences of *H. capsulatum* reference strains, whose genomes are available at the National Center for Biotechnology Information (<https://www.ncbi.nlm.nih.gov/bioproject>) were considered in all phylogenetic analyses of the present study: G-217B (accession number PRJNA12653) from the NAm 2 clade; H143 (accession number PRJNA29161) and H88 (accession number PRJNA29163) from the African clade; and G-186A (accession number PRJNA12635) from the Panama lineage. In this study, it is important to remark that the *H. capsulatum* strains named by Kasuga et al. [20] as H8, H81, H82, and H83, here are reported as G-217B, G-184B, G-186A, and G-186B, respectively.

Table 1. Data about the new *H. capsulatum* isolates reported in the present study.

Isolate Related		Phylogenetic-	Origin	GenBank (Accession Numbers)			
Acronym	Source	Species/Lineage ^a		arf	H-anti	ole1	tub1
1558	Human	LAm B (*)	AR	KT601344	KT601418	KT601381	KT601463
1739	Human	LAm B (*)	AR	KT601345	KT601419	KT601382	KT601464
92590	Human	LAm B (LAm B1)	AR	KT601346	KT601420	KT601383	KT601465
951814	Human	LAm B (LAm B1)	AR	KT601347	KT601421	KT601384	KT601466
993444	Human	LAm B (LAm B1)	AR	KT601348	KT601423	KT601385	KT601467
993445	Human	LAm B (LAm B1)	AR	KT601349	KT601424	KT601386	KT601468
993446	Human	LAm B (LAm B1)	AR	KT601350	KT601425	KT601387	KT601469
993267	Human	LAm B (LAm B1)	AR	KT601351	KT601422	KT601388	KT601470
AP	Human	LAm A (LAm A1)	CO	KT601352	KT601427	KT601389	KT601471
DS	Human	LAm A (*)	CO	KT601353	KT601428	KT601390	KT601472
GeM	Human	LAm A (LAm A1)	CO	KT601354	KT601445	KT601391	KT601473
GLi	Human	LAm A (LAm A2)	CO	KT601355	KT601446	KT601392	KT601474
Hz	Human	LAm B (LAm B1)	CO	KT601356	KT601449	KT601393	KT601475
JG	Human	LAm B (LAm B1)	CO	KT601357	KT601450	KT601394	KT601476
LA	Human	LAm A (LAm A2)	CO	KT601358	KT601451	KT601395	KT601477
LF	Human	LAm A (*)	CO	KT601359	KT601452	KT601396	KT601478
MZ2	Human	LAm A (LAm A2)	CO	KT601360	KT601426	KT601397	KT601479
RG	Human	LAm A (LAm A1)	CO	KT601361	KT601453	KT601398	KT601480
WCh	Human	LAm A (LAm A1)	CO	KT601362	KT601454	KT601399	KT601481
H1.02.W	Human	LAm A (LAm A2)	GT	KT601363	KT601447	KT601400	KT601482
H1.12.96	Human	LAm A (LAm A2)	GT	KT601364	KT601448	KT601401	KT601483
EH-323	Human	LAm A (*)	MX	KT601365	KT601429	KT601402	KT601484
EH-324	Human	LAm A (*)	MX	KT601366	KT601430	KT601403	KT601485
EH-326	Human	LAm A (*)	MX	KT601367	KT601431	KT601404	KT601486
EH-327	Human	LAm A (*)	MX	KT601368	KT601432	KT601405	KT601487
EH-328	Human	LAm A (LAm A1)	MX	KT601369	KT601433	KT601406	KT601488
EH-355	Human	LAm A (*)	MX	KT601370	KT601434	KT601407	KT601489
EH-356	Human	LAm A (*)	MX	KT601371	KT601435	KT601408	KT601490
EH-357	Human	LAm A (*)	MX	KT601372	KT601436	KT601409	KT601491
EH-3831 ^b	<i>L. nivalis</i>	LAm A (LAm A1)	MX	AF495619	AF495620	AF495621	F495622
EH-383P ^b	<i>L. nivalis</i>	LAm A (LAm A1)	MX	AF495623	AF495624	AF495625	AF495626
EH-384I ^b	<i>T. brasiliensis</i>	NAm 3 (BAC1)	MX	AF495627	AF495628	AF495629	AF495630
EH-384P ^b	<i>T. brasiliensis</i>	NAm 3 (BAC1)	MX	AF495631	AF495632	AF495633	AF495634
EH-408H ^b	<i>L. nivalis</i>	LAm A (LAm A1)	MX	AF495644	AF495645	AF495645	AF495646
EH-449B	<i>L. nivalis</i>	LAm A (LAm A1)	MX	KT601373	KT601437	KT601410	KT601455
EH-655P	<i>T. brasiliensis</i>	NAm 3 (BAC1)	MX	KT601374	KT601438	KT601411	KT601458
EH-658H	<i>T. brasiliensis</i>	NAm 3 (BAC1)	MX	KT601375	KT601439	KT601412	KT601459
EH-670B	<i>T. brasiliensis</i>	NAm 3 (BAC1)	MX	KT601376	KT601440	KT601414	KT601460
EH-670H	<i>T. brasiliensis</i>	NAm 3 (BAC1)	MX	KT601377	KT601441	KT601415	KT601461
EH-672B	<i>T. brasiliensis</i>	NAm 3 (*)	MX	KT601378	KT601442	KT601413	KT601456
EH-672H	<i>T. brasiliensis</i>	NAm 3 (*)	MX	KT601379	KT601443	KT601416	KT601457
EH-696P	<i>T. brasiliensis</i>	H153-lineage (*)	MX	KT601380	KT601444	KT601417	KT601462

^a Phylogenetic species of the new isolates studied, based on the classification as Kasuga et al. [20] and, in parenthesis, as Teixeira et al. [26].

^b Isolates previously studied by Taylor et al. [21], without phylogenetic classification. (*) *H. capsulatum* isolates not included previously in any phylogenetic species. Bat species: *L. nivalis* = *Leptonycteris nivalis*; *T. brasiliensis* = *Tadarida brasiliensis*. NAm 3: North American 3. AR: Argentina; CO: Colombia; GT: Guatemala; MX: Mexico.

2.3. DNA Extraction, PCR, and Sequencing of *Histoplasma capsulatum* Isolates

DNA extraction was performed on the 42 new isolates, according to Taylor et al. [9]. We processed PCR products of the *H. capsulatum* gene fragments (*arf*, *H-anti*, *ole1*, and *tub1*) as described by Kasuga et al. [20] with minor modifications as per Taylor et al. [21]. Amplicons were sequenced at the High-Throughput Genomics Center (University of Washington, Seattle, WA, USA). DNA sequencing reactions were implemented for both DNA strands and a consensus sequence was generated for each gene fragment using MESQUITE version 3.01 (<http://mesquiteproject.org>) and Chromas Lite version 2.1.1 (<http://technelysium.com.au/>). Sequences of the 42 new *H. capsulatum* isolates were deposited in the GenBank (see Table 1). The sequences from Kasuga et al. [20] are available on the TreeBASE database (study ID S1063).

2.4. *Histoplasma capsulatum* Sequence Alignments and BLASTn Analyses

The sequences of 176 isolates were assembled and aligned manually using MESQUITE (<http://mesquiteproject.org>). A concatenated matrix containing the four gene fragments studied was used for phylogenetic reconstruction.

A BLASTn analysis [33] was conducted with the complete genes reported in the GenBank (accession numbers: L25117.1, U20346.1, X85962.1, and M28358.1 for *arf*, *H-anti*, *ole1*, and *tub1*, respectively) for the G-217B strain (American Type Culture Collection-26032) from Louisiana/USA, which is considered the most representative strain of the NAm 2 phylogenetic species.

2.5. Congruence Analysis

Congruence of the four gene genealogies was evaluated with the incongruence length difference (ILD) test developed by Farris et al. [34] and implemented in PAUP* version 4.2003 as the partition homogeneity test (<http://paup.csit.fsu.edu/downl.html>). For each test, uninformative characters were excluded, and the sum of tree lengths of the actual partition was compared to the sum of tree lengths of 1000 randomly assigned partitions, where the null hypothesis is that the *arf*, *H-anti*, *ole1*, and *tub1* partitions are congruent (the sequences are drawn from a single, homogeneous group of characters). The percent of instances where the sum of the tree lengths of each random partition exceeded that of the true partition was used to detect incongruence between data sets.

2.6. Phylogenetic Reconstruction

The four gene regions were subjected to two-way comparisons in all possible combinations and analyzed by different methods. (1) Parsimony analysis was performed with TNT version 1.1 [35] using a random starting tree with 1000 ratchet iterations [36]; all characters were treated as unordered and assigned equal weights. (2) Probabilistic analyses were performed with maximum likelihood (ML) and Bayesian inference (BI). ML analysis was conducted in RAxMLGUI version 1.31 [37] using the general time reversible (GTR) substitution model with a gamma distribution. BI was performed in MrBayes version 3.2 [38] using four chains with a total of 100,000,000 generations and sampling trees every 10,000 generations. Convergence of the chains was evaluated with the effective sample size (ESS) values and corroborated with Tracer version 1.6 (<http://beast.bio.ed.ac.uk/Tracer>). Both probabilistic analyses were implemented in jModeltest version 2.1.4 [39]. Based on the results of the Bayesian information criterion of jModeltest, the substitution models considered for each partition were K80 (*H-anti*), K80 + G (*arf* and *tub1*), and K80 + I (*ole1*).

Bootstrap (bt) values for parsimony and ML analyses were based on the heuristic search of 1000 replicates, using tree-bisection-reconnection. For the BI, the maximum clade credibility tree was selected with a posterior probability (pp) limit of 0.95, using TreeAnnotator version 1.8.2, implemented with *BEAST [40]. Unrooted trees were constructed using concatenated and individual sequence alignments. In special cases, rooted trees were generated with *Blastomyces dermatitidis* as an outgroup, using the sequences available in the GenBank database (accession numbers: *arf*-XM002628904.1; *ole1*-XM002625814.1; and

tub1-JN562337.1). In the concatenated analyses, the *H-anti* gene fragment was considered as missing data.

2.7. Coalescence Analysis

A coalescence-based analysis was conducted using the *BEAST method, which was implemented in BEAST version 1.8.2 [40,41]. An XML file was generated for the alignments of the four loci using BEAUti version 1.8.2 [41]. The K80 substitution model with empirical base frequencies was applied to the four loci, and the gamma distribution was included for *arf* and *tub1*, whereas invariant sites were included in the model for *ole1*. The remaining parameters used in the *BEAST coalescence analysis were the same as those used in the BI phylogenetic analysis. The final run of the coalescence analysis assumed a strict molecular clock based on the results of the stepping-stone and marginal likelihoods methods implemented in MrBayes software version 3.2 [38,41], which tested strict clock vs. no clock or strict clock vs. some sort of relaxed clock. Here, we used the nucleotide substitution rates reported by Kasuga et al. [20], which were estimated considering two divergence times from Eurotiomycetes, 127.8 million years ago for *Histoplasma* and 31.8 million years ago for *Blastomyces*; *arf*: 0.86×10^{-9} , *H-anti*: 1.17×10^{-9} , *ole1*: 0.87×10^{-9} , and *tub1*: 1.63×10^{-9} substitutions/site/year.

2.8. Concatenated Sequence-Types (CSTs) Network

The concatenated matrix of four nuclear genes was used to generate an unrooted network constructed by the median-joining algorithm [42] with Network version 4.613 (www.fluxus-engineering.com).

2.9. Nucleotide Diversity (π)

Estimation of intraspecific π values for *arf*, *H-anti*, *ole1*, and *tub1* gene fragments of the *H. capsulatum* isolates studied was performed on the concatenated alignment using DnaSP version 5.10 [43].

3. Results

Of the 42 newly reported isolates, 13 were obtained from naturally infected bats captured in different Mexican regions and 29 were isolated from human clinical samples (8 from Argentina, 11 from Colombia, 2 from Guatemala, and 8 from Mexico) (see Table 1).

3.1. *Histoplasma capsulatum* BLASTn Analysis

High similarity (95–99%) was found by BLASTn among all the sequences studied, when compared with the sequences of the four complete genes (*arf*, *H-anti*, *ole1*, and *tub1*) of the G-217B reference strain.

3.2. Congruence Analysis

The concatenated matrix of the four gene fragments had a total of 1538 nucleotides (nt), of which 321 sites were variable and 226 were parsimony informative (Table 2). The length of each gene fragment studied was as follows: *arf*-457 nt, *H-anti*-397 nt, *ole1*-414 nt, and *tub1*-270 nt.

Table 2. Genetic diversity of each gene fragment analyzed.

	Gene Fragments		Nucleotide Sites		Parsimonious
	Size (nt)	^a Start/End (nt)	Variable	Informative	
<i>arf</i>	457	415/871	70	44	26
<i>H-anti</i>	397	394/789	91	59	32
<i>ole1</i>	414	37/450	69	49	20
<i>tub1</i>	270	590/862	91	74	17
Total	1538		321	226	95

^a Reference data came from each complete gene of the G-217B *H. capsulatum* strain deposited in GenBank (see Materials and Methods).

The ILD test found no significant heterogeneity among the four gene genealogies (Table 3).

Table 3. Data for the incongruence length difference test using the sequences of the four genes studied.

Partition	Sum of Tree Lengths		
	Original Partition	Range of Replicates	p Value
Four genes	1243	1243–1242	0.997
<i>arf</i> vs. <i>H-anti</i>	161	161–0	1
<i>arf</i> vs. <i>ole1</i>	156	156–157	0.941
<i>arf</i> vs. <i>tub1</i>	193	193–194	0.997
<i>H-anti</i> vs. <i>ole1</i>	168	168–169	0.748
<i>H-anti</i> vs. <i>tub1</i>	217	217–0	1
<i>ole1</i> vs. <i>tub1</i>	202	202–0	1

The ILD test was performed with the 176 *H. capsulatum* isolates.

3.3. Phylogenetic Reconstruction

In all phylogenetic analyses of the concatenated alignments, using the sequences of the 176 *H. capsulatum* isolates studied, the eight clades described by Kasuga et al. [20] and the LAm A1, LAm A2, LAm B1, and BAC1 clades named by Teixeira et al. [26] were recognized (see Figure 1A–C).

Due to the ML and BI trees have similar topologies in the individual analysis for the alignments of each locus studied; they were represented as BI trees. The support for each branch was included as bt values for ML/pp values for BI analyses (see Supplementary Material, Figures S1–S4).

The parsimony analysis of the concatenated alignment resulted in eight most parsimonious trees, a tree length of 514 steps, a consistency index of 0.654, and a retention index of 0.934 (Figure 1A).

According to our data, most of the new *H. capsulatum* isolates analyzed match with LAm A phylogenetic species described by Kasuga et al. [20]. In addition, 28 of these new isolates clustered together with some isolates previously classified by Teixeira et al. [26] as belonging to the phylogenetic species LAm A1, LAm A2, LAm B1, and BAC1, with the exception of isolates 1558 and 1739 from Argentina, DS and LF from Colombia, as well as EH-323, EH-324, EH-326, EH-327; EH-355, EH-356, EH-357, EH-672B, EH-672H, and EH-696 from Mexico, which formed different independent groups (see Table 1).

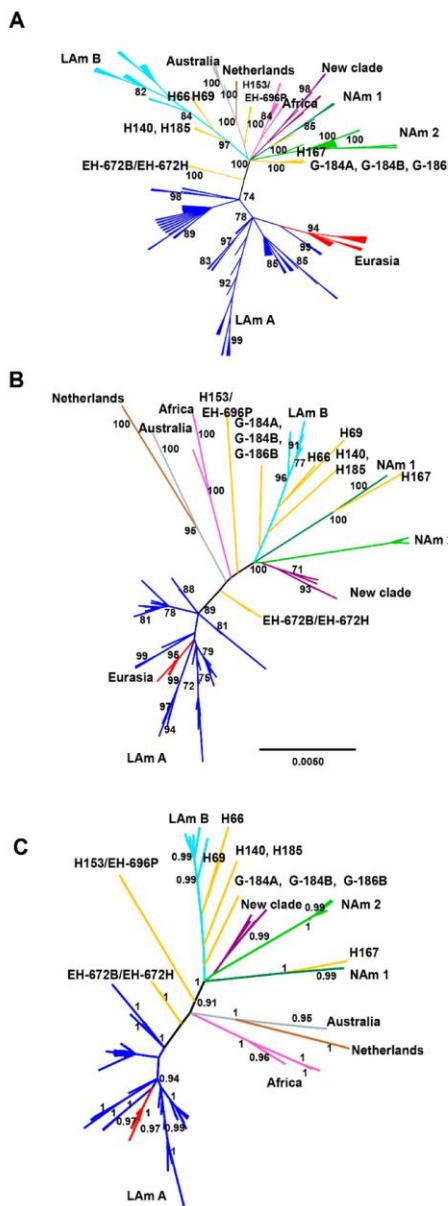


Figure 1. Unrooted phylogenetic trees of *H. capsulatum* isolates generated by different inference methods. The analyses were performed with a concatenated matrix of 1538-nt constructed with four gene fragments (*arf*, *H-anti*, *ole1*, and *tub1*). (A) Parsimony strict consensus tree with a bt $\geq 70\%$; (B) maximum likelihood tree with a bt $\geq 70\%$; (C) Bayesian inference maximum clade credibility tree was selected with a pp limit of 0.95. The support values of bt and pp are indicated on their corresponding tree nodes (details under Materials and Methods).

In agreement with the results by Kasuga et al. [20], the present data showed that LAm A forms a clade that also contains the Eurasian isolates. Furthermore, LAm A is connected to almost all the other isolates by a long and well-supported internal branch. A branch leading to the two isolates, EH-672B and EH-672H, is always attached to this long internal branch in the concatenated analyses (Figure 1A–C).

Unrooted phylogenetic trees (Figure 1A–C) had similar topologies and showed slight differences between parsimony (Figure 1A) and BI (Figure 1C) trees.

In the present analyses, the EH-315 isolate obtained from a *M. megalophylla* bat captured in Mexico and classified as a lone lineage by Kasuga et al. [20], forms a particular clade ($bt > 70\%$ and $pp > 0.95$), together with six *H. capsulatum* isolates (EH-384I, EH-384P, EH-655P, EH-658H, EH-670B, and EH-670H) obtained from *T. brasiliensis* bats captured in different regions of Mexico (Figure 1A–C); although isolates EH-384I, EH-384P, and EH-315 were slightly divergent. This clade forms a polytomy with several others in the parsimony tree (Figure 1A), including LAm B, Netherlands–Australian, African, and NAm 1, as well as NAm 2; however, notably in the ML and BI analyses, this clade is the sister group of NAm 2 (Figure 1B,C). Given its relationship to NAm 2, we propose naming this new clade formed here with seven *H. capsulatum* isolates as NAm 3, highlighting that this clade incorporated three *H. capsulatum* isolates that had been previously described by Taylor et al. [21] and later considered as a new phylogenetic species denominated BAC1 by Teixeira et al. [26].

Another of the new *H. capsulatum* isolates, EH-696P, obtained from a *T. brasiliensis* bat captured in the state of Nuevo León in northwestern Mexico had similar sequences to the isolate H153 (100% bt ; 1.0 pp) from a Brazilian patient, which had formerly been classified as a lone lineage by Kasuga et al. [20] and Teixeira et al. [26].

Here, we also found a new lone lineage composed of *H. capsulatum* isolates EH-672B and EH-672H, both obtained from a *T. brasiliensis* bat captured in the state of Hidalgo, Mexico. This lone lineage had high support values in parsimony ($bt = 100$, Figure 1A) and BI ($pp = 1$, Figure 1C) analyses, although a $bt < 70\%$ was found in the ML analysis. The relationships of the EH-672B/EH-672H isolates to all other clades and lone lineages are unclear in the analyses using the concatenated matrix (Figure 1A–C), and in *H-anti*, *ole1*, and *tub1* individual trees, these isolates are included in different clades (see Supplementary Material, Figures S2–S4); regarding the *arf* gene, the amplified fragments generated for these isolates showed a lower query cover than the compared reference sequences of the GenBank, affecting their analyses.

All phylogenetic rooted trees were constructed using *B. dermatitidis* sequences as an outgroup. The results showed similar topologies to those for unrooted trees, although the branch between the outgroup and the *H. capsulatum* isolates was longer in the individual gene trees (Supplementary Material, Figures S5–S8).

3.4. Coalescence Analysis

Convergence among runs was found in the *BEAST analysis using a strict molecular clock; the ESS values were >200 . The *BEAST analysis was also performed using a relaxed molecular clock, and the same topology was recovered. However, the topology of the resulting species tree (Figure 2) was different from those of all phylogenetic analyses. It showed that the NAm 3 clade and most of the lone lineages were closely related with the Latin American and the Eurasian clades (0.84 pp) described by Kasuga et al. [20], except for a lone lineage H167 from Argentina that was sister to NAm 1 (0.99 pp) and for the lone lineage formed by H153 and EH-696P isolates (0.99 pp), which was sister to all other phylogenetic species. The Australian and Netherlands clades grouped together (0.94 pp), as found in the MLST analyses performed by Kasuga et al. [20]. In the coalescence analysis (Figure 2), the EH-672B/EH-672H lone lineage is a close relative of the newly-named NAm 3 clade (0.99 pp).

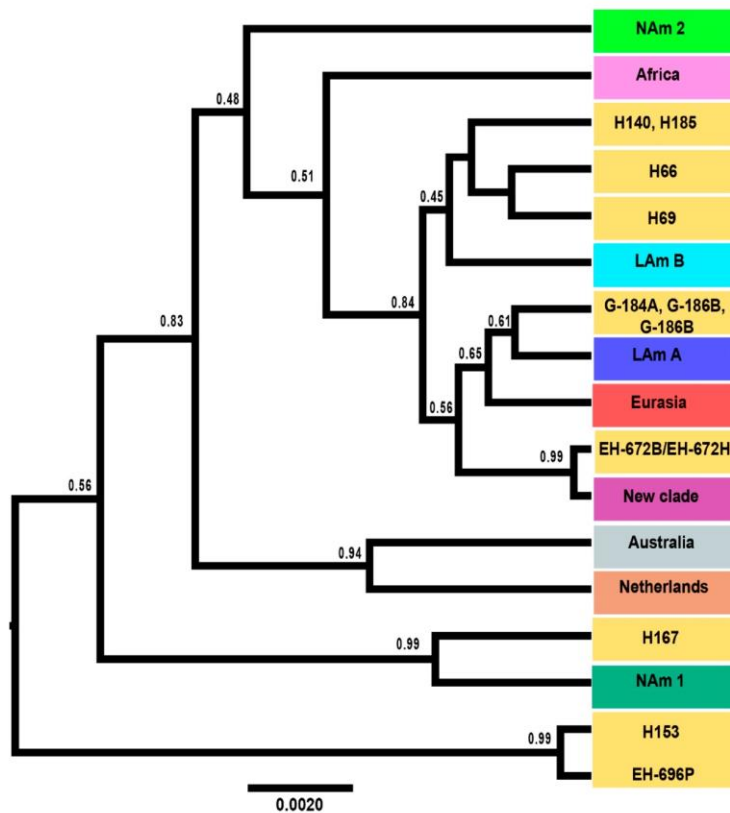


Figure 2. Species tree generated by coalescent-based species delimitation methods of the *H. capsulatum* complex. Maximum-clade-credibility tree of the concatenated gene fragments *arf*, *H-anti*, *ole1*, and *tub1* was selected from the *BEAST analysis, using a strict molecular clock (see Materials and Methods). The values of pp are indicated on their corresponding branches of the tree nodes.

3.5. Concatenated Sequence-Types (CSTs) Network

Concatenated sequence-types (CSTs) network analysis found a total of 110 distinctive CSTs from the four loci concatenated matrix of the 176 *H. capsulatum* isolates (Figure 3). In the CSTs analysis it was possible to confirm that the LAm A clade was the most genetically differentiated (52 CSTs), followed by the LAm B (13 CSTs), NAm 2 (11 CSTs), Eurasian (9 CSTs), NAm 3 (6 CSTs), and African (5 CSTs) clades. The least genetically differentiated clades were NAm 1 (2 CSTs), Netherlands (2 CSTs), and Australian (2 CSTs). Of the 110 CSTs, nine occurred as lone lineages (Figure 3).

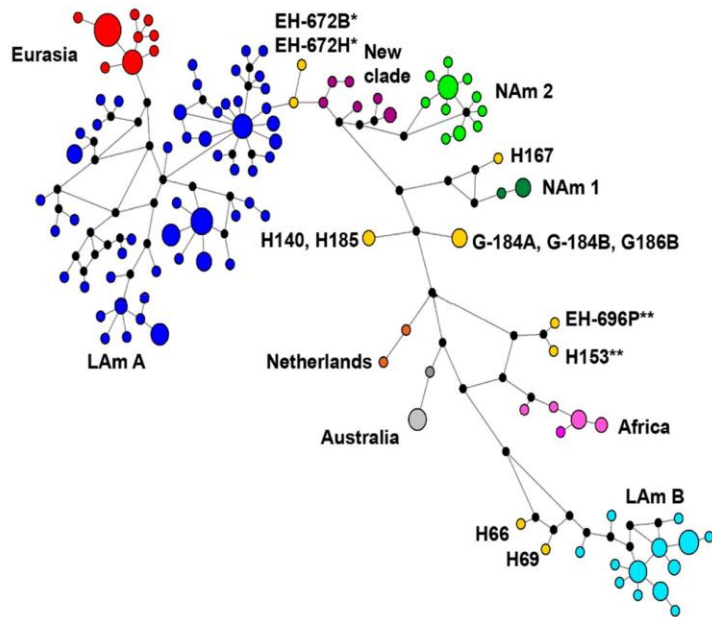


Figure 3. Dispersion of the *H. capsulatum* complex associated with concatenated sequence-types (CSTs) from the 176 isolates studied. A total of 110 CSTs were generated using a median-joining network based on the analysis of the 1538-nt alignment of four concatenated gene fragments. The branch lengths are proportional to the number of substitutions, and the relative sizes of circles are proportional to their corresponding CST frequencies. Each node (black circle) indicates a hypothetical missing CST. The CST colors correspond to different *H. capsulatum* clades and the lone lineages are in yellow.

In terms of distance among CSTs, the LAm A and the LAm B clades were the most distant, the Eurasian CSTs emerged from LAm A, the new EH-672B/EH-672H lone lineage was connected to LAm A, and the NAm 3 clade was associated to NAm 2. The African, Netherlands and Australian clades were closely grouped (Figure 3). These last relationships can also be seen in all phylogenetic analyses using a concatenated matrix (Figure 1A–C).

3.6. Nucleotide Diversity (π)

In regard to genetic diversity, intraspecific π values for clades ranged from the most diverse (LAm A = 0.00835) to the least diverse (Australian = 0.00027). The NAm 3 clade had a π value of 0.0061 rather the African clade (π = 0.00622). The nucleotide diversity of the lone lineages revealed π values in the range of 0.00528 (EH-672B/EH-672H) to 0.00342 (H153/EH-696P).

4. Discussion

The role of bats in spreading *H. capsulatum* in the environment was proposed many years ago, particularly by Hoff and Bigler [7]; however, the relationship between the behavior of bats and *H. capsulatum* ecology remains ambiguous, especially the potential connection of their movements and migrations with this pathogen's dispersion in nature [8].

Regarding the bat–*Histoplasma* interplay, the first important finding to this binomial relationship concerns a lone lineage (EH-315) described by Kasuga et al. [20], which was formed by one *H. capsulatum* isolate from an infected *M. megalophylla* bat captured in Mexico. According to our novel data and major sequence analyses, a cluster comprising

six *H. capsulatum* isolates (EH-384I, EH-384P, EH-655P, EH-658H, EH-670B, and EH-670H) associated with *T. brasiliensis* bats, together with the EH-315 isolate, formed a NAm 3 clade that was supported in the phylogenetic reconstruction analyses with values of $bt > 70\%$ and $pp > 0.95$ and was well defined in the CSTs network. Thus, it is reasonable to consider the NAm 3 clade as a phylogenetic species, based on the GCPSR concept recognized by Taylor et al. [29] and Mayden [44], in agreement with Kasuga et al. [20] and Teixeira et al. [26]. The two wild bat species from which these *H. capsulatum* isolates were recovered are colonial and share some attributes, such as insectivorous feeding, habitats, and migratory behavior [45,46].

Considering the inclusion of an important number of new *H. capsulatum* isolates from different sources, our results support the high genetic diversity of this pathogen by using multifaceted methods for phylogenetic and species tree inference. The present study confirms the earlier molecular phylogenetic relationships of the *H. capsulatum* species complex, reported by Kasuga et al. [20] and Teixeira et al. [26], and it replaces the BAC1 clade (with only three isolates) proposed by Teixeira [26] with the NAm 3 clade (containing seven isolates), which revealed itself to be more closely related to the NAm 2 phylogenetic species, by concatenated sequence analyses and CSTs network findings.

Tadarida brasiliensis was the major bat species associated with *H. capsulatum* isolates from the NAm 3 phylogenetic species, the lone lineage EH-672B/EH-672H, and the EH-696P isolate that clustered together with the lone lineage H153, previously described by Kasuga et al. [20]. This bat species was captured in different states of the Mexican territory included in North or Central America (see Figure 4). In the past, Taylor et al. [9] described that the GACG(GA)11GA haplotype of the (GA)n microsatellite and its flanking regions is associated with nine *H. capsulatum* isolates from *T. brasiliensis* captured in the southern region of Mexico (Chiapas and Oaxaca states); of these nine *H. capsulatum* isolates, six (EH-384I, EH-384H, EH-655P, EH-658H, EH-670B, and EH-670H) were classified here as belonging to the NAm 3 phylogenetic species. Based on these findings, it is reasonable to consider that gene flow mechanisms could displace *H. capsulatum* genetic patterns in the environment, mainly associated with special wild hosts. Particularly, according to our findings, it is possible to expect that *T. brasiliensis* has at least three different migratory routes in the Mexican territory (see Figure 4), based on the genetic diversity of the *H. capsulatum* isolates recovered from this bat species. Interestingly, the subspecies *T. brasiliensis mexicana* has a migratory route that extends from the southwestern regions of the USA to the northern and central-southeastern regions of Mexico [47]. Thus, the geographic distribution of *H. capsulatum* could be related to the migratory behavior of infected bats, considering their possible evolutionary history with this pathogen in shared natural habitats [9,20,21,26].

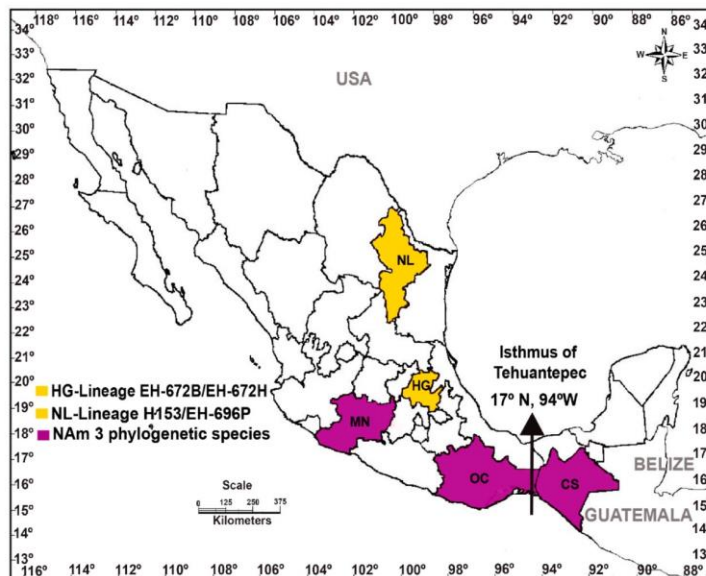


Figure 4. Distribution of *H. capsulatum* isolated from the migratory bat *T. brasiliensis* in Mexico. Geographically, Mexico is in North and Central America, and the boundary of both regions is delimited by the Isthmus of Tehuantepec (arrowhead). *T. brasiliensis* bats were captured in different states of Mexico, which are distributed in either the Northern or Central American regions of the Mexican territory. CS: Chiapas; HG: Hidalgo; MN: Michoacán; NL: Nuevo León; OC: Oaxaca.

In regard to the motivating data published by Sepúlveda et al. [27], who by using phylogenomic species recognition, which presented the *Histoplasma* American phylogenetic species as *H. capsulatum sensu stricto*, *H. mississippiense*, *H. ohense*, and *H. suramericanum*, it is noteworthy that none of the new *H. capsulatum* isolates analyzed here were compatible with the phylogenetic species reported by Sepúlveda et al. [27], probably because we followed different methodologies for species recognition.

With respect to the congruence analysis, in contrast to the report by Kasuga et al. [17], we found no evidence of incongruence among individual gene trees by the ILD test [34] (see Table 3). This discrepancy may be due to our inclusion of additional isolates, which may increase support for branches among species and reduce it within species. Besides, even if incongruence is detected, it may not provide a conclusive demonstration that concatenation of data produces phylogenetic error [48].

The present results also improve our understanding of Latin American *H. capsulatum* phylogeographic distribution. Based on phylogenetic reconstruction and coalescence analyses, it was found that most of the *H. capsulatum* isolates from Mexico and Colombia here studied are in the LAm A clade. However, two new *H. capsulatum* isolates from Colombia and all the new isolates from Argentina detailed in Table 1 were shown to belong to the LAm B clade according to Kasuga et al. [20] or LAm B1 considering the modified classification of Teixeira et al. [26]. In consequence, there may be an association between Latin American clades and geography in South America.

In our study, unrooted phylogenetic trees were primarily generated; additionally, rooted trees were also constructed using *B. dermatitidis* as an outgroup and only considering the accessible sequences for *arf*, *ole1*, and *tub1*. It is important to comment that *H-anti* was not used in the construction of the rooted trees because its sequences were not available for *B. dermatitidis* or any fungus that could be used as an outgroup, such as *B. parvus*,

Paracoccidioides brasiliensis, *P. lutzii* or *Emmonsia crescens*. Overall, the topologies of rooted trees agreed with each clade generated by unrooted trees, as mentioned in the results section. Slight discrepancies in the topologies of unrooted trees, involving short internal branches of some clades, could be explained by the different phylogenetic analyses used, which is consistent with an early and short period of *H. capsulatum* radiation.

The *H. capsulatum* isolates from the NAm 3 phylogenetic species share a high similarity among their CSTs (see Figure 3) and in their phylogenetic reconstruction (see Figure 1A–C). Our data also highlight that NAm 3 has strong support in the four unrooted individual gene trees and does not contain other taxa.

The CST network is a general evolutionary representation that infers ancestral types, variants, and estimates dating and provides strong support to investigate the relationships among all *H. capsulatum* isolates studied. Based on the number of CSTs found for each clade, LAm A was the most diverse and the best sampled. Besides, NAm 3 was also diverse, irrespective of the number of isolates analyzed.

The coalescence analysis using the *BEAST method is a useful tool for inferring relationships among groups of isolates, but in a few cases, it revealed conflicting relationships when compared with other phylogenetic and network methods, which have somewhat lower support. However, the lower *bt* and *pp* values shown in this coalescent-based method are possibly due to the lack of more molecular data. This occurred in the present analyses as well as in other reports [20].

Regarding the independent lineages previously described by Kasuga et al. [20], the present results also support a close relationship between the lone lineages H81 (G-184B), H66, and H69 and the LAm B clade (see Figure 1A–C) even though branch support is low. Considering the results reported by Kasuga et al. [20], the discrepancy in branch support reported here could be explained by the use of different methods that often give contrasting results for the same organism, as sustained by Sites and Marshall [49]. In addition, the sister relationship between the Brazilian H153 and the Mexican EH-696P isolates is well supported in the species tree as a lone lineage, although the phylogenetic position of this lineage with respect to other *H. capsulatum* isolates remains unclear. This latter issue should be investigated further with more loci.

Intraspecific π values were obtained for *H. capsulatum* isolates only to detect gene diversity among isolates of the same clade or the same lone lineage, whereas determination of interspecific π values were unnecessary because divergences among clades and lineages were well sustained by all phylogenetic analyses reported here. Our data indicate that the intraspecific variation in NAm 3 ($\pi = 0.0061$), LAm A ($\pi = 0.00835$), and African ($\pi = 0.00622$) clades was homogeneous. Finally, considering the number of CSTs (6 CSTs) and the π value ($\pi = 0.0061$), the existence of a different evolutionary line supports the new phylogenetic species NAm 3.

5. Conclusions

The present information about the interaction between the fungal pathogen *H. capsulatum* and one of its most important wild hosts is unique. We analyzed sequences of nine *H. capsulatum* isolates from *T. brasiliensis*: six (EH-384I, EH-384P, EH-655P, EH-658H, EH-670B, and EH-670H) belong to the NAm 3 phylogenetic species, while the other three (EH-672B, EH-672H, and EH-696P) are proposed as lone lineages. Concatenated sequence analyses and the CSTs network support these findings in the *H. capsulatum* complex. Interestingly, the NAm 3 phylogenetic species and the EH-672B/EH-672H lineage reported here are known only from naturally infected bats captured in Mexico, which may suggest that specific mammals are susceptible to particular genotypes of *H. capsulatum*, a possibility that warrants future comparison of their genomes. Thus, the detection of fungal genotypes associated with geographical patterns in infected bats randomly captured in the environment could contribute as a molecular biomarker to monitor the movements and migrations of bats and also to generate an epidemiological map of *H. capsulatum*, according to its distribution in nature. Furthermore, our results highlight the importance

of histoplasmosis as a global health issue, including the unusual aspects of the pathogen *H. capsulatum* involving naturally infected bats.

Supplementary Materials: The following are available online at <https://www.mdpi.com/article/10.3390/jof7070529/s1>. Figure S1: Unrooted phylogenetic tree of the *arf* gene fragment for *H. capsulatum* isolates. The Bayesian inference maximum clade credibility tree was selected with a pp limit of 0.95. The bt and pp values are indicated on their corresponding tree nodes (details under Materials and Methods). Supporting values are indicated as follows: bt/pp in maximum likelihood/Bayesian inference, respectively. Figure S2: Unrooted phylogenetic tree of the *H-anti* gene fragment for *H. capsulatum* isolates. The Bayesian inference maximum clade credibility tree was selected with a pp limit of 0.95. The bt and pp values are indicated on their corresponding tree nodes (details under Materials and Methods). Supporting values are indicated as follows: bt/pp in maximum likelihood/Bayesian inference, respectively. Figure S3: Unrooted phylogenetic tree of the *ole1* gene fragment for *H. capsulatum* isolates. The Bayesian inference maximum clade credibility tree was selected with a pp limit of 0.95. The bt and pp values are indicated on their corresponding tree nodes (details under Materials and Methods). Supporting values are indicated as follows: bt/pp in maximum likelihood/Bayesian inference, respectively. Figure S4: Unrooted phylogenetic tree of the *tub1* gene fragment for *H. capsulatum* isolates. The Bayesian inference maximum clade credibility tree was selected with a pp limit of 0.95. The bt and pp values are indicated on their corresponding tree nodes (details under Materials and Methods). Supporting values are indicated as follows: bt/pp in maximum likelihood/Bayesian inference, respectively. Figure S5: Rooted phylogenetic tree of the *arf* gene fragment for *H. capsulatum* isolates. A Bayesian inference maximum clade credibility tree was selected with a pp limit of 0.95. The pp values are indicated on their corresponding tree nodes. A *B. dermatitidis* sequence was used as an outgroup (see Materials and Methods). Figure S6: Rooted phylogenetic tree of the *ole1* gene fragment for *H. capsulatum* isolates. A Bayesian inference maximum clade credibility tree was selected with a pp limit of 0.95. The pp values are indicated on their corresponding tree nodes. A *B. dermatitidis* sequence was used as an outgroup (see Materials and Methods). Figure S7: Rooted phylogenetic tree of the *tub1* gene fragment for *H. capsulatum* isolates. A Bayesian inference maximum clade credibility tree was selected with a pp limit of 0.95. The pp values are indicated on their corresponding tree nodes. A *B. dermatitidis* sequence was used as an outgroup (see Materials and Methods). Figure S8: Rooted phylogenetic tree of the concatenated *arf*, *ole1*, and *tub1* genes of *H. capsulatum* isolates generated by a Bayesian inference method. Maximum-clade-credibility tree was constructed with a concatenated matrix with three gene fragments. The pp ≥ 0.95 values are indicated on their corresponding branches of the tree nodes. *B. dermatitidis* sequences of the three gene fragments available in the GenBank were used as an outgroup.

Author Contributions: M.L.T. and T.V.-G. were involved in the study design, they analyzed and interpreted the results and drafted the manuscript. T.V.-G., M.d.R.R.-M. and C.E.C. performed the experiments. T.V.-G., D.A.E.-B. and D.S.G. conducted data analysis; and they participated in drafting the manuscript and provided a critical review of the same. G.R.-A., J.H.S., L.S.-D. and J.A.R. processed the fungal samples for DNA extraction. M.L.T., J.W.T. and R.M.Z.-O. participated in the study design and provided a critical review of the manuscript. M.L.T. conceptualized and coordinated the project. All authors have read and agreed to the published version of the manuscript.

Funding: The present research was funded by a grant from the “Programa de Apoyo a Proyectos de Investigación e Innovación Tecnológica-Dirección General de Asuntos del Personal Académico” from UNAM-Mexico (PAPIIT-DGAPA/UNAM-MX, Reference Number-IN213515).

Institutional Review Board Statement: Not applicable.

Informed Consent Statement: Not applicable.

Data Availability Statement: Not applicable.

Acknowledgments: This paper constitutes partial fulfillment of the requirements for the Graduate Program in Biological Science of the UNAM. TVG thanks the Graduate Program in Biological Science of the UNAM and the scholarship of the Consejo Nacional de Ciencia y Tecnología-Mexico (Reference Number-231985). RMZ-O is supported in part by Conselho Nacional de Desenvolvimento Científico e Tecnológico- Brazil (Reference Number-304976/2013-0).

Conflicts of Interest: The authors declare that they have no conflict of interest.

References

1. Taylor, M.L.; Chávez-Tapia, C.B.; Vargas-Yáñez, R.; Rodríguez-Arellanes, G.; Peña-Sandoval, G.R.; Toriello, C.; Pérez, A.; Reyes-Montes, M.R. Environmental conditions favoring bat infection with *Histoplasma capsulatum* in Mexican shelters. *Am. J. Trop. Med. Hyg.* **1999**, *61*, 914–919. [[CrossRef](#)]
2. Canteros, C.E.; Iachini, R.H.; Rivas, M.C.; Vaccaro, O.; Madariaga, J.; Galarza, R.; Snaiderman, L.; Martínez, M.; Paladino, M.; Cicuttin, G.; et al. Primer aislamiento de *Histoplasma capsulatum* de murciélagos urbanos *Eumops bonariensis*. *Rev. Argent. Microbiol.* **2005**, *37*, 46–56. [[PubMed](#)]
3. González-González, A.E.; Aliouat-Denis, C.M.; Carreto-Binaghi, L.E.; Ramírez, J.A.; Rodríguez-Arellanes, G.; Demanche, C.; Chabé, M.; Aliouat, E.M.; Dei-Cas, E.; Taylor, M.L. An *Hcp100* gene fragment reveals *Histoplasma capsulatum* presence in lungs of *Tadarida brasiliensis* migratory bats. *Epidemiol. Infect.* **2012**, *140*, 1955–1963. [[CrossRef](#)]
4. González-González, A.E.; Ramírez, J.A.; Aliouat-Denis, C.M.; Demanche, C.; Aliouat, E.M.; Dei-Cas, E.; Chabé, M.; Taylor, M.L. Molecular detection of *Histoplasma capsulatum* in the lung of a free-ranging common Noctule (*Nyctalus noctula*) from France using the *Hcp100* gene. *J. Zoo Wildl. Med.* **2013**, *44*, 15–20. [[CrossRef](#)] [[PubMed](#)]
5. González-González, A.E.; Aliouat-Denis, C.M.; Ramírez-Bárcenas, J.A.; Demanche, C.; Pottier, M.; Carreto-Binaghi, L.E.; Akbar, H.; Derouiche, S.; Chabé, M.; Aliouat, E.M.; et al. *Histoplasma capsulatum* and *Pneumocystis* spp. co-infection in wild bats from Argentina, French Guyana, and Mexico. *BMC Microbiol.* **2014**, *14*, 1–8. [[CrossRef](#)] [[PubMed](#)]
6. Suárez-Alvarez, R.O.; Sahaza, J.H.; Berzunza-Cruz, M.; Becker, I.; Curiel-Quesada, E.; Pérez-Torres, A.; Reyes-Montes, M.R.; Taylor, M.L. Dimorphism and dissemination of *Histoplasma capsulatum* in the upper respiratory tract after intranasal infection of bats and mice with mycelial propagules. *Am. J. Trop. Med. Hyg.* **2019**, *101*, 716–723. [[CrossRef](#)] [[PubMed](#)]
7. Hoff, G.L.; Bigler, W.J. The role of bats in the propagation and spread of histoplasmosis: A review. *J. Wildl. Dis.* **1981**, *17*, 191–196. [[CrossRef](#)] [[PubMed](#)]
8. Taylor, M.L.; Chávez-Tapia, C.B.; Reyes-Montes, M.R. Molecular typing of *Histoplasma capsulatum* isolated from infected bats, captured in Mexico. *Fungal Genet. Biol.* **2000**, *30*, 207–212. [[CrossRef](#)]
9. Taylor, M.L.; Hernández-García, L.; Estrada-Bárcenas, D.A.; Salas-Lizana, R.; Zancopé-Oliveira, R.M.; García de la Cruz, S.; Galvão-Dias, M.A.; Curiel-Quesada, E.; Canteros, C.E.; Bojórquez-Torres, G.; et al. Genetic diversity of microsatellite (GA)_n and their flanking regions of *Histoplasma capsulatum* isolated from bats captured in three Latin-American countries. *Fungal Biol.* **2012**, *116*, 308–317. [[CrossRef](#)]
10. Vincent, R.D.; Goewert, R.; Goldman, W.E.; Kobayashi, G.S.; Lambowitz, A.M.; Medoff, G. Classification of *Histoplasma capsulatum* isolates by restriction fragment polymorphisms. *J. Bacteriol.* **1986**, *165*, 813–818. [[CrossRef](#)]
11. Spitzer, E.D.; Lasker, B.A.; Travis, S.J.; Kobayashi, G.S.; Medoff, G. Use of mitochondrial and ribosomal DNA polymorphisms to classify clinical and soil isolates of *Histoplasma capsulatum*. *Infect. Immun.* **1989**, *57*, 1409–1412. [[CrossRef](#)] [[PubMed](#)]
12. Spitzer, E.D.; Keath, E.J.; Travis, S.J.; Painter, A.A.; Kobayashi, G.S.; Medoff, G. Temperature-sensitive variants of *Histoplasma capsulatum* isolated from patients with acquired immunodeficiency syndrome. *J. Infect. Dis.* **1990**, *162*, 258–261. [[CrossRef](#)]
13. Keath, E.J.; Kobayashi, G.S.; Medoff, G. Typing of *Histoplasma capsulatum* by restriction fragment length polymorphisms in a nuclear gene. *J. Clin. Microbiol.* **1992**, *30*, 2104–2107. [[CrossRef](#)]
14. Poonwan, N.; Imai, T.; Na, M.; Yazawa, K.; Mikami, Y.; Ando, A.; Nagata, Y. Genetic analysis of *Histoplasma capsulatum* strains isolated from clinical specimens in Thailand by a PCR-based random amplified polymorphic DNA method. *J. Clin. Microbiol.* **1998**, *36*, 3073–3076. [[CrossRef](#)] [[PubMed](#)]
15. Reyes-Montes, M.R.; Bobadilla-Del Valle, M.; Martínez-Rivera, M.A.; Rodríguez-Arellanes, G.; Maravilla, E.; Sifuentes-Osornio, J.; Taylor, M.L. Relatedness analyses of *Histoplasma capsulatum* isolates from Mexican patients with AIDS-associated histoplasmosis by using histoplasmin electrophoretic profiles and randomly amplified polymorphic DNA patterns. *J. Clin. Microbiol.* **1999**, *37*, 1404–1408. [[CrossRef](#)]
16. Muniz, M. de M.; Pizzini, C.V.; Peralta, J.M.; Reiss, E.; Zancopé-Oliveira, R.M. Genetic diversity of *Histoplasma capsulatum* strains isolated from soil, animals, and clinical specimens in Rio de Janeiro State, Brazil, by a PCR-based random amplified polymorphic DNA assay. *J. Clin. Microbiol.* **2001**, *39*, 4487–4494. [[CrossRef](#)]
17. Kasuga, T.; Taylor, J.W.; White, T.J. Phylogenetic relationships of varieties and geographical groups of the human pathogenic fungus *Histoplasma capsulatum* Darling. *J. Clin. Microbiol.* **1999**, *37*, 653–663. [[CrossRef](#)]
18. Jiang, B.; Bartlett, M.; Allen, S.D.; Smith, J.W.; Wheat, L.J.; Connolly, P.A.; Lee, C.H. Typing of *Histoplasma capsulatum* isolates based on nucleotide sequence variation in the Internal Transcribed Spacer regions of rRNA genes. *J. Clin. Microbiol.* **2000**, *38*, 241–245. [[CrossRef](#)] [[PubMed](#)]
19. Carter, D.A.; Taylor, J.W.; Dechairo, B.; Burt, A.; Koenig, G.L.; White, T.J. Amplified single-nucleotide polymorphisms and a (GA)_n microsatellite marker reveal genetic differentiation between populations of *Histoplasma capsulatum* from the Americas. *Fungal Genet. Biol.* **2001**, *34*, 37–48. [[CrossRef](#)]
20. Kasuga, T.; White, T.J.; Koenig, G.; McEwen, J.; Restrepo, A.; Castañeda, E.; Da Silva Lacaz, C.; Heins-Vaccari, E.M.; De Freitas, R.S.; Zancopé-Oliveira, R.M.; et al. Phylogeography of the fungal pathogen *Histoplasma capsulatum*. *Mol. Ecol.* **2003**, *12*, 3383–3401. [[CrossRef](#)]
21. Taylor, M.L.; Chávez-Tapia, C.B.; Rojas-Martínez, A.; Reyes-Montes, M.R.; Bobadilla-Del Valle, M.; Zúñiga, G. Geographical distribution of genetic polymorphism of the pathogen *Histoplasma capsulatum* isolated from infected bats, captured in a central zone of Mexico. *FEMS Immunol. Med. Microbiol.* **2005**, *45*, 451–458. [[CrossRef](#)]

22. De Muniz, M.M.; Morais, P.M.S.; Meyer, W.; Nosanchuk, J.D.; Zancopé-Oliveira, R.M. Comparison of different DNA-based methods for molecular typing of *Histoplasma capsulatum*. *Appl. Environ. Microbiol.* **2010**, *76*, 4438–4447. [CrossRef]
23. Balajee, S.A.; Hurst, S.F.; Chang, L.S.; Miles, M.; Beeler, W.; Hale, C.; Kasuga, T.; Benedict, K.; Chiller, T.; Lindsley, M.D. Multilocus sequence typing of *Histoplasma capsulatum* in formalin-fixed paraffin-embedded tissues from cats living in non-endemic regions reveals a new phylogenetic clade. *Med. Mycol.* **2013**, *51*, 345–351. [CrossRef]
24. Galo, C.; Sanchez, A.L.; Fontecha, G.A. Genetic diversity of *Histoplasma capsulatum* isolates from Honduras. *Sci. J. Microbiol.* **2013**. [CrossRef]
25. Vite-Garín, T.; Estrada-Bárcenas, D.A.; Cifuentes, J.; Taylor, M.L. The importance of molecular analyses for understanding the genetic diversity of *Histoplasma capsulatum*: An overview. *Rev. Iberoam. Micol.* **2014**, *31*, 11–15. [CrossRef]
26. Teixeira, M.M.; Patané, J.S.L.; Taylor, M.L.; Gómez, B.L.; Theodoro, R.C.; de Hoog, S.; Engelthaler, D.M.; Zancopé-Oliveira, R.M.; Felipe, M.S.S.; Barker, B.M. Worldwide phylogenetic distributions and population dynamics of the genus *Histoplasma*. *PLoS Negl. Trop. Dis.* **2016**, *10*, e0004732. [CrossRef]
27. Sepúlveda, V.E.; Márquez, R.; Turissini, D.A.; Goldman, W.E.; Matute, D.R. Genome sequences reveal cryptic speciation in the human pathogen *Histoplasma capsulatum*. *MBio* **2017**, *8*, e01339-17. [CrossRef] [PubMed]
28. Maxwell, C.S.; Sepúlveda, V.E.; Turissini, D.A.; Goldman, W.E.; Matute, D.R. Recent admixture between species of the fungal pathogen *Histoplasma*. *Evol. Lett.* **2018**, *2*, 210–220. [CrossRef] [PubMed]
29. Taylor, J.W.; Jacobson, D.J.; Kroken, S.; Kasuga, T.; Geiser, D.M.; Hibbett, D.S.; Fisher, M.C. Phylogenetic species recognition and species concepts in fungi. *Fungal Genet. Biol.* **2000**, *31*, 21–32. [CrossRef] [PubMed]
30. Tibayrenc, M. Towards a unified evolutionary genetics of microorganisms. *Annu. Rev. Microbiol.* **1996**, *50*, 401–429. [CrossRef] [PubMed]
31. Rodríguez-Arellanes, G.; Pérez-Mejía, A.; Duarte-Escalante, E.; Taylor, M.L. Organización de la colección de cepas de *Histoplasma capsulatum* del Laboratorio de Inmunología de Hongos, Facultad de Medicina, UNAM. *Rev. Inst. Nal. Enf. Resp. Mex.* **1998**, *11*, 243–246.
32. Gannon, W.L.; Sikes, R.S. The Animal Care and Use Committee of the American Society of Mammalogists: Guidelines of the American Society of Mammalogists for the use of wild mammals in research. *J. Mammal.* **2007**, *88*, 809–823. [CrossRef]
33. Altschul, S.F.; Gish, W.; Miller, W.; Myers, E.W.; Lipman, D.J. Basic local alignment search tool. *J. Mol. Biol.* **1990**, *215*, 403–410. [CrossRef]
34. Farris, J.S.; Källersjö, M.; Kluge, A.G.; Bult, C. Testing significance of incongruence. *Cladistics* **1994**, *10*, 315–319. [CrossRef]
35. Goloboff, P.A.; Farris, J.S.; Nixon, K.C. TNT, a free program for phylogenetic analysis. *Cladistics* **2008**, *24*, 774–786. [CrossRef]
36. Nixon, K.C. The parsimony ratchet, a new method for rapid parsimony analysis. *Cladistics* **1999**, *15*, 407–414. [CrossRef]
37. Silvestro, D.; Michalak, I. RAxMLGUI: A graphical front-end for RAxML. *Org. Divers. Evol.* **2012**, *12*, 335–337. [CrossRef]
38. Ronquist, F.; Teslenko, M.; van der Mark, P.; Ayres, D.L.; Darling, A.; Hohnä, S.; Larget, B.; Liu, L.; Suchard, M.A.; Huelsenbeck, J.P. MrBayes 3.2: Efficient Bayesian phylogenetic inference and model selection across a large model space. *Syst. Biol.* **2012**, *61*, 539–542. [CrossRef] [PubMed]
39. Posada, D. JModelTest: Phylogenetic model averaging. *Mol. Biol. Evol.* **2008**, *25*, 1253–1256. [CrossRef] [PubMed]
40. Heled, J.; Drummond, A.J. Bayesian inference of species trees from multilocus data. *Mol. Biol. Evol.* **2010**, *27*, 570–580. [CrossRef]
41. Drummond, A.J.; Suchard, M.A.; Xie, D.; Rambaut, A. Bayesian phylogenetics with BEAUTi and the BEAST 1.7. *Mol. Biol. Evol.* **2012**, *29*, 1969–1973. [CrossRef]
42. Bandelt, H.J.; Forster, P.; Röhl, A. Median-joining networks for inferring intraspecific phylogenies. *Mol. Biol. Evol.* **1999**, *16*, 37–48. [CrossRef] [PubMed]
43. Librado, P.; Rozas, J. DnaSP v5: A software for comprehensive analysis of DNA polymorphism data. *Bioinformatics* **2009**, *25*, 1451–1452. [CrossRef] [PubMed]
44. Mayden, R.L. A hierarchy of species concepts: The denouement in the saga of the species problem. In *Species. The Units of Biodiversity*; Oraridge, M.F., Dawah, H.A., Wilson, M.R., Eds.; Chapman and Hall: London, UK, 1997; pp. 381–424.
45. Arita, H.T.; Ortega, J. *Tadarida brasiliensis* (L. Geoffroy, 1824). In *Los Mamíferos Silvestres de México*; Ceballos, G., Oliva, G., Eds.; Fondo de Cultura Económica/CONABIO: Ciudad de México, MX, USA, 2005; pp. 335–337.
46. Iñiguez-Dávalos, L.I. *Mormoops megalophylla* (Peters, 1864). In *Los Mamíferos Silvestres de México*; Ceballos, G., Oliva, G., Eds.; Fondo de Cultura Económica/CONABIO: Ciudad de México, MX, USA, 2005; pp. 178–179.
47. Russel, A.L.; Medellin, R.A.; McCracken, G.F. Genetic variation and migration in the Mexican free-tailed bat *Tadarida brasiliensis mexicana*. *Mol. Ecol.* **2005**, *14*, 2207–2222. [CrossRef] [PubMed]
48. Hipp, A.L.; Hall, J.C.; Sytsma, K.J. Congruence versus phylogenetic accuracy: Revisiting the incongruence length difference test. *Syst. Biol.* **2004**, *53*, 81–89. [CrossRef] [PubMed]
49. Sites, J.W., Jr.; Marshall, J.C. Operational criteria for delimiting species. *Annu. Rev. Ecol. Evol. Syst.* **2004**, *35*, 199–227. [CrossRef]

2. OTROS ARTÍCULOS, CAPÍTULO DE LIBRO Y MEMORIAS PUBLICADAS, CONGRESOS

Rodríguez-Arellanes, G., Nascimento de Sousa, C., Medeiros-Muniz, M., Ramírez, J.A., Pizzini, C.V., De Abreu-Almeida, M., Evangelista De Oliveira, M.M., Fusco-Almeida, A.M., **Vite-Garín, T.**, Pitangui, N.S., Estrada-Bárcenas, D.A., González-González, A.E., Mendes-Giannini, M.J.S., Zancopé-Oliveira, R.M. y Taylor, M.L. (2013). Frequency and genetic diversity of the *MAT1* locus of *Histoplasma capsulatum* isolates in Mexico and Brazil. *Eukaryot. Cell* 12(7):1033-1038. <https://doi.org/10.1128/EC.00012-13>.

Vite-Garín, T., Estrada-Bárcenas, D.A., Cifuentes, J. y Taylor, M.L. (2014). The importance of molecular analyses for understanding the genetic diversity of *Histoplasma capsulatum*: an overview. *Rev. Iberoam. Micol.* 31(1):11-15, <https://doi.org/10.1016/j.riam.2013.09.013>.

Estrada-Bárcenas, D.A., **Vite-Garín, T.**, Navarro-Barranco, H., De La Torre Arciniega, R., Pérez-Mejía, A., Rodríguez-Arellanes, G., Ramirez, J.A., Sahaza, J.H., Taylor, M.L. y Toriello, C. (2014). Genetic diversity of *Histoplasma* and *Sporothrix* complexes based on sequences of their ITS1-5.8S-ITS2 regions from the Bold System. *Rev. Iberoam. Micol.* 31(1):90-94. <https://doi.org/10.1016/j.riam.2013.10.003>.

Damasceno, L.S., **Vite-Garín, T.**, Ramírez, J.A., Rodríguez-Arellanes, G., Abreu De Almeida, M., Muniz, Mdm., Lima De Mesquita, J.R., Silva Leitão T.M.J., Taylor, M.L. y Zancopé-Oliveira, R.M. (2018). Mixed infection by *Histoplasma capsulatum* isolates with different mating types in Brazilian AIDS-patients. *Rev. Inst. Med. Trop. São Paulo* 61:e8. <https://doi.org/10.1590/S1678-9946201961008>

Carreto-Binaggi, L.E., Morales-Villarreal, F.R., García-De La Torre, G., **Vite-Garín, T.**, Ramirez, J.A., Aliouat, El-M., Martínez-Orozco, J.A. y Taylor, M.L. (2019). *Histoplasma capsulatum* and *Pneumocystis jirovecii* coinfection in hospitalized HIV and non-HIV patients from a tertiary care hospital in Mexico. *Inter. J. Infect. Dis.* 85:1-24, <https://doi.org/10.1016/j.ijid.2019.06.010>.

Damasceno, L.S., Teixeira, M.D.M., Barker, B.M., Almeida, M.A., Muniz, Mdm., Pizzini, C.V., Lima Mesquita, J.R., Rodríguez-Arellanes, G., Ramírez, J.A., **Vite-Garín, T.**, Silva Leitão, T.M.J., Taylor, M.L., Almeida-Paes, R. y Zancopé-Oliveira, R.M. (2019). Novel clinical and dual infection by *Histoplasma capsulatum* genotypes in HIV patients from northeastern, Brazil. *Sci. Rep.* 9:11789, <https://doi.org/10.1038/s41598-019-48111-6>.

Toriello, C., De La Torre, R., Estrada-Bárcenas, D.A., Ramírez, J.A., Rodríguez-Arellanes, G., **Vite-Garín, T.M.**, Navarro-Barranco, H., Pérez-Mejía, A., Reyes-Montes, M.R. y Taylor, M.L. (2012). Genetic diversity of *Histoplasma* and *Sporothrix* species complexes using the internal transcribed spacer (ITS) region. Abstracts of the 18th Congress of the International Society for Human and Animal Mycology, Berlin, Germany. June 11-15, 2012. *Mycoses* 55 (Suppl. 4): 239 (P459).

Sahaza, J.H., Estrada-Bárcenas, D.A., **Vite-Garín, T.M.**, Ramírez, J.A., Rodríguez-Arellanes, G.; González-González, A.E. y Taylor, M.L. (2012). Multilocus analyses of *Histoplasma capsulatum* isolated of cave-dwelling bats from Mexico reveals a new probable genetic population of this fungal pathogen. Abstracts of the 18th Congress of the International Society for Human and Animal Mycology, Berlin, Germany. June 11-15, 2012. *Mycoses* 55 (Suppl. 4): 239 (P460).

Taylor, M.L., Rodríguez-Arellanes, G., Ramírez, J.A., González-González, A.E., Sahaza, J.H., **Vite-Garín, T.** y Estrada-Bárcenas, D.A. (2012). Capítulo 31. Características relevantes de *Histoplasma capsulatum* y de la epidemiología molecular de la histoplasmosis. En: Méndez-Tovar, L.J.; López-Martínez, R. y Hernández-Hernández, F. (eds.). Actualidades en Micología Médica. Editoriales: Sefirot, S.A. de C.V. 1^a ed. (ISBN SEFIROT: 9786077728337); UNAM 6^a ed. (ISBN UNAM: 9786070232794), México, D.F. 2012, pg. 144-149

Frequency and Genetic Diversity of the *MAT1* Locus of *Histoplasma capsulatum* Isolates in Mexico and Brazil

Gabriela Rodríguez-Arellanes,^a Carolina Nascimento de Sousa,^b Mauro de Medeiros-Muniz,^b José A. Ramírez,^a Cláudia V. Pizzini,^b Marcos de Abreu-Almeida,^b Manoel M. Evangelista de Oliveira,^b Ana-Marisa Fusco-Almeida,^c Tania Vite-Garín,^a Nayla S. Pitanguí,^c Daniel A. Estrada-Bárcenas,^d Antonio E. González-González,^a María José Soares Mendes-Giannini,^c Rosely M. Zancopé-Oliveira,^b María-Lucía Taylor^a

Departamento de Microbiología-Parasitología, Facultad de Medicina, Universidad Nacional Autónoma de México (UNAM), México DF, Mexico^a; Instituto de Pesquisa Clínica Evandro Chagas, Fundação Oswaldo Cruz, Rio de Janeiro, Brazil^b; Faculdade de Ciências Farmacêuticas, Universidade Estadual Paulista, Araraquara, São Paulo, Brazil^c; Colección Nacional de Cultivos Micrbianos, Centro de Investigación y de Estudios Avanzados, Instituto Politécnico Nacional, México DF, Mexico^d

The *MAT1-1* and *MAT1-2* idiomorphs associated with the *MAT1* locus of *Histoplasma capsulatum* were identified by PCR. A total of 28 fungal isolates, 6 isolates from human clinical samples and 22 isolates from environmental (infected bat and contaminated soil) samples, were studied. Among the 14 isolates from Mexico, 71.4% (95% confidence interval [95% CI], 48.3% to 94.5%) were of the *MAT1-2* genotype, whereas 100% of the isolates from Brazil were of the *MAT1-1* genotype. Each *MAT1* idiomorphic region was sequenced and aligned, using the sequences of the G-217B (+ mating type) and G-186AR (- mating type) strains as references. BLASTn analyses of the *MAT1-1* and *MAT1-2* sequences studied correlated with their respective + and - mating type genotypes. Trees were generated by the maximum likelihood (ML) method to search for similarity among isolates of each *MAT1* idiomorph. All *MAT1-1* isolates originated from Brazilian bats formed a well-defined group; three isolates from Mexico, the G-217B strain, and a subgroup encompassing all soil-derived isolates and two clinical isolates from Brazil formed a second group; last, one isolate (EH-696P) from a migratory bat captured in Mexico formed a third group of the *MAT1-1* genotype. The *MAT1-2* idiomorph formed two groups, one of which included two *H. capsulatum* isolates from infected bats that were closely related to the G-186AR strain. The other group was formed by two human isolates and six isolates from infected bats. Concatenated ML trees, with internal transcribed spacer 1 (ITS1) -5.8S-ITS2 and *MAT1-1* or *MAT1-2* sequences, support the relatedness of *MAT1-1* or *MAT1-2* isolates. *H. capsulatum* mating types were associated with the geographical origin of the isolates, and all isolates from Brazil correlated with their environmental sources.

Histoplasma capsulatum is a heterothallic ascomycete that has an anamorphic or asexual stage with two types of sexual compatibility, + and -, represented at the mating locus (*MAT1*) by the idiomorphic regions *MAT1-1* and *MAT1-2*, respectively. The teleomorphic (sexual) stage that results from + and - mating was first described as *Emmonsiella capsulata* by Kwon-Chung (1–4). Nowadays it is known as *Ajellomyces capsulatus*, which temporarily exhibits the dikaryotic and diploid phases that form haploid ascospores after two meiotic reductions. Thus, the species *H. capsulatum* and *A. capsulatus* constitute the same holomorph organism. The classical studies of sexual compatibility in *H. capsulatum* were performed by mating fungal specimens in culture plates. However, this procedure is difficult because *H. capsulatum* isolates rapidly lose the ability to mate *in vitro* (5); therefore, molecular methods were developed to identify the mating type in this microorganism (6–8).

To date, there have been a few relevant studies in the United States about the use of genetic tools to determine sexual compatibility in *H. capsulatum*, in which the - mating type predominates (6–8). Recent findings have involved the product of the Velvet A gene (VeA), which belongs to the proteins of the Velvet family, in mating structure formation (cleistothelial) and virulence of *H. capsulatum* (9). *H. capsulatum* isolates exhibit a wide distribution and an important genetic diversity, as has been documented in Latin America (10–16). However, the frequency and genetic diversity of the + and - mating types are not well documented in most countries where *H. capsulatum* is found, and data reported

in the United States are not necessarily representative of other geographical areas.

In the present work, we studied indigenous *H. capsulatum* isolates from Mexico (North America) and Brazil (South America) to determine the frequency and genetic diversity of the sexual compatibility types of *H. capsulatum* in these two distant geographical areas. Most of the isolates studied were obtained from naturally infected bats and contaminated soils, although some isolates from human clinical cases were also analyzed. PCR was used to identify and to perform genetic analyses of the *MAT1-1* and *MAT1-2* idiomorphs. The internal transcribed spacer 1 (ITS1)-5.8S-ITS2 region of the *H. capsulatum* isolates of each *MAT1* idiomorph was used for concatenated phylogenetic analyses of both genomic regions to increase the genetic relatedness of *H. capsulatum* isolates from different mating types. Therefore, our contribution is original, mainly for its frequency data and because it is the first one to use the *MAT1* locus as a geographical marker for *H. capsulatum*.

Received 17 January 2013 Accepted 17 May 2013

Published ahead of print 24 May 2013

Address correspondence to María-Lucía Taylor, emello@unam.mx.

Copyright © 2013, American Society for Microbiology. All Rights Reserved.

doi:10.1128/EC.00012-13

TABLE 1 General data and sexual compatibility of the *H. capsulatum* isolates studied

Isolate	Associated clinical form ^a	Source ^b	Geographical origin ^c	Mating type ^d
EH-46	D	Human (liver)	GR-Mexico	—
EH-53	D	Human (blood)	HG-Mexico	—
EH-317	D/HIV+	Human (blood)	MS-Mexico	+
EH-315	NA	<i>Mormoops megalophylla</i> (gut)	GR-Mexico	+
EH-373	NA	<i>Artibeus hirsutus</i> (lung)	MS-Mexico	—
EH-374	NA	<i>Artibeus hirsutus</i> (spleen)	MS-Mexico	—
EH-376	NA	<i>Artibeus hirsutus</i> (lung)	MS-Mexico	—
EH-378	NA	<i>Artibeus hirsutus</i> (lung)	MS-Mexico	—
EH-391	NA	<i>Leptonycteris nivalis</i> (liver)	MS-Mexico	—
EH-405	NA	<i>Leptonycteris nivalis</i> (lung)	PL-Mexico	—
EH-449B	NA	<i>Leptonycteris nivalis</i> (spleen)	MS-Mexico	—
EH-521	NA	<i>Artibeus hirsutus</i> (lung)	MS-Mexico	+
EH-672H	NA	<i>Tadarida brasiliensis</i> (liver)	HG-Mexico	—
EH-696P	NA	<i>Tadarida brasiliensis</i> (lung)	NL-Mexico	+
18H	D/HIV+	Human (blood)	RJ-Brazil	+
37307	D/HIV+	Human (bone marrow)	RJ-Brazil	+
247BL	ND	Human (ND)	MS-Brazil	+
M396/08	NA	<i>Molossus molossus</i> (NR)	SP-Brazil	+
M1084/08	NA	<i>Molossus molossus</i> (NR)	SP-Brazil	+
M487/08	NA	<i>Molossus molossus</i> (NR)	SP-Brazil	+
M975/08	NA	<i>Molossus molossus</i> (NR)	SP-Brazil	+
AC05	NA	Soil	RJ-Brazil	+
TI01	NA	Soil	RJ-Brazil	+
IGS19	NA	Soil	RJ-Brazil	+
RPS51	NA	Soil	RJ-Brazil	+
C02	NA	Soil	RJ-Brazil	+
C04	NA	Soil	RJ-Brazil	+
Igs4/5	NA	Soil	RJ-Brazil	+

^a Abbreviations: D, Disseminated histoplasmosis; HIV+, human immunodeficiency virus positive; NA, not applicable; ND, not determined.

^b ND, not determined; NR, not registered.

^c The state and country are shown. The country is shown after the hyphen, and the state is shown before the hyphen as follows: in Mexico, GR, Guerrero; HG, Hidalgo; MS-Mexico, Morelos, Mexico; PL, Puebla; NL, Nuevo León; in Brazil, RJ, Rio de Janeiro; MS-Brazil, Mato Grosso do Sul, Brazil; SP, São Paulo.

^d The + mating type has the *MATI-1* idiomorphic region, and the — mating type has the *MATI-2* idiomorphic region.

MATERIALS AND METHODS

***Histoplasma capsulatum*.** We studied 28 *Histoplasma capsulatum* isolates (14 from Mexico and 14 from Brazil) obtained from different infectious sources (Table 1). The isolates were maintained in the yeast phase by culture at 37°C in brain heart infusion broth (Bioxon; Becton, Dickinson, Mexico City, Mexico) supplemented with 0.1% l-cysteine and 1% glucose.

Identification of sexual compatibility types. We followed the protocols for yeast DNA extraction and the processing of PCR products of Bubnick and Smulian (6) with minor modifications. We used two sets of primers designed for the *MATI* locus: (i) for the *MATI-1* sequence, *MATI-1S* (5'-CGTGGTTAGTTACGGAGCA-3') and *MATI-1AS* (5'-TGAGGATCGAGTGTGGGA-3'), which generated an amplicon of 440 bp; and (ii) for the *MATI-2* sequence, *MATI-2S* (5'-ACACAGTAG CCCAACCTCTC-3') and *MATI-2AS* (5'-TCGACAATCCCATCCAAT ACCG-3'), which generated an amplicon of 528 bp. The PCR was performed in a 25-μl reaction mixture, containing 200 μM each deoxyribonucleoside triphosphate (dNTP) (Applied Biosystems Inc., Foster City, CA, USA), 1.5 mM MgCl₂, 50 ng/μl of each primer, 2.5 U *Taq* DNA polymerase (New England BioLabs Inc., MA, USA), 1× *Taq* commercial buffer, and 75 ng/μl of each DNA sample.

PCR assays were performed in a Thermal iCycler (Bio-Rad Laboratories Inc., Hercules, CA, USA) programmed as follows: (i) 3 min at 95°C; (ii) 35 cycles, consisting of 30 s at 95°C, 30 s at 58°C, and 1 min 30 s at 72°C; and (iii) 10 min at 72°C. The PCR products were resolved by 1.5% agarose

TABLE 2 Database accession numbers of *H. capsulatum* *MATI* sequences analyzed

Isolate	GenBank accession no.
<i>MATI-1</i> isolates	
EH-696P	KC282441
EH-315	KC282442
EH-317	KC282443
EH-521	KC282444
37307	KC282445
18H	KC282446
RPS51	KC282447
IGS19	KC282448
AC05	KC282449
Igs4/5	KC282450
TI01	KC282451
C02	KC282452
C04	KC282453
247BL	KC282454
M396/08	KC282455
M975/08	KC282456
M487/08	KC282457
M1084/08	KC282458
<i>MATI-2</i> isolates	
EH-46	KC282431
EH-53	KC282432
EH-373	KC282433
EH-374	KC282434
EH-376	KC282435
EH-378	KC282436
EH-672H	KC282437
EH-391	KC282438
EH-449B	KC282439
EH-405	KC282440

gel electrophoresis under the same conditions described by Bubnick and Smulian (6). The 100-bp DNA ladder was used as a molecular marker.

ITS1-5.8S-ITS2 PCR. The PCR assay was performed by the method of Muniz et al. (13), using the following primers: ITS4 (5'-TCCTCCGCTT ATTGATATGC-3') and ITS5 (5'-GGAAGTAAAGTCGTAACAAGG-3'), which generated an amplicon of 607 bp.

Sequencing. The resolved PCR products were purified using the Montage PCR centrifugal filter device kit (Millipore Corporation, Bedford, MA, USA). The purified products were sent to the Molecular Biology Unit of the Cellular Physiology Institute, Universidad Nacional Autónoma de México (UNAM)-Mexico, for sequencing in an ABI automated apparatus (Applied Biosystems). Sequencing was performed for both DNA strands. The generated consensus *MATI-1* and *MATI-2* or ITS1-5.8S-ITS2 sequences for each isolate are deposited in GenBank or in the Fungi Barcode of Life Database (Bold System) and their available accession numbers are shown in Tables 2 and 3.

Genetic analyses. Sequences were aligned with Clustal-W in MEGA version 5.0 (MEGA-5) (<http://www.megasoftware.net>) and edited manually.

The sequences of the *MATI-1* and *MATI-2*-idiomorphs from all the *H. capsulatum* isolates studied were compared by searching the GenBank database for homologous nucleotide sequences with the BLASTn algorithm. The sequence of the G-217B strain from Louisiana-United States, ATCC 22636 (GenBank accession number EF433757), was used as a reference for the *MATI-1* idiomorphic region. The sequence of the G-186AR strain from Panama, ATCC 22635 (GenBank accession number EF433756), was used as a reference for the *MATI-2* idiomorphic region.

The aligned sequences were submitted to evolutionary analyses to assume the similarity or divergence among isolates of each mating type, using the maximum likelihood (ML) method. Concatenated ML trees, with ITS1-5.8S-ITS2 and *MATI-1* or *MATI-2* sequences, were processed to provide more-robust phylogenetic data. Unrooted ML trees were constructed in MEGA-5, based on the Hasegawa-Kishino-Yano (HKY) model (17) for *MATI* idiomorphs and Tamura-Nei (TrN) model for con-

TABLE 3 Database accession numbers of *H. capsulatum* ITS1-5.8S-ITS2 sequences analyzed

Isolate	Accession no. ^a
Mexican isolates	
EH-46	HIST019-13
EH-53	HIST001-13
EH-315	HIST002-13
EH-317	HIST003-13
EH-373	HIST004-13
EH-374	HIST020-13
EH-376	HIST021-13
EH-378	HIST022-13
EH-391	HIST006-13
EH-449B	HIST025-13
EH-521	HIST026-13
EH-672H	HIST029-13
EH-696P	HIST018-13
Brazilian isolates	
IgS4/5	GU320945.1
T101	GU320964.1
CO2	KF114466
CO4	KF114465
37307	KF114464
247BL	KF114463
18H	KF114471
M396/08	KF114467
RPS51	GU320962.1
M975/08	KF114469
IGS19	GU320944.1
M487/08	KF114468
AC05	GU320980.1
M1084/08	KF114470

^aThe Mexican isolates were deposited in the Fungi Barcode of Life Database (Bold System), and the Brazilian isolates were deposited in GenBank.

catenated analyses (18). Gaps and missing data were eliminated. A bootstrapping algorithm was implemented on the data set for 1,000 replicates. The highest bootstrap values were registered in each node of each ML tree.

Statistics. The *MAT1-1* and *MAT1-2* idiomorph frequencies were estimated in relation to each mating genotype, taking into account all *H. capsulatum* isolates from Mexico or Brazil studied. In regard to frequency data, the 95% confidence interval (95% CI) was calculated by normal distribution.

RESULTS AND DISCUSSION

Previous studies of the clinical and environmental *H. capsulatum* strains in the United States using conventional mating tests with the fungal mycelial phase reported a higher frequency of the – mating type in clinical strains than in strains isolated from soil samples (5, 19). However, the predominance of the – genotype in clinical strains in the United States, even if supported by a large number of *H. capsulatum* samples from different sources as indicated by Kwon-Chung et al. (5, 19), is not necessarily true in other geographical areas. Although the above-published data have emphasized interesting findings about the disequilibrium of the – and + mating types in human clinical isolates associated with the clinical form of the disease (5, 6, 19), these findings may not apply to clinical isolates from other geographical areas, since *H. capsulatum* isolates exhibit a wide distribution and a significant genetic diversity as has been documented in Latin America (11). On the basis of our present results, it was impossible to infer a disequilibrium of – and + mating types due to the small number of human clinical isolates studied, and in regard to the environmental isolates, we did not find any evidence of disequilibrium.

TABLE 4 Variable sites within the *MAT1-1* idiomorph sequences of *H. capsulatum*

Variable site in the <i>MAT1-1</i> idiomorph sequence
Noninformative sites common to all <i>MAT1-1</i> isolates
Transitions
Guanine to adenine at nt 807, 813, and 822
Cytosine to thymine at nt 856
Informative sites for nine isolates from RJ, Brazil ^a
Transitions
Cytosine to thymine at nt 782 and 1127
Thymine to cytosine at nt 865
Guanine to adenine at nt 1023
Informative sites for five isolates (four from SP, Brazil, and one from MS, Brazil) ^a
Transition
Guanine to adenine at nt 1000

^aRJ, Rio de Janeiro; SP, São Paulo; MS, Mato Grosso do Sul.

Currently, DNA-based mating studies have been used to evaluate the distribution of the sexual compatibility types of *Ophiostoma quercus* in different geographical areas (20). According to this antecedent, in the present paper, by PCR of the *MAT1* locus, we determined the mating types of 6 autochthonous clinical isolates and 22 native environmental isolates (infected bats and contaminated soil) of *H. capsulatum* from two distant regions within the Americas (Mexico and Brazil) (Table 1). The *MAT1-2* genotype was predominant in Mexico, representing 71.4% (95% CI, 48.3 to 94.5%) of the isolates, whereas 100% of the isolates originating in Brazil were of the *MAT1-1* genotype.

Hence, the frequencies of *H. capsulatum* mating types were mainly associated with the geographical origin of the isolates and most likely correlate with their environmental sources. Given that the – mating type is more widely distributed in the *H. capsulatum* isolates from the United States and Mexico (North America) and the + mating type is more frequent in Brazil (South America), as revealed by the present results, we suggest that the different mating types of *H. capsulatum* are distinctively spread across the American continent. In addition, the presence of two sexual compatibility types in the same geographical region, albeit unequally distributed, suggest that genetic dispersion of the *MAT1* locus in the environment could be associated with natural reservoirs of *H. capsulatum*.

For the *MAT1-1* idiomorph, 18 sequences from nucleotide (nt) 778 to 1171 were analyzed, whereas 10 sequences from nt 3038 to 3,584 were analyzed for the *MAT1-2* idiomorph. The sequences obtained for each idiomorph were aligned with the matching sequences of the *H. capsulatum* reference strains obtained from GenBank, G-217B (*MAT1-1*) or G-186AR (*MAT1-2*).

Based on the known sequence of reference strain G-217B, the sequences of the *MAT1-1* idiomorph region (14 from Brazilian *H. capsulatum* isolates and four from Mexican *H. capsulatum* isolates) were aligned by using MEGA-5, showing four noninformative sites common to all isolates (Table 4). In the *MAT1-1* genotype, four informative sites stand out, these sites were shared by nine isolates (seven isolates from soil samples and two isolates

TABLE 5 Variable sites within the *MATI-2* idiomorph sequences of *H. capsulatum*

Variable site in the <i>MATI-2</i> idiomorph sequence
Noninformative sites common to all <i>MATI-2</i> isolates
Transitions
Cytosine to thymine at nt 3098 and 3248
Adenine to guanine at nt 3125 and 3285
Thymine to cytosine at nt 3200
Transversion
Thymine to adenine at nt 3068
Informative sites for eight isolates from MS, Mexico ^a
Transitions
Thymine to cytosine at nt 3156
Guanine to adenine at nt 3284
Adenine to guanine at nt 3449
Transversions
Thymine to adenine at nt 3130 and 3212
Cytosine to adenine at nt 3163 and 3188

^a MS, Morelos.

from human clinical samples) from Rio de Janeiro, Brazil. In addition, one informative site was shared by four isolates recovered from *Molossus molossus* bats from São Paulo State and one human isolate from Mato Grosso do Sul State, Brazil (Table 4).

Two isolates from Mexico (EH-317 from a clinical case and EH-315 from an infected bat) with the *MATI-1* genotype exhibited the same mutations, a transition (cytosine to thymine at nt 940) and a transversion (guanine to thymine at nt 955). The Mexican *H. capsulatum* isolate EH-521 was the most similar to reference strain G-217B, whereas the *H. capsulatum* isolate EH-696P, from the migratory *Tadarida brasiliensis* bat captured in Mexico, was the most divergent from all *MATI-1* *H. capsulatum* isolates studied (data not shown).

The *MATI-2* sequences of the 10 Mexican isolates were compared to the *MATI-2* sequence of reference strain G-186AR (GenBank) using MEGA-5, showing six noninformative sites common to all isolates (Table 5). In addition, eight isolates from Morelos State, Mexico, shared three transitions and four transversions (Table 5). However, four out of these eight *H. capsulatum* isolates, which were recovered from bats captured in the same cave of Morelos, diverge from this group by the absence of mutations between nt 3510 and 3513 (data not shown).

Two informative sites (both transversions, adenine to thymine at nt 3052 and guanine to thymine at nt 3480) were found only in isolates EH-374 and EH-672H (data not shown).

Alignment analysis showed that isolate EH-696P from Mexico, which had been recovered from a bat captured at the northeastern Mexican border, exhibited the greatest number of point mutations in its *MATI-1* sequence, whereas the EH-374 and EH-672H isolates showed fewer mutations among the *MATI-2* sequences (data not shown).

BLASTn analysis of nucleotide sequences of the *MATI-1* idiomorph region of 18 *H. capsulatum* isolates demonstrated that five of the Brazilian isolates exhibited 99% similarity to the sequence of reference strain G-217B. The fact that these isolates came from a circumscribed geographical region in Brazil, that four of the isolates (M396/08, M487/08, M975/08, and M1084/08) were recovered from *M. molossus* bats from São Paulo and one isolate (247BL) came from a human clinical sample from Mato

Grosso do Sul State, which borders São Paulo State, suggest that an unusual *MATI-1* genotype is prevalent in this particular region. Likewise, nine Brazilian isolates from Rio de Janeiro (seven isolates from soil, isolates AC05, CO2, CO4, IgS4/5, IGS19, RPS51, and TI01, and two isolates from human samples, isolates 18H and 37307) exhibited 98% similarity. Three Mexican isolates (EH-315, EH-317, and EH-521) showed 98% similarity and the Mexican EH-696P isolate from the migratory bat *T. brasiliensis* was detected to have 96% similarity to the G-217B reference strain. The BLASTn algorithm search for similarities among sequences of the *MATI-1* genotype revealed only a very low similarity of 6.8% with the gene sequence of a hypothetical protein of the ascomycete *Pyrenopora teres* f. sp. *teres*, which supports the close relationship of all *MATI-1* *H. capsulatum* isolates studied.

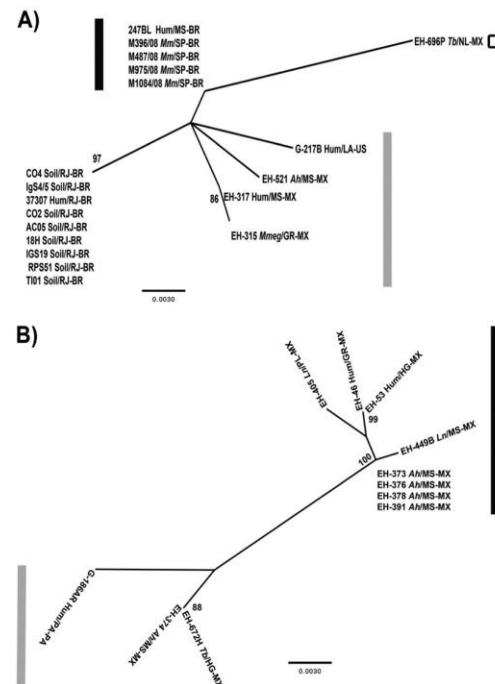


FIG 1 Maximum likelihood trees for the *MATI* locus of the *H. capsulatum* isolates studied. (A) *MATI-1* tree. (B) *MATI-2* tree. The ML analysis was based on the HKY model. The trees were generated by 1,000 replications, as outlined in Materials and Methods. The bootstrap values that were $\geq 70\%$ are shown at the nodes. The G-217B (*MATI-1*) and G-186AR (*MATI-2*) sequences were obtained from the GenBank database and were used as reference strains. The black and gray bars indicate the different isolate groups. The isolates are named by their biological and geographical sources. The source (soil or biological) of the isolate is shown before the slash as follows: Hum, human; Ah, *Arietibes hirsutus*; Ln, *Leptonycteris nivalis*; Mm, *Molossus molossus*; Mmeg, *Mormoops megalophylla*; Tb, *Tadarida brasiliensis*. The geographical source of the isolate is shown after the slash. The state is shown after the slash and before the hyphen as follows: GR, Guerrero; HG, Hidalgo; LA, Louisiana; MS, Morelos (Mexico); NL, Mato Grosso do Sul (Brazil); NL, Nuevo León; PL, Puebla; PA, Panama; RJ, Rio de Janeiro; SP, São Paulo. The country is shown after the hyphen (Brazil [BR], Mexico [MX], United States [US]).

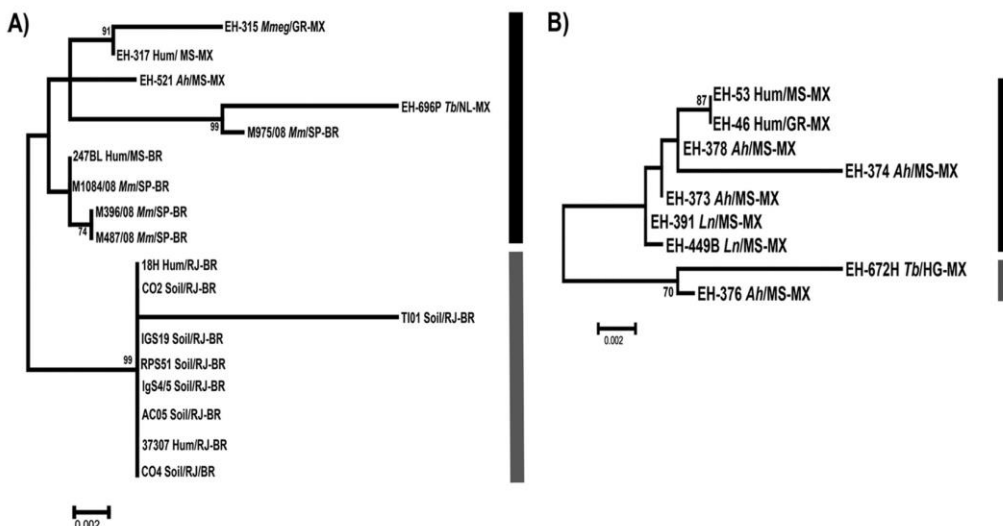


FIG 2 Concatenated maximum likelihood trees for the ITS1-5.8S-ITS2 region and each *MAT1* locus of the *H. capsulatum* isolates studied. (A) ITS1-5.8S-ITS2 and *MAT1*-1 concatenated tree. (B) ITS1-5.8S-ITS2 and *MAT1*-2 concatenated tree. The ML analysis was based on the TrN model. The trees were generated by 1,000 replications, as outlined in Materials and Methods. The bootstrap values that were $\geq 70\%$ are shown at the nodes. The black and dark gray bars indicate the different isolate groups. For abbreviations, see the legend to Fig. 1.

BLASTn analysis of 10 sequences from Mexican *H. capsulatum* isolates of the *MAT1*-2 idiomorph region revealed their high similarity with the sequence of reference strain G-186AR. This reference sequence shared 98% similarity with sequences of two isolates from different bat species (EH-374 and EH-672H). The other eight Mexican isolates from the central zone of the country (EH-46 and EH-53 from human clinical samples; EH-373, EH-376, EH-378, EH-391, EH-405, and EH-449B from different bat species) showed 97% similarity with the sequence of the G-186AR reference strain. The BLASTn algorithm search for similarities among *MAT1*-2 genotype sequences showed 49.1% similarity with the gene sequence of a predicted protein, with a high-mobility-group (HMG) DNA binding domain, of the fungal pathogen *Paracoccidioides brasiliensis* (clone 60855 isolate C4-PS3) and 44.4% similarity with the gene sequence of a protein, with an HMG DNA binding domain, of *Ajellomyces dermatitidis* (strain SLH14081). These data also confirm the relationship among all *MAT1*-2 *H. capsulatum* isolates studied.

The ML analysis of the sequences of the *MAT1*-1 idiomorph demonstrated that our Brazilian isolates from infected bats captured in São Paulo State (Table 1) and the human clinical isolate from Mato Grosso do Sul, Brazil, constitute a well-defined group, representing a probable clonal population of *H. capsulatum*. In addition, seven *H. capsulatum* isolates from contaminated soil and two clinical isolates, all from Rio de Janeiro, Brazil (Table 1), formed a distinct subgroup that shared a probably clonal *MAT1*-1 genotype, which is in agreement with previous data using different molecular markers published by Muniz et al. (12, 13). This subgroup clustered with three *MAT1*-1 isolates from Mexico and the G-217B reference strain. The EH-696P isolate from a migratory

bat captured in Mexico constituted a third group of the *MAT1*-1 genotype and showed the largest genetic distance to all the *H. capsulatum* isolates with the *MAT1*-1 genotype studied (Fig. 1A).

In contrast, ML analysis of the *MAT1*-2 idiomorph, which included most sequences from Mexican isolates, demonstrated that these sequences could be categorized into two major groups. The first group was formed by two isolates from bats (EH-374 and EH-672H) and the G-186AR reference strain (Fig. 1B). The other group was formed by two human clinical isolates and six isolates from infected bats, four of which (EH-373, EH-376, EH-378, and EH-391) belong to a probably clonal population of *H. capsulatum*, as reported by Kasuga et al. (11).

Our results reveal a preferential distribution of *H. capsulatum* isolates with respect to the sequences of the idiomorphic regions of the *MAT1* locus, encompassing two distant geographical areas of the Americas, Mexico and Brazil. Moreover, our findings demonstrated a close relationship between the fungal isolation source and geographical origin within Brazil and also in the central states of Mexico (Guerrero, Morelos, Puebla, and Hidalgo), where most of the Mexican samples were isolated.

Regarding the population structure of the *H. capsulatum* isolates studied, some of the Mexican isolates classified by Kasuga et al. (11) were characterized as possibly recombinant, and others, such as environmental isolates from the Morelos State of Mexico, were characterized as a clonal population (11, 14–16).

Undoubtedly, understanding the *H. capsulatum* mating type distribution in areas of the Americas with a high prevalence of histoplasmosis would contribute to our knowledge of the *H. capsulatum* genetic plasticity generated by sexual recombination

events, which could eventually occur under environmental conditions.

Results of concatenated analyses, using ITS1-5.8S-ITS2 region and each *MAT1* idiomorph, support the relatedness of *MAT1-1* or *MAT1-2* isolates with robust data (Fig. 2A and B, respectively). In addition, ML concatenated analyses generated similar tree topologies as Fig. 1A and B, despite the fact that only two major groups were found. In these analyses, G-217B and G-186AR reference strains were not included because their ITS1-5.8S-ITS2 sequences were not available in different databases. The ITS1-5.8S-ITS2 sequence of the Mexican EH-405 isolate was not obtained due to the loss of this isolate and its DNA.

In conclusion, knowledge regarding the distribution of the *MAT1* locus in *H. capsulatum* and its genetic diversity should contribute to a better understanding of the biology of this fungus and the actual impact of its sexual compatibility genes distributed in natural conditions. We emphasize that in this paper we incorporated two completely new aspects. (i) We studied isolates from two very distant geographical areas to use the *MAT1* locus as a geographical marker. (ii) Most of the *H. capsulatum* isolates studied came from natural sources (wild infected bats), which makes our contribution unique as a result of its geographical frequency data.

ACKNOWLEDGMENTS

This study was funded by the PAPIIT-DGAPA project from UNAM (IN204210), the Bilateral Collaboration Agreement between CONACYT-Mexico (B330/099/11) and CNPq-Brazil (490110/2009-6), the Bilateral Collaboration Agreement between UNAM-Mexico (15090-563-24-V-04) and UNESP-Brazil (000528/04/01/2005), and the FAPERJ E-26/111.532/2010. R.M.Z.-O. is supported in part by CNPq 350338/2000-0. C.N.D.S. is supported by INOVATEC FIOCRUZ/FAPERJ. T.V.-G. thanks CONACYT for scholarship 231985.

M.-L.T. thanks Ingrid Mascher for editorial assistance.

Rosely M. Zancopé-Oliveira and María-Lucía Taylor participated in the design and coordination of the study.

REFERENCES

- Kwon-Chung KJ. 1972. Sexual stage of *Histoplasma capsulatum*. *Science* 175:326.
- Kwon-Chung KJ. 1972. *Emmonsia capsula*: perfect state of *Histoplasma capsulatum*. *Science* 177:368–369.
- Kwon-Chung KJ. 1973. Studies on *Emmonsia capsula*. I. Heterothallicism and development of the ascocarp. *Mycologia* 65:109–121.
- Kwon-Chung KJ, Bennett JE. 1992. Medical mycology. Lea and Febiger, Philadelphia, PA.
- Kwon-Chung KJ, Weeks RJ, Larsh HW. 1974. Studies on *Emmonsia capsula* (*Histoplasma capsulatum*). II. Distribution of the two mating types in 13 endemic states of the United States. *Am. J. Epidemiol.* 99:44–49.
- Bubnick M, Smulian AG. 2007. The *MAT1* locus of *Histoplasma capsulatum* is responsive in a mating type-specific manner. *Eukaryot. Cell* 6:616–621.
- Fraser JA, Stajich JE, Tarcha EJ, Cole GT, Inglis DO, Sil A, Heitman J. 2007. Evolution of the mating type locus: insights gained from the dimorphic primary fungal pathogens *Histoplasma capsulatum*, *Coccidioides immitis*, and *Coccidioides posadasii*. *Eukaryot. Cell* 6:622–629.
- Laskowski MC, Smulian AG. 2010. Insertional mutagenesis enables cleistothelial formation in a non-mating strain of *Histoplasma capsulatum*. *BMC Microbiol.* 10:49–64. doi:10.1186/1471-2180-10-49.
- Laskowski-Peak MC, Calvy AM, Rohrsen J, Smulian AG. 2012. VEA1 is required for cleistothelial formation and virulence in *Histoplasma capsulatum*. *Fungal Genet. Biol.* 49:838–846.
- Kasuga T, Taylor JW, White TJ. 1999. Phylogenetic relationships of varieties and geographical groups of the human pathogenic fungus *Histoplasma capsulatum* Darling. *J. Clin. Microbiol.* 37:653–663.
- Kasuga T, White TJ, Koenig G, McEwen J, Restrepo A, Castañeda E, Da Silva-Lacaz C, Heins-Vaccari EM, De Freitas RS, Zancopé-Oliveira RM, Qin Z, Negroni R, Carter DA, Mikami Y, Tamura M, Taylor ML, Miller GF, Poomwan N, Taylor JW. 2003. Phylogeography of the fungal pathogen *Histoplasma capsulatum*. *Mol. Ecol.* 12:3383–3401.
- Muniz MM, Pizzini CV, Peralta JM, Reis E, Zancopé-Oliveira RM. 2001. Genetic diversity of *Histoplasma capsulatum* strains isolated from soil, animals, and clinical specimens in Rio de Janeiro State, Brazil, by a PCR-based random amplified polymorphic DNA assay. *J. Clin. Microbiol.* 39:4438–4449.
- Muniz MM, Morais e Silva Tavares P, Meyer W, Nosanchuk JD, Zancopé-Oliveira RM. 2010. Comparison of different DNA-based methods for molecular typing of *Histoplasma capsulatum*. *Appl. Environ. Microbiol.* 76:4438–4447.
- Taylor ML, Chávez-Tapia CB, Reyes-Montes MR. 2000. Molecular typing of *Histoplasma capsulatum* isolated from infected bats, captured in Mexico. *Fungal Genet. Biol.* 30:207–212.
- Taylor ML, Chávez-Tapia CB, Rojas-Martínez A, Reyes-Montes MR, Bobadilla del Valle M, Zuhiga G. 2005. Geographical distribution of genetic polymorphism of the pathogen *Histoplasma capsulatum* isolated from infected bats, captured in a central zone of Mexico. *FEMS Immunol. Med. Microbiol.* 45:451–458.
- Taylor ML, Hernández-García L, Estrada-Bárcenas D, Salas-Lizana R, Zancopé-Oliveira RM, García de La Cruz S, Galvão-Dias MA, Curiel-Quesada E, Canteros CE, Bojórquez-Torres G, Bogard-Fuentes CA, Zamora-Tehozol E. 2012. Genetic diversity of *Histoplasma capsulatum* isolated from infected bats randomly captured in Mexico, Brazil and Argentina, using the polymorphism of (GA)_n microsatellite and its flanking regions. *Fungal Biol.* 116:308–317.
- Hasegawa M, Kishino H, Yano T. 1985. Dating of the human-ape splitting by a molecular clock of mitochondrial DNA. *J. Mol. Evol.* 22:160–174.
- Tamura K, Nei M. 1993. Estimation of the number of nucleotide substitutions in the control region of mitochondrial DNA in humans and chimpanzees. *Mol. Biol. Evol.* 10:512–526.
- Kwon-Chung KJ, Bartlett MS, Wheat LJ. 1984. Distribution of the two mating types among *Histoplasma capsulatum* isolates obtained from an urban histoplasmosis outbreak. *Sabouraudia* 22:155–157.
- Wilken PM, Steenkamp ET, Hall TA, De Beer ZW, Wingfield MJ, Wingfield BD. 2012. Both mating types in the heterothallic fungus *Ophiostoma quercus* contain *MAT1-1* and *MAT1-2* genes. *Fungal Biol.* 116:427–437.



ELSEVIER
DOYMA

Revista Iberoamericana de Micología

www.elsevier.es/reviberoammicol



Mycologic Forum

The importance of molecular analyses for understanding the genetic diversity of *Histoplasma capsulatum*: An overview



Tania Vite-Garín^a, Daniel Alfonso Estrada-Bárcenas^b, Joaquín Cifuentes^c, María Lucía Taylor^{a,*}

^a Departamento de Microbiología y Parasitología, Facultad de Medicina, Universidad Nacional Autónoma de México (UNAM), México DF, Mexico

^b Colección Nacional de Cultivos Microbianos, Centro de Investigación y de Estudios Avanzados, Instituto Politécnico Nacional, México DF, Mexico

^c Herbario FCME (Hongos), Facultad de Ciencias, Universidad Nacional Autónoma de México (UNAM), México DF, Mexico

ARTICLE INFO

Article history:

Received 21 August 2013

Accepted 27 September 2013

Available online 16 November 2013

Keywords:

Histoplasma capsulatum

Molecular tools

Multi-locus analyses

Genetic diversity

ABSTRACT

Advances in the classification of the human pathogen *Histoplasma capsulatum* (*H. capsulatum*) (ascomycete) are sustained by the results of several genetic analyses that support the high diversity of this dimorphic fungus. The present mini-review highlights the great genetic plasticity of *H. capsulatum*. Important records with different molecular tools, mainly single- or multi-locus sequence analyses developed with this fungus, are discussed.

Recent phylogenetic data with a multi-locus sequence analysis using 5 polymorphic loci support a new clade and/or phylogenetic species of *H. capsulatum* for the Americas, which was associated with fungal isolates obtained from the migratory bat *Tadarida brasiliensis*.

This manuscript is part of the series of works presented at the "V International Workshop: Molecular genetic approaches to the study of human pathogenic fungi" (Oaxaca, Mexico, 2012).

© 2013 Revista Iberoamericana de Micología. Published by Elsevier España, S.L. All rights reserved.

Importancia de los análisis moleculares en la comprensión de la diversidad genética de *Histoplasma capsulatum*: revisión

RESUMEN

Los resultados de diversos análisis genéticos que respaldan la alta diversidad de este hongo dimorfo confirman los progresos en la clasificación del patógeno humano *Histoplasma capsulatum* (*H. capsulatum*) (un ascomiceto). La presente revisión destaca la importante plasticidad genética de *H. capsulatum*. Se describen los datos importantes con los diferentes instrumentos moleculares, sobre todo, los análisis de las secuencias individuales o multi-loci establecidos con este hongo.

Datos filogenéticos recientes con un análisis multi-loci de secuencias utilizando 5 loci polimorfos respaldan un nuevo clado y/o especie filogenética de *H. capsulatum* del continente americano, asociado a aislamientos fúngicos obtenidos del murciélagos migratorio *Tadarida brasiliensis*.

Este artículo forma parte de una serie de estudios presentados en el «V International Workshop: Molecular genetic approaches to the study of human pathogenic fungi» (Oaxaca, México, 2012).

© 2013 Revista Iberoamericana de Micología. Publicado por Elsevier España, S.L. Todos los derechos reservados.

The scientific history of the pathogenic fungus *Histoplasma capsulatum* began with the histopathological findings, published by Samuel Taylor Darling in 1906, in tissues of a patient from Martinique, who was working on the construction of the Panama Channel. Darling observed intracellular parasites with 1–6 µm in diameter surrounded by a translucent halo.⁵ Due to its resemblance to *Leishmania*, it was described as a protozoan, and was named

"*H. capsulatum*" because of the similarity of its halo with a capsule. Later, in 1912, Henrique da Rocha Lima inferred the mycotic nature of this pathogen, characterizing it as a yeast.⁶ The fungus is a saprobe-geophilic organism that utilizes two nomenclatures depending on its sexual state: *H. capsulatum* (anamorph or asexual state) and *Ajellomyces capsulatus* (teleomorph or sexual state); both constitute the same holomorph organism, which is the causative agent of histoplasmosis, a systemic mycosis with primary respiratory compromise.

Before the description of the sexual state of *H. capsulatum* by Kwon-Chung,^{18,19} this pathogen was classified into the

* Corresponding author.

E-mail addresses: emello@unam.mx, luciataylor@yahoo.com.mx (M.L. Taylor).

Division Deuteromycota, Order Moniliales, and Family Moniliaceae, based on the morphological criteria proposed in 1899 by Saccardo.²⁴ Currently, *H. capsulatum* is classified into the Kingdom Fungi, Subkingdom Dikarya, Phylum Ascomycota, Class Eurotiomycetes, Order Onygenales, and Family Onygenaceae and/or Ajellomycetaceae,^{10–12} according to the analyses of six loci: 18S, 5.8S and 28S of the rRNA genes; *EF1α* (Elongation factor-1α); *RPB1* and *RPB2* (RNA polymerase II subunits 1 and 2).

In the environment, this organism grows preferentially in bat and bird guano that contains high concentrations of nitrogen and phosphorus in addition to other micronutrients. These conditions, together with optimal air and soil temperatures (18–28 °C), humidity (>60%), and darkness (fosters sporulation), characterize the ideal ecological niche of *H. capsulatum*, which favors the development of its multicellular infective mycelial phase (M-phase).^{27,29,34–36}

Classification of *Histoplasma capsulatum*

The biological species *H. capsulatum* comprised three taxonomic varieties: *H. capsulatum* var. *capsulatum* Darling, 1906; *H. capsulatum* var. *duboisii* (Vanbreuseghem, 1957) – Ciferrí, 1960; and *H. capsulatum* var. *farcininosum* (Rivolta, 1873) – Weeks, Padhye, et Ajello, 1985. These varieties were identified by their micromorphologies, geographic distribution, host-association, and clinical forms of the disease. Currently, with the advent of molecular techniques to classify fungal species, these taxonomic varieties have been included in a molecular taxonomy based on the phylogenetic species concept.¹⁵

Taylor et al.³³ indicated that the concepts and/or criteria of species recognition often used in mycology are the biological and morphological ones, and most of the described species have been identified with phenotypic characters. However, some pathogenic fungi show few informative characters thereby leading to skewed, controversial, and erroneous classifications.^{8,9} To overcome these inconveniences, most authors have promoted genetic and molecular statements for genotypic and phylogenetic classifications of pathogenic fungi.

Genotyping of *Histoplasma capsulatum*

H. capsulatum isolates have been grouped based on their genotype patterns using different molecular assays (Table 1). First, Vincent et al.³⁷ grouped clinical strains in three classes according to their Restriction Fragment Length Polymorphism (RFLP) profiles and hybridization with mtDNA and rDNA probes. Class 1 included only the Downs strain of *H. capsulatum* var. *capsulatum* from North America; Class 2 was formed by 14 *H. capsulatum* var. *capsulatum* strains from North America and two *H. capsulatum* var. *duboisii* strains from Africa; finally, Class 3 grouped four *H. capsulatum* var. *capsulatum* strains from Central America and two *H. capsulatum* var. *capsulatum* strains from South America. Spitzer et al.,²⁵ using the same methodology, proposed a new Class 4; one

year later, a Class 5 based on hybridization with a probe of the YPS-3 gene was recorded.²⁶

Keath et al.,¹⁶ in accordance with Spitzer et al.,²⁶ increased the number of strains studied and expanded the fungus genotyping to six classes, including four subclasses within Class 5. It is noteworthy that, from the initial proposal of Vincent et al.³⁷ until the classification of Keath et al.,¹⁶ most of the studied strains came from restricted geographic areas of North America, and very few strains were isolated in Central (Panama) and South America (Colombia).

Later, Poonwan et al.,²² analyzed 13 clinical isolates of *H. capsulatum* from Thailand with Random Amplification of Polymorphic DNA (RAPD-PCR), using three oligonucleotides separately, and found that isolates from Thailand formed two to four homogeneous groups that were clearly separated from the G-217B reference strain from North America.

Jiang et al.¹³ genotyped 24 fungal isolates from the United States of America through the nucleotide sequence analysis of the ITS1-5.8S-ITS2 region of the rDNA, and found 10 different *H. capsulatum* sequence patterns. As a result, they suggested that this method could be useful for reorganizing isolates from other classifications.

Based on a RAPD-PCR assay with the single random primer 1281, Reyes-Montes et al.²³ distinguished four groups (I–IV) and two subgroups (Ia and Ib) of *H. capsulatum* from different origins in Latin America (Mexico, Guatemala, Panama, and Colombia), which were isolated from clinical and environmental sources. In this study, the reference strain G-186B from Panama (Class 3, according to Vincent et al.³⁷) formed a single group. The latter authors suggested that RAPD-PCR profiles with suitable random primers could be used for classifying fungal isolates in accordance with their source and geographic distribution. The RAPD-PCR method with four independent random primers was used by Muniz et al.²¹ to analyze 48 *H. capsulatum* samples from Rio de Janeiro State (Brazil) isolated from different sources (soil, animal, and human clinical samples), which were grouped according to the genetic polymorphism generated for each primer. The RAPD-PCR profiles were able to separate the Brazilian isolates from the North American (United States of America) isolates in accordance with their percentage of similarity. Afterwards, Zancopé-Oliveira et al.,³⁸ using a similar procedure, analyzed 22 Brazilian *H. capsulatum* isolates, mostly from human clinical samples, and identified three clusters: cluster I, with isolates from the Brazilian north-eastern region; a major cluster II, with isolates from the Brazilian south-eastern and south regions; and cluster III (48% similarity), with isolates from Goias State in the central region of Brazil.

Additional molecular studies by Carter et al.,^{2–4} Kasuga et al.,¹⁴ and Taylor et al.³¹ have referred differences in the population structures of *H. capsulatum* (clonal and recombinant). The analyses of *H. capsulatum* genetic populations, mainly with the (GA)_n, (GT)_n and GT(A)_n multiallelic markers (microsatellites), enabled the possibility of distinguishing *H. capsulatum* isolates from the United States of America and Colombia, suggesting the separation of these fungal populations in distinct phylogenetic species.^{2,4} Recently, Taylor et al.,³² based on the sequences of a 240-nt fragment of the (GA)_n microsatellite and its flanking regions, found

Table 1
Relevant molecular classifications of *Histoplasma capsulatum* isolates.

<i>H. capsulatum</i> classifications	No. of isolates	Sources	Assays
3 Classes ³⁷	20	Human and naturally infected animal	RFLP, hybridization with mtDNA and rDNA probes
5 Classes ²⁶	9	Human	RFLP, hybridization with mtDNA, rDNA and YPS-3 probes
6 Classes ¹⁶ and 4 subclasses	76	Human and soil	<i>Idem</i> above
2–4 Groups ²⁴	13	Human	RAPD-PCR using three primers
10 Patterns ¹³	24	Human	RFLP with ITS region
4 Groups ²³	14	Human and soil	RAPD-PCR using the 1281 primer
8 Clades ¹⁵ (7 phylogenetic species)	137	Human, soil and naturally infected animal	MLS analysis with four markers (<i>arf</i> , <i>H-anti</i> , <i>ole1</i> , and <i>tub1</i>)
3–4 Clades ²⁰	51	Human, soil and naturally infected animal	<i>Idem</i> above and ITS region

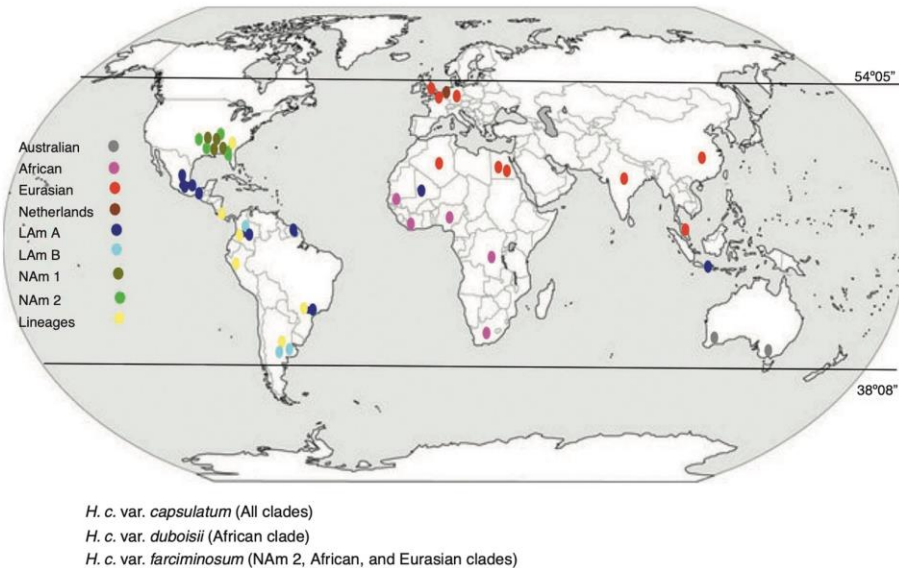


Fig. 1. Geographic distribution of the *H. capsulatum* clades and lineages based on their actual phylogeographic classification. Data were obtained from Kasuga et al.,¹⁵ who proposed this classification based on the partial sequences of four protein-coding genes, using 137 fungal isolates from 25 countries; most were of the taxonomic variety *H. capsulatum* var. *capsulatum*. Some individuals of the taxonomic varieties *H. capsulatum* var. *duboisii* and *H. capsulatum* var. *farciminosum* were also included in different clades.

two major clusters, I and II, according to the genetic diversity of *H. capsulatum* isolated from nine distinct bat species captured in different geographic regions from Mexico and Brazil, emphasizing a sub-cluster grouped in cluster I that carried a unique haplotype of *H. capsulatum* samples that were isolated from the migratory bat *Tadarida brasiliensis*.

Today, advances in fungal classification are supported by robust analyses of the sequences of gene fragments that provide important genetic informative sites to separate clusters of isolates. The statement of a large number of these sites associated with several loci would establish a clear relatedness among fungi and would contribute to a better understanding of the intra- and inter-specific diversity of fungal species. In the last ten years, Multi-Locus Sequence Typing (MLST) has been used to group or classify pathogenic fungi.³⁰ MLST or Multi-Locus Sequence (MLS) analyses utilize sequences of several genes with sufficient polymorphism for differentiating isolates of the same fungal species. It is an excellent molecular tool to characterize genetic diversity in different microorganisms.

Phylogenetic classification of *Histoplasma capsulatum*: Multi-Locus Sequence analyses

In some circumstances, the molecular markers have been useful for identifying species that remained cryptic under morphological and/or biological criteria. Currently, the identification of these species are revealed by phylogenetic, genealogic, or gene concordance species concepts, which group the organisms according to the changes in their nucleic acids.^{6,9,33} Taking into consideration the aforementioned concepts, *H. capsulatum* must be considered a cryptic phylogenetic species complex.³³

Two pioneer MLS studies, which contributed to the phylogenetic classification of *H. capsulatum*, were reported by Kasuga et al.^{14,15} (Table 1). In the last report, using 137 isolates from 25 countries, Kasuga et al.¹⁵ proposed a phylogeographic classification of *H. capsulatum* based on the partial sequences of four protein-coding genes (*arf*, *H-anti*, *ole1*, and *tub1*), which include eight genetic populations (clades) named as: North America class 1 (NAm 1), North America class 2 (NAm 2), Latin America group A (LAm A), Latin America group B (LAm B), Australian, Netherlands, Eurasian, and African. With the exception of the Eurasian clade, seven clades were considered to be phylogenetic species. Consistent with the Kasuga et al.¹⁵ data, Fig. 1 was constructed to represent the *H. capsulatum* clades and lineages around the world.

Following the Kasuga et al.^{14,15} contributions, several authors have used the same gene fragments to advance in the phylogenetic study of *H. capsulatum*. Taylor et al.²⁸ conducted an MLS analysis with 14 isolates of the fungus obtained from naturally infected bats captured in Mexico with different migratory habits (*Artibeus hirsutus*-non-migratory and *Leptonycteris nivalis*, *Leptonycteris curasaoae*, *T. brasiliensis*-migratory), which suggested the existence of a new clade of *H. capsulatum* related to isolates from the infected *T. brasiliensis* bats. Later, Muniz et al.,²⁰ using the same aforementioned protein-coding genes, analyzed 51 isolates of *H. capsulatum* from different sources and Brazilian geographic areas, and revealed three to four clades according to the phylogenetic trees generated; furthermore, the authors suggested different population structures in the isolates from Brazil. Finally, Balajee et al.¹ conducted an MLS analysis with *arf*, *H-anti*, and *tub1* gene fragments, and the ITS region. These authors extracted the DNA of *H. capsulatum* from paraffin-embedded tissue samples from cats diagnosed with histoplasmosis, living in three cities localized in non-endemic areas of the disease in the

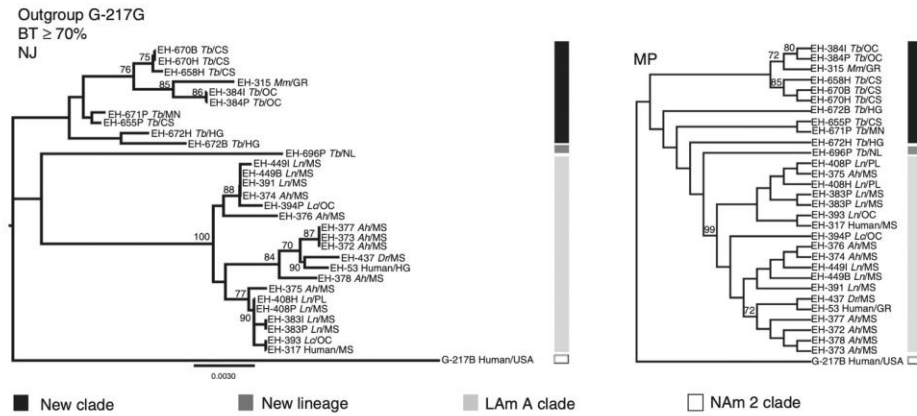


Fig. 2. Concatenated phylogenetic trees of Mexican *H. capsulatum* isolates using an MLS analysis. Trees were constructed with MEGA5 software considering the sequences, from 30 *H. capsulatum* samples, of the polymorphic loci: *arf*, *H-anti*, *ole1*, *tub1*, and the $(GA)_n$ microsatellite. Phylogenetic analyses were conducted as follows: (1) the neighbor-joining (NJ) method using the Kimura two-parameter model¹⁷; and (2) the maximum parsimony (MP) method using the close-neighbor-interchange algorithm.⁷ Data of parsimony were: MPT = 99; LT = 188; CI = 0.584615; RI = 0.881569. Trees were generated with 1000 replicates. Fourteen of the Mexican *H. capsulatum* isolates were previously classified by Kasuga et al.¹⁵ as belonging to the LAm A clade. Abbreviations: Tb (*T. brasiliensis*), Ah (*A. hirsutus*), Ln (*L. nivalis*), Lc (*L. curasaoe*), Mm (*M. megalophylla*), Dr (*Desmodus rotundus*), CS (Chiapas), GR (Guerrero), HG (Hidalgo), Mn (Michoacán), MS (Morelos), NL (Nuevo León), OC (Oaxaca), PL (Puebla), and USA (United States of America).

United States of America. This study included, as reference, 82 sequences of the fungal strains previously reported by Kasuga et al.¹⁵ representing their eight described clades, and the authors suggested that their results demonstrated a new phylogenetic clade associated with all *H. capsulatum* strains causing cat infections.

Based on unpublished results from our laboratory, with 28 *H. capsulatum* isolates obtained from wild bats captured in Mexico and two reference strains from Mexican histoplasmosis patients, it was possible to generate more robust data to classify these fungal samples by using an MLS analysis with various informative sites of highly polymorphic loci [*arf*, *H-anti*, *ole1*, *tub1*, and the $(GA)_n$ microsatellite]. Similarities and genetic distances among their sequences demonstrated that fungal isolates recovered from cave-dwelling bats and the two clinical reference strains from the central states of Mexico (Morelos, Puebla, and Hidalgo) were grouped independently from most *H. capsulatum* isolated from the migratory bat *T. brasiliensis* (captured in the Mexican states of Chiapas, Hidalgo, and Michoacán) and from one isolate from a *Mormoops megalophylla* bat captured in Guerrero (Fig. 2). This finding matches previous data published by Taylor et al.,^{28,32} who had proposed that fungal isolates from *T. brasiliensis* form a new clade because these isolates did not group with any isolate from the Kasuga et al.¹⁵ clades. In addition, a single *H. capsulatum* isolate from a *T. brasiliensis* captured in the Northwest of Mexico (Nuevo León State) forms a new lineage. Thus, the topology of the two concatenated trees that were generated by an MLS analysis using the five aforementioned polymorphic loci were able to discriminate the high genetic diversity of this fungus, thereby contributing to the knowledge of the pathogen (Fig. 2).

Conflict of interest

The authors declare that they have no conflict of interests.

Acknowledgments

This paper constitutes partial fulfillment of the requirements of the Graduate Program in Biological Sciences of the UNAM. TVG

thanks the scholarship No. 324232 provided by the National Council of Science and Technology (CONACyT).

References

- Balajee SA, Hurst SF, Chang LS, Miles M, Beeler E, Hale C, et al. Multilocus sequence typing of *Histoplasma capsulatum* in formalin-fixed paraffin-embedded tissues from cats living in non-endemic regions reveals a new phylogenetic clade. *Mem Mycol*. 2012;50:91–8.
- Carter DA, Burt A, Taylor JW, Koenig GL, Dechairo BM, White TJ. A set of electrophoretic molecular markers for strain typing and population genetic studies of *Histoplasma capsulatum*. *Electrophoresis*. 1997;18:1047–53.
- Carter DA, Burt A, Taylor JW, Koenig GL, White TJ. Clinical isolates of *Histoplasma capsulatum* from Indianapolis, Indiana, have a recombining population structure. *J Clin Microbiol*. 1996;34:2577–84.
- Carter DA, Taylor JW, Dechairo B, Burt A, Koenig GL, White TJ. Amplified single-nucleotide polymorphisms and a $(GA)_n$ microsatellite marker reveal genetic differentiation between populations of *Histoplasma capsulatum* from the Americas. *Fungal Genet Biol*. 2001;34:37–48.
- Darling ST. A protozoan general infection producing pseudotubercles in the lungs and focal necroses in the liver, spleen and lymph nodes. *JAMA*. 1906;46:1283–5.
- Da Rocha-Lima H. Histoplasmosis and epizootic lymphangitis. *Arch Schiffs Tropenhyg*. 1912;16:79–85.
- Eck RV, Dayhoff MO, editors. *Atlas of protein sequence and structure*. Silver Spring: National Biomedical Research Foundation; 1966.
- Fréalle E, Noël C, Viscogliosi E, Camus D, Delcas E, Delhaes L. Manganese superoxide dismutase in pathogenic fungi: an issue with pathophysiological and phylogenetic involvements. *FEMS Immunol Med Microbiol*. 2005;45: 411–22.
- Gazis R, Rehner S, Chaverri P. Species delimitation in fungal endophyte diversity studies and its implications in ecological and biogeographic inferences. *Mol Ecol*. 2011;20:3001–13.
- Hibbett DS, Binder M, Bischoff JF, Blackwell M, Cannon PF, Eriksson OE, et al. A higher-level phylogenetic classification of the fungi. *Mycol Res*. 2007;111:509–47.
- Index Fungorum.org. Centre for Agriculture and Bioscience International (CABI); c2003–04 [update; 2012 referenced 15th January 2013]. Available at: <http://www.indexfungorum.org/Names/Names.asp?RecordID=102749>
- Jones TY, Kauff F, Schöch CL, Matheny PB, Hofstetter V, Cox CJ, et al. Reconstructing the early evolution of fungi using a six-gene phylogeny. *Nature*. 2006;443:818–22.
- Jiang B, Bartlett M, Allen SD, Smith JW, Wheat LJ, Connolly PA, et al. Typing of *Histoplasma capsulatum* isolates based on nucleotide sequence variation in the internal transcribed spacer regions of rRNA genes. *J Clin Microbiol*. 2000;38:241–5.
- Kasuga T, Taylor JW, White TJ. Phylogenetic relationships of varieties and geographical groups of the human pathogenic fungus *Histoplasma capsulatum*. *Darling J Clin Microbiol*. 1999;37:653–63.

15. Kasuga T, White TJ, Koenig G, McEwen J, Restrepo A, Castañeda E, et al. Phylogeography of the fungal pathogen *Histoplasma capsulatum*. *Mol Ecol*. 2003;12:3383–401.
16. Keath EJ, Kobayashi GS, Medoff G. Typing of *Histoplasma capsulatum* by restriction fragment length polymorphisms in a nuclear gene. *J Clin Microbiol*. 1992;30:2104–7.
17. Kimura M. A simple method for estimating evolutionary rates of base substitutions through comparative studies of nucleotide sequences. *J Mol Evol*. 1980;16:111–20.
18. Kwon-Chung KJ. Sexual stage of *Histoplasma capsulatum*. *Science*. 1972;175:326.
19. Kwon-Chung KJ. *Emmonsella capsulata*: perfect state of *Histoplasma capsulatum*. *Science*. 1972;177:368–9.
20. Muniz MM, Morais e Silva Tavares P, Meyer W, Nosanchuk JD, Zancope-Oliveira RM. Comparison of different DNA-based methods for molecular typing of *Histoplasma capsulatum*. *Appl Environ Microbiol*. 2010;76:4438–47.
21. Muniz MM, Pizzini CV, Peralta JM, Reiss E, Zancope-Oliveira RM. Genetic diversity of *Histoplasma capsulatum* strains isolated from soil, animals, and clinical specimens in Rio de Janeiro State, Brazil, by a PCR-based random amplified polymorphic DNA assay. *J Clin Microbiol*. 2001;39:4487–94.
22. Poomwan N, Imai T, Mekha N, Yazawa K, Mikami Y, Ando A, et al. Genetic analysis of *Histoplasma capsulatum* strains isolated from clinical specimens Thailand by a PCR-based random amplified polymorphic DNA method. *J Clin Microbiol*. 1998;36:3073–6.
23. Reves-Montes MR, Bobadilla-Del Valle M, Martínez-Rivera MA, Rodríguez-Arellanes G, Maravilla E, Sifuentes-Osornio J, et al. Relatedness analyses of *Histoplasma capsulatum* isolates from Mexican patients with AIDS-associated histoplasmosis by using histoplasmin electrophoretic profiles and randomly amplified polymorphic DNA patterns. *J Clin Microbiol*. 1999;37:1404–8.
24. Saccardo PA, editor. *Sylloge Fungorum Omnium Hucusque Cognitorum*. Pavia; 1899.
25. Spitzer ED, Keath EJ, Travis SJ, Painter AA, Kobayashi GS, Medoff G. Temperature-sensitive variants of *Histoplasma capsulatum* isolated from patients with acquired immunodeficiency syndrome. *J Infect Dis*. 1990;258–61.
26. Spitzer ED, Lasker BA, Travis SJ, Kobayashi GS, Medoff G. Use of mitochondrial and ribosomal DNA polymorphisms to classify clinical and soil isolates of *Histoplasma capsulatum*. *Infect Immun*. 1989;57:1409–12.
27. Taylor ML, Chávez-Tapia CB, Reyes-Montes MR. Molecular typing of *Histoplasma capsulatum* isolated from infected bats, captured in Mexico. *Fungal Genet Biol*. 2000;30:207–12.
28. Taylor ML, Chávez-Tapia CB, Rojas-Martínez A, Reyes-Montes MR, Bobadilla-Del Valle M, Zúñiga G. Geographical distribution of genetic polymorphism of the pathogen *Histoplasma capsulatum* isolated from infected bats, captured in a central zone of Mexico. *FEMS Immunol Med Microbiol*. 2005;45:451–8.
29. Taylor ML, Chávez-Tapia CB, Vargas-Yáñez R, Rodríguez-Arellanes G, Peña-Sandoval GR, Torriello C, et al. Environmental conditions favoring bat infection with *Histoplasma capsulatum* in Mexican shelters. *Am J Trop Med Hyg*. 1999;61:914–9.
30. Taylor JW, Fisher MC. Fungal multilocus sequence typing—it's not just for bacteria. *Curr Opin Microbiol*. 2003;6:351–6.
31. Taylor JW, Geiser DM, Burt A, Koufopanou V. The evolutionary biology and population genetics underlying fungal strain typing. *Clin Microbiol Rev*. 1999;12:126–46.
32. Taylor ML, Hernández-García L, Estrada-Bárcenas DA, Salas-Lizana R, Zancopé-Oliveira RM, García de la Cruz S, et al. Genetic diversity of microsatellite (GA)_n and their flanking regions of *Histoplasma capsulatum* isolated from bats captured in three Latin-American countries. *Fungal Biol*. 2012;116:308–17.
33. Taylor JW, Jacobson DJ, Kroken S, Kasuga T, Geiser DM, Hibbett DS, et al. Phylogenetic species recognition and species concepts in fungi. *Fungal Genet Biol*. 2000;31:21–32.
34. Taylor ML, Reyes-Montes MR, Chávez-Tapia CB, Curiel-Quesada E, Duarte-Escalante E, Rodríguez-Arellanes G, et al. Ecology and molecular epidemiology findings of *Histoplasma capsulatum*, in Mexico. In: Moján RM, Benedik M, editors. *Research advances in microbiology*. Kerala: Global Research Network; 2000. p. 29–35.
35. Taylor ML, Rodríguez-Arellanes G, Duarte-Escalante E, editors. *Catálogo de Cepas de "Histoplasma capsulatum"*. México DF: Editorial Facultad de Medicina-Universidad Nacional Autónoma de México; 1999.
36. Tewari J, Wheat LJ, Ajello L. Agents of histoplasmosis. In: Ajello L, Hay RJ, editors. *Topley & Wilson's microbiology and microbial infections. Medical mycology*. New York: Arnold and Oxford University Press; 1998. p. 373–407.
37. Vincent RD, Goewert R, Goldman WE, Kobayashi GS, Lambowitz AM, Medoff G. Classification of *Histoplasma capsulatum* isolates by restriction fragment polymorphisms. *J Bacteriol*. 1986;165:813–8.
38. Zancopé-Oliveira RM, Morais e Silva Tavares P, Muniz MM. Genetic diversity of *Histoplasma capsulatum* strains in Brazil. *FEMS Immunol Med Microbiol*. 2005;45:443–9.



Mycologic Forum

Genetic diversity of *Histoplasma* and *Sporothrix* complexes based on sequences of their ITS1-5.8S-ITS2 regions from the BOLD System



Daniel Alfonso Estrada-Bárcenas^a, Tania Vite-Garín^b, Hortensia Navarro-Barranco^c, Raúl de la Torre-Arciniega^b, Amelia Pérez-Mejía^c, Gabriela Rodríguez-Arellanes^b, Jose Antonio Ramirez^b, Jorge Humberto Sahaza^{b,d}, María Lucia Taylor^{b,e}, Conchita Toriello^{c,*e}

^a Colección Nacional de Cultivos Microbianos, Centro de Investigación y de Estudios Avanzados, Instituto Politécnico Nacional, México DF, Mexico

^b Laboratorio de Inmunología de Hongos, Departamento de Microbiología y Parasitología, Facultad de Medicina, UNAM, México DF, Mexico

^c Laboratorio de Micología Básica, Departamento de Microbiología y Parasitología, Facultad de Medicina, UNAM, México DF, Mexico

^d Unidad de Micología Médica y Experimental, Corporación para Investigaciones Biológicas, Medellín, Colombia

ARTICLE INFO

Article history:

Received 30 August 2013

Accepted 9 October 2013

Available online 20 November 2013

Keywords:

Histoplasma capsulatum

Sporothrix schenckii

ITS region

iBOL

ABSTRACT

High sensitivity and specificity of molecular biology techniques have proven usefulness for the detection, identification and typing of different pathogens. The ITS (Internal Transcribed Spacer) regions of the ribosomal DNA are highly conserved non-coding regions, and have been widely used in different studies including the determination of the genetic diversity of human fungal pathogens. This article wants to contribute to the understanding of the intra- and interspecific genetic diversity of isolates of the *Histoplasma capsulatum* and *Sporothrix schenckii* species complexes by an analysis of the available sequences of the ITS regions from different sequence databases. ITS1-5.8S-ITS2 sequences of each fungus, either deposited in GenBank, or from our research groups (registered in the Fungi Barcode of Life Database), were analyzed using the maximum likelihood (ML) method. ML analysis of the ITS sequences discriminated isolates from distant geographic origins and particular wild hosts, depending on the fungal species analyzed.

This manuscript is part of the series of works presented at the "V International Workshop: Molecular genetic approaches to the study of human pathogenic fungi" (Oaxaca, Mexico, 2012).

© 2013 Revista Iberoamericana de Micología. Published by Elsevier España, S.L. All rights reserved.

Diversidad genética de los complejos *Histoplasma* y *Sporothrix* en función de las secuencias de sus regiones ITS1-5.8S-ITS2 del BOLD System

RESUMEN

Las técnicas de biología molecular han proporcionado instrumentos de alta sensibilidad y especificidad, útiles para la detección, identificación y tipificación de diferentes patógenos. Las regiones ITS (Internal Transcribed Spacer) del ADN ribosómico están altamente conservadas y no son codificantes. Estas regiones se han utilizado ampliamente en diferentes tipos de estudios, incluida la determinación de la diversidad genética de hongos patógenos del ser humano. La finalidad de este artículo es contribuir al conocimiento de la diversidad genética intra- e interespecífica de aislamientos de los complejos de *Histoplasma capsulatum* y *Sporothrix schenckii* a través del análisis de las secuencias disponibles de las regiones ITS en distintos bancos de secuencias. Las secuencias de las regiones ITS1-5.8S-ITS2, de cada hongo, depositadas en el GenBank, junto con las obtenidas por nuestros grupos de investigación (depositadas en la Fungal Barcoding of Life Database), se analizaron con el método de máxima probabilidad (ML, por sus

* Corresponding author.

E-mail addresses: toriello@unam.mx, c.toriellonajera@gmail.com (C. Toriello).

^e These authors participated in the design and coordination of the Mexican Thematic Net for Fungi Barcode of Life (MEXBOL) of the Consejo Nacional de Ciencia y Tecnología (CONACYT)-MEXICO and have equally contributed to this review.

siglas en inglés). El análisis ML de las secuencias de las regiones ITS discriminó aislamientos de orígenes geográficos distantes y de huéspedes salvajes particulares, de acuerdo con la especie fúngica analizada. Este artículo forma parte de una serie de estudios presentados en el «VI International Workshop: Molecular genetic approaches to the study of human pathogenic fungi» (Oaxaca, México, 2012).

© 2013 Revista Iberoamericana de Micología. Publicado por Elsevier España, S.L. Todos los derechos reservados.

Reliable identification of pathogenic fungal species is fundamental to epidemiology in terms of biodiversity, geographical variation, and environmental changes. Species identification in fungi is particularly challenging because of their transient nature. Limitations to the studies of diversity in mammalian pathogenic fungi exist due to a lack of taxonomic specialists, and scarce and incomplete data for many taxonomic characters, which has been suggested by Suwannasai et al.¹⁷ and Tantichareon.¹⁹

Pheno- and genotyping of fungal strains have been used as important tools for identifying environmental sources of outbreaks as well as confirming the existence of pathogens in natural habitats. These different typing methods have used both conventional and molecular techniques.

Although phenotyping has continuously been used to study fungi, sensitive and specific genotyping methods are being developed to characterize fungal species, but different criteria must be met to be accepted by specialists. In many cases, genotyping methods compare DNA polymorphisms and classify fungal organisms according to the principles of molecular systematic. For *Histoplasma capsulatum* (etiological agent of the systemic mycosis histoplasmosis) and *Sporothrix schenckii* (etiological agent of the subcutaneous mycosis sporotrichosis) typing and classification, different molecular techniques have been applied, among them, various PCR methods using genomic sequences.^{7,8}

There is a wide array of molecular markers for microorganism identification and genotyping or molecular classification. Among them, the Internal Transcribed Spacer (ITS) regions stand out for the study of closely related taxa, due to genetic diversity associated with the high rate of evolutionary changes characteristic of these regions.¹² ITS consist of two variable non-coding regions (ITS1 and ITS2) inserted between the highly conserved small subunit 18S, the 5.8S, and the large subunit 28S of the rDNA gene cluster.¹²

ITS as a molecular target for fungal identification are supported by several unique characteristics: (i) The complete ITS region has a length between 600 and 800 bp and can be easily amplified, using universal primers that are complementary to rDNA sequences. (ii) The multicopy nature of the repeat regions of the rDNA allows for the amplification of the ITS regions from small, diluted or degraded DNA samples. (iii) Several studies have demonstrated that the ITS regions are highly variable among morphologically distinct fungal species.¹²

The usefulness of ITS markers has been documented in several studies of phylogeny and genotyping of *H. capsulatum*^{1,5,6,11} and *S. schenckii*.^{2–4,22}

The Mexican Barcode of Life project for the *H. capsulatum* and *S. schenckii* species complexes

The Mexican Barcode of Life (MEXBOL) resulted from the work of Mexican investigators as part of the international DNA barcoding (iBOL) project. MEXBOL is now part of a network with funding from the Consejo Nacional de Ciencia y Tecnología (CONACyT) and the Comisión Nacional para el Conocimiento y Uso de la Biodiversidad (CONABIO). The Natural Sciences and Engineering Research Council of Canada (NSERC) developed a Barcode of Life Database (BOLD) based on a specific informatics infrastructure. The cytochrome oxidase subunit 1 (COI), ribulose-bisphosphate

carboxylase (rbcl), maturase K (matK), and ITS regions are among the Barcode sequences used. In addition to the assembly of barcode information and maintenance of these records by the BOLD system, a copy of all sequence and key specimen data is archived at the National Center for Biotechnology Information (NCBI) or its sister genomic repositories, the DNA Data Bank of Japan (DDBJ) and the European Molecular Biology Laboratory (EMBL), when results are ready for public release.¹³

The identification of *H. capsulatum* and *S. schenckii* isolates from different sources and origins by the sequences of the ITS regions started in 2010 as a project for the MEXBOL network for fungi. To date there are 19 ITS1–5.8S–ITS2 sequences of *H. capsulatum* from the Laboratorio de Inmunología de Hongos and 10 sequences of *Sporothrix* spp. from the Laboratorio de Micología Básica, Departamento de Microbiología y Parasitología, Facultad de Medicina, UNAM, deposited in the BOLD System. Sequences were obtained from isolates that were previously pheno- and genetically well identified.^{10,14,15}

Data regarding the natural hosts, sources, and samples of the 19 *H. capsulatum* and 10 *Sporothrix* spp. isolates are shown in Table 1. Fungal specimens are deposited in the Culture Collection of *H. capsulatum* from the Laboratorio de Inmunología de Hongos and the Culture Collection of Fungal Pathogens of the Laboratorio de Micología Básica, from the Departamento de Microbiología y Parasitología, Facultad de Medicina, UNAM. In addition, they are registered in the database of the World Federation for Culture Collection, with code number LIH-UNAM WDCM817 for *H. capsulatum* (http://www.wfcc.info/ccinfo/index.php/collection/by_id/817) and code number BMFM-UNAM WDCM834 for *Sporothrix* spp. (http://www.wfcc.info/ccinfo/index.php/collection/by_id/834).

Analysis of the genetic diversity of *H. capsulatum* and *S. schenckii* species complexes based on ITS sequences from MEXBOL project

Current data from our laboratory teams, using evolutionary and genetic distance analyses by maximum likelihood (ML) of ITS1–5.8S–ITS2 sequences of *H. capsulatum* or *Sporothrix* spp. from the BOLD System and GenBank datasets, produced robust results to aid in understanding the similarities and diversities among isolates either of *H. capsulatum* or *Sporothrix* spp. from different sources and geographic origins.

Sequences were generated by PCR assays with ITS5/ITS4 primers⁹ for *H. capsulatum* and ITS1F/ITS4 primers⁹ for *Sporothrix* spp. Fig. 1 shows the predicted products, 607 bp for *H. capsulatum* and 575 bp for *Sporothrix* spp., amplified by their respective primers. The ML trees generated are shown in Fig. 2.

Concerning *H. capsulatum*, Fig. 2A highlights the sequences of all isolates from different geographic origins and phylogenetic species that clustered together in a major group sustained by 99% of bootstrap values (BT). This finding confirms the high similarity of the isolates analyzed, separates a reference strain of *Ajellomyces dermatitidis* (nearby sister), and underlines the genetic distance from a heterologous pathogenic fungus, *Paracoccidioides brasiliensis*, used as an outgroup in the ML analysis. The ML tree topology of *H. capsulatum* sequences in Fig. 2A clearly confirms that inter-specific diversity among fungal pathogens that cause respiratory diseases

Table 1
Data of isolates of *Histoplasma* and *Sporothrix* complexes analyzed using the ITS1-5.8S-ITS2 region.

Isolate	Host or source sample	Species	Barcode accession number
EH-53	Human/Blood	<i>H. capsulatum</i> LAm A ^a	HIST001-13
EH-315 ^b	Bat/Intestine	<i>H. capsulatum</i> Lineage ^c	HIST002-13
EH-317	Human/Blood	<i>H. capsulatum</i> LAm A ^d	HIST003-13
EH-373 ^b	Bat/Lung	<i>H. capsulatum</i> LAm A ^d	HIST004-13
EH-375 ^b	Bat/Lung	<i>H. capsulatum</i>	HIST005-13
EH-378 ^b	Bat/Lung	<i>H. capsulatum</i>	"-----"
EH-391 ^c	Bat/Liver	<i>H. capsulatum</i> LAm A ^e	HIST006-13
EH-393 ^d	Bat/Spleen	<i>H. capsulatum</i>	HIST007-13
EH-394P ^d	Bat/Spleen	<i>H. capsulatum</i>	HIST008-13
EH-398P ^d	Bat/Lung	<i>H. capsulatum</i>	HIST009-13
EH-449 ^c	Bat/Intestine	<i>H. capsulatum</i>	HIST010-13
EH-449P ^c	Bat/Lung	<i>H. capsulatum</i>	HIST011-13
EH-655P ^e	Bat/Lung	<i>H. capsulatum</i>	HIST012-13
EH-658H ^f	Bat/Liver	<i>H. capsulatum</i>	HIST013-13
EH-670B ^g	Bat/Spleen	<i>H. capsulatum</i>	HIST014-13
EH-670H ^g	Bat/Liver	<i>H. capsulatum</i>	HIST015-13
EH-671P ^g	Bat/Lung	<i>H. capsulatum</i>	HIST016-13
EH-672B ^g	Bat/Spleen	<i>H. capsulatum</i>	HIST017-13
EH-696P ^e	Bat/Lung	<i>H. capsulatum</i>	HIST018-13
EH-143	Human/Cutaneous	<i>S. schenckii</i>	BMFM001-13
EH-194	Environmental/Rose plant	<i>S. schenckii</i>	BMFM002-13
EH-195	Environmental/Coffee soil	<i>S. schenckii</i>	BMFM003-13
EH-197	Human/Cutaneous	<i>S. schenckii</i>	BMFM004-13
EH-230	Human/Cutaneous	<i>S. globosa</i>	BMFM005-13
EH-234	Human/Cutaneous	<i>S. schenckii</i>	BMFM006-13
EH-251	Environmental/Soil	<i>S. schenckii</i>	BMFM007-13
EH-252	Environmental/Soil	<i>S. schenckii</i>	BMFM008-13
EH-253	Environmental/Soil	<i>S. schenckii</i>	BMFM009-13
EH-254	Environmental/Soil	<i>S. schenckii</i>	BMFM010-13

^a Phylogenetic species reported by Kasuga et al.⁷

^b The sequence of this isolate has not yet been deposited in the BOLD System.

^c *Mormoops megalophylla*.

^d *Artibeus hirsutus*.

^e *Leptonycteris nivalis*.

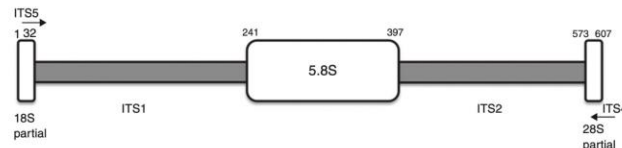
^f *L. curasaoae*.

^g *Tadarida brasiliensis*.

is well sustained using ITS1-5.8S-ITS2 region sequence analyses. Besides, it should be emphasized that ITS could also distinguish intra-specific diversity among *H. capsulatum* isolates, evidenced by the formation of a subgroup sustained by 89% BT, which contains six fungal isolates recovered from a particular wild host (*Tadarida brasiliensis* bats), together with one isolate recovered from an

infected *Mormoops megalophylla* bat. This conclusion is consistent with results for these particular isolates using other molecular markers.^{20,21} In contrast, the ITS1-5.8S-ITS2 region sequence analysis in Fig. 2A could not discriminate cryptic species or clades of the *H. capsulatum* complex (NAm 1, NAm 2, LAm A, LAm B, African, Eurasian, and some lineages) and the taxonomic varieties

Histoplasma capsulatum (EH-658H)



Sporothrix schenckii (EH-234)



Fig. 1. ITS1-5.8S-ITS2 regions amplified from *Histoplasma* and *Sporothrix* samples. The schema depicts the regions amplified by the primers: ITS5 (5'-GGAAGTAAAGTCGTAACAAAGC-3') and ITS4 (5'-TCCTCCGCTTATTTGATATGC-3') for *H. capsulatum*, and ITS1F (CTGGTCATTAGAGGAAGTAA) and ITS4 for *Sporothrix* spp. The figure was modified from Saar and Polans,¹⁰ according to *H. capsulatum* and *Sporothrix* spp. ITS region data.

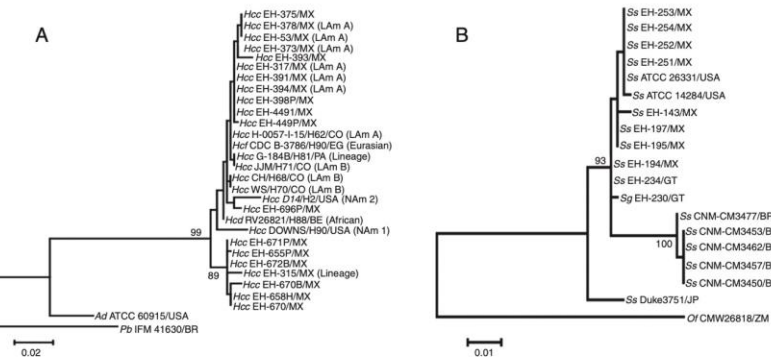


Fig. 2. Maximum likelihood (ML) trees of ITS1-5.8S-ITS2 regions amplified for *Histoplasma* (A) and *Sporothrix* (B) samples. PCR products using primers aforementioned in Fig. 1 for each fungal species were sequenced and aligned by MUSCLE program (MEGA version 5). The best model of evolution to generate the ML phylogenetic trees was obtained by Tamura and Nei gamma distribution.¹⁸ A bootstrapping algorithm was achieved on the dataset for 1000 replicates, and values $\geq 70\%$ were recorded for each tree node. BOLD System sequence accession numbers are referenced in table 1. GenBank sequences for both fungal species were included as reference strains or as outgroups in the ML analyses. Accession numbers are as follows: for *H. capsulatum*: *H. capsulatum* var. *farcininosum* (*Hcf*) H90 (AF322387.1), *H. capsulatum* var. *capsulatum* (*Hcc*) H81 (AF322385.1), H71 (AF322384.1), H62 (AF322379.1), H2 (AF322378.1), H9 (AF322377.1), H68 (AF322382.1), *H. capsulatum* var. *duboisi* (*Hcd*) H88 (AF322386.1); for *S. schenckii* (*Ss*): ATCC 14284 (AF364061.1), ATCC 26331 (FJ455232.1), CNM-CM3477 (EU126945.1), CNM-CM3453 (EU126941.1), CNM-CM3462 (EU126943.1), CNM-CM3457 (EU126942.1), CNM-CM3450 (EU126940.1), Duke3751 (AB089138.1). The GenBank sequence of *A. dermatitidis* (*Ad*) ATCC 60915 (AF322388.1) was used as reference strain, and *P. brasiliensis* (*Pb*) IFM 41630 (AB304423.1) as the outgroup for *H. capsulatum*; *O. fumigatum* (*Of*) CMW26818 (HM051415.1) was used as outgroup for *Sporothrix* spp. Parenthesis indicate *H. capsulatum* clades or lineages as Kasuga et al.⁷ Abbreviations: *Sg* = *S. globosa*; BE = Belgium; BR = Brazil; CO = Colombia; EG = Egypt; GT = Guatemala; JP = Japan; MX = Mexico; PA = Panama; USA = United States of America; ZM = Zambia.

H. capsulatum var. *farcininosum*, *H. capsulatum* var. *capsulatum*, and *H. capsulatum* var. *duboisi*.

The tree generated for *Sporothrix* (Fig. 2B) shows three groups in relation with the outgroup, *Ophiostoma fumigatum*. The first group was formed by two isolates from the United States of America, eight *S. schenckii* from Mexico, and one isolate of *S. schenckii* and one of *Sporothrix globosa* from Guatemala, with a BT of 93%. The second group was formed by five isolates of *S. schenckii*, all from Brazil, which was sustained by a BT of 100%. Finally, the third group included only one isolate of *S. schenckii* from Japan (Fig. 2B). Therefore, the ITS1-5.8S-ITS2 region sequence is a molecular marker that could discriminate *Sporothrix* species from different geographic regions; however, this marker could not discriminate between *Sporothrix* species.

Conclusions

ITS1-5.8S-ITS2 region sequences deposited in different databases could be utilized as a broad molecular marker for inter- and intraspecific genetic diversity of the *H. capsulatum* and *S. schenckii* species complexes. The intraspecific diversity of this genetic region could discriminate *H. capsulatum* or *Sporothrix* isolates according to their geographic distribution and association with environmental sources. However, ITS regions were unable to distinguish neither *H. capsulatum* species nor *Sporothrix* spp. among their respective phylogenetic, biological and/or taxonomic species complexes.

Conflict of interests

The authors have no conflict of interests.

Acknowledgments

MLT and CT thank the MEXBOL program of CONACyT-Mexico, ref. numbers: 122896 and 122481, respectively. RTA thanks

MEXBOL program of CONACyT, ref. 122481, for his scholarship. The authors thank Ingrid Mascher for editorial assistance.

References

- Balajee SA, Hurst SF, Chang LS, Miles M, Beeler E, Hale C, et al. Multilocus sequence typing of *Histoplasma capsulatum* in formalin-fixed paraffin-embedded tissues from cats living in non-endemic regions reveals a new phylogenetic clade. *Med Mycol*. 2012;50:91–8.
- de Beer ZW, Harrington TC, Vismer HF, Wingfield BD, Wingfield MJ. Phylogeny of the *Ophiostoma stenoraceas*-*Sporothrix schenckii* complex. *Mycologia*. 2003;95:434–41.
- de Meyer EM, de Beer W, Summerbell RC, Moharram AM, de Hoog GS, Vismer HF, et al. Taxonomy and phylogeny of new wood- and soil-inhabiting *Sporothrix* species in the *Ophiostoma stenoraceas*-*Sporothrix schenckii* complex. *Mycologia*. 2008;100:647–61.
- Gutiérrez-Galhardo MC, Zancopé-Oliveira RM, Francesconi Do Valle AC, de Almeida-Paes R, Morais P, Silva Tavares E, et al. Molecular epidemiology and antifungal susceptibility patterns of *Sporothrix schenckii* isolates from a cat-transmitted epidemic of sporotrichosis in Rio de Janeiro, Brazil. *Med Mycol*. 2008;46:141–51.
- Jiang B, Bartlett M, Allen SD, Smith JW, Wheat LJ, Connolly PA, et al. Typing of *Histoplasma capsulatum* isolates based on nucleotide sequence variation in the Internal Transcribed Spacer regions of rRNA genes. *J Clin Microbiol*. 2000;38:241–5.
- Kasuga T, Taylor JW, White TJ. Phylogenetic relationships of varieties and geographical groups of the human pathogenic fungus *Histoplasma capsulatum* Darling. *J Clin Microbiol*. 1999;37:653–63.
- Kasuga T, White TJ, Koenig G, McEwen J, Restrepo A, Castañeda E, et al. Phylogeography of the fungal pathogen *Histoplasma capsulatum*. *Mol Ecol*. 2003;12:3383–401.
- Marimon R, Gené J, Cano J, Trilles L, Dos Santos Lazera M, Guarro J. Molecular phylogeny of *Sporothrix schenckii*. *J Clin Microbiol*. 2006;44:3251–6.
- Martin KJ, Rygiewicz PT. Fungal-specific PCR: primers developed for analysis of the ITS region of environmental DNA extracts. *BMC Microbiol*. 2005;5:28.
- Mesa-Arango AC, Reyes-Montes MR, Pérez-Mejía A, Navarro-Barranco H, Souza V, Zúñiga G, et al. Phenotypic and genotypic of *Sporothrix schenckii* isolates according to geographic origin and clinical forms of Sporotrichosis. *J Clin Microbiol*. 2002;40:3004–11.
- Muniz MM, Morais e Silva Tavares P, Meyer W, Nosanchuk JD, Zancopé-Oliveira RM. Comparison of different DNA-based methods for molecular typing of *Histoplasma capsulatum*. *Appl Environ Microbiol*. 2010;76:4438–47.
- Nilsson RH, Kristiansson E, Ryberg M, Hallenberg N, Larsson KH. Intraspecific ITS variability in the kingdom fungi as expressed in the international sequence databases and its implications for molecular species identification. *Evol Bioinformatics*. 2008;4:193–201.

13. Ratnasingham S, Hebert PDN. Bold: the barcode of life data system (<http://www.barcodinglife.org>). Mol Ecol Notes. 2007;7:355–64.
14. Reyes-Montes MR, Rodríguez-Arellanes G, Flores-Robles E, Taylor ML. Tipificación de aislados clínicos de *Histoplasma capsulatum* por métodos fenotípicos y genotípicos. Rev Inst Nal Enf Resp Mex. 1998;11:195–201.
15. Reyes-Montes MR, Taylor ML, Curiel-Quesada E, Mesa-Arango AC. Estado actual de la tipificación del hongo patógeno *Histoplasma capsulatum* var. *capsulatum*: una revisión de los hallazgos. Rev Iberoam Micol. 2000;17:121–6.
16. Saar DE, Polans NO. ITS sequence variation in selected taxa of *Pisum*. Pisum Genet J [Electronic Journal]. 2000;32. Available at: <http://pisum.bionet.nsc.ru/pg/32/42.htm> [consulted on 15.01.13].
17. Suwannasai N, Martin MP, Phosri C, Sihanonth P, Whalley AJS, Spouge JL. Fungi in Thailand: a case study of the efficacy of an ITS barcode for automatically identifying species within the *Annulohypoxylon* and *Hypoxylon* genera. PLoS One. 2013;8:e54529.
18. Tamura K, Nei M. Estimation of the number of nucleotide substitutions in the control region of mitochondrial DNA in humans and chimpanzees. Mol Biol Evol. 1993;10:512–26.
19. Tantichareon M. Introduction to Thai biodiversity. In: Jones EBG, Tantichareon M, Hyde KD, editors. Thai fungal diversity. Pathum Thani: Biotec; 2004. p. 1–16.
20. Taylor ML, Chávez-Tapia CB, Rojas-Martínez A, Reyes-Montes MR, Bobadilla-Del Valle M, Zúñiga G. Geographical distribution of genetic polymorphism of the pathogen *Histoplasma capsulatum* isolated from infected bats, captured in a central zone of Mexico. FEMS Immunol Med Microbiol. 2005;45:451–8.
21. Taylor ML, Hernández-García L, Estrada-Bárcenas DA, Salas-Lizana R, Zancopé-Oliveira RM, García de la Cruz S, et al. Genetic diversity of microsatellite (GA)_n and their flanking regions of *Histoplasma capsulatum* isolated from bats captured in three Latin-American countries. Fungal Biol. 2012;116:308–17.
22. Watanabe S, Kawasaki M, Mochizuki T, Ishizaki H. RFLP analysis of the internal transcribed spacer regions of *Sporothrix schenckii*. Jpn J Med Mycol. 2004;45:165–75.

Mixed infection by *Histoplasma capsulatum* isolates with different mating types in Brazilian AIDS-patients

Lisandra Serra Damasceno^{1,2}, Tania Vite-Garín³, José Antonio Ramírez³, Gabriela Rodríguez-Arellanes³, Marcos Abreu de Almeida¹, Mauro de Medeiros Muniz¹, Jacó Ricarte Lima de Mesquita², Terezinha do Menino Jesus Silva Leitão^{2,4}, Maria Lucia Taylor³, Rosely Maria Zancopé-Oliveira¹

ABSTRACT

Mixed infection by *Histoplasma capsulatum* isolates with different mating types, in AIDS-patients are described in this study. Morphological, mating type-specific PCR assay and multilocus sequencing type analysis of *H. capsulatum* isolates recovered from two Brazilian AIDS-patients were performed. Five *H. capsulatum* isolates were recovered at different times from the two patients. Three isolates were obtained from bone marrow (day 1 – CE0411) and from buffy coat cultures (day 1 – CE0311; day 2 – CE0511) of patient 1, and two isolates were isolated from buffy coat cultures (day 3 – CE2813; day 12 – CE2513) of patient 2. The mycelial colonies depicted different textures and pigmentation features. Dimorphic conversion to the yeast-phase in ML-Gema medium was achieved in all isolates. MAT1-1 idiomorph was identified in CE0311, CE0411 and CE2813 isolates; MAT1-2 idiomorph was found in CE0511 and CE2513 isolates. These *H. capsulatum* isolates were grouped within LAm A clade, highlighting that CE0311 and CE0411 isolates formed a subgroup supported by a high bootstrap value. The CE0511, CE2513, and CE2813 isolates clustered together with a Brazilian H151 isolate. This research reports mixed infections caused by *H. capsulatum* isolates with different mating types in Brazilian AIDS-patients for the first time in the literature.

KEYWORDS: Mixed infection. *Histoplasma capsulatum*. Mating types. Multilocus sequence typing. Histoplasmosis. HIV coinfections.

INTRODUCTION

Histoplasma capsulatum is a dimorphic fungus found in the form of mold in the environment and *in vitro* at 25–28 °C. The yeast form is observed during parasitism conditions or in cultures at 34–37 °C in enriched media¹. *Histoplasma* infection can occur in individuals that are exposed to fungal micro-niches rich in bat guano or bird droppings¹. Severe forms of histoplasmosis usually occur in individuals with immunosuppression, such as AIDS-patients².

The asexual stage or anamorph (*H. capsulatum*) is an eukaryotic and heterothallic microorganism found in the environment as haploid mycelium associated with + or – mating types³. *Ajellomyces capsulatus* is the sexual stage or teleomorph of *H. capsulatum*, resulting from the sexual compatibility + and – of *H. capsulatum* isolates⁴. Both fungal stages represent the same holomorph^{3–5}.

H. capsulatum has a bipolar mating system that expresses transcription factors encoded at the *MAT1* locus^{6,7}. In this fungus, this locus presents two idiomorphs, MAT1-1 and MAT1-2, which define the + and – mating types, respectively⁶. In

¹Fundação Oswaldo Cruz, Instituto Nacional de Infectologia Evandro Chagas, Laboratório de Micologia, Setor Imunodiagnóstico, Rio de Janeiro, Rio de Janeiro, Brazil

²Hospital São José de Doenças Infecciosas, Fortaleza, Ceará, Brazil

³Universidad Nacional Autónoma de México, Facultad de Medicina, Departamento de Microbiología y Parasitología, Laboratorio de Inmunología de Hongos, Ciudad de México, México

⁴Universidade Federal do Ceará, Faculdade de Medicina, Departamento de Saúde Comunitária, Fortaleza, Ceará, Brazil

Correspondence to: Lisandra Serra Damasceno
Fundação Oswaldo Cruz, Instituto Nacional de Infectologia Evandro Chagas, Laboratório de Micologia, Setor Imunodiagnóstico, Av. Brasil, 4365, Manguinhos, CEP 21040-360, Rio de Janeiro, RJ, Brazil
Tel: +55 21 3865-9557
Fax: +55 21 2590-9988

E-mail: lisainfesto@gmail.com

Received: 25 August 2018

Accepted: 20 December 2018

some fungi as *Cryptococcus neoformans* and *Aspergillus fumigatus*, the mating type is associated with the virulence^{8,9}. In addition, mixed infections with different mating types have been rarely described in pathogenic fungi¹⁰.

A high genetic diversity of *H. capsulatum* has been reported worldwide¹¹⁻¹³. In 2003, the performance of multilocus sequencing type (MLST) by partial amplification of four nuclear protein-coding genes, ADP-ribosylation factor (*arf*), H antigen precursor (*H-anti*), delta-9 fatty acid desaturase (*oleI*) and alpha-tubulin (*tubI*) indicated the presence of eight phylogenetic clades among 149 *H. capsulatum* isolates from 25 countries¹¹. The results of these analyses revealed the presence of NAm 1 and NAm 2 clades in North America; LAm A and LAm B clades in Latin America; Africa clades restrict to Africa; Euroasian clades constituted from fungal isolates from Egypt, India, China, Thailand and England; Netherlands clades; an Australian clade¹¹. In addition, diverse new lineages have also been identified in different geographic regions of the world^{11,12}. A recent study performed with a broad number of fungal isolates (n=234) and more robust phylogenetic analyses identified five new phylogenetic clades, with a great admixture among *H. capsulatum* isolates from Latin America¹⁴. The LAm A clade was regrouped in LAm A1, LAm A2 and LAm B clade was reclassified in LAm B1 and LAm B2¹⁴. In addition, two new phylogenetic clades (RJ from Southeastern Brazil and BCA1 from Mexico), and four monophyletic clusters in Brazil (BR1-4) were identified.

Here, two cases of mixed infection with different mating types of *H. capsulatum* in AIDS-patients are reported. In addition, the five *H. capsulatum* isolates obtained from these cases of histoplasmosis in AIDS-patients were evaluated by morphological criteria, mating type determination and phylogenetic classification by MLST analysis.

MATERIAL AND METHODS

Medical records

Clinical data of patients with histoplasmosis and AIDS from São José Hospital, Fortaleza city, Ceará State, Brazil, were retrospectively retrieved from medical records. Only patients that had positive cultures for *H. capsulatum* in two or more different samples or in different hospitalization time, between 2011 to 2014 period were included. A total of 13 biological samples of six patients were studied by mating type-PCR. Only two patients were selected because they presented more than one *H. capsulatum* isolate with different mating types during their period of hospitalization and treatment. The study was approved by the Research

Ethics Committee at the Instituto Nacional de Infectologia Evandro Chagas/FIOCRUZ (Nº 19342513.2.0000.5262), Rio de Janeiro State, Brazil.

Fungal isolation and phenotypic characterization

Fungal isolates (buffy coat from whole blood and bone marrow aspirate) from patients were cultured on Potato Dextrose Agar (Difco, Detroit, MI, USA) at 25 °C during 21 days. The macromorphology of filamentous fungal cultures were visually examined and recorded. Colonies were described according to pigmentation (albino and scale beige - light beige, dark beige, and beige) and texture (cottony or powdery). Their micromorphologies were observed in 10 different fields by optical microscopy at a 40 X magnification of *H. capsulatum* colonies, stained with Lactophenol Cotton Blue (Fluka Analyzed, France). Dimorphism was demonstrated by conversion to the yeast-like form on ML- Gema agar medium¹⁵, for 7 to 14 days at 37 °C.

Mating type determination

Yeast cells were submitted to limiting dilution and a single colony was used for DNA extraction as previously reported¹⁶. The *MAT1* locus of *H. capsulatum* isolates was identified by polymerase chain reaction (PCR) using specific pair of primers for *MAT1-1* and *MAT1-2* idiomorphs based in a previous protocol, with minor modifications¹⁷. Briefly, PCR was performed in a 25 µL reaction mixture, containing 200 µM of each deoxynucleoside triphosphate (dNTP) (Applied Biosystems Inc., Foster City, CA, USA), 1.5 mM MgCl₂, 50 ng/µL of each primer, 1.5 U *Taq* DNA polymerase (New England BioLabs Inc., MA, USA), 1 X *Taq* commercial buffer and 75 ng (25 ng/µL) of each DNA template. G-217B from USA (*MAT1-1*) and G-186AR from Panama (*MAT1-2*) are reference strains and were used as controls.

PCR assays were performed in a Thermal iCycler (Bio-Rad Laboratories Inc., Hercules, CA, USA) programmed as follows: (a) 3 min at 95 °C; (b) 35 cycles, consisting of 30 s at 95 °C, 30 s at 58 °C, and 1 min and 30 s at 72 °C; and (c) 10 min at 72 °C. Amplicons were visualized on 1.5% agarose gel electrophoresis. The 100-bp DNA ladder was used as a molecular marker. Amplicons were sequenced at the High-Throughput Genomics Center (University of Washington, Seattle, WA, USA). The obtained sequences were deposited in GenBank database (<http://www.ncbi.nlm.nih.gov>). They were edited and aligned for BLASTn analysis¹⁸, using as reference the sequence of the strains G-217B from USA (*MAT1-1*, GenBank accession

Nº EF433757) and G-186AR from Panama (MAT1-2, GenBank accession Nº EF433756).

Phylogenetic relationship among the studied isolates

The genetic reconstruction analysis was performed by MLST using PCR amplification of partial DNA sequences from four nuclear genes (*arf*, *H-anti*, *ole1*, and *tub1*) according to the protocol described by Kasuga *et al.*¹¹ with some modifications. PCR was performed in 25 µL of reaction mixture, containing 200 µM of each deoxynucleoside triphosphate (dNTP) (Applied Biosystems Inc., Foster City, CA, USA), 2.0 mM MgCl₂, 50 ng/µL of each primer, 1.0 U *Taq* DNA polymerase (New England BioLabs Inc., MA, USA), 1 X *Taq* commercial buffer, and 20 ng (10 ng/µL) of each DNA template. The G-217B from USA reference strains was used as a control. PCR assays were performed in a Thermal iCycler (Bio-Rad Laboratories Inc., Hercules, CA, USA) programmed as follows: (a) 3 min at 95 °C; (b) 32 cycles, consisting of 15 sec at 94 °C, 30 sec at 65 °C in the first cycle, which was subsequently reduced by 0.7 °C/cycle for the next 12 cycles, and 1 min at 72 °C. In the remaining 20 cycles, the annealing temperature was kept at 56 °C; (c) a final extension cycle of 5 min at 72 °C – touchdown PCR¹⁹.

Generated amplicons were also sequenced at the High-Throughput Genomics Center (University of Washington) and the sequences were deposited in the GenBank database (<http://www.ncbi.nlm.nih.gov>). The resulting sequences were analyzed by BLASTn¹⁷, using the sequences of the G-217B strain as reference (GenBank accession Nº L25117.1, U20346.1, X85962.1, and M28358.1).

To identify the relationships of the five studied isolates with other *H. capsulatum* isolates previously characterized by the four aforementioned nuclear genes, a combined matrix using partial sequences of these genes was generated and edited manually by MESQUITE ver. 2.75²⁰. This matrix was constructed with 260 sequences, considering four genes per isolate, out of 65 analyzed *H. capsulatum* isolates: 57 isolates from TreeBASE (<http://treebase.org>, study ID S1063) reported by Kasuga *et al.*¹¹; three from GenBank with their respective accession numbers for *arf*, *H-anti*, *ole1*, and *tub1* genes (EH-3831 isolate- AF495619, AF495620, AF495621, and AF495622; and EH-375 isolate- AF495607, AF495608, AF495609, and AF495610; and the G-217B strain, see the aforementioned GenBank accession numbers); and the five *H. capsulatum* clinical isolates reported in this study. Details of the 65 *H. capsulatum* isolates are in Tables 1 and 2.

Table 1 - Major data of *H. capsulatum* strains/isolates whose sequences were acquired from databases of the MLST analysis of the present study. (continues on the next page)

Strain/isolate	Phylogenetic clade	Source	Origin	Year of isolation
Downs (H9)*	NAm 1	Human	USA	1968
H79*	NAm 1	Skunk	USA	1967 or before
H126*	NAm 1	Human/HIV+	USA	1987
H127*	NAm 1	Human/HIV+	USA	1987
G-217B (H8)†	NAm 2	Human	USA	1973 or before
H11*	NAm 2	Human	USA	1993 or before
H97*	NAm 2	Human	USA	1995 or before
H139*	NAm 2	Soil	USA	1975
H179*	NAm 2	Human	USA	Not known
H146*	LAm A	Human	Brazil	1979
H149*	LAm A	Human/HIV+	Brazil	1996
H150*	LAm A	Human	Brazil	1996
H151*	LAm A	Human/HIV+	Brazil	1997
H152*	LAm A	Human/HIV+	Brazil	1997
H155*	LAm A	Human/HIV+	Brazil	1998
H67*	LAm A	Human	Colombia	1993
H61*	LAm A	Human	Colombia	1993
H62*	LAm A	Human	Colombia	1993
H63*	LAm A	Human	Colombia	1989

Table 1 - Major data of *H. capsulatum* strains/isolates whose sequences were acquired from databases of the MLST analysis of the present study. (cont.)

Strain/isolate	Phylogenetic clade	Source	Origin	Year of isolation
EH-46*	LA _m A	Human	Mexico	1979
EH-53*	LA _m A	Human	Mexico	1977
EH-317*	LA _m A	Human/HIV+	Mexico	1992
L-100-91 (EH-333)*	LA _m A	Black bird excreta	Guatemala	1991
EH-383†	LA _m A	Bat	Mexico	1997
CEPA 2 (EH-362)*	LA _m A	Black bird excreta	Guatemala	1996
CEPA 3 (EH-363)*	LA _m A	Human	Guatemala	1996
H.1.04.91 (EH-304)*	LA _m A	Human	Guatemala	1991
H.1.11.94 (EH-332)*	LA _m A	Human	Guatemala	1994
EH-375†	LA _m A	Bat	Mexico	1997
H162 *	LA _m B	Human/HIV+	Argentina	1998-1999
H163*	LA _m B	Human/HIV+	Argentina	1998-1999
H164*	LA _m B	Human/HIV+	Argentina	1998-1999
H165*	LA _m B	Human/HIV+	Argentina	1998-1999
H166*	LA _m B	Human/HIV+	Argentina	1998-1999
H148*	Eurasia	Horse	Not known	1935
H178*	Eurasia	Human	China	Not known
H192*	Eurasia	Human	India	Not known
H194*	Eurasia	Horse	Egypt	Not known
H206*	Eurasia	Human	Thailand	1994
H87*	Africa	Human	Guinea-Liberian border	1970
H137*	Africa	Human	Zaire	1962
H147*	Africa	Human	Senegal	1957
H187*	Africa	Bat guano	Nigeria	1991
H189*	Africa	Not known	Not known	Not known
H157*	Australia	Human	Australia	1970s
H158*	Australia	Soil/bat guano	Australia	1984
H159*	Australia	Human	Australia	1984
H160*	Australia	Human/HIV+	Australia	1988
H161*	Australia	Human/HIV+	Australia	1990
H144*	Netherlands	Human	Netherlands	1965
H176*	Netherlands	Human	Netherlands	1969
H66*	Lineage	Human	Colombia	1986
H69*	Lineage	Human	Colombia	1991
H153*	Linage	Human	Brazil	1997
G-186B (H83)*	Lineage	Human	Panama	1967 or before
G-186A (H82)*	Lineage	Human	Panama	1967 or before
G-184B (H81)*	Lineage	Human	Panama	1967 or before
H140*	Lineage	Owl monkey	USA/Peru	1997
H185*	Lineage	Owl monkey	USA/Peru	1999
EH-315*	Lineage	Bat	Mexico	1994

The sequences of all *H. capsulatum* strains/isolates in this table were obtained from *TreeBase and †GenBank. Numbers in parenthesis are acronyms.

Table 2 - Characteristics of *H. capsulatum* isolates associated with mixed infections.

Characteristics of fungal isolates	Patient 1			Patient 2	
	CE0311	CE0411	CE0511	CE2813	CE2513
Source	Buffy coat	Bone marrow	Buffy coat	Buffy coat	Buffy coat
Day of hospitalization	1°	1°	2°	3°	12°
Pigmentation of colonies	Albino	Light-beige	Beige	Dark-beige	Light-beige
Texture of colonies	Cottony	Cottony	Cottony	Powdery	Powdery
Mating type	MAT1-1	MAT1-1	MAT1-2	MAT1-1	MAT1-2

The generated combined matrix containing 1539-nt was analyzed through two methods: a) Maximum likelihood (ML) in RaxMLGUI ver. 1.31²¹ through the General Time Reversible substitution model gamma distribution; and b) Bayesian inference (BI) by MrBayes ver. 3.2²² with a final run using four chains for a total of 100,000,000 generations and sampling trees every 10,000 generations. The substitution models considered in BI for each partition were K80 (H-anti), K80+G with four categories (arf and tub1), and K80+I (ole1). The substitution models for ML and BI methods were selected according to Akaike Information Criterion and Bayesian information criterion tests, implemented in Jmodeltest ver. 2.1.4 for ML and BI²³, respectively.

Bootstrap values (bt) for ML analysis were based on 1000 heuristic search replicates, using Tree-Bisection-Reconnection. For the BI analysis, the maximum clade credibility tree was selected with a posterior probability (pp) limit of 0.95, using TreeAnnotator ver. 1.8.2, implemented in BEAST - Bayesian Evolutionary Analysis Sampling Trees^{24,25}. An unrooted tree was constructed using the combined matrix.

RESULTS

During the study period, 40 AIDS-patients were hospitalized in the São José Hospital with histoplasmosis diagnosis confirmed by culture in different biologic samples. For this study, six patients were recruited and 13 biologic samples of these six patients, which were available for mating type – PCR. Four patients presented the same mating type, two patients with MAT 1-1 and two patients with MAT 1-2. However, for this report we selected only the two patients presenting with *H. capsulatum* isolates with different mating types.

Patient 1

A 22-year-old male AIDS-patient was admitted in an infectious diseases hospital with fever, diarrhea,

asthenia, and a weight loss of 6 kg. He was a craftsman and lived in an urban area of Baturite, Ceará State, Brazil. Physical examination revealed cervical adenomegaly and hepatosplenomegaly. Pulmonary and cardiac auscultation as well as vital signs were normal. He used antiretroviral drugs irregularly (estavudine, lamivudine, and efavirenz). Laboratory evaluations revealed hemoglobin level of 9.3g/dL, white blood cells count 1,200/mm³ (neutrophils = 80%; lymphocytes = 10.8%; monocytes = 4.2%; eosinophils = 5%), and platelets count 65,000/mm³. Renal function was normal. The level of lactate dehydrogenase (LDH) was high (2,086 U/L). Aspartate aminotransferase (AST) level was 274 U/L, alanine aminotransferase (ALT) level was 67 U/L and alkaline phosphate (AP) was 184 U/L. The patient had CD4+ lymphocytes count of 273 cells/mm³ and plasma HIV-RNA of 127,240 copies/mL. *H. capsulatum* yeast-like was visualized by Giemsa staining of buffy coat smear. Therapy with amphotericin B (1 mg/kg per day) was administered and the patient was discharged after 35 days of hospitalization. In the clinical follow-up, the antifungal therapy was maintained with amphotericin B once a week for 6 month.

Patient 2

A 52-year-old male AIDS-patient was admitted in an infectious diseases hospital with fever, abdominal pain, cough, dyspnea, hematochezia, and weight loss. He had a history of an oral mucosa lesion for the last 2 months. He was engaged in farming activities and lived in a rural area of Maracanau, Ceará State, Brazil. His vital signs were as follows: temperature 37.2 °C; pulse rate 106/min, respiratory frequency 30/min, and blood pressure 70/30 mm Hg. A physical examination revealed pallor, oral ulcer with partial destruction of uvula, and oral candidiasis. Cardiac auscultation detected crackles in the base of the left lung. The abdominal examination revealed hepatosplenomegaly. He used antiretroviral drugs irregularly (zidovudine, lamivudine, atazanavir, and ritonavir). Laboratory

evaluations revealed hemoglobin level of 4.3 g/dL, white blood cells count 3,860/mm³ (1%; neutrophils = 64%; lymphocytes = 24%; monocytes = 8%; eosinophils = 2%; basophiles = 1%), and platelets count 34,000/mm³. Renal function was normal. A high level of LDH was observed (1,402 U/L). Hepatic function was altered (AST = 97 U/L, ALT = 32 U/L, AP = 908 U/L, γGT = 197 U/L). The patient had CD4+ lymphocytes count of 80 cells/mm³. A chest X-ray showed diffuse reticulonodular pulmonary infiltrate. Empiric therapy with amphotericin B (1 mg/kg per day) was started on day 1. However, the patient presented respiratory and renal failure. He died after 18 days of hospitalization.

Fungal cultures and morphological identification

H. capsulatum were isolated from patients' clinical samples during their hospitalization and treatment. Three *H. capsulatum* isolates were obtained from patient 1, one from bone marrow (day 1 – CE0411) and two from buffy coat (day 1 – CE0311; day 2 – CE0511). Two *H. capsulatum* isolates were recovered from buffy coat of patient 2 on day 3 (CE2813) and day 12 (CE2513) of hospitalization. *H. capsulatum* mycelial cultures of patient 1 presented

a cottony texture macromorphology, whereas mycelial cultures of patient 2 were powdery. Different pigmentations were observed in the fungal cultures of both patients. These morphological characteristics are in Table 2. In regard to micromorphology, all fungal isolates had hyaline, septated and branched thin hyphae, microconidia and tuberculate macroconidia. Dimorphic conversion occurred in all *H. capsulatum* isolates, with typical budding yeast cells. Figure 1 shows a representative micromorphology of the five fungal isolates recovered in this study.

Mating types of *H. capsulatum* isolates recovered from the AIDS-patients

The *MAT1-1* idiomorph was identified in *H. capsulatum* isolates CE0311 and CE0411 (patient 1) as well as in CE2813 (patient 2) isolates; whereas the *MAT1-2* idiomorph was found in CE0511 (patient 1) and CE2513 (patient 2) isolates. The sequences of the *MAT1* locus for these five fungal isolates are available in the GenBank (accession numbers in Table 3) and they were compatible with *A. capsulatum* through BLASTn analysis¹⁸. The CE0311 and CE0411 isolates showed 99% similarity and CE2813 isolate



Figure 1 - Representative micromorphology of *H. capsulatum* mycelium and yeast phases of CE0411 isolate from an AIDS-patient. Both fungal phases were stained by Lactophenol Cotton Blue. Magnification of 40 X.

Table 3 - GenBank accession numbers of the sequences from each gene used to characterize the five *H. capsulatum* isolates in the present study.

Fungal isolate	MAT1	Arf	H-anti	ole1	tub1
CE 0311	KX058315	KX058302	KX058322	KX058307	KX058312
CE0411	KX058314	KX058301	KX058321	KX058306	KX058311
CE0511	KX058317	KX058300	KX058320	KX058305	KX058310
CE2813	KX058313	KX058298	KX058318	KX058303	KX058309
CE2513	KX058316	KX058299	KX058319	KX058304	KX058308

showed 100% similarity with the sequence of the G-217B reference strain (*MATI-1*), whereas CE0511 and CE2513 isolates showed 97% similarity with the sequence of the G-186AR reference strain (*MATI-2*).

Phylogenetic analyses of the *H. capsulatum* isolates

These partial sequences obtained from the five *H. capsulatum* isolates were deposited in GenBank (accession numbers in Table 3). The phylogenetic trees for the four genes analyzed by either ML or BI methods presented similar topologies. A BI phylogenetic tree was constructed to support both ML and BI data, where bt and pp values were represented in each tree node (Figure 2).

The five *H. capsulatum* isolates from the AIDS-associated histoplasmosis patients were grouped in the LAm A clade together with other LAm A isolates included in the present study (Table 1, Figure 2). The CE0311 and CE0411 isolates from patient 1 share the same branch with the H146 isolate from Brazil, supported by $bt = 74\%$ (ML) and $pp = 1.0$ (BI) values. On the other hand, CE0511 (patient 1), CE2513 and CE2813 (patient 2) isolates were clustered together and share a branch with Brazilian H151 and H149 isolates ($bt = 56\%$ in ML, $pp = 1.0$ in BI) (Figure 2). In regard to the sequences of other isolates used to develop the MLST analyses, Figure 2 shows that they clustered according to Kasuga *et al.*¹¹ criterion, representing the different clades reported in Table 1.

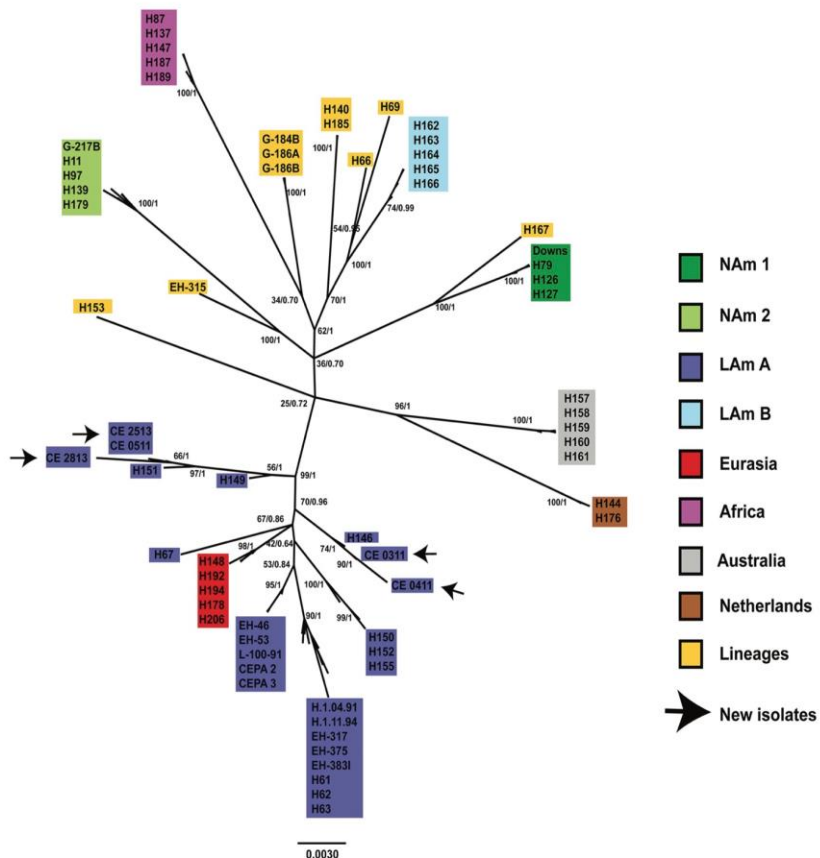


Figure 2 - Unrooted phylogenetic tree of *H. capsulatum* isolates. The tree was constructed with a concatenated matrix of 1539-nt using four gene fragments (*arf*, *H-anti*, *ole1*, and *tub1*). It was generated by BI and is representative of both ML and BI analyses. The values of bt/pp are indicated on their corresponding tree nodes.

DISCUSSION

This study reports for the first time in the literature, two cases of mixed infection caused by *H. capsulatum* isolates with different mating types in AIDS-patients, highlighting the genetic diversity among the five fungal isolates recovered from clinical samples. The *H. capsulatum* isolates associated with mixed infections were from the Ceará State, which is an endemic area of histoplasmosis in Northeast Brazil. This mycosis usually occurs in AIDS-patients, and a high mortality rate has been recorded (30-40%) among them^{2,26}.

Mixed infections caused by microorganisms with different genetic profiles have been described mainly with pathogenic bacteria^{27,28}. Fungal mixed infection with different mating types of the same species was described in individuals colonized or infected by *Aspergillus fumigatus*¹⁰. However, the clinical consequences of this event are still unknown. It is suggested that the mechanisms driving mixed infections include microevolution of pre-existing clones, simultaneous coinfection by recently acquired strains, and superinfection by a new strain different from preexisting clones^{29,30}. Here, mixed infections caused by different isolates were supported by the finding of different *H. capsulatum* mating type's idiomorphs in the same patient, at different time points of the histoplasmosis treatment.

Some studies have also shown that the mating system of *Cryptococcus neoformans* and *A. fumigatus* is associated with virulence of these pathogens as well as with the severity of infections^{8,9,31}. *MAT1-1* has been associated with invasive aspergillosis³² and in *C. neoformans* infections, the α -mating type has been described as more virulent than the a-mating type^{8,31}. However, more recently, experimental studies revealed that there is not association between mating type and virulence of *C. neoformans* and *A. fumigatus*^{33,34}.

The sexual reproduction by meiosis between strains with different mating types can generate genetic variability, which is very important for lineage survival. In addition, this process can lead to the formation of hypervirulent strains, as well as strains with the ability to evade the host's immune response and with increased resistance to antifungal drugs^{7,30}.

Few studies have investigated the mating type of *H. capsulatum* isolates and its impact on the virulence of the pathogen^{5,35}. Conventional methods, such as *in vitro* cross mating between isolates of *H. capsulatum*, identified a predominance of *MAT1-2* in clinical isolates from USA patients with acute pulmonary histoplasmosis³⁵. In 2007, a molecular study identified *MAT1-1* in strains from USA isolated from a patient with unusual histoplasmosis (G-217B) and UH1 isolate obtained from a transplanted patient with disseminated histoplasmosis. *MAT1-2* was

related to the strain G-186AR from Panama and the strains VA1 and T-3-1 from USA⁶.

More recently, several environmental and clinical *H. capsulatum* isolates from Mexico and Brazil were characterized concerning their *MAT1* locus by PCR¹⁷. Six out of 28 studied fungal isolates were obtained from patients with disseminated histoplasmosis, where three isolates came from HIV-patients (two from Brazil and one from Mexico). The *MAT1-1* was found in all (11 environmental and three clinical) isolates studied from Brazil, whereas the *MAT1-2* was predominantly identified in most of the Mexican *H. capsulatum* isolates, including two clinical isolates. Interestingly, *MAT1-1* idiomorph was also identified in four isolates from Mexico, where one of these was isolated from an HIV-patient¹⁷. As new data, it was reported here two *MAT1-2* *H. capsulatum* isolates from Brazil. Undoubtedly, more studies are necessary to characterize the distribution and the impact of mating types in *H. capsulatum* isolates from different regions of the Americas.

Among the morphological characteristics recorded for the studied *H. capsulatum* isolates, pigmentation was the sole divergent factor. It is well known that pigmentation of fungal isolates depends on the culture medium, age of strain and melanin production. Even though the melanization of *H. capsulatum* protects the fungus against antifungal drugs such as amphotericin B³⁶, experimental studies did not find any difference in virulence between albino (non-melanized) and brown (melanized) *H. capsulatum* strains³⁷.

All *H. capsulatum* isolates of this study were identified within the former LAm A clade by MLST analyses, which also revealed genetic diversities among the fungal isolates of each patient. According to the new phylogenetic clusters proposed by Teixeira *et al.*¹⁴, the isolates CE0311 and CE0411 would be classified within the BR4 clade together with H146; and CE0511, CE2513, and CE2813 within the BR2 clade together H151. Thus, isolates from patient 1, CE0311 and CE0411, grouped in a different cluster from that of isolate CE0511; whereas isolate CE2513 from patient 2 showed a high genetic similarity with the CE0511 isolate from patient 1, supported by bt and pp values of ML and BI trees, respectively (Figure 2). Based on these genetic findings and considering the differences in the *MAT1* locus described in the *H. capsulatum* isolates of the same patient, it is possible to assume that these fungal mixed infections could be explained by simultaneous coinfection with a new isolate that diverged and coexists in the same area, or by superinfection with a latent *Histoplasma* infection. Previous phylogenetic studies with different molecular markers have demonstrated that there is a high genetic diversity among *H. capsulatum* isolates from diverse regions, as well as in the same region^{11-14,38-40}. Therefore, coinfection and

superinfection are events that can occur in mixed infections and cannot be discarded in *H. capsulatum* infections. In spite of all this, more studies aiming at evaluating the consequences of mixed infections with *H. capsulatum* harboring different genetic and morphologic characteristics are necessary to better understand the pathogenesis of histoplasmosis.

CONCLUSIONS

This research indicates that mixed infection caused by *H. capsulatum* isolates with different mating types can occur due to different mechanisms as microevolution, coinfection or superinfection. More studies are necessary to evaluate the results this coinfection in the virulence of pathogen and in the pathogenesis of histoplasmosis.

ACKNOWLEDGMENTS

LSD thanks the *Programa de Pós-Graduação Stricto Sensu em Pesquisa Clínica em Doenças Infectocontagiosas do Instituto Nacional de Infectologia Evandro Chagas*, FIOCRUZ and the scholarship Nº 99999.002336/2014-06 provided by the *Programa Institucional de Bolsas de Doutorado Sanduíche no Exterior* from the *Coordenação de Aperfeiçoamento de Pessoal de Nível Superior (CAPES)*, Brazil. The authors thank Ingrid Mascher and Rodrigo de Almeida Paes for their editorial assistance.

FINANCIAL SUPPORT

RMZ-O was supported in part by CNPq [304976/2013-0] and FAPERJ [E-26/103.157/2011]. This research was also partially supported by a grant provided by *Programa de Apoyo a Proyectos de Investigación e Innovación Tecnológica-Dirección General de Asuntos del Personal Académico* from UNAM [PAPIIT-DGAPA/UNAM, Reference Nº IN213515].

CONFLICT OF INTERESTS

The authors declare that there is no conflict of interests among them and with any financial organization regarding the material discussed in the present manuscript.

AUTHORS' CONTRIBUTIONS

LSD, TVG, JAR, GRA, MAA, JRLM carried out the laboratory work of the study; LSD, TVG, MMM, MLT, RMZO evaluated and interpreted data; LSD, TMJSL, MLT, RMZO drafted the manuscript; All authors participated in the design of the study and revised manuscript. All authors

have contributed intellectually during the writing process and have read and approved the final manuscript.

REFERENCES

1. Taylor ML, Reyes-Montes MR, Chávez-Tapia CB, Curiel-Quesada E, Duarte-Escalante E, Rodríguez-Arellanes G, et al. Ecology and molecular epidemiology findings of *Histoplasma capsulatum*, in Mexico. In: Moján RM, Benedik M, editors. Research advances in microbiology. Kerala : Global Research Network; 2000. p.29-35.
2. Dasmasceno LS, Novaes Jr AR, Alencar CH, Lima DT, Sidrim JJ, Gonçalves MV, et al. Disseminated histoplasmosis and AIDS: relapse and late mortality in endemic area in North-Eastern Brazil. Mycoses. 2013;56:520-6.
3. Kwon-Chung KJ. Sexual stage of *Histoplasma capsulatum*. Science. 1972;175:326.
4. Kwon-Chung KJ. *Emmonsia capsulata*: perfect state of *Histoplasma capsulatum*. Science. 1972;177:368-9.
5. Kwon-Chung KJ, Weeks RJ, Lash HW. Studies on *Emmonsia capsulata* (*Histoplasma capsulatum*). II. Distribution of the two mating types in 13 endemic states of the United States. Am J Epidemiol. 1974;99:44-9.
6. Bubnick M, Smulian AG. The MAT1 locus of *Histoplasma capsulatum* is responsive in a mating type-specific manner. Eukaryot Cell. 2007;6:616-21.
7. Muniz MM, Sousa CN, Oliveira MM, Pizzini CV, Almeida MA, Rodríguez-Arellanes G, et al. Sexual variability in *Histoplasma capsulatum* and its possible distribution: what is going on? Rev Iberoam Micol. 2014;31:7-10.
8. Kwon-Chung KJ, Edman JC, Wickes BL. Genetic association of mating types and virulence in *Cryptococcus neoformans*. Infect Immun. 1992;60:602-5.
9. Cheema MS, Christians JK. Virulence in an insect model differs between mating types in *Aspergillus fumigatus*. Med Mycol. 2011;49:202-7.
10. Alvarez-Perez S, Garcia ME, Bouza E, Pelaez T, Blanco JL. Characterization of multiple isolates of *Aspergillus fumigatus* from patients: genotype, mating type and invasiveness. Med Mycol. 2009;47:601-8.
11. Kasuga T, White TJ, Koenig G, McEwen J, Restrepo A, Castañeda E, et al. Phylogeography of the fungal pathogen *Histoplasma capsulatum*. Mol Ecol. 2003;12:3383-401.
12. Vite-Garín T, Estrada-Bárcenas DA, Cifuentes J, Taylor ML. The importance of molecular analyses for understanding the genetic diversity of *Histoplasma capsulatum*: an overview. Rev Iberoam Micol. 2014;31:11-5.
13. Damasceno LS, Leitão TM, Taylor ML, Muniz MM, Zancopé-Oliveira RM. The use of genetic markers in the molecular epidemiology of histoplasmosis: a systematic review. Eur J Clin Microbiol Infect Dis. 2016;35:19-27.

14. Teixeira MM, Patané JS, Taylor ML, Gómez BL, Theodoro RC, de Hoog S, et al. Worldwide phylogenetic distributions and population dynamics of the genus *Histoplasma*. *PLoS Negl Trop Dis.* 2016;10:e0004732.
15. Fressatti R, Dias-Siqueira L, Svidzinski TI, Herrero F, Klemmleier C. A medium for inducing conversion of *Histoplasma capsulatum* var. *capsulatum* into its yeast-like form. *Mem Inst Oswaldo Cruz.* 1992;87:53-8.
16. Muniz MM, Tavares PM, Meyer W, Nosanchuk JD, Zancopé-Oliveira RM. Comparison of different DNA-based methods for molecular typing of *Histoplasma capsulatum*. *Appl Environ Microbiol.* 2010;76:4438-47.
17. Rodríguez-Arellanes G, Sousa CN, Medeiros-Muniz M, Ramírez JA, Pizzini CV, Almeida MA, et al. Frequency and genetic diversity of the MAT1 locus of *Histoplasma capsulatum* isolates in Mexico and Brazil. *Eukaryot Cell.* 2013;12:1033-8.
18. Altschul SF, Gish W, Miller W, Myers EW, Lipman DJ. Basic local alignment search tool. *J Mol Biol.* 1990;215:403-10.
19. Don RH, Cox PT, Wainwright BJ, Baker K, Mattick JS. 'Touchdown' PCR to circumvent spurious priming during gene amplification. *Nucleic Acids Res.* 1991;19:4008.
20. Maddison DR, Maddison WP. Mesquite: a modular system for evolutionary analysis. [cited 2019 Jan 14]. Available from: <http://mesquiteproject.org>
21. Stamatakis A. RAxML version 8: a tool for phylogenetic analysis and post-analysis of large phylogenies. *Bioinformatics.* 2014;30:1312-3.
22. Ronquist F, Teslenko M, van der Mark P, Ayres DL, Darling A, Hohna S, et al. MrBayes 3.2: efficient Bayesian phylogenetic inference and model selection across a large model space. *Syst Biol.* 2012;61:539-42.
23. Darriba D, Taboada GL, Doallo R, Posada D. jModelTest 2: more models, new heuristics and parallel computing. *Nat Methods.* 2012;9:772.
24. Drummond AJ, Suchard MA, Xie D, Rambaut A. Bayesian phylogenetics with BEAUTi and the BEAST 1.7. *Mol Biol Evol.* 2012;29:1969-73.
25. Heled J, Drummond AJ. Bayesian inference of species trees from multilocus data. *Mol Biol Evol.* 2010;27:570-80.
26. Brilhante RS, Fechine MA, Mesquita JR, Cordeiro RA, Rocha MF, Monteiro AJ, et al. Histoplasmosis in HIV-positive patients in Ceará, Brazil: clinical-laboratory aspects and in vitro antifungal susceptibility of *Histoplasma capsulatum* isolates. *Trans R Soc Trop Med Hyg.* 2012;106:484-8.
27. Martin IM, Ison CA. Detection of mixed infection of *Neisseria gonorrhoeae*. *Sex Transm Infec.* 2003;79:56-8.
28. García de Viedma D, Alonso Rodriguez N, Andrés S, Ruiz Serrano MJ, Bouza E. Characterization of clonal complexity in tuberculosis by mycobacterial interspersed repetitive unit-variable-number tandem repeat typing. *J Clin Microbiol.* 2005;43:5660-4.
29. Ene IV, Bennett RJ. The cryptic sexual strategies of human fungal pathogens. *Nat Rev Microbiol.* 2014;12:239-51.
30. García de Viedma D, Marín M, Ruiz Serrano MJ, Alcalá L, Bouza E. Polyclonal and compartmentalized infection by *Mycobacterium tuberculosis* in patients with both respiratory and extrarespiratory involvement. *J Infect Dis.* 2003;187:695-9.
31. Nielsen K, Marra RE, Hagen F, Boekhout T, Mitchell TG, Cox GM, et al. Interaction between genetic background and the mating-type locus in *Cryptococcus neoformans* virulence potential. *Genetics.* 2005;171:975-83.
32. Alvarez-Perez S, Blanco JL, Alba P, Garcia ME. Mating type and invasiveness are significantly associated in *Aspergillus fumigatus*. *Med Mycol.* 2010;48:273-7.
33. Zhai B, Zhu P, Foyle D, Upadhyay S, Idnurm A, Lin X. Congenic strains of the filamentous form of *Cryptococcus neoformans* for studies of fungal morphogenesis and virulence. *Infect Immun.* 2013;81:2626-37.
34. Losada L, Sugui JA, Eckhaus MA, Chang YC, Mouaud S, Figat A, et al. Genetic analysis using an isogenic mating pair of *Aspergillus fumigatus* identifies azole resistance genes and lack of mat locus's role in virulence. *PLoS Pathog.* 2015;11:e1004834.
35. Kwon-Chung KJ, Bartlett MS, Wheat LJ. Distribution of the two mating types among *Histoplasma capsulatum* isolates obtained from an urban histoplasmosis outbreak. *Sabouraudia.* 1984;22:155-7.
36. Gómez BL, Nosanchuk JD. Melanin and fungi. *Curr Opin Infect Dis.* 2003;16:91-6.
37. Campbell CC, Berliner MD. Virulence differences in mice of type a and b *Histoplasma capsulatum* yeasts grown in continuous light and total darkness. *Infect Immun.* 1973;8:677-8.
38. Muniz MM, Pizzini CV, Peralta JM, Reiss E, Zancopé-Oliveira RM. Genetic diversity of *Histoplasma capsulatum* strains isolated from soil, animals, and clinical specimens in Rio de Janeiro State, Brazil, by a PCR-based random amplified polymorphic DNA assay. *J Clin Microbiol.* 2001;39:4487-94.
39. Taylor ML, Hernández-García L, Estrada-Bárcenas D, Salazar-Lizana R, Zancopé-Oliveira RM, García de la Cruz S, et al. Genetic diversity of *Histoplasma capsulatum* isolated from infected bats randomly captured in Mexico, Brazil and Argentina, using the polymorphism of (GA)_n microsatellite and its flanking regions. *Fungal Biol.* 2012;116:308-17.
40. Taylor ML, Chávez-Tapia CB, Rojas-Martínez A, de Rocio Reyes-Montes M, Bobadilla del Valle M, Zuñiga G. Geographical distribution of genetic polymorphism of the pathogen *Histoplasma capsulatum* isolated from infected bats, captured in a central zone of Mexico. *FEMS Immunol Med Microbiol.* 2005;45:451-8.



Histoplasma capsulatum and Pneumocystis jirovecii coinfection in hospitalized HIV and non-HIV patients from a tertiary care hospital in Mexico



Laura E. Carreto-Binaghi^{a,b}, Fernando R. Morales-Villarreal^c, Guadalupe García-de la Torre^d, Tania Vite-Garín^a, Jose-Antonio Ramirez^a, El-Moukhtar Aliouat^e, Jose-Arturo Martínez-Orozco^c, María-Lucía Taylor^{a,*}

^aLaboratorio de Inmunología de Hongs, Unidad de Micología, Departamento de Microbiología-Parasitología, Facultad de Medicina, Universidad Nacional Autónoma de México (UNAM), CDMX, 04510, Mexico

^bDepartamento de Investigación en Microbiología, Instituto Nacional de Enfermedades Respiratorias "Ismael Cosío Villegas" (INER), CDMX, 14080, Mexico

^cDepartamento de Microbiología Clínica, INER, CDMX, 14080, Mexico

^dDepartamento de Salud Pública, Facultad de Medicina, UNAM, CDMX, 04510, Mexico

^eUniv. Lille, CNRS, Inserm, CHU Lille, Institut Pasteur de Lille, U1019 – UMR 8204 – CIL – Centre d'Infection et d'Immunité de Lille, Lille, France

ARTICLE INFO

Article history:

Received 30 January 2019

Received in revised form 10 June 2019

Accepted 11 June 2019

Corresponding Editor: Eskild Petersen, Aarhus, Denmark

Keywords:

Histoplasmosis

Pneumocystosis

Coinfection

Molecular diagnosis

Bronchoalveolar lavage

ABSTRACT

Background: *Histoplasma capsulatum* and *Pneumocystis jirovecii* are respiratory fungal pathogens that principally cause pulmonary disease. Coinfection with both pathogens is scarcely reported. This study detected this coinfection using specific molecular methods for each fungus in the bronchoalveolar lavage (BAL) of patients from a tertiary care hospital.

Materials and methods: BAL samples from 289 hospitalized patients were screened by PCR with specific markers for *H. capsulatum* (Hcp100) and *P. jirovecii* (mtLSUrRNA and mtSSUrRNA). The presence of these pathogens was confirmed by the generated sequences for each marker. The clinical and laboratory data for the patients were analyzed using statistical software.

Results: The PCR findings separated three groups of patients, where the first was represented by 60 (20.8%) histoplasmosis patients, the second by 45 (15.6%) patients with pneumocystosis, and the last group by 12 (4.2%) patients with coinfection. High similarity among the generated sequences of each species was demonstrated by BLASTn and neighbor-joining algorithms. The estimated prevalence of *H. capsulatum* and *P. jirovecii* coinfection was higher in HIV patients.

© 2019 The Authors. Published by Elsevier Ltd on behalf of International Society for Infectious Diseases. This is an open access article under the CC BY-NC-ND license (<http://creativecommons.org/licenses/by-nc-nd/4.0/>).

Introduction

Histoplasma capsulatum is the causative agent of histoplasmosis, one of the most important systemic mycoses in humans; this disease is particularly related to endemic regions in America, and autochthonous outbreaks have been described from latitude 54° north (Alberta, Canada) (Anderson et al., 2006) to 38° south (Neuquén, Argentina) (Calanni et al., 2013). The epidemic form of

histoplasmosis commonly implies an occupational risk, as reported in some Latin American countries, but currently, it represents a human immunodeficiency virus (HIV)-defining condition (Centers for Disease Control and Prevention, 2008). Thus, *H. capsulatum* could be considered a primary fungal pathogen because it infects healthy people, although it also shows an opportunistic behavior since it causes more severe disease in immunocompromised individuals.

H. capsulatum is a dimorphic fungus with two morphotypes, a mycelial infective phase found mainly in bat and bird guano and a yeast virulent phase, which can survive within macrophages and depicts a chronic granulomatous inflammation in host tissues (Köhler et al., 2017; Pomerville, 2018). Infection occurs by inhalation of aerosolized mycelial propagules (mainly microconidia and small hyphal fragments), which become yeasts upon entering the hosts respiratory tract.

* Corresponding author.

E-mail addresses: lauraelena_c@yahoo.com (L.E. Carreto-Binaghi), fernando62fmv@gmail.com (F.R. Morales-Villarreal), gsgarciaadelatorre@gmail.com (G. García-de la Torre), tania.vite.garin@gmail.com (T. Vite-Garín), anton100559@hotmail.com (J.-A. Ramírez), elmoukhtar.aliouat-3@univ-lille2.fr (E.-M. Aliouat), jarturoinfectologia@iner.gob.mx (J.-A. Martínez-Orozco), emello@unam.mx (M.-L. Taylor).

<https://doi.org/10.1016/j.ijid.2019.06.010>
1201-9712/© 2019 The Authors. Published by Elsevier Ltd on behalf of International Society for Infectious Diseases. This is an open access article under the CC BY-NC-ND license (<http://creativecommons.org/licenses/by-nc-nd/4.0/>).

Pneumocystis jirovecii, which was first described by Frenkel (1976), is currently accepted as the specific fungal agent of human pneumocystosis (Morris and Norris, 2012). During the acquired immunodeficiency syndrome (AIDS) epidemic in the 1980s, this fungal species was associated with the primary cause of mortality in HIV/AIDS patients, despite the use of antiretroviral therapy. Pneumocystosis is distributed worldwide, and it can also be diagnosed in other immunocompromised patients and in chronic obstructive pulmonary disease exacerbations (Morris et al., 2008). In immunocompetent human hosts, *P. jirovecii* has been reported as an asymptomatic infection or colonization, suggesting it can be the source of infection transmission for other individuals (Morris and Norris, 2012). All *Pneumocystis* spp. depict two morphotypes: the trophic and the ascospore forms. The ascospores typically contain ascospores, which are rounded or elongated and can be aerosolized, acting as probable transmission propagules from one individual to another (Hauser and Cushion, 2018). Each *Pneumocystis* sp. is host-specific for one mammal species (a characteristic known as stenoxenism) and cannot be grown in laboratory artificial media (Akbar et al., 2012; Hauser and Cushion, 2018).

H. capsulatum and *P. jirovecii* coinfection was previously reported in a few studies (Baughman et al., 1994; Gago et al., 2014; Huber et al., 2008; Le Gal et al., 2013; Velásquez et al., 2010; Wheat et al., 1985). Most of these studies were developed in samples from hospitalized AIDS patients, where *Histoplasma* was diagnosed by culture growth and *Pneumocystis* by Grocott staining of bronchoalveolar lavage (BAL) or pulmonary biopsies. Three studies have described *H. capsulatum* and *Pneumocystis* sp. coinfection using molecular methods: Gago et al. (2014), who used a multiplex PCR assay in human BAL or biopsy samples; González-González et al. (2014), who used specific nested PCRs in lung samples of randomly captured *Tadarida brasiliensis* bats from Argentina, Mexico, and French Guyana; and Almeida-Silva et al. (2016), who reported an HIV patient with several opportunistic fungal infections detected by nested PCR and multiplex qPCR.

H. capsulatum and *Pneumocystis* sp. share different characteristics that support the possibility of coinfection in the same individual. They are ascomycete fungi that infect through the host's respiratory tract. The lung is the main target organ for both fungi, causing the pulmonary disease representative of their most common clinical form. However, some biological, pathogenic, and clinical differences are remarkable between both parasites. For *H. capsulatum*, yeasts are preferentially found in the host's intracellular space (primarily within macrophages). For *Pneumocystis* sp., the two morphotypes are particularly found in the host extracellular space, and the trophic forms develop strong interactions with alveolar epithelial cells. *H. capsulatum* is found in natural habitats, whereas *Pneumocystis* spp. have only been described in infected hosts. *H. capsulatum* does not colonize healthy or immunocompetent individuals, and no possible respiratory transmission from one individual to another has been reported, whereas both features are common for *Pneumocystis* sp. (Köhler et al., 2017; Pomerville, 2018; Skalski et al., 2015). Overall, histoplasmosis patients can develop disseminated disease (rarely seen in pneumocystosis).

The aim of this study was to detect the frequency of *H. capsulatum* and *P. jirovecii* coinfection, using specific molecular methods for each fungus, in BAL samples of patients from a tertiary care hospital focused on respiratory diseases in Mexico.

Materials and methods

Patients

This study was developed in two periods: from June to October 2014, and from May to September 2016. We considered a total of

289 patients hospitalized for acute pulmonary diseases at the Instituto Nacional de Enfermedades Respiratorias "Ismael Cosío Villegas" (INER), in Mexico City, CDMX, Mexico, who required a bronchoscopy diagnostic procedure due to hypoxicemic pneumonia. We also analyzed eight samples collected in 2011 from healthy volunteers, which were kindly donated by the team of Dr. Eduardo Sada Díaz, from the "Departamento de Investigación en Microbiología" at INER, as noninfected controls for molecular diagnosis of *H. capsulatum* and *P. jirovecii*. No samples were obtained ex professo for this study.

Clinical data processed from the medical record of each patient were sex, age, place of birth, lactate dehydrogenase (LDH) levels, smoking status, guano exposure, travel history, and main outcome at hospital discharge. Laboratory data evaluated included complete blood count, HIV status (including viral load and CD4⁺ cell count), and BAL sample laboratory procedures, such as bacterial and fungal cultures (for *H. capsulatum*), Grocott staining (for *P. jirovecii*), as well as multiplex viral PCR and other specific tests for the diagnosis of infectious diseases, which were performed according to physician requests.

BAL samples

From all patients considered for this study, we analyzed one BAL sample. After BAL collection, samples were centrifuged at 2850 × g for 20 min, the supernatant was aliquoted in 600-μl microtubes (Eppendorf, Inc., Enfield, CT, USA) and frozen at -80 °C in less than one hour for other studies, and the pellet was processed for DNA extraction to search for *H. capsulatum* and *P. jirovecii*.

DNA extraction

The pellet of each BAL sample was processed for DNA extraction using a commercial kit (Molecular Biology Kit, Bio Basic Inc., Toronto, ON, CA), according to manufacturer's instructions. DNA samples were quantified in an Epoch microplate spectrophotometer (BioTek Instruments Inc., Winooski, VT, USA) at 260–280 nm and then stored at -80 °C until required. To avoid contamination during molecular screening, all DNA samples were processed in specialized cabinets for each step of the molecular assays performed.

Molecular screening for *H. capsulatum* in DNA samples

Fungal presence was investigated in each extracted DNA sample using a nested PCR for a fragment of the *Hcp100* gene encoding a 100-kDa protein, a molecular marker highly specific for this pathogen (Bialek et al., 2002; Taylor et al., 2005). Two sets of primers were used; the outer primer set included HcI (5'-GCG-TTC-CGA-GCC-TTC-CAC-CTC-AAC-3') and HcII (5'-ATG-TCC-CAT-CGG-GCG-CCG-TGT-AGT-3'); the inner primers were HcIII (5'-GAG-ATC-TAG-TGGCGG-CCA-GGT-TCA-3') and HcIV (5'-AGG-AGA-GAA-CTG-TAT-CGG-TGG-CTT-G-3'), delimiting a 210-bp fragment unique to *H. capsulatum*. Details of the amplification are provided in González-González et al. (2012). DNA from the EH-53 *H. capsulatum* strain from a Mexican clinical case was used as a positive control, and milli-Q water (Milli-Q water purifier, Merck KGaA, Darmstadt, DE) was always processed as a negative control.

Molecular screening for *P. jirovecii* in DNA samples

We used nested PCR for the amplification of two genes that are reliable markers for *Pneumocystis* detection: the mitochondrial ribosomal large subunit (mtLSURNA) and the mitochondrial ribosomal small subunit (mtSSURNA) (Wakefield et al., 2003). For the mtLSURNA locus, we used the outer primer set pAZ102-H

(5'-GTG-TAC-GTT-GCA-AAG-TAG-TC-3') and pAZ102-E (5'-GAT-GGC-TGT-TTC-CAA-GCC-CA-3'). The inner primers, pAZ102-X (5'-GTG-AAA-TAC-AAA-TCG-GAC-TAG-G-3') and pAZ102-Y (5'-TCA-CIT-AAT-ATT-AAT-TGG-GGA-GC-3'), delimit a 267-bp fragment specific for *Pneumocystis* sp. Nested PCR for the mtSSUrRNA locus was performed with the outer primers, pAZ112-10F (5'-GGG-AAT-TCT-AGA-CGG-TCA-CAG-AGA-TCA-G-3') and pAZ112-10R (5'-GGG-AAT-TCT-AGC-AAC-GAT-TAC-TAG-CAA-CCC-3'). The inner primers, pAZ112-13RI (5'-GGG-AAT-TCG-AAG-CAT-GTT-GTT-TAA-TTC-G-3') and pAZ112-14RI (5'-GGG-AAT-TCT-TCA-AAG-AAT-CGA-GTT-TCA-G-3'), delimit a 300-bp fragment specific for *Pneumocystis* sp. (González-González et al., 2014). A DNA sample obtained from a pulmonary biopsy from a patient diagnosed by Grocott staining with pneumocystosis was used as a positive control. Milli-Q water (Merck) was always used as a negative control for both *Pneumocystis* molecular markers.

Amplified products (amplicons)

Amplicons from each nested PCR were electrophoresed on a 1.8% agarose gel in 0.5X Tris-borate-EDTA buffer. Electrophoresis was conducted at 120V for 50 min using a 100-bp DNA ladder (Gibco Laboratories, Grand Island, NY, USA) as a molecular size marker. The amplicons were visualized using a UV transilluminator after GelRed Nucleic Acid Gel Stain (Thermo Fisher Scientific Inc., Waltham, MA, USA) staining (0.5 µg/100 ml). The amplicons were purified using the Nucleotrap PCR Purification Kit (BD Biosciences, Palo Alto, CA, USA) and sent to the High-Throughput Genomics Center (University of Washington, Seattle, WA, USA) for sequencing of the sense and antisense DNA strands; a consensus sequence for each amplified sample was generated.

Sequence analyses

The generated sequences were aligned and manually edited using MEGA software, version 7, <http://www.megasoftware.net> (Kumar et al., 2016), and their alignments are provided in the electronic supplementary material (Supplementary files 1, 2 and 3) for the readers' reference.

Sequences were analyzed to confirm their high homology for each marker, which was the main criterion for the molecular identification of each fungus in BAL samples, considering for *P. jirovecii* at least one of the two markers used. First, the sequences were analyzed using the BLASTn algorithm (<http://blast.ncbi.nlm.nih.gov/Blast.cgi>) to search in the GenBank database for all homologous sequences corresponding to the nested PCR products of *H. capsulatum* and *P. jirovecii* gene fragments. Afterward, sequence analysis with the neighbor-joining (NJ) method was used to construct the respective genetic relationship trees for each marker using MEGA7 (Kumar et al., 2016). To infer the NJ trees, genetic distances were conducted using the Kimura two-parameter model, considering gaps/missing data and mutation rates between the analyzed nucleotide sites. Bootstrap values (bt) for NJ analyses were based on 1000 replicates (Kumar et al., 2016). To construct the NJ trees, Hcp100 sequences were aligned with the sequence of the G-217B reference strain from Louisiana, USA (GenBank accession no. AJ005963); mtLSUrRNA sequences were aligned with the reference sequence of *P. jirovecii* EH1-PAZ102E (GenBank accession no. JF733748); and mtSSUrRNA sequences were aligned with the reference sequence of *P. jirovecii* (GenBank accession no. HQ228547).

Statistical analyses

The total infection rate was estimated considering all patients. The Chi-Square (χ^2) test was used to detect significant differences

between the groups of patients infected with *H. capsulatum*, *P. jirovecii* or both fungi. The prevalence odds ratio test and its corresponding 95% confidence interval (95% CI) were calculated to evaluate the possible strength of the association between each different analyzed variable and the occurrence of histoplasmosis, pneumocystosis or their coinfection. Both statistical analyses were performed using SPSS Statistics version 21.0 (SPSS Inc., Chicago, IL, USA). Values of $P < 0.05$ were considered significant.

Results

We analyzed BAL samples from 289 patients: 84 (29.1%) were from HIV patients and 205 (70.9%) were from non-HIV patients. Seventy-one HIV patients were male and 13 were female with a median age of 34 years, showing a median HIV viral load of 246 852 copies/ml and a median CD4⁺ count of 23 cells/ml of peripheral blood. One hundred and ten non-HIV patients were male and 95 were female with a median age of 54 years. Most individuals (66.4%) lived in Mexico City and the surrounding conurbation, whereas the rest of patients (33.6%) came from rural areas.

Out of 289 patient BAL samples, the amplified Hcp100 marker diagnosed the presence of *H. capsulatum* infection in 60 patients (20.8%), which included four patients with positive cultures for *H. capsulatum*. The amplification of either mtLSUrRNA or mtSSUrRNA locus diagnosed the presence of *P. jirovecii* infection in 45 cases (15.6%) (Table 1). Regarding *P. jirovecii* detection using two independent molecular markers (mtLSUrRNA and mtSSUrRNA) for its identification, it is important to remark that both markers were amplified in 34 samples, whereas the mtLSUrRNA marker generated more sequences (47) than the mtSSUrRNA (33). None of these markers was amplified in any of the samples from noninfected controls (healthy volunteers). Milli-Q water was always negative in each assay performed.

The BLASTn analysis for Hcp100 sequences showed a range from 94 to 100% similarity between them and the GenBank reference sequence from *H. capsulatum*, whereas mtLSUrRNA and mtSSUrRNA sequences showed a range from 98 to 100% similarity between them and the reference sequences from *P. jirovecii*.

All *H. capsulatum* Hcp100 sequences analyzed by NJ are represented in Figure 1, and the cluster of these sequences supports a close genetic relationship among them. Figure 2 shows the sequence trees analyzed by NJ for the *P. jirovecii* mtSSUrRNA (Figure 2a) and mtLSUrRNA (Figure 2b) markers, respectively, and the topologies of these trees sustained a close genetic relationship among the sequences.

The molecular tools used in this study revealed that 12 (4.2%) patients presented both *H. capsulatum* and *P. jirovecii* infections simultaneously. Out of these 12 coinfecting patients, nine samples belonged to HIV patients (10.7% of 84 HIV patients) and the other three to non-HIV patients (1.5% of 205 non-HIV patients) (Table 1).

The main data for all studied patients, such as sex, age, HIV status, LDH levels, smoking status, guano exposure, mechanical ventilation, and lethality, are provided in Table 1. The last column shows the results of the χ^2 test for each variable to detect significant differences among the groups of patients infected with *H. capsulatum*, *P. jirovecii* or both fungi, and P values are shown in Table 1. Demographic and clinical data such as sex, LDH levels, mechanical ventilation, and lethality did not show significant differences between groups. Two important risk factors were assessed for the fungal infections studied, such as smoking status (for *H. capsulatum* and *P. jirovecii*) or guano exposure (for *H. capsulatum* only). Significant differences were found between smoking and nonsmoking patients ($P=0.002$), considering the *H. capsulatum*, *P. jirovecii* and coinfecting groups of patients. No significant differences ($P=0.270$) were found among patients exposed to guano in the environment in regard to *H. capsulatum*

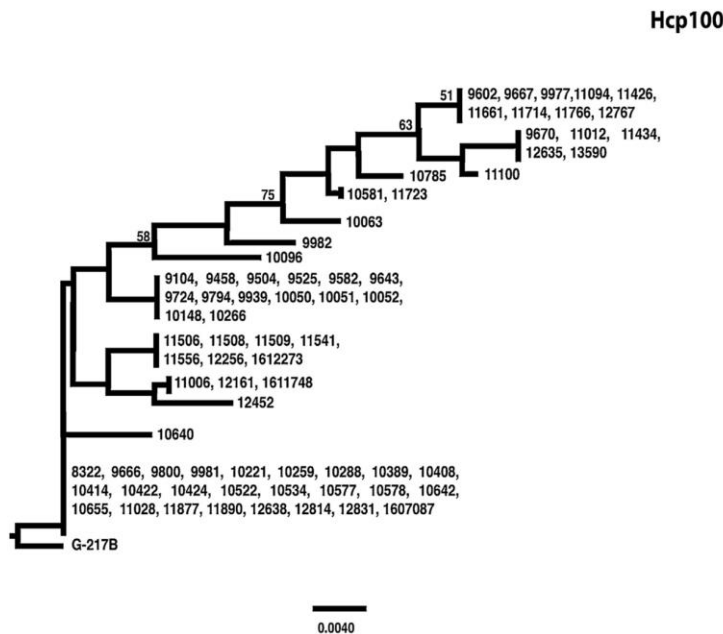
Table 1

Main data from histoplasmosis, pneumocystosis and coinfected patients.

Demographic and clinical data	<i>H. capsulatum</i> infection only n=60	<i>P. jirovecii</i> infection only n=45	Coinfection n=12	P
Age ^a (years)	46 [32–66]	37 [30–47]	34 [30–44]	
Sex				0.212
Female	21 (35%)	15 (33%)	2 (16.7%)	
Male	39 (65%)	30 (66.7%)	10 (83.3%)	
HIV patients	16 (26.7%)	32 (71%)	9 (75%)	<0.0001
Viral load ^a (copies/ml)	293 479 [24 064–848 244]	427 572 [34 951–851 138]	462 080 [228 922–933 417]	
CD4+ count ^a (cells/ml)	42 [10–56]	21 [7–42]	25 [7–42]	
Non-HIV patients	44 (73.3%)	13 (28.9%)	3 (25%)	
LDH ^a (U/l)	186 [140–273]	227 [152–341]	279 [140–396]	0.070
Smoking				0.002
Active	26 (43.3%)	19 (42.2%)	3 (25%)	
Passive	12 (20%)	4 (8.9%)	0 (0%)	
None	16 (26.7%)	16 (35.6%)	8 (66.7%)	
No data	6 (10%)	6 (13.3%)	1 (8.3%)	
Guano exposure				0.270
Yes	17 (28.3%)	11 (24.5%)	2 (16.7%)	
No	37 (61.7%)	28 (62.2%)	9 (75%)	
No data	6 (10%)	6 (13.3%)	1 (8.3%)	
Mechanical ventilation				0.129
Yes	17 (28.3%)	14 (31.1%)	6 (50%)	
No	37 (61.7%)	25 (55.6%)	5 (41.7%)	
No data	6 (10%)	6 (13.3%)	1 (8.3%)	
Lethality				0.088
Yes	10 (16.7%)	6 (13.3%)	4 (33.3%)	
No	44 (73.3%)	33 (73.4%)	7 (58.4%)	
No data	6 (10%)	6 (13.3%)	1 (8.3%)	

LDH: Lactate dehydrogenase.

Percentages in parentheses were estimated considering the number of patients in each infected group.

^a Median values of these clinical data are shown, with the corresponding interquartile range (IQR 25–75) in brackets.**Figure 1.** NJ analysis of the *H. capsulatum* sequences. The NJ tree was constructed using a matrix of 142-nt of the Hcp100 gene fragments. The NJ analysis was conducted as described in Materials and methods. Supporting bt values ≥50% are indicated on their corresponding tree branches.

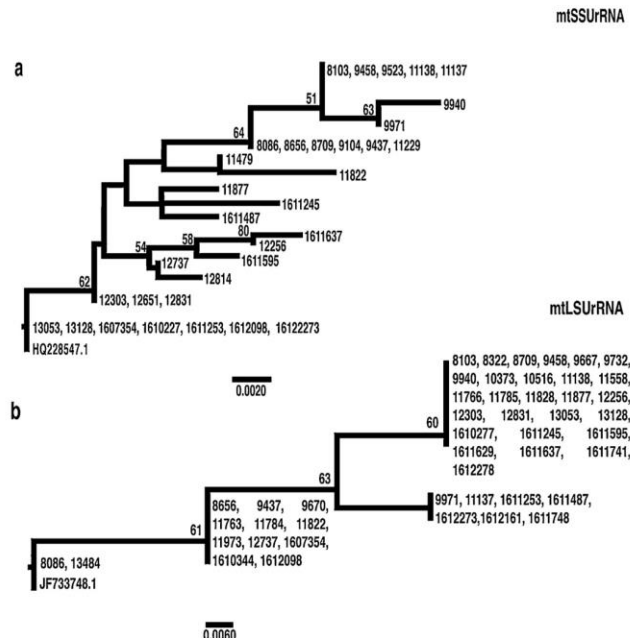


Figure 2. NJ analyses of the *P. jirovecii* sequences. (a) For the mtSSUrRNA sequences, the NJ tree was constructed using a matrix of 274-nt. (b) For the mtLSUrRNA sequences, the NJ tree was constructed using a matrix of 176-nt. The NJ analyses were conducted as described in Materials and methods. Supporting bt values $\geq 50\%$ are indicated on their corresponding tree branches.

and coinfected groups of patients. Based on additional information from the hospital records, we found that *H. capsulatum* was detected in 25.5% of the patients from urban areas and in 23.7% of the patients from rural areas, whereas *P. jirovecii* was detected in 18.2% of the patients from urban areas and in 22.6% of the patients from rural areas, and no significant differences were detected. Other laboratory data (hemoglobin, hematocrit, total leukocyte count, and platelet count) for each group of patients studied revealed no significant differences among patients with histoplasmosis, pneumocystosis and coinfection (data not shown).

According to laboratory reports, *H. capsulatum* cultures were positive only in four BAL samples of HIV/AIDS patients, corresponding to 5.6% of all the *H. capsulatum*-positive samples detected by PCR, whereas *P. jirovecii* was observed by Grocott staining only in 14 BAL samples, representing 24.6% of all the *P. jirovecii*-positive samples detected by PCR.

Microorganisms distinct from the studied fungi were detected only in 44 out of 289 patients, by culture (for bacteria and other fungi) and by multiplex PCR (for viruses), as reported in the clinical records. Eight patients were infected with *M. tuberculosis*, 14 with Gram-negative bacteria and four with Gram-positive bacteria. Mixed infections with different microorganisms (virus-bacteria, bacteria-bacteria, bacteria-fungi or virus-fungi) were found in 19 patients; 11 patients presented more than two types of microorganisms. Interestingly, out of the 12 patients coinfected with *H. capsulatum* and *P. jirovecii*, three were infected with other microorganisms that could be part of the normal microbiota of the upper respiratory tract: one patient had *Pseudomonas aeruginosa*, the second had *P. aeruginosa* and *Klebsiella pneumoniae*, and the third had *P. aeruginosa*, parainfluenza 2 virus and rhinovirus.

Details about the different microorganisms found in the studied groups are available in the Supplementary Table.

Figure 3 shows a detailed description of the statistical analyses for histoplasmosis, pneumocystosis and coinfection in HIV vs. non-HIV patients.

The prevalence of histoplasmosis infection in the whole studied population was 20.8% (60 of 289 patients), whereas the prevalence in HIV patients was slightly lower (19%) than in non-HIV patients (21.5%); however, this difference was not significant ($P=0.64$) (Figure 3a).

The prevalence of pneumocystosis infection in the whole studied population was 15.6% (45 of 289 patients), and it was significantly higher in HIV patients with $P < 0.0001$ (38.1%) when compared to non-HIV patients (6.3%). Moreover, the estimated prevalence odds ratio for pneumocystosis was 9.08 (95% CI, 4.45–18.56), which suggested that infection with *P. jirovecii* was 9.08-fold more possible in HIV patients (Figure 3b).

The prevalence of coinfection with both fungi was 4.2% (12 of 289 patients), and the frequency of coinfection in HIV patients (10.7%) was significantly higher than in non-HIV patients (1.5%) with $P=0.001$. Therefore, the prevalence odds ratio estimated for coinfection was 8.08 (95% CI, 2.13–30.6), revealing that HIV patients had an 8.08-fold greater probability of becoming infected with both fungi (Figure 3c).

In particular, it is remarkable that the lethality rate for patients in the histoplasmosis-pneumocystosis coinfection group (33.3%, 4 of 12 patients) was higher than the lethality rate for patients with only histoplasmosis infection (16.6%, 10 of 60 patients) or only pneumocystosis infection (13.3%, 6 of 45 patients), even though these results were not statistically significant (see Table 1).



Histoplasma capsulatum and *Pneumocystis jirovecii* coinfection in hospitalized HIV and non-HIV patients from a tertiary care hospital in Mexico



Laura E. Carreto-Binaghi^{a,b}, Fernando R. Morales-Villarreal^c, Guadalupe García-de la Torre^d, Tania Vite-Garín^a, Jose-Antonio Ramirez^a, El-Moukhtar Aliouat^e, Jose-Arturo Martínez-Orozco^c, María-Lucía Taylor^{a,*}

^aLaboratorio de Inmunología de Hongs, Unidad de Micología, Departamento de Microbiología-Parasitología, Facultad de Medicina, Universidad Nacional Autónoma de México (UNAM), CDMX, 04510, Mexico

^bDepartamento de Investigación en Microbiología, Instituto Nacional de Enfermedades Respiratorias "Ismael Cosío Villegas" (INER), CDMX, 14080, Mexico

^cDepartamento de Microbiología Clínica, INER, CDMX, 14080, Mexico

^dDepartamento de Salud Pública, Facultad de Medicina, UNAM, CDMX, 04510, Mexico

^eUniv. Lille, CNRS, Inserm, CHU Lille, Institut Pasteur de Lille, U1019 – UMR 8204 – CIL – Centre d'Infection et d'Immunité de Lille, Lille, France

ARTICLE INFO

Article history:

Received 30 January 2019

Received in revised form 10 June 2019

Accepted 11 June 2019

Corresponding Editor: Eskild Petersen, Aarhus, Denmark

Keywords:

Histoplasmosis

Pneumocystosis

Coinfection

Molecular diagnosis

Bronchoalveolar lavage

ABSTRACT

Background: *Histoplasma capsulatum* and *Pneumocystis jirovecii* are respiratory fungal pathogens that principally cause pulmonary disease. Coinfection with both pathogens is scarcely reported. This study detected this coinfection using specific molecular methods for each fungus in the bronchoalveolar lavage (BAL) of patients from a tertiary care hospital.

Materials and methods: BAL samples from 289 hospitalized patients were screened by PCR with specific markers for *H. capsulatum* (Hcp100) and *P. jirovecii* (mtLSUrRNA and mtSSUrRNA). The presence of these pathogens was confirmed by the generated sequences for each marker. The clinical and laboratory data for the patients were analyzed using statistical software.

Results: The PCR findings separated three groups of patients, where the first was represented by 60 (20.8%) histoplasmosis patients, the second by 45 (15.6%) patients with pneumocystosis, and the last group by 12 (4.2%) patients with coinfection. High similarity among the generated sequences of each species was demonstrated by BLASTn and neighbor-joining algorithms. The estimated prevalence of *H. capsulatum* and *P. jirovecii* coinfection was higher in HIV patients.

© 2019 The Authors. Published by Elsevier Ltd on behalf of International Society for Infectious Diseases. This is an open access article under the CC BY-NC-ND license (<http://creativecommons.org/licenses/by-nc-nd/4.0/>).

Introduction

Histoplasma capsulatum is the causative agent of histoplasmosis, one of the most important systemic mycoses in humans; this disease is particularly related to endemic regions in America, and autochthonous outbreaks have been described from latitude 54° north (Alberta, Canada) (Anderson et al., 2006) to 38° south (Neuquén, Argentina) (Calanni et al., 2013). The epidemic form of

histoplasmosis commonly implies an occupational risk, as reported in some Latin American countries, but currently, it represents a human immunodeficiency virus (HIV)-defining condition (Centers for Disease Control and Prevention, 2008). Thus, *H. capsulatum* could be considered a primary fungal pathogen because it infects healthy people, although it also shows an opportunistic behavior since it causes more severe disease in immunocompromised individuals.

H. capsulatum is a dimorphic fungus with two morphotypes, a mycelial infective phase found mainly in bat and bird guano and a yeast virulent phase, which can survive within macrophages and depicts a chronic granulomatous inflammation in host tissues (Köhler et al., 2017; Pomerville, 2018). Infection occurs by inhalation of aerosolized mycelial propagules (mainly microconidia and small hyphal fragments), which become yeasts upon entering the hosts respiratory tract.

* Corresponding author.

E-mail addresses: lauraelena_c@yahoo.com (L.E. Carreto-Binaghi), fernando62fmv@gmail.com (F.R. Morales-Villarreal), gsgarciaadelatorre@gmail.com (G. García-de la Torre), tania.vite.garin@gmail.com (T. Vite-Garín), anton100559@hotmail.com (J.-A. Ramirez), elmoukhtar.aliouat-3@univ-lille2.fr (E.-M. Aliouat), jarturoinfectologia@iner.gob.mx (J.-A. Martínez-Orozco), emello@unam.mx (M.-L. Taylor).

we estimated a coinfection rate of 13.3%. Later, Baughman et al. (1994) screened opportunistic infections in 894 BAL samples from AIDS patients; they found 420 (46.97%) patients with *Pneumocystis*, five of whom were coinfecte with *H. capsulatum* (0.55% according to our estimation). In French Guiana, Huber et al. (2008) described 200 cases of AIDS-associated histoplasmosis over 25 years; seven were coinfecte with *Pneumocystis* (3.5% according to our estimation). Velásquez et al. (2010) studied 44 HIV/AIDS patients with histoplasmosis and found concomitant pneumocystosis in 11.4% of the cases. Caceres et al. (2018) reported three cases of pneumocystosis in 45 HIV patients with histoplasmosis (6.7% with coinfection, according to our estimation). Interestingly, Le Gal et al. (2013) described the intracellular coexistence of *H. capsulatum* and *P. jirovecii* in an alveolar macrophage from a BAL sample of one AIDS patient.

The abovementioned reports were entirely focused on HIV patients, and most of the frequencies of coinfection that we estimated from their results were similar to our reported rate of 10.7% (9 of 84 HIV patients). Coinfection could be explained by the virus-related immunocompromised condition, which makes the patients more susceptible to concomitant infections.

In regard to the LDH levels, which is a marker associated with the prognosis of patients with disseminated histoplasmosis (Butt et al., 2002; Ramos et al., 2018) and more frequently used to distinguish bacterial from *Pneumocystis pneumonia* (Sun et al., 2016), our results showed that the serum LDH levels were not significant to support the diagnosis of either histoplasmosis or pneumocystosis.

Other risk factors assessed in this study were smoking and guano exposure. Smoking has been previously reported as a risk factor for complications in the ocular histoplasmosis syndrome (Chheda et al., 2012; Ganley, 1973). Additionally, smoking is a presumed risk factor for presenting *P. jirovecii* pneumonia in HIV patients (Blount et al., 2013; Miguez-Burbano et al., 2005) and in non-HIV patients (Santos et al., 2017). Regarding the lack of significance in the analysis concerning guano exposure related to *H. capsulatum* infection, it is important to emphasize that histoplasmosis outbreaks might occur both in rural and urban areas because the fungus has been found in several niches where people could be inadvertently exposed. (Corcho-Berdugo et al., 2011; Muñoz et al., 2010; Taylor et al., 2005). However, other risk factors associated with histoplasmosis or pneumocystosis, such as previous treatment with immunosuppressive drugs, were scarcely referred for the studied patients.

It would be fascinating to identify the influence of one pathogen in regard to the other on the coinfection outcome; however, it was not possible to detect this association because some patients' medical records were incomplete. It is crucial to underline the higher lethality rate associated with coinfection, suggesting a contribution of both pathogens in the fatal clinical course of the patients (Table 1). In general, most of the causes of death referred for histoplasmosis, pneumocystosis and coinfecte patients were pneumonia with sepsis and/or septic shock.

An important feature to consider from most studies is the diagnostic procedure used for histoplasmosis (culture) and pneumocystosis (microscopic observation), which require specialized supplies and technical experience for successful diagnosis. Therefore, new methods should be implemented to detect coinfection with these fungi. To date, only a few studies have used molecular methods. Gago et al. (2014) reported one of 14 HIV patients with *H. capsulatum* and *P. jirovecii* coinfection (7.14% according to our estimation) while developing a multiplex PCR assay for fungi. González-González et al. (2014) described coinfection with *H. capsulatum* and *Pneumocystis* spp. in 122 randomly captured bats (35.2% of cases), supporting a high frequency of both pathogens in this particular host (González-González et al., 2014). Thus, we

chose molecular methods for histoplasmosis and pneumocystosis diagnosis due to their rapid, specific and accurate detection, emphasizing that these methods were very useful to reveal *H. capsulatum* and *P. jirovecii* in BAL samples. We would like to emphasize that the four HIV/AIDS patients with positive *H. capsulatum* cultures also amplified the specific marker Hcp100, which highlights the efficiency of the molecular method used. Fungal sequences generated by PCR, using DNA extracted from BAL samples, reflected active mycotic disease, and the specificity of the molecular markers used in the present study makes misdiagnosis very improbable. In contrast, immunological diagnostic procedures sometimes are unable to differentiate past from present infection. For both fungi, we selected nested PCR protocols, which have been demonstrated to be very sensitive, reproducible for the identification of pathogens in different clinical samples, and able of avoiding molecular contamination under well-controlled laboratory conditions. Moreover, nested PCR is a useful tool for epidemiological studies, where this method serves as a great screening technique when compared to real-time PCR (Seo et al., 2014; Sharifdini et al., 2015).

We considered the generated sequence of each marker as a unique criterion for diagnosis because the single visualization of the amplified PCR products could lead to misinterpretation or overdiagnosis of the results and because non-specific products could sometimes be produced. Although our criterion is very strict, it is undoubtedly precise and reliable, as demonstrated by BLASTn and NJ genetic analyses of the generated sequences. Thus, the close genetic relationship among the sequences of Hcp100 for *H. capsulatum* and among the sequences of mtLSUrRNA and mtSSUrRNA for *P. jirovecii* confirmed their respective fungal molecular identification. The scientific literature has reported mtLSUrRNA marker as a better diagnostic tool for *P. jirovecii*; however, based on our previous experience (González-González et al., 2014), we also selected the mtSSUrRNA marker because the fungus was identified in a few samples in which only this marker was amplified.

In conclusion, statistical analyses support the highest prevalence of pneumocystosis and coinfection in HIV patients, and based on our findings, *H. capsulatum* and *P. jirovecii* coinfection is a more common medical problem than expected, not only in immunocompromised patients. Searching for both pathogens at the initial stages of disease should be routinely performed to establish adequate treatments for both fungi to improve patient outcomes and diminish the risk for complications. Basic research studies on this coinfection are still needed to explain the interaction of the two pathogens in vivo.

Funding

This paper was only supported by the internal funding of the Laboratorio de Inmunología de Hongos, Facultad de Medicina, UNAM.

Ethical approval

Patients' and volunteers' BAL samples were obtained in accordance with the ethical standards of the Helsinki Declaration (1964, amended in 2008). Written consent was obtained and kept in the hospital's individual medical records. This work was approved by the School of Medicine Research and Ethics Committee (UNAM, report 132/2015) and by the INER Ethics Research Committee (protocol B13-14).

Conflict of interest

The authors declare that they have no conflicts of interest.

Authors' contributions

LECB and MLT conceived the study, participated in its design and coordination and helped to draft the manuscript. LECB and FRMV collected the samples. LECB and JAR performed the experimental procedures. MLT, LECB, GGT, TVG, and JAR analyzed the data. EMA and JAMO drafted the manuscript and revised it critically for important intellectual content. JAMO and MLT share the academic responsibility for this manuscript. All authors read and approved the final manuscript.

Acknowledgments

LECB thanks the "Programa de Doctorado en Ciencias Biológicas", Universidad Nacional Autónoma de México (UNAM) and fellowship No. 329884 from "Consejo Nacional de Ciencia y Tecnología Mexico (CONACYT-Mexico)". The authors thank I. Mascher for editorial assistance and Dr. Olivia Sánchez Cabral, Dr. Berenice López González, Dr. Iván Rodolfo García Izquierdo, Dr. Miguelina Altgracia Jaquez Carrasco, and the bronchoscopy team from INER for their valuable help during the BAL collection.

Appendix A. Supplementary data

Supplementary material related to this article can be found, in the online version, at doi:<https://doi.org/10.1016/j.ijid.2019.06.010>.

References

- Akbar H, Pinçon C, Aliouat-Denis CM, Derouiche S, Taylor ML, Pottier M, et al. Characterizing *Pneumocystis* in the lungs of bats: understanding *Pneumocystis* evolution and the spread of *Pneumocystis* organisms in mammal populations. *Appl Environ Microbiol* 2012;78(22):8122–36.
- Almeida-Silva F, Damasceno LS, Serna MJ, Valero C, Quintella LP, Almeida-Paes R, et al. Multiple opportunistic fungal infections in an individual with severe HIV disease: a case report. *Rev Iberoam Microl* 2016;33(2):118–21.
- Anderson H, Honish L, Taylor G, Johnson M, Tovstuk C, Fanning A, et al. Histoplasmosis cluster, golf course, Canada. *Emerg Infect Dis* 2006;12(1):163–5.
- Baughman RP, Dohn MN, Frame PT. The continuing utility of bronchoalveolar lavage to diagnose opportunistic infection in AIDS patients. *Am J Med* 1994;97(6):515–22.
- Bialek R, Feucht A, Aepinus C, Just-Nübling G, Robertson VJ, Knobloch J, et al. Evaluation of two nested PCR assays for detection of *Histoplasma capsulatum* DNA in human tissue. *J Clin Microbiol* 2002;40:1644–7.
- Blount RJ, Djawe K, Daly KR, Jarlsberg LG, Fong S, Balmes J, et al. Ambient air pollution associated with suppressed serologic responses to *Pneumocystis jirovecii* in a prospective cohort of HIV-infected patients with *Pneumocystis* pneumonia. *PLoS One* 2013;8(11):e80795.
- Butt AA, Michaels S, Greer D, Clark R, Kissinger P, Martin DH. Serum LDH level as a clue to the diagnosis of histoplasmosis. *AIDS Read* 2002;12(7):317–21.
- Caceres DH, Tobón AM, Restrepo A, Chiller T, Gómez BL. The important role of coinfections in patients with AIDS and progressive disseminated histoplasmosis (PDH): a cohort from Colombia. *Med Mycol Case Rep* 2018;19:41–4.
- Calamini LM, Pérez RA, Brasil S, Schmidt NG, Iovannitti CA, Zuliani MF, et al. Outbreak of histoplasmosis in province of Neuquén, Patagonia Argentina. *Rev Iberoam Microl* 2013;30(3):193–9 [in Spanish].
- Centers for Disease Control and Prevention. AIDS-defining conditions. 2008. [Accessed 15 November 2018] <https://www.cdc.gov/mmwr/preview/mmwrhtml/rr5710a2.htm>.
- Chheda LV, Ferketic AK, Carroll CP, Moyer PD, Kurz DE, Kurz PA. Smoking as a risk factor for choroidal neovascularization secondary to presumed ocular histoplasmosis syndrome. *Ophthalmology* 2012;119(2):333–8.
- Corcho-Berdugo A, Muñoz-Hernández B, Palma-Cortés G, Ramírez-Hernández A, Martínez-Rivera M, Fries-de León M, et al. [An unusual outbreak of histoplasmosis in residents of the state of Mexico]. *Gac Med Mex* 2011;147(5):377–84 [in Spanish].
- Frenkel JK. *Pneumocystis jirovecii* n. sp. from man: morphology, physiology, and immunology in relation to pathology. *Natl Cancer Inst Monogr* 1976;43:13–30.
- Gago S, Esteban C, Valero C, Zaragoza O, Puig de la Bellacasa J, Buitrago MJ. A multiplex real-time PCR assay for identification of *Pneumocystis jirovecii*, *Histoplasma capsulatum*, and *Cryptococcus neoformans/Cryptococcus gattii* in samples from AIDS patients with opportunistic pneumonia. *J Clin Microbiol* 2014;52(4):1168–76.
- Ganley JP. Epidemiologic characteristics of presumed ocular histoplasmosis. *Acta Ophthalmol Suppl* 1973;119:1–63.
- González-González AE, Aliouat-Denis CM, Carreto-Binaghi LE, Ramírez JA, Rodríguez-Arellanes G, Demanche C, et al. An Hcp100 gene fragment reveals *Histoplasma capsulatum* presence in lungs of *Tadarida brasiliensis* migratory bats. *Epidemiol Infect* 2012;140(11):1955–63.
- González-González AE, Aliouat-Denis CM, Ramírez-Bárcenas JA, Demanche C, Pottier M, Carreto-Binaghi LE, et al. *Histoplasma capsulatum* and *Pneumocystis* spp. co-infection in wild bats from Argentina, French Guyana, and Mexico. *BMC Microbiol* 2014;14:23. doi:<http://dx.doi.org/10.1186/1471-2180-14-23>.
- Hauser PM, Cushion MT. Is sex necessary for the proliferation and transmission of *Pneumocystis*? *PLoS Pathog* 2018;14(12):e1007409.
- Huber F, Nacher M, Aznar C, Pierre-Demar M, El Guedj M, Vaz T, et al. AIDS-related *Histoplasma capsulatum* var. *capsulatum* infection: 25 years experience of French Guiana. *AIDS* 2008;22(9):1047–53.
- Köhler JR, Huber B, Puccia R, Casadevall A, Perfect JR. Fungi that infect humans. In: Heitman J, Howlett B, Crous P, Stukenbrock E, James T, Gow N, editors. *The fungal kingdom*. Washington: ASM Press; 2017. p. 813–43.
- Kumar S, Stecher G, Tamura K. MEGA7: Molecular Evolutionary Genetics Analysis Version 7.0 for bigger datasets. *Mol Biol Evol* 2016;33(7):1870–4.
- Le Gal S, Damiani C, Virmaux M, Schmit JL, Totet A, Nevez G. Photo quiz: a 39-year-old man with human immunodeficiency virus infection presenting with an alveolo-interstitial pulmonary syndrome. *J Clin Microbiol* 2013;51(9):3165 2809.
- Miguez-Burbaro MJ, Ashkin D, Rodriguez A, Duncan J, Pitchenik A, Quintero N, et al. Increased risk of *Pneumocystis carinii* and community-acquired pneumonia with tobacco use in HIV disease. *Int J Infect Dis* 2005;9(4):208–17.
- Morris A, Norris KA. Colonization by *Pneumocystis jirovecii* and its role in disease. *Clin Microbiol Rev* 2012;25(2):297–317.
- Morris A, Scurba FC, Norris KA. *Pneumocystis*: a novel pathogen in chronic obstructive pulmonary disease? *COPD* 2008;5(1):43–51.
- Muñoz B, Martínez MA, Palma GH, Ramírez A, Fries MG, Reyes MR, et al. Molecular characterization of *Histoplasma capsulatum* isolated from an outbreak in treasure hunters. *BMC Infect Dis* 2010;10:264.
- Pomeroville JC. *Eukaryotic microorganisms: the fungi*. Fundamentals of microbiology. 11th ed. Burlington: Jones & Bartlett Learning; 2018. p. 621–2.
- Ramos IC, Soares YC, Damasceno LS, Libório MP, Farias LABG, Heukelbach J, et al. Predictive factors for disseminated histoplasmosis in AIDS patients with fever admitted to a reference hospital in Brazil. *Rev Soc Bras Med Trop* 2018;51(4):479–84.
- Santos CR, de Assis ÂM, Luz EA, Lyra L, Toro IF, Seabra JCC, et al. Detection of *Pneumocystis jirovecii* by nested PCR in HIV-negative patients with pulmonary disease. *Rev Iberoam Microl* 2017;34(2):83–8.
- Seo AN, Park HJ, Lee HS, Park JO, Chang HE, Nam KH, et al. Performance characteristics of nested polymerase chain reaction vs real-time polymerase chain reaction methods for detecting *Mycobacterium tuberculosis* complex in paraffin-embedded human tissues. *Am J Clin Pathol* 2014;142(3):384–90.
- Sharafidini M, Mirehendi H, Ashrafi K, Hosseini M, Mohebali M, Khodadadi H, et al. Comparison of nested polymerase chain reaction and real-time polymerase chain reaction with parasitological methods for detection of *Strongyloides stercoralis* in human fecal samples. *Am J Trop Med Hyg* 2015;93(6):1285–91.
- Skalski JH, Kottom TJ, Limper AH. Pathobiology of *Pneumocystis* pneumonia: life cycle, cell wall and cell signal transduction. *FEMS Yeast Res* 2015;15(6): pii: foy046.
- Sun J, Su J, Xie Y, Yin MT, Huang Y, Xu L, et al. Plasma IL-6/IL-10 ratio and IL-8, LDH, and HBsD level predict the severity and the risk of death in AIDS patients with *Pneumocystis* pneumonia. *J Immunol Res* 2016;2016:1583951.
- Taylor ML, Ruiz-Palacios GM, Reyes-Montes MR, Rodríguez-Arellanes G, Carreto-Binaghi LE, Duarte-Escalante E, et al. Identification of the infectious source of an unusual outbreak of histoplasmosis, in a hotel in Acapulco, state of Guerrero, Mexico. *FEMS Immunol Med Microbiol* 2005;45:435–41.
- Velasquez G, Rueda ZV, Vélez LA, Aguirre DA, Gómez-Arias RD. Histoplasmosis in AIDS patients. A cohort study in Medellín, Colombia. *Infectio* 2010;14:S99–S106.
- Wakefield AE, Lindley AR, Ambrose HE, Denis CM, Miller RF. Limited asymptomatic carriage of *Pneumocystis jirovecii* in human immunodeficiency virus-infected patients. *J Infect Dis* 2003;187:901–8.
- Wheat LJ, Slama TG, Zeckel ML. Histoplasmosis in the acquired immune deficiency syndrome. *Am J Med* 1985;78(2):203–10.

OPEN

Novel clinical and dual infection by *Histoplasma capsulatum* genotypes in HIV patients from Northeastern, Brazil

Received: 19 November 2018

Accepted: 30 July 2019

Published online: 13 August 2019

Lisandra Serra Damasceno¹, Marcus de Melo Teixeira^{1,2,3}, Bridget Marie Barker^{1,2,3}, Marcos Abreu Almeida⁴, Mauro de Medeiros Muniz³, Cláudia Vera Pizzini³, Jacó Ricarte Lima Mesquita¹, Gabriela Rodríguez-Arellanes⁵, José Antonio Ramírez⁵, Tania Vite-Garín⁵, Terezinha do Menino Jesus Silva Leitão^{1,6}, Maria Lucia Taylor⁵, Rodrigo Almeida-Paes⁴ & Rosely Maria Zancopé-Oliveira¹

Histoplasmosis is a worldwide-distributed deep mycosis that affects healthy and immunocompromised hosts. Severe and disseminated disease is especially common in HIV-infected patients. At least 11 phylogenetic species are recognized and the majority of diversity is found in Latin America. The northeastern region of Brazil has one of the highest HIV/AIDS prevalence in Latin America and Ceará State has one of the highest death rates due to histoplasmosis in the world, where the mortality rate varies between 33–42%. The phylogenetic distribution and population genetic structure of 51 clinical isolates from Northeast Brazil was studied. For that morphological characteristics, exoantigens profile, and fungal mating types were evaluated. The genotypes were deduced by a MSLT in order to define local population structure of this fungal pathogen. In addition, the relationships of *H. capsulatum* genotypes with clinically relevant phenotypes and clinical aspects were investigated. The results suggest two cryptic species, herein named population Northeast BR1 and population Northeast BR2. These populations are recombining, exhibit a high level of haplotype diversity, and contain different ratios of mating types MAT1-1 and MAT1-2. However, differences in phenotypes or clinical aspects were not observed within these new cryptic species. A HIV patient can be co-infected by two or more genotypes from Northeast BR1 and/or Northeast BR2, which may have significant impact on disease progression due to the impaired immune response. We hypothesize that co-infections could be the result of multiple exposure events and may indicate higher risk of disseminated histoplasmosis, especially in HIV infected patients.

Histoplasmosis is a worldwide-distributed systemic mycosis caused by several cryptic species nested within the *Histoplasma capsulatum* complex¹. *H. capsulatum* has a dimorphic life cycle; the mycelial phase (MP) develops in an environmental milieu with high concentrations of nitrogen and phosphorus, humidity above 60%, darkness, and near watercourses². Upon inhalation of microconidia or macroconidia from *Histoplasma* spp. by susceptible hosts, the fungus differentiates into the yeast phase (YP), composed by budding yeast cells. Both MP and YP can be obtained by *in vitro* cultivation of the fungus at 25–28 °C and 34–37 °C, respectively. *Histoplasma*

¹Hospital São José de Doenças Infectosas – Secretaria de Saúde do Ceará, Fortaleza, Ceará, Brazil. ²Núcleo de Medicina Tropical, Faculdade de Medicina, Universidade de Brasília, Brasília, Distrito Federal, Brazil. ³Pathogen and Microbiome Institute, Northern Arizona University, Flagstaff, Arizona, United States of America. ⁴Instituto Nacional de Infectologia Evandro Chagas (INI), FIOCRUZ – Fundação Oswaldo Cruz, Laboratório de Micologia, 21045-900, Rio de Janeiro, RJ, Brazil. ⁵Facultad de Medicina, UNAM – Universidad Nacional Autónoma de México, Departamento de Microbiología y Parasitología, Laboratorio de Inmunología de Hongos, 04510, Ciudad de México, Mexico. ⁶Faculdade de Medicina, UFC – Universidade Federal do Ceará, Departamento de Saúde Comunitária, 60430-140, Fortaleza, Ceará, Brazil. Lisandra Serra Damasceno, Marcus de Melo Teixeira, Maria Lucia Taylor and Rosely Maria Zancopé-Oliveira contributed equally. Correspondence and requests for materials should be addressed to L.S.D. (email: lisainfecto@gmail.com)

infections have been reported on all continents with exception of Antarctica¹. The course of histoplasmosis varies from asymptomatic infection to mild-to-severe disease. High incidence of human *Histoplasma* infection has been reported mainly in tropical and subtropical areas of the Americas. However, the true disease range is likely larger, as this mycosis has also been found in Canada and in the Patagonia desert in Argentina^{3,4}.

This pathogen can cause disease in different animal hosts, such as bats, domestic cats, and several wild mammals^{2,4,5}. In humans, histoplasmosis outbreaks have been described in immunocompetent individuals linked to activities such as visiting caves and archeological sites, or working on a construction site. These exposures are often associated with environments containing high levels of bat or bird guano, which may favor the development of MP that harbors infectious microconidia⁶.

In last years, an increase of disseminated histoplasmosis has been reported, mainly associated with AIDS-patients throughout the Americas^{7,8}. A major challenge is that mortality rate, presence of skin and mucosal lesions, and relapse frequency of these infections vary in individuals from distinct geographic areas of the disease^{9,10}. In addition, experimental studies have demonstrated that variation in virulence may be associated with different genetic lineages of *H. capsulatum*¹¹.

Multilocus sequence typing (MLST) is the main molecular tool currently used to evaluate genetic diversity at the species level of *H. capsulatum*¹². The first analysis of isolates across the global distribution of the species defined 8 phylogenetic clades^{13,14}. The LAm A and LAm B clades harbor isolates primarily from Latin America; the Nam 1 and Nam 2 clades from North America; the Eurasian clade from Egypt, India, China, Thailand, and England; the Netherlands clade; the Africa clade; and the Australian clade¹⁴. Recently, a more robust MLST study evaluating 234 isolates of *H. capsulatum* lead to the identification of at least 11 species-level clades, the majority of them found in Latin America. The former LAm A and LAm B species were divided into four different genetic clusters as follows: LAm A1, LAm A2, LAm B1 and LAm B2. Two new phylogenetic species, RJ (Southeast of Brazil) and BAC-1 (Mexico), and four different monophyletic and cryptic clades from Brazil (BR1-4) were also identified¹.

Brazil presents one of the highest global incidences of histoplasmosis, and also presents the greatest genetic variability of *Histoplasma* and could be considered the center of origin of this important pathogen^{1,15}. It is estimated that 2.19 individuals had a histoplasmosis diagnosis per 1,000 hospitalizations in Brazil¹⁶. However, the true incidence of this mycosis in Brazil is unknown, especially because it is not a notifiable disease.

Studies performed by histoplasmin skin-test between 1940 and 1990 have found different levels of prevalence of histoplasmosis in Brazil¹⁷. A prevalence rate of 93.2% was observed in southeastern Brazil^{17,18}. In Ceará, a state located in the northeastern of Brazil, the prevalence rates varied from 23.6% to 61.5% among residents in rural areas^{19,20}. Among HIV-positive individuals from Ceará without severe immunosuppression (lymphocyte T CD4+ >350 cells/mm³), the histoplasmosis prevalence reached 11.8%²¹. In the last three decades, the Ceará State has presented a large number of cases of disseminated histoplasmosis (DH) described mainly in AIDS-patients⁹. Between 1995 and 2004, 164 cases of co-infection of DH and AIDS were observed in a single hospital²². Moreover, 134 cases of the disease were found during a 7 year medical surveillance²³; 208 cases in another 5 years⁸ and, more recently, 264 new cases in 7 years⁹ in this single state. These studies clearly demonstrate that northeastern Brazil, particularly Ceará State, is a highly endemic area of histoplasmosis, and is associated with a high annual death rate among HIV patients²⁴. In Fortaleza (the capital of Ceará State), many cases of histoplasmosis are associated with low sanitation capacity, ecotourism, and fishing²⁵.

Although antiretroviral therapy has modified the course of AIDS, a mortality rate between 33–42% associated with histoplasmosis has been observed in this region of Brazil^{8,9}, unlike other endemic regions such as Panama (12.5%)²⁶ and French Guiana (8%)^{24,27}. The genetic background of *Histoplasma* in northeastern Brazil is poorly explored, especially considering the high mortality rates of DH so far reported for this particular area.

The aim of this study was to assemble the epidemiological, clinical, and laboratory data of histoplasmosis patients diagnosed in Ceará, Northeastern of Brazil. The phenotypes of clinical strains such as morphological characteristics, exoantigen profiles, and fungal mating types were evaluated. The genotypes of clinical isolates of *H. capsulatum* obtained from patients were deduced by a MLST in order to define local population structure of this fungal pathogen. In addition, the relationships of *H. capsulatum* genotypes with clinically relevant phenotypes and clinical aspects were investigated. Finally, it was demonstrated the occurrence of recurrent infections by multiple genotypes of *H. capsulatum* in HIV patients.

Results

Clinical data. Relevant clinical data were evaluated in 43 hospitalizations of 40 individuals with DH from 2011 to 2014 (Table 1). Thirty-one cases occurred in males and nine in females. Patient's age varied from 19 to 56 years old (median 31 years; interquartile range: 28–39 years). Only a single patient was HIV-negative. Hospitalizations were more frequent in individuals living in the metropolitan area of Fortaleza (75%). Other Ceará regions, such as the central wilderness, mountain region, and east coast, had smaller number of histoplasmosis cases (Table S1). All patients received amphotericin B deoxycholate (1 mg/Kg/day) until the clinical improvement, followed by itraconazole (400 mg/day). Co-infections with tuberculosis were detected in 15% of the cases. Fever, cough, and dyspnea were the most common clinical manifestations observed in the herein described patients (Table 1). Data revealed a high mortality ratio among the AIDS-patients (33%) included in this study. Moreover, presence of skin lesions ($p = 0.003$) and acute renal failure ($p = 0.010$) were risk factors associated with deaths.

Macro and micromorphological characteristics of MP. Fifty-one clinical fungal isolates were obtained from the included patients. Fungi were isolated from buffy coat (n = 30), blood (n = 14), bone marrow (n = 6), and bronchoalveolar lavage (n = 1) (Table S1). The overall morphological characteristics of the *H. capsulatum* isolates are reported in Table S2, where differences in colony texture, color, and micromorphologies were recorded.

Epidemiological data	
Gender	
Man	31 (77.5%)
Woman	9 (22.5%)
Origin	
Fortaleza, Ceará	23 (57.5%)
Other cities of Ceará	17 (42.5%)
HIV/AIDS test	
Positive	39 (97.5%)
Negative	1 (2.5%)
Drug addictive	
Yes	6 (15.0%)
No	34 (85.0%)
Co-infection with tuberculosis	
Positive	6 (15.0%)
Negative	34 (85.0%)
Clinical characteristics	
Fever	40 (100%)
Weight loss	33 (82.5%)
Cough	27 (67.5%)
Dyspnea	27 (67.5%)
Hepatomegaly	26 (65%)
Diarrhea	25 (62.5%)
Asthenia	22 (55%)
Splenomegaly	20 (50%)
Vomit	18 (45%)
Abdominal pain	12 (30%)
Headache	11 (27.5%)
Mucosa hemorrhage	10 (25%)
Skin lesion	09 (22%)
Adenomegaly	08 (20%)
Acute renal failure	06 (15%)

Table 1. Baseline measurements of the histoplasmosis cases ($n = 40$) evaluated in the São José Hospital from Fortaleza, Ceará, Brazil, between 2011 to 2014.

The surface of *H. capsulatum* colonies varied from pale (white to beige) (36/51–70.6%) to dark (brown) (15/51–29.4%) and the texture of colonies ranged from cottony (42/51–82.4%) to powdery (9/51–17.6%). Microconidia were observed in all isolates while macroconidia were identified in 74.5% (38/51) of *H. capsulatum* isolates. There was no association between texture and presence of tuberculate macroconidia, as the majority of cottony (30/42–71.4%) and powdery colonies (8/9–89%) produced tuberculate macroconidia ($p = 0.417$).

Dimorphism. The MP-YP conversion occurred in 88.2% (45/51) of *H. capsulatum* isolates in the first cultivation on ML-Gema Agar between 7 to 14 days. Five isolates (9.8%) presented a delayed MP-YP conversion, since the dimorphic switch took place after 3 or 4 sub-cultivations at the same conditions. Just one isolate (CE 0613) did not convert from MP to YP (2%) under the studied conditions (Table S2). All YP colonies presented smooth and moist texture, and showed characteristic oval-shaped yeast cells ranging from 2 to 5 μm in size.

Exoantigen profiles. ID tests revealed that 17.6% of *H. capsulatum* exoantigens (9/51) yielded precipitin bands. Eight fungal isolates had single M band, and only one isolate had both H and M precipitin bands. By using Western blot, a more sensitive technique, the exoantigens were detected in all fungal isolates (Table S2). Both H and M antigens were observed in 29 (54.9%) isolates; 18 (35.2%) had single M band (corresponding to a 94 kDa protein), and 4 (7.9%) isolates just presented the H antigen (corresponding to a 114 kDa protein). There was no association between isolates that produced the both H and M antigens with texture ($p = 0.268$) or pigmentation ($p = 0.167$) of colonies, as well as with the presence or absence of macroconidia ($p = 0.106$).

Phylogenetic distribution, population structure, and clinical/phenotype correlation. Phylogenetic analysis revealed two new clades within Latin America, comprised mainly of the *H. capsulatum* isolates recovered from HIV-infected patients, named the Northeast clade BR1 and Northeast clade BR2 (Fig. 1). Both clades appear to be monophyletic using both maximum likelihood (ML) (Fig. 1A) and Bayesian inference (BI) methods (Fig. 1B). According to Teixeira *et al.*¹, the strains from BR2 clade (84476, 84502, 84564, H151, and JIEF) and BR4 clade (H146, RE5646, and RE9463) nested within the herein proposed Northeast BR1 and Northeast BR2 populations, respectively. For that study, those clades were not classified as phylogenetic species due to the low taxon sampling (1). Therefore, the

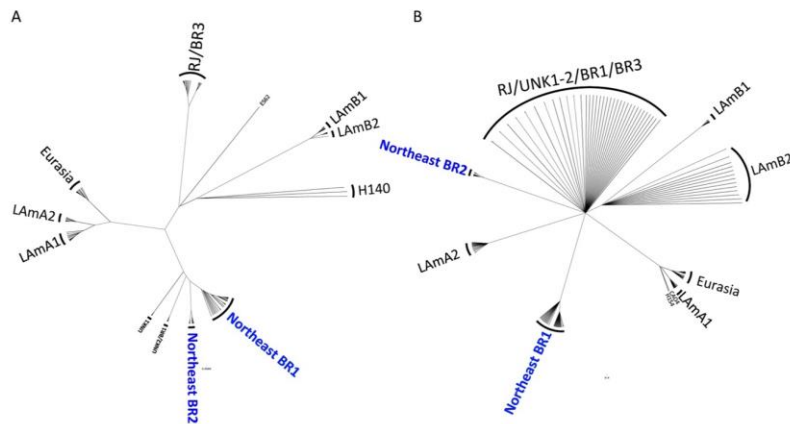


Figure 1. Phylogenetic distribution of the isolates from Northeast Brazil. Two cryptic clades Northeast BR1 and Northeast BR2 are revealed. Unrooted trees were generated by (A) Maximum Likelihood and (B) Bayesian analysis using K2P+ Inv Gamma DNA substitution model. Brach supports are proportion to the thickness of each branch.

clades found in the Northeast region of Brazil were renamed in order to clarify nomenclature, Northeast clade BR1 and Northeast clade BR2. According to both ML and BI unrooted trees, the Northeast BR1 and BR2 clades are monophyletic; however, they have low bootstrap and posterior probability values (Fig. 1).

Initially, the whole population structure of Latin American (former LAm A, LAm B and Eurasia clades)¹ was assessed via Bayesian Analysis of Population Structure using a Kmax value of 50. Initial admixture analysis revealed at least four clusters: Eurasia/LAm A1/LAm A2, RJ, LAm B1/LAm B2, and a fourth population composed mainly of isolates from the northeastern Brazil confirming the monophly achieved in the phylogenetic analyses (Fig. 2). Gene flow between the RJ and Northeast BR1 and BR2 populations was noted, as the isolates JIEF, RE9463, and RE5646 share alleles from both populations (Fig. 2). Allele exchange has been extensively reported in the former LAm A clade, which is compatible with a sexually recombining species. Recombination analysis for the Northeast population was positive ($p = 2.345 \times 10^{-12}$) using the PHI-test analysis, and a cluster network analysis demonstrated gene flow between isolates within this population (Supplementary Fig. S1).

A deep investigation of the phylogenetic and population distribution of the 59 strains [51 from the present study and eight from Teixeira *et al.*¹] belonging to the *Histoplasma* Northeast populations showed two monophyletic clades strongly supported by bootstrap values as represented by the ML tree (Fig. 2). Admixture analysis using a fixed K model revealed an optimal partition of $K = 3$: Northeast BR1, Northeast BR2, and a third population composed of two isolates (RE9463 and RE5646) from Pernambuco State, Brazil (a state that borders Ceará) and a third isolate (JIEF) from Ceará shares alleles with Northeast BR1 population and is likely a hybrid strain (Fig. 3).

Haplotype networks revealed that the two Northeast populations are highly diverse (Fig. 4A). The haplotype diversity index for these populations is comparable to the highly recombinant RJ population ($Hd = 0.9269$)¹. At least 30 haplotypes were observed within the subset of 59 isolates from northeastern Brazil (Fig. 4A). Northeast BR1 and Northeast BR2 are separated by nine mutations that are fixed in each population. The isolates RE9463 and RE5646 from Pernambuco form a unique haplotype (Hap2) derived from a median vector from a population Northeast BR2 (Fig. 4A). The isolates 84476, 84502, and 84564 were isolated in Rio de Janeiro in 1998 and represent cases diagnosed outside northeastern of Brazil belonging to Northeast BR1. Importantly, the population Northeast BR2 is widely spread across Ceará state while the Northeast BR1 is more restricted to the metropolitan area of the capital Fortaleza (Fig. 4B). This is evident as haplotypes 17 and 18 and their derivations (Hap19-23, Hap29, and Hap30) are clustered in Fortaleza and adjacent regions. Finally, it was observed that haplotype 18 is widely distributed in at least four municipalities and may represent a broadly distributed genotype (Fig. 4B). Associations between Northeast BR1 and Northeast BR2 populations and clinical manifestations such as dyspnea, mucosa hemorrhage, skin lesion, acute renal failure, and deaths were not observed ($p > 0.05$). Additionally, relationships between the genetic populations and their phenotypes were not detected either (Table 2, Supplementary Fig. S2). However, there was a slightly predominance of *MAT1-1* (68.7%) in Northeast BR2 and *MAT1-2* (62.9%) in Northeast BR1 ($p = 0.036$ – Table 2).

Dual *Histoplasma* infections in HIV patients. Seven patients included in this study yielded more than one *H. capsulatum* strain for analysis (Table S2). The phenotypic analyses of these strains revealed one patient (number 17) that yielded three isolates (CE 0313, CE 0713, CE 1013) with pale colonies, and one with dark pigmentation (CE 2713). The textures of *H. capsulatum* colonies obtained from two patients were cottony in some isolates (CE 0313, CE 0713, and CE 1013 from patient 17; CE 0513, and CE 0814 from patient 19) and powdery

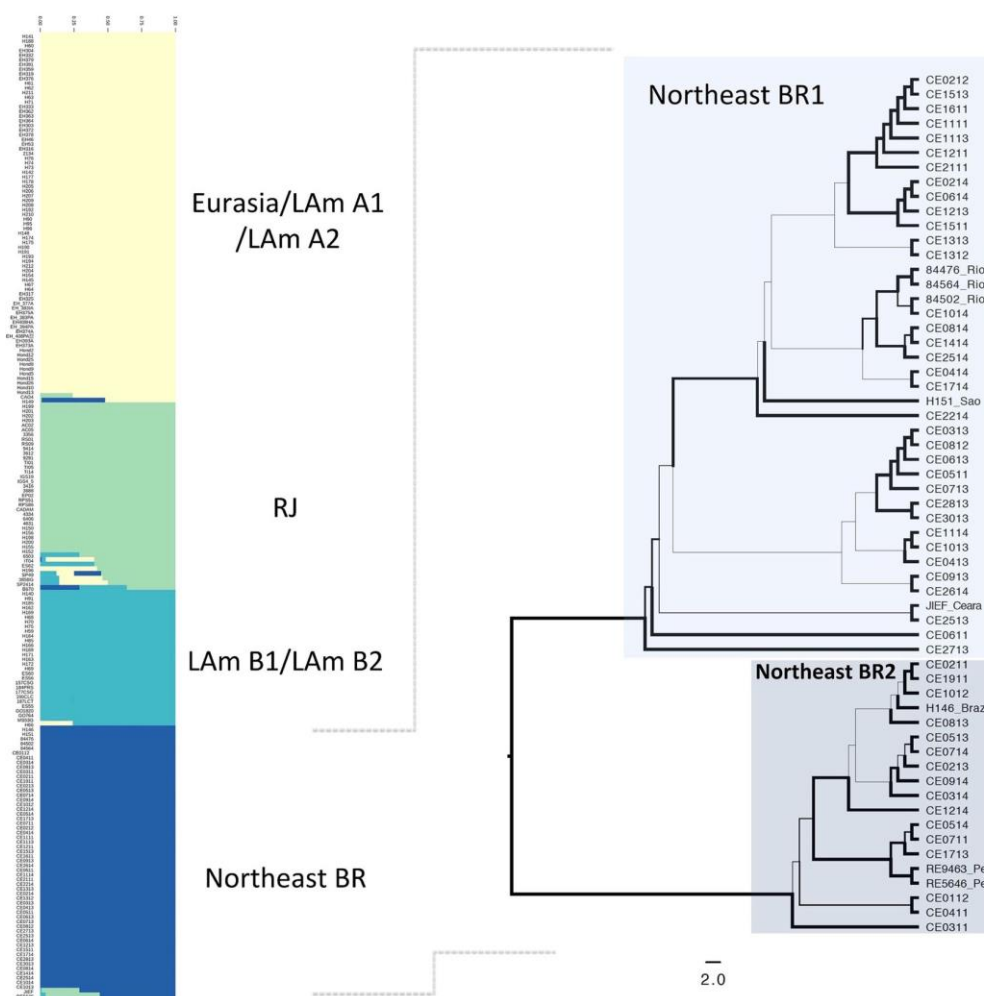


Figure 2. Population distribution of *H. capsulatum* in Latin America. (A) Admixture plots revealed a cryptic *H. capsulatum* population (green) harboring isolates from Northeast Brazil. Gene flow between Latin American populations is evidenced by admixed plots in RJ, LAm B and Northeast populations. (B) Phylogenetic analysis using the Maximum Likelihood methods of the Northeast population revealed two cryptic species Northeast1 and Northeast 2.

in others (CE 2713 from patient 17 and CE 0914 from patient 19). Tuberculate macroconidia were present in all isolates recovered from patients 2, 22 and 28; however, three patients (1, 17, and 19) were infected with fungal isolates with and without tuberculate macroconidia. The macroconidia were not observed on the isolates CE 0614 and CE 1014 from patient number 33. Moreover, the *H. capsulatum* isolates recovered from patients 2, 17, 19, 28, and 33 expressed different exoantigen profiles under the same experimental conditions.

The genotypic analyses revealed that sequential isolates belonging to the same haplotype were recovered from two patients (1 and 22). It is noteworthy that isolates CE0211 and CE1911 from patient 1, comprising the haplotype 9 within the Northeast BR2 population (Fig. 4), are phenotypically distinct, since CE1911 did not produce macroconidia. On the other hand, isolates CE1113 and CE1513 recovered from patient 22 are identical by means of genotypic (haplotype 17, Northeast BR1 population) and phenotypic analyses (Supplementary Fig. S2).

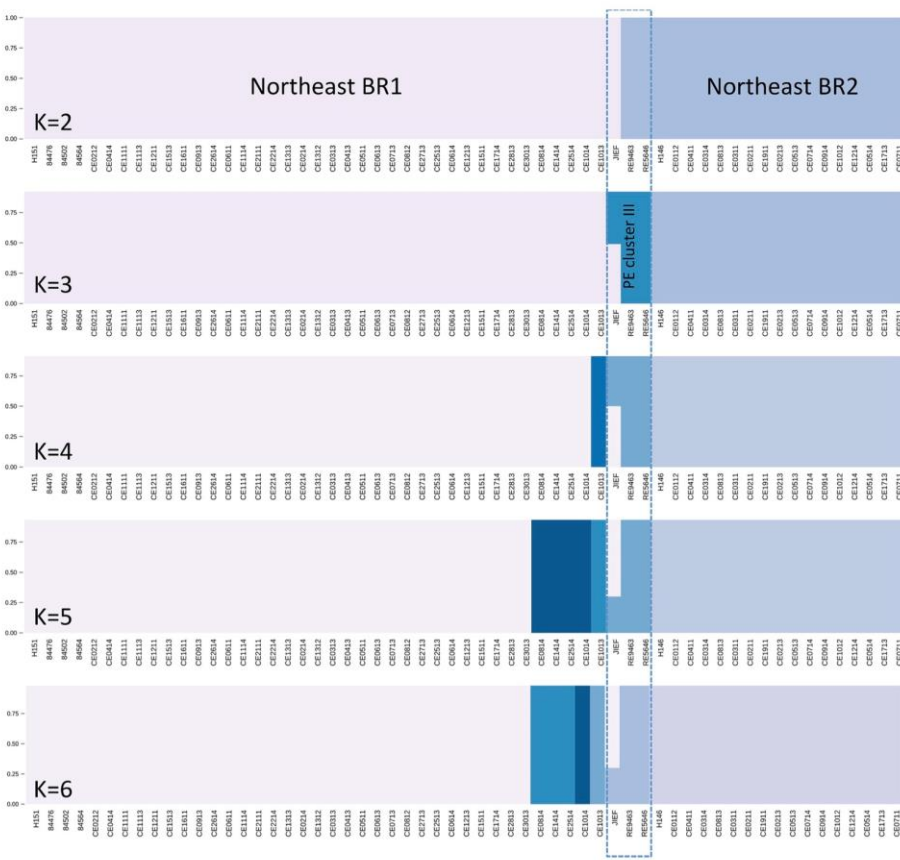


Figure 3. Sub-population distribution of Northeast isolates. Admixtures plots show the percentage of alleles unique or shares between Northeast BR1 and Northeast BR2 populations. At least three populations were found within Northeast isolates: The previous phylogenetic proposed Northeast BR1 and Northeast BR2 and an additional one composed by isolates of the neighbor state of Pernambuco, Brazil.

For the other five patients, more than one genotype was recovered from successive isolations (Table 3). Patients 2 and 19 were infected by isolates from the Northeast BR1 population (CE0511 and CE0814, respectively) and from the Northeast BR2 population (CE0112 and CE0311 from patient 2; CE0513 and CE0914, from patient 19), while three patients (17, 28, and 33) were infected by different haplotypes within the Northeast BR1 population (Supplementary Fig. S3).

Of five patients affected with dual infection, all individuals were men, with average age of 34.6 years. Three patients had risk activity for histoplasmosis. Dyspnea was observed in all patients, and only one patient had skin lesions, mucosa bleeding and renal failure (patient 28). The first opportunistic infection in 4 among these 5 patients was histoplasmosis or disseminated histoplasmosis was AIDS defining illness in 4 among these 5 patients. Only one patient had AIDS before this mycosis (patient 33), and this individual had irregular adhesion to HAART. One patient had tuberculosis co-infection (patient 2). Four patients had discharged and one died. Mortality of patients harboring different genotypes was similar to those infected with a single genotype ($p = 1.000$).

Three patients were re-hospitalized with the new hospitalization one to five months apart the first: patient 17 yielded four isolates with different phenotypic characteristics (Supplementary Figure 2) but all of them belonging to three distinct haplotypes from the Northeast BR1 population; patient 19 yielded three isolates from three different haplotypes, interestingly the two isolates from the first hospitalization (CE0513 and CE0914) were from the Northeast BR2 population and the isolate from the second hospitalization (CE0814) was from the Northeast

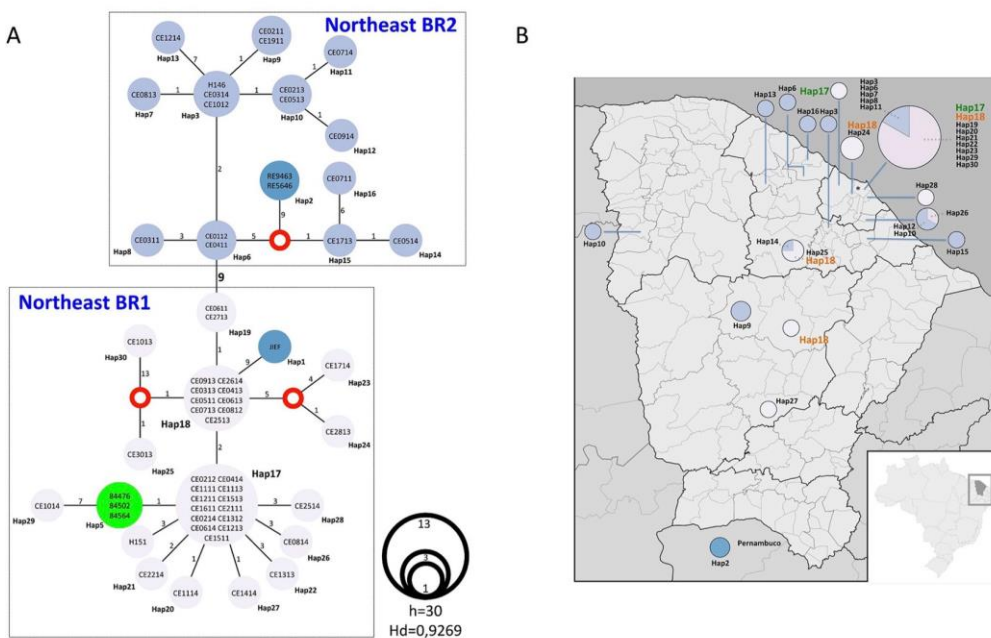


Figure 4. Haplotype network analysis using the Median-Joining method. (A) The haplotypes are proportional to the number of individuals and the number of mutations between each haplotype is displayed to each correspondent vertices. We identified 2 main population correspondent to Northeast BR1 and Northeast BR2 genotypes. (B) The haplotypes were plotted against each corresponding location in the map of Ceará state.

Phenotype	BR1 genotype	BR2 genotype	p-value
Color			
Pale	25 (71.4%)	11 (68.8%)	0.846
Dark	10 (28.6%)	5 (31.2%)	
Texture			
Cotony	30 (85.7%)	12 (75%)	0.352
Powdery	5 (14.3%)	4 (25%)	
Micromorfolgy			
Macroconidia+	26 (64.3%)	12 (75%)	0.957
Macroconidia-	9 (25.7%)	4 (25%)	
Exoantigen			
M antigen	15 (42.8%)	7 (43.8%)	0.952
M and H antigen	20 (57.2%)	9 (56.2%)	
Mating			
<i>MAT1-1</i>	13 (37.1%)	11 (68.8%)	0.036
<i>MAT1-2</i>	22 (62.9%)	5 (31.2%)	

Table 2. Associations between phenotype and genotype of *H. capsulatum* isolates from Ceará, Brazil.

BR1 population; finally patient 33 was infected by isolates with different haplotypes and mating types (CE0614 – Hap17, *MAT1-1*; CE1014 – Hap29, *MAT1-2*, from first and second hospitalizations, respectively), but both belonging to the Northeast BR1 population (Supplementary Figs S2 and S3).

Patients	Sex	Age	Risk activity	Symptoms	CD4+ (cells/mm ³)	HAART at admission	Outcome
Patient 2	Man	22	no	Dyspnea	273	No	Discharged
Patient 17	Man	38	no	Dyspnea	Not performed	No	Discharged
Patient 19	Man	31	yes	Dyspnea	36	No	Discharged
Patient 28	Man	52	yes	Dyspnea, renal failure, skin lesions, mucosa bleeding	Not performed	No	Death
Patient 33*	Man	30	yes	Dyspnea	117	Poor adhesion	Discharged

Table 3. Clinical and epidemiological features of patients infected with different genotypes of *Histoplasma capsulatum*. *This individual was re-hospitalized with histoplasmosis and severe immunodeficiency (CD4+ 29 cells/mm³).

Discussion

Histoplasmosis has been considered an AIDS defining illness since 1987²⁸, and a disease responsible for thousands of deaths in Latin America among people living with HIV/AIDS. The Ceará state, Northeastern Brazil, is considered the area with the highest mortality due to histoplasmosis in South America^{8,9,24}, far surpassing rates in other endemic areas, such as Panama²⁶ and French Guiana^{24,27}. Thirty-one cases occurred in males and nine in females. These data has been previously demonstrated by Damasceno and collaborators (2013)⁹ where the majority of the subjects included in their studies were male with a mean age of 35 years (SD = 2.2; 95% CI = 3.01–3.75) and were born in the capital of Ceará. A lack of early diagnosis for the disease contributes to the high rates of mortality. The high mortality rate observed in this study, which unfortunately is expected for this disease among immunocompromised patients at this area, is in accordance with other studies conducted at Ceará, Brazil.

Currently, *H. capsulatum* is thought to be a complex of different species, containing at least 11 phylogenetic species and/or cryptic lineages¹. Latin America presents higher diversity than other endemic areas, and diversity is highest in Brazil^{1,29}. Additionally, the majority of *H. capsulatum* Brazilian clinical isolates previously studied were obtained from residents of southeastern Brazil^{1,14}.

Fungal infections may contain multiple genotypes of the same pathogen, but still are usually considered as uniform entities. For the first time, we show strong support for two new populations, Northeast BR1 and Northeast BR2 that could cause mixed infections in HIV-positive individuals. The co-infection concept in virology is characterized by patients infected with two different virus strains simultaneously. On the other hand, the superinfection concept represents a condition in which an individual with established viral infection acquires a secondary infection provoked by a second genotype and this phenomenon is widely studied in viruses³⁰. Similar event was observed in this research. Possibly, there were two different exposure events in the patients that presented different genotypes. Another explanation is that different genotypes share similar ecologic niches. Further studies are necessary to address these issues.

In bacteriology, this concept is slightly different; a secondary infection overcomes the earlier one caused by a different species and may be resistant to primary antibacterial treatment. Either way, mixed infections of *Mycobacterium tuberculosis* also have shown effects on both treatment and disease control³¹. Multiple infections due *Cryptococcus neoformans*³² and *Pneumocystis jirovecii*³³ were also reported on HIV patients, however the incubation periods of fungal, bacterial and viral infections varies and whether the herein reported mixed infections are either co-infection or superinfections must be deeply revised in the medical mycology field.

Different genotypes may display divergent host cell tropism, immunologic evasion, or even antifungal-drug resistance, which is critical for patients with disseminated histoplasmosis and other endemic mycosis³⁴. Thus, heterogeneous *H. capsulatum* infections may have significant consequences for immunologic escape and histoplasmosis progression. The competence of a previously cleared or ongoing *Histoplasma* infection to protect against a subsequent infection by a novel *Histoplasma* genotype may decrease the ability of the adaptive immune response to provide adequate and broad protection. The immunity induced by a prior *Histoplasma* infection could be insufficient to prevent a new infection. This directly challenges our current understanding of protective immunity, and impacts the development of vaccines for histoplasmosis and other endemic fungal pathogens in certain patient populations.

The genotyped isolates from Northeastern Brazil are contained in the previously delineated BR2 clade and BR4 clade respectively (Figs 1–4)¹. The BR2 and BR4 clades were not previously ranked as phylogenetic species due to the low taxon sampling. However, we herein propose to elevate the status of “cryptic clades” to phylogenetic species of the former BR2 and BR4 (Fig. 1). The newly described *Histoplasma* Northeast BR1 and Northeast BR2 clades are monophyletic in both phylogenetic methods evaluated. However low bootstrap support for these monophyletic branches, likely due to homoplasy, were detected in both species so it is clear that more in depth analyses, such as whole genome sequencing, would resolve this question. Phylogenetic methods were coupled with population genetics analysis and it was identified the same population structure for the Northeast BR1 and Northeast BR2 clades mentioned above (Figs 2 and 3). Moreover, further investigation may reveal new populations in Northeast Brazil as evidenced by an isolated population of *H. capsulatum* in the Pernambuco state of Brazil (Fig. 3).

Additionally, this is the first study that evaluates the relationships between genotypes with clinical and phenotypic aspects of *H. capsulatum* isolates. It is known that DH can present with differential clinical characteristics in individuals from different endemic areas. For example, skin lesions and deaths are more frequent in individuals from Brazil than in patients from North America¹⁰. These differences may be related to different

circulating genotypes on these two regions but also by phenotypic traits of the strains, such as different tolerances to cooler temperatures found in the skin. In fact the development and progression of histoplasmosis is very sophisticated and depend of differences in fungal burden, disease kinetics, cytokine responses, and many virulence factors. Experimental studies have also found differences in the virulence of the pathogen, gene expression, and pathogenesis of disease between *H. capsulatum* from different phylogenetic clades^{35–37}. Despite this, associations between genetic populations and phenotypic features were not detected (Table 2). Neither morphology nor exoantigen profile were associated with population/species, revealing that the phenotypic plasticity of those isolates is a process independent of speciation/population subdivision, and more likely due to intrinsic variation^{38,39}.

Mixed mating types were identified with a slight predominance of one mating type in each group. Consequently, we hypothesize that both Northeast BR1 and Northeast BR2 are sexually recombining populations as evidenced by recombination analysis (phi-test), recombination networks, homoplasy, and admixture profiles (Figs 1, 3 and S1). Sexual reproduction can increase genetic diversity and may have consequences for pathogenesis by creating progeny with novel traits such as the ability to evade the host immune responses, a greater resistance to antifungal drugs, biofilm formation, or hyper virulence⁴⁰. Thus, recombination events can facilitate shifts in lifestyles, which can persist in successive successful lineages⁴¹. In *Toxoplasma gondii*, mating crosses between type II and III virulent strains revealed that the recombinant f1 progeny had a virulence increased by 1,000-fold in a mice model⁴². More studies are necessary to characterize the impact of natural variation found within *H. capsulatum* populations and its influence on virulence and pathogenesis. Additionally, it was demonstrated that a single patient (patient #17) was infected by different mating types from the same phylogenetic species (Northeast BR1). We hypothesize that co-infections could be the result of multiple exposure events and may indicate higher risk of disseminated histoplasmosis, especially in HIV infected patients.

In summary, *H. capsulatum* clinical isolates from Ceará are genetically distinct from isolates from southern Brazil and Latin America, which demonstrates the high genetic diversity this pathogen. It is unclear how this relates to variation in phenotypes, and additional investigation is greatly needed in this area, such as a GWAS approach.

Methods

Histoplasmosis patients. The study was approved in the Research Ethical Committee of INI/FIOCRUZ (protocol number 19342513.2.0000.5262) and it is in accordance with the suggestions of the Ethics Committee of the School of Medicine, UNAM (protocol number 057–2014). Forty patients hospitalized at São José Hospital from Fortaleza, Ceará, Brazil, from 2011 to 2014 were included in this study. All patients had proven histoplasmosis by the isolation of *H. capsulatum* from clinical samples cultures. A retrospective study was conducted by reviewing medical records including epidemiological (sex, age, origin, occupational risk of histoplasmosis infection, drug addiction, and co-infection with tuberculosis), clinical (fever, weight loss, cough, dyspnea, hepatomegaly, diarrhea, asthenia, splenomegaly, vomit, abdominal pain, headache, mucosa hemorrhage, skin lesion, adenomegaly, and acute renal failure - ARF), and laboratory data (HIV serological test). Patient data entries were anonymously handled with Epi-Info software, version 7.1.5 (Centers for Disease Control and Prevention, Atlanta, GA, USA).

Informed consent. Informed consent was obtained from all individual participants included in the study.

Fungal isolates and DNA extraction. Fifty-one fungal isolates were obtained from the 40 patients seen at São José Hospital, located in Fortaleza (Ceará, Brazil), as mentioned above. *Histoplasma* colonies were isolated from diverse samples [blood, bone marrow, buffy coat and bronchoalveolar lavage (BAL)] by *in vitro* culture. YP or MP cells were grown in Ham's F12 broth at 37 °C and 25 °C for 3–5 days, respectively. A total of 500 µl of YP/MP liquid cultures were used for DNA extraction. Briefly, the cells were harvested by centrifugation, washed three times with distilled deionized water, and kept at –4 °C for DNA extraction as previously described⁴³. DNA was quantified by spectrophotometry using the Epoch™ Multi-Volume Spectrophotometer System (Biotek Instruments, Inc., USA).

Phenotypic assays. Fungal isolates were maintained for 21 days on Potato Dextrose Agar plates (PDA – Difco, Detroit, MI, USA) at 25 °C in order to obtain the MP. Macromorphological features of *H. capsulatum* MP cultures, such as texture and color of colonies, were described. Micromorphological characteristics of MP were observed by optical microscopy (Zeiss PrimoStar, Oberkochen, Germany) by sampling 10 fields randomly with a magnification of 400X, after Lactophenol Cotton Blue (Fluka Analytical, France) staining. Dimorphism was demonstrated by MP-YP conversion in the ML-Gema Agar at 37 °C, for 7 to 14 days⁴³.

Exoantigens were obtained from the 51 *H. capsulatum* isolates included in this study. Briefly, a fragment of 2–4 cm² of *H. capsulatum* MP grown for 14 days on PDA slants was transferred to Erlenmeyer flasks containing 25 ml of Brain Heart Infusion broth (BHI - Difco, Detroit, MI, USA). Flasks were incubated at 25 °C in a gyratory shaker at 150 rpm for 7 days (New Brunswick Scientific, Edison, NJ). Thimerosal 1% was added in the seventh day to inactivate fungal cells, and the flasks were re-incubated overnight at 25 °C. Cultures were centrifuged at 1,050 × g for 10 min, and the supernatants were filtered through 0.45 µm pore size filter membranes (Nalgene Co., Rochester, NY). The pooled filtrate was concentrated to 50X in a Minicon Macrosolute B-15 Concentrator (Amicon Corp., Lexington, MA, USA)⁴⁴. To evaluate the presence of the specific H and/or M antigens in the exoantigens from each *H. capsulatum* isolate, double immunodiffusion (ID) and western blot (WB) were performed. The ID assay was performed as previously described¹³. For the WB experiments, *H. capsulatum* exoantigens were initially separated by sodium dodecyl sulfate-polyacrylamide gel electrophoresis (SDS-PAGE), on 10% polyacrylamide resolving gels with a 4% polyacrylamide stacking gel. The gels were then processed for WB according to the protocol previously established⁴⁵ and revealed against a pool of sera from human patients with proven histoplasmosis.

Mating type identification. The *MAT* locus of the *H. capsulatum* isolates was identified by a polymerase chain reaction (PCR) using previously described primers and reaction conditions^{46,47}, where amplicons with 440 and 528 bp are expected after the amplification of *H. capsulatum MAT1-1* and *MAT1-2* loci, respectively. The G-217B (ATCC® Number: MYA-2455™) from USA (*MAT1-1*) and G-186A (ATCC® Number: 26029™) from Panama (*MAT1-2*) reference strains were respectively used as controls for each mating type. Amplicons were resolved by 1.5% agarose gel electrophoresis. The 100-bp DNA ladder was used as a molecular size marker.

Multi locus sequencing typing. Amplification of partial DNA sequences of four nuclear genes (*arf*, *H-anti*, *ole1*, and *tub1*) was performed according to the protocol described by Kasuga *et al.*¹³, with some modifications. The PCR reactions were achieved in a final volume of 25 µl, containing 200 µM of each deoxynucleoside triphosphate (dNTP) (Applied Biosystems Inc., Foster City, CA, USA), 2 mM of MgCl₂, 0.45 µM of each primer, 1.0 U of *Taq* DNA polymerase (New England BioLabs Inc., MA, USA), 1 X of *Taq* commercial buffer (New England BioLabs Inc., MA, USA) and 20 ng of each DNA template. The G-217B reference strain was used as positive control for the PCR reactions. PCR assays were performed in a Thermal iCycler (Bio-Rad Laboratories Inc., Hercules, CA, USA) programmed as follows: (a) 3 min at 95 °C; (b) 32 cycles consisting of 15 sec at 94 °C, 30 sec at 65 °C in the first cycle, which was subsequently reduced by 0.7 °C/cycle for next 12 cycles, and 1 min at 72 °C. The remaining 20 cycles, the annealing temperature was continued at 56 °C; (c) a final extension cycle of 5 min at 72 °C (touchdown PCR)⁴⁸. Generated amplicons were then sequenced by Sanger method at the High-Throughput Genomics Center (University of Washington) and the sequences were deposited in the GenBank database (<http://www.ncbi.nlm.nih.gov>) – (Table S3). The Asparagin Platform (<http://asparagin.cenargen.embrapa.br/phph/>) was used to analyze the electropherograms.

Phylogenetic analysis. The obtained sequences were first checked by BLASTn⁴⁹ to evaluate the genetic similarity with other *H. capsulatum* sequences deposited at GenBank. The sequences were aligned using the ClustalW⁵⁰ algorithm implemented in the Mega 6.0 software⁵¹. We included the same dataset evaluated by Teixeira *et al.*¹ to compare to the entire diversity of the genus *Histoplasma* so far reported (Table S3). The combined matrix was analyzed through two phylogenetic methods. First, maximum likelihood (ML) trees were generated using the IQ-TREE program⁵² using the –m MODEL function that allowing an automatic best-fit model selection (ModelFinder – K2P+ Inv Gamma was used in all tested phylogenies). The ultrafast bootstrap (UFBoot) approximation described by Minh *et al.*⁵³ was employed to test branch confidence. Second, Bayesian inference (BI) was conducted using the MrBayes ver. 3.2 software⁵⁴. Bayesian analysis was performed through 300,000 generations and samples were collected every 100 generations using 4 independent Markov Chain Monte Carlo (MCMC) to compute the posterior probability density. Twenty-five percent of the initial samples were discarded as *burn-in* and the remaining samples were used to build the consensual Bayesian tree. The consensus tree obtained by both methods was visualized in FigTree v1.3.1⁵⁵.

Recombination and population structure analysis. Recombination within Northeast populations was assessed using pairwise homoplasy index, (PHI-test). Cluster network analysis was inferred using the software SplitsTree 4⁵⁶. Population distribution of Northeast *H. capsulatum* isolates was inferred using a Bayesian Analysis of Population Structure (BAPS)⁵⁷. The haplotypic networks were inferred to visualize diversity both Northeast *H. capsulatum* populations. The distribution and diversity of haplotypes for the concatenated dataset was estimated using the software DnaSP, v 5⁵⁸, and Median-joining networks were built and visualized in Network, v 4, software (Fluxus Technology, Clare, Suffolk, England). We conducted mixture and admixture analysis setting K-max to 50 hypothetical populations within the former LamA, LAmB as well as the Eurasian clade. In addition, fixed K model analysis (K = 2–5) was used for mixture analysis in order to infer the population sub-structuring within the Northeast population. In the admixture analysis (K = 3), 200 interactions were used to infer the admixture coefficient. Fifty references individuals were assumed for each cluster and admixture analyses were repeated 10 times per individual.

Statistical analysis. The statistical analysis was carried out using the software STATA 11.2 (StataCorp LP, College Station, TX, USA). A bivariate analysis was performed to evaluate clinical data, phenotypic aspects, and genetic populations, using the Chi-square or Fisher exact test, if any value in the cells of the contingency table was less than five. A significance level of 5% ($\alpha = 0.05$) was applied in all tests.

Data Availability

The datasets correspondent to the sequenced genes generated during the current study are available in the GenBank repository (<https://www.ncbi.nlm.nih.gov/genbank/>). Accession numbers and all other data generated or analysed during this study are included in this published article and its Supplementary Information files.

References

- Teixeira, M. M. *et al.* Worldwide Phylogenetic distributions and population dynamics of the genus *Histoplasma*. *PLoS Negl. Trop. Dis.* **10**, e0004732 (2016).
- Taylor, M. L. *et al.* Environmental conditions favoring bat infection with *Histoplasma capsulatum* in Mexican shelters. *Am. J. Trop. Med. Hyg.* **61**, 914–919 (1999).
- Calanni, L. M. *et al.* Brote de histoplasmosis en la provincia de Neuquén, Patagonia Argentina. *Rev. Iberoam. Micol.* **30**, 193–199 (2013).
- Burek-Huntington, K. A., Gill, V. & Bradway, D. S. Locally acquired disseminated histoplasmosis in a northern sea otter (*Enhydra lutris kenyoni*) in Alaska, USA. *J. Wildl. Dis.* **50**, 389–392 (2014).
- Brilhante, R. S. *et al.* Feline histoplasmosis in Brazil: clinical and laboratory aspects and a comparative approach of published reports. *Mycopathologia.* **173**, 193–197 (2012).

6. Benedict, K. & Mody, R. K. Epidemiology of histoplasmosis outbreaks, United States, 1938–2013. *Emerg. Infect. Dis.* **22**, 370–378 (2016).
7. Colombo, A. L., Tobon, A., Restrepo, A., Queiroz-Telles, F. & Nucci, M. Epidemiology of endemic systemic fungal infections in Latin America. *Med. Mycol.* **49**, 785–798 (2011).
8. Brilhante, R. S. et al. Histoplasmosis in HIV-positive patients in Ceará, Brazil: clinical-laboratory aspects and *in vitro* antifungal susceptibility of *Histoplasma capsulatum* isolates. *Trans. R. Soc. Trop. Med. Hyg.* **106**, 484–488 (2012).
9. Damasceno, L. S. et al. Disseminated histoplasmosis and aids: relapse and late mortality in endemic area in North-Eastern Brazil. *Mycoses.* **56**, 520–526 (2013).
10. Couprie, P., Aznar, C., Carme, B. & Nacher, M. American histoplasmosis in developing countries with a special focus on patients with HIV: diagnosis, treatment, and prognosis. *Curr. Opin. Infect. Dis.* **19**, 443–449 (2006).
11. Sepulveda, V. E., Williams, C. L. & Goldman, W. E. Comparison of phylogenetically distinct *Histoplasma* strains reveals evolutionarily divergent virulence strategies. *MBio.* **5**, e01376–14 (2014).
12. Damasceno, L. S., Leitão, T. M., Taylor, M. L., Muniz, M. M. & Zancopé-Oliveira, R. M. The use of genetic markers in the molecular epidemiology of histoplasmosis: a systematic review. *Eur. J. Clin. Microbiol. Infect. Dis.* **35**, 19–27 (2016).
13. Kasuga, T., Taylor, J. W. & White, T. J. Phylogenetic relationships of varieties and geographical groups of the human pathogenic fungus *Histoplasma capsulatum* Darling. *J. Clin. Microbiol.* **37**, 653–663 (1999).
14. Kasuga, T. et al. Phylogeography of the fungal pathogen *Histoplasma capsulatum*. *Mol. Ecol.* **12**, 3383–3401 (2003).
15. Wheat, L. J. et al. Histoplasmosis. *Infect. Dis. Clin. North Am.* **30**, 207–227 (2016).
16. Giacomazzi, J. et al. The burden of serious human fungal infections in Brazil. *Mycoses.* **59**, 145–150 (2016).
17. Fava, S. C. & Netto, C. F. Epidemiologic surveys of histoplasmin and paracoccidioidin sensitivity in Brazil. *Rev. Inst. Med. Trop. S. Paulo.* **40**, 155–164 (1998).
18. Guimaraes, A. J., Nosanchuk, J. D. & Zancopé-Oliveira, R. M. Diagnosis of histoplasmosis. *Braz. J. Microbiol.* **37**, 1–13 (2006).
19. Diógenes, M. J. et al. Reações à histoplasmina e paracoccidioidina na Serra de Pereiro (estado do Ceará-Brasil). *Rev. Inst. Med. Trop. S. Paulo.* **32**, 116–120 (1990).
20. Faganha, M. C. et al. Estudo soroprevalente de paracoccidioidomicose em Palmácia, Ceará. *Rev. Soc. Bras. Med. Trop.* **24**(Supl 2), 28 (1991).
21. Bezerra, F. S. et al. Histoplasmin survey in HIV-positive patients: results from an endemic area in northeastern Brazil. *Rev. Inst. Med. Trop. S. Paulo.* **55**, 261–265 (2013).
22. Daher, F. E. et al. Risk factors for death in acquired immunodeficiency syndrome-associated disseminated histoplasmosis. *Am. J. Trop. Med. Hyg.* **74**, 600–603 (2006).
23. Pontes, L. B., Leitão, T. M. J. S., Lima, G. G., Gerhard, E. S. & Fernandes, T. A. Características clínico-evolutivas de 134 pacientes com histoplasmosse disseminada associada a SIDA no Estado do Ceará. *Rev. Soc. Bras. Med. Trop.* **43**, 27–31 (2010).
24. Prado, M., Silva, M. B., Laurenti, R., Travassos, L. R. & Taborda, C. P. Mortality due to systemic mycoses as a primary cause of death or in association with AIDS in Brazil: a review from 1996 to 2006. *Mem. Inst. Oswaldo Cruz.* **104**, 513–521 (2009).
25. Correia, F. G. S. et al. Spatial distribution of disseminated histoplasmosis and AIDS co-infection in an endemic area of Northeastern Brazil. *Rev. Soc. Bras. Med. Trop.* **49**, 227–231 (2016).
26. Gutierrez, M. E., Canton, A., Sosa, N., Puga, E. & Talavera, L. Disseminated histoplasmosis in patients with AIDS in Panama: a review of 104 cases. *Clin. Infect. Dis.* **40**, 1199–1202 (2005).
27. Adenis, A. et al. HIV-associated histoplasmosis early mortality and incidence trends: from neglect to priority. *PLoS Negl. Trop. Dis.* **8**, e3100 (2014).
28. CDC. Revision of the CDC surveillance case definition for acquired immunodeficiency syndrome. Council of State and Territorial Epidemiologists; AIDS Program, Center for Infectious Diseases. *MMWR Suppl.* **36**, 1S–15S (1987).
29. Vite-Garin, T., Estrada-Barcenas, D. A., Cifuentes, J. & Taylor, M. L. The importance of molecular analyses for understanding the genetic diversity of *Histoplasma capsulatum*: an overview. *Rev. Iberoam. Mycol.* **31**, 11–15 (2014).
30. Blackard, J. T. & Sherman, K. E. Hepatitis C virus coinfection and superinfection. *J. Infect. Dis.* **195**, 519–524 (2007).
31. Cohen, T. et al. Mixed-strain *Mycobacterium tuberculosis* infections and the implications for tuberculosis treatment and control. *Clin. Microbiol. Rev.* **25**, 708–719 (2012).
32. van Wyk, M., Govender, N. P., Mitchell, T. G., Litvintseva, A. P. & Germs, S. A. Multilocus sequence typing of serially collected isolates of *Cryptococcus* from HIV-infected patients in South Africa. *J. Clin. Microbiol.* **52**, 1921–1931 (2014).
33. Helweg-Larsen, J. et al. Clinical correlation of variations in the internal transcribed spacer regions of rRNA genes in *Pneumocystis carinii* f.sp. *hominis*. *AIDS.* **15**, 451–459 (2001).
34. Sil, A. & Andrianopoulos, A. Thermally dimorphic human fungal pathogens—polyphyletic pathogens with a convergent pathogenicity trait. *Cold Spring Harb. Perspect. Med.* **5**, a019794 (2014).
35. Durkin, M. M. et al. Pathogenic differences between North American and Latin American strains of *Histoplasma capsulatum* var. *capsulatum* in experimentally infected mice. *J. Clin. Microbiol.* **42**, 4370–4373 (2004).
36. Karimi, K. et al. Differences in histoplasmosis in patients with acquired immunodeficiency syndrome in the United States and Brazil. *J. Infect. Dis.* **186**, 1655–1660 (2002).
37. Sahaza, J. H., Perez-Torres, A., Zenteno, E. & Taylor, M. L. Usefulness of the murine model to study the immune response against *Histoplasma capsulatum* infection. *Comp. Immunol. Microbiol. Infect. Dis.* **37**, 143–152 (2014).
38. Nieduszynski, C. A. & Liti, G. From sequence to function: Insights from natural variation in budding yeasts. *Biochim. Biophys. Acta.* **1810**, 959–966 (2011).
39. Wohlbach, D. J. et al. Comparative genomics of *Saccharomyces cerevisiae* natural isolates for bioenergy production. *Gen. Biol. Evol.* **6**, 2557–2566 (2014).
40. Ene, I. V. & Bennett, R. J. The cryptic sexual strategies of human fungal pathogens. *Nat. Rev. Microbiol.* **12**, 239–251 (2014).
41. Tibayrenc, M. & Ayala, F. J. Reproductive clonality of pathogens: a perspective on pathogenic viruses, bacteria, fungi, and parasitic protists. *Proc. Nat. Acad. Sci. USA* **109**, E3305–E3313 (2012).
42. Grigg, M. E., Bonnfoy, S., Hehl, A. B., Suzuki, Y. & Boothroyd, J. C. Success and virulence in *Toxoplasma* as the result of sexual recombination between two distinct ancestries. *Science.* **294**, 161–165 (2001).
43. Fressatti, R., Dias-Siqueira, V. L., Svidzinski, T. I. E., Herrero, F. & Kemmelmeyer, C. A medium for inducing conversion of *Histoplasma capsulatum* var. *capsulatum* into a yeast-like form. *Mem. Inst. Oswaldo Cruz.* **87**, 53–58 (1992).
44. Standard, P. G. & Kaufman, L. Specific immunological test for the rapid identification of members of the genus *Histoplasma*. *J. Clin. Microbiol.* **3**, 191–199 (1976).
45. Pizzini, C. V. et al. Evaluation of a western blot test in an outbreak of acute pulmonary histoplasmosis. *Clin. Diagn. Lab. Immunol.* **6**, 20–23 (1999).
46. Bubnick, M. & Smulian, A. G. The MAT1 locus of *Histoplasma capsulatum* is responsive in a mating type-specific manner. *Eukaryot. Cell.* **6**, 616–621 (2007).
47. Rodriguez-Arellanes, G. et al. Frequency and genetic diversity of the MAT1 locus of *Histoplasma capsulatum* isolates in Mexico and Brazil. *Eukaryot. Cell.* **12**, 1033–1038 (2013).
48. Don, R. H., Cox, P. T., Wainwright, B. J., Baker, K. & Mattick, J. S. ‘Touchdown’ PCR to circumvent spurious priming during gene amplification. *Nucleic Acids Res.* **19**, 4008 (1991).

49. Altschul, S. F., Gish, W., Miller, W., Myers, E. W. & Lipman, D. J. Basic Local Alignment Search Tool (BLASTn). *J. Mol. Biol.* **215**, 403–410 (1990).
50. Thompson, J. D., Higgins, D. G. & Gibson, T. J. CLUSTAL W: improving the sensitivity of progressive multiple sequence alignment through sequence weighting, position-specific gap penalties and weight matrix choice. *Nucleic Acids Res.* **22**, 4673–4680 (1994).
51. Tamura, K., Stecher, G., Peterson, D., Filipski, A. & Kumar, S. MEGA6: Molecular Evolutionary Genetics Analysis version 6.0. *Mol. Biol. Evol.* **30**, 2725–2729 (2013).
52. Nguyen, L. T., Schmidt, H. A., von Haeseler, A. & Minh, B. Q. IQ-TREE: a fast and effective stochastic algorithm for estimating maximum-likelihood phylogenies. *Mol. Biol. Evol.* **32**, 268–274 (2015).
53. Minh, B. Q., Nguyen, M. A. & von Haeseler, A. Ultrafast approximation for phylogenetic bootstrap. *Mol. Biol. Evol.* **30**, 1188–1195 (2013).
54. Ronquist, F. et al. MrBayes 3.2: efficient Bayesian phylogenetic inference and model choice across a large model space. *Syst. Biol.* **61**, 539–542 (2012).
55. Rambaut, A. FigTree v1.3.1: Tree figure drawing tool. Preprint at <http://tree.bio.ed.ac.uk/software/figtree/> (2009).
56. Huson, D. H. & Bryant, D. Application of phylogenetic networks in evolutionary studies. *Mol. Biol. Evol.* **23**, 254–267 (2006).
57. Corander, J., Cheng, L., Marttinen, P., Sirén, J. & Tang, J. BAPS: Bayesian Analysis of Population Structure. BAPS, <http://www.helsinki.fi/bgs/software/BAPS/> (2011).
58. Librado, P. & Rozas, J. DnaSP v5: a software for comprehensive analysis of DNA polymorphism data. *Bioinformatics* **25**, 1451–1452 (2009).

Acknowledgements

Lisandra Serra Damasceno thanks the “Programa de Pós-graduação *Stricto Sensu* em Pesquisa Clínica em Doenças Infectuosas do Instituto Nacional de Infectologia Evandro Chagas”, FIOCRUZ and the scholarship No. 99999.002336/2014-06 provided by the “Programa Institucional de Bolsas de Doutorado Sanduíche no Exterior” from the “Coordenação de Aperfeiçoamento de Pessoal de Nível Superior (Capes)”, Brazil, which was realized in the Laboratorio de Inmunología de Hongos, Unidad de Micología, Departamento de Microbiología y Parasitología, Facultad de Medicina, UNAM, Mexico. RMZ-O was supported in part by CNPq [302796/2017-7] and FAPERJ [E-26/203.076/2016]. This research was also partially supported by a grant provided by “Programa de Apoyo a Proyectos de Investigación e Innovación Tecnológica-Dirección General de Asuntos del Personal Académico” from UNAM [PAPIIT-DGAPA/UNAM, Reference Number-IN213515] as well for Bridget Barker Startup funding from Northern Arizona University. PRINT-FIOCRUZ-CAPES was responsible for payment for this publication.

Author Contributions

Conceptualization: Rosely Maria Zancopé-Oliveira. Data curation: Lisandra Serra Damasceno, Jacó Ricarte Lima de Mesquita, Terezinha do Menino Jesus Silva Leitão. Formal analysis: Lisandra Serra Damasceno, Marcus de Melo Teixeira, Bridget Marie Barker, Rodrigo Almeida-Paes. Funding acquisition: Rosely Maria Zancopé-Oliveira, María Lucia Taylor. Investigation: Lisandra Serra Damasceno. Methodology: Lisandra Serra Damasceno, Marcus de Melo Teixeira, Marcos Abreu de Almeida, Mauro de Medeiros Muniz, Claudia Vera Pizzini, Jacó Ricarte Lima de Mesquita, Gabriela Rodríguez-Arellanes, José Antonio Ramírez, Tania Vite-Garín. Project Administration: Terezinha do Menino Jesus Silva Leitão, María Lucia Taylor, Rosely Maria Zancopé-Oliveira. Resources: Lisandra Serra Damasceno, Jacó Ricarte Lima de Mesquita, Terezinha do Menino Jesus Silva Leitão, María Lucia Taylor, Rodrigo Almeida-Paes, Rosely Maria Zancopé-Oliveira. Supervision: Rosely Maria Zancopé-Oliveira. Validation: Rodrigo Almeida-Paes. Visualization: Lisandra Serra Damasceno, Marcus de Melo Teixeira, Gabriela Rodríguez-Arellanes, José Antonio Ramírez, Tania Vite-Garín. Writing – original draft: Lisandra Serra Damasceno, Marcus de Melo Teixeira, Bridget Marie Barker. Writing, review, and editing: María Lucia Taylor, Rodrigo Almeida-Paes, Rosely Maria Zancopé-Oliveira.

Additional Information

Supplementary information accompanies this paper at <https://doi.org/10.1038/s41598-019-48111-6>.

Competing Interests: The authors declare no competing interests.

Publisher's note: Springer Nature remains neutral with regard to jurisdictional claims in published maps and institutional affiliations.



Open Access This article is licensed under a Creative Commons Attribution 4.0 International License, which permits use, sharing, adaptation, distribution and reproduction in any medium or format, as long as you give appropriate credit to the original author(s) and the source, provide a link to the Creative Commons license, and indicate if changes were made. The images or other third party material in this article are included in the article's Creative Commons license, unless indicated otherwise in a credit line to the material. If material is not included in the article's Creative Commons license and your intended use is not permitted by statutory regulation or exceeds the permitted use, you will need to obtain permission directly from the copyright holder. To view a copy of this license, visit <http://creativecommons.org/licenses/by/4.0/>.

© The Author(s) 2019

powerful tool for epidemiological investigation of PCP outbreaks, being as effective and less time-consuming than the 8-loci procedure.

P459

Genetic diversity of *Histoplasma* and *Sporothrix* species complexes using the internal transcribed spacer (ITS) region

C. Toriello, R. de la Torre, D. A. Estrada-Bárcenas, J. A. Ramírez, G. Rodríguez-Arellanes, T. M. Vite-Garín, H. Navarro-Barranco, A. Pérez-Mejía, M. R. Reyes-Montes and M. L. Taylor
Universidad Nacional Autónoma de México, Microbiología-Parasitología, Facultad de Medicina, México D.F., México

The internal transcribed spacer (ITS) region contains two variable non-coding regions that are nested within the rDNA. It is a convenient target region for molecular identification and disease diagnosis of pathogenic fungi. Two dimorphic and relevant fungi, *Histoplasma capsulatum* (Hc) and *Sporothrix schenckii* (Ss), causing histoplasmosis and sporotrichosis, respectively, are important mycoses in Mexico, with particular severe clinical course in immunocompromised patients. From two fungal pathogen collections of the World Data Centre for Microorganisms (WDCM), one of Hc (LH-UNAM WDCM817) and another from Ss (BMFM-UNAM WDCM834), 20 and 10 strains, respectively, were selected and ITS1-5.8S-ITS2 regions amplified by PCR. Primers ITS4 5'-TCCTCCGCTTATTGATATGC-3' and ITS5 5'-GGAAGTAAAAGTCGTAAAGG-3' were used for ITS fragment amplification of *Histoplasma*. Primers ITS1 5'-CTGGTCATTAGAG-GAAGTAA-3' and ITS4 5'-TCCTCCGCTTATTGATATGC-3' were used for *Sporothrix*. PCR amplified products (approximately 600 bp for Hc and 700 bp for Ss) were purified and sequenced. The generated sequences were aligned and edited with program MEGA v.5. Phylogenetic trees were constructed using neighbor-joining (NJ) and maximum parsimony (MP) analyses. For *Histoplasma*, the generated trees gave two well defined groups, I and II, with two subgroups in II, discriminating strains from different hosts and geographic origin. For *Sporothrix*, the generated trees gave two well defined groups, discriminating strains of America from Japan as observed by the genetic distance between them, but did not discriminate among Ss different species.

P460

Multilocus analyses of *Histoplasma capsulatum* isolated of cave-dwelling bats from Mexico reveals a new probable genetic population of this fungal pathogen

J. H. Sahaza,¹ D. A. Estrada-Bárcenas,^{1,2} T. M. Vite-Garín,¹ J. A. Ramírez,¹ G. Rodríguez-Arellanes,¹ A. E. González-González¹ and M. L. Taylor¹

¹Universidad Nacional Autónoma de México, Microbiología-Parasitología, Facultad de Medicina, México D.F., México; ²Instituto Politécnico Nacional, Colección Nacional de Cultivos Microbianos, Centro de Investigación y Estudios Avanzados, México D.F., México

Histoplasma capsulatum isolates from naturally infected bats captured randomly in different caves of Mexico were studied by means of a phylogenetic multilocus analysis using sequence fragments of five molecular markers [arf, H-anti, ole1, tub1, and (GA)n]. The MBGA vers. 5.0 software generated individual or concatenated trees for the five markers, using the neighbor-joining (NJ) and the maximum parsimony (MP) methods. The NJ and MP trees of the five individual or concatenated markers defined two major groups of *H. capsulatum* isolates. The first group was integrated by most of the isolates from the migratory bat *Tadarida brasiliensis* together with one *H. capsulatum* isolate from *Mormoops megalophylla* (previously described as a lineage). The second group was formed with all *H. capsulatum* isolates obtained from other different bat species (migratory and non-migratory). These

results suggest that the first group of isolates from *T. brasiliensis* and *M. megalophylla* can be proposed as a new genetic population (clade) of *H. capsulatum* in the Americas.

P461

Phylogenetic relationship of *Malassezia* species isolated from seborrheic dermatitis

Y. Amado,¹ A. Patiño-Uzcátegui,¹ M. C. Cepero de García,¹ J. Tabima,¹ A. Motta,² M. Cardenas,¹ A. Bernal,¹ S. Restrepo¹ and A. Celis¹

¹Universidad de los Andes, Bogotá, Colombia; ²Universidad El Bosque, Bogotá, Colombia

Scaling, inflammation and redness are the main characteristics of the widespread chronic skin pathology, Seborrheic Dermatitis (SD). It occurs mainly in body areas rich in sebaceous glands such as the scalp, face and chest. The disorder is present in 3 to 5% of the immunocompetent adults. In AIDS patients prevalence ranges from 30 to 85%; and it is considered an early marker of the evolutionary trend of HIV infection.

The etiology of this pathology is unknown but it has been related to opportunistic activity of yeasts of the genus *Malassezia*, which are normally human skin commensals. *Malassezia* spp comprises 14 species, 9 of them isolated from human skin. For several years, their identification was based on phenotypic traits but recently due to variability of interpretation of these traits, molecular methods have been implemented. Consequently, new species have been discovered and phylogenetic studies have been developed to support these discoveries. The results from these analyses show intraspecific variation within some species of *Malassezia*. Additionally, recent reports have shown that these species are differentially distributed around the world. In Colombia, previous studies found a high frequency of *M. globosa* and *M. restricta* in individuals with SD.

In order to determine the most frequently isolated species in Colombia from SD lesions, we performed a phylogenetic characterization based on morphological and physiological traits. A monotypic characterization was conducted by PCR amplification of 5.8S rDNA-ITS2 regions of *Malassezia* isolates from immunocompetent and HIV/AIDS individuals, both with and without active SD. To assess phylogenetic relationships, maximum-parsimony, maximum likelihood and Bayesian inference assessments were used. Furthermore, due to ITS primary sequence analysis of *Malassezia* spp has shown a high rate of change, we propose a comparative analysis of ITS2 sequences using a RNA secondary structure model.

Our results showed that *M. restricta* (37.5%) are the species more often isolated from individuals with SD while *M. furfur* (46.7%) was frequently isolated from healthy individuals. Moreover, we reported the isolation of *M. yamatoensis* from a healthy individual, for the first time in Colombia. We found a different phylogenetic signal from ITS secondary structure in relation to primary sequence. Information provided by phylogenetic analysis extends the knowledge about the genetic variability that has this genus.

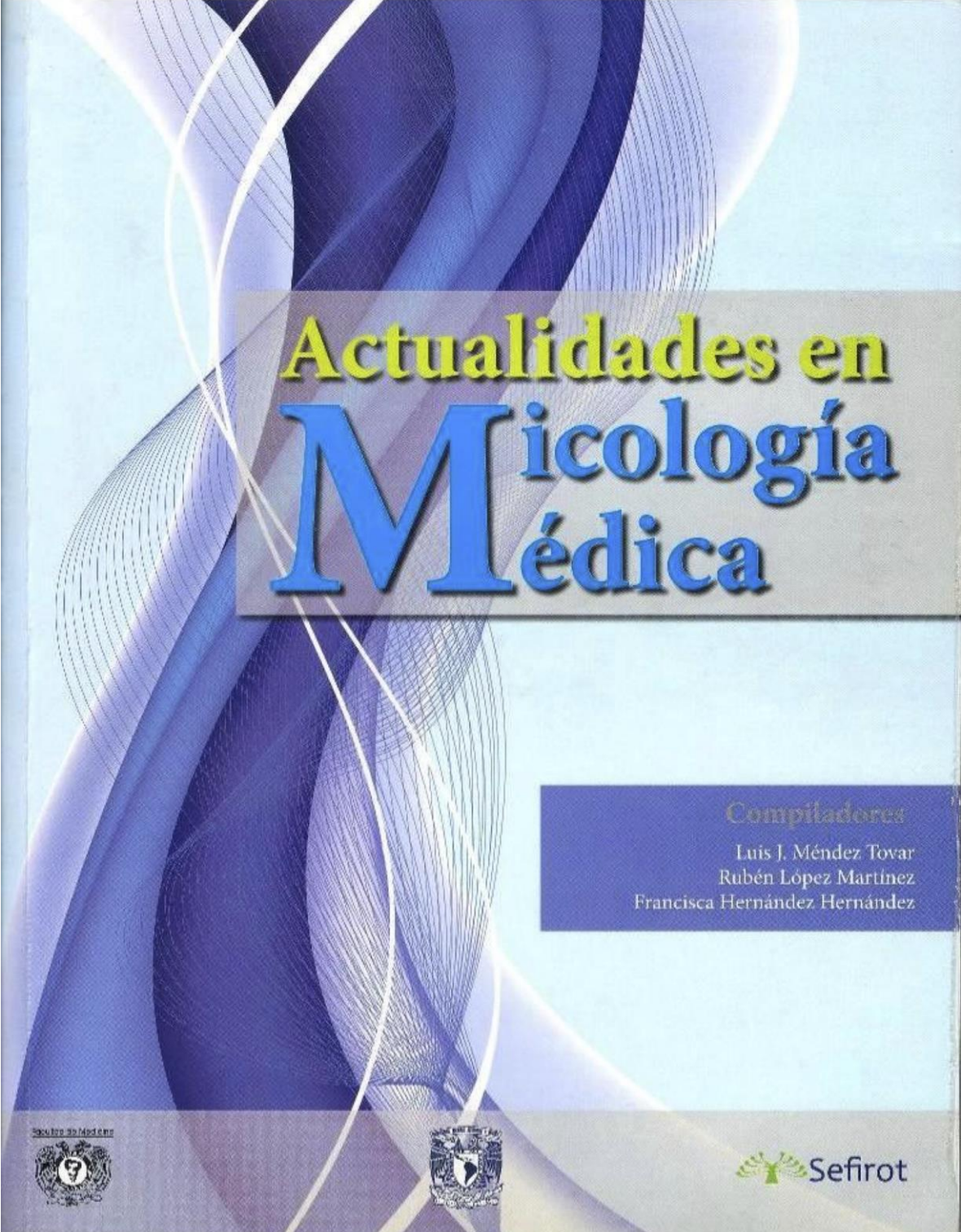
P462

Genetic diversity of environmental *Cryptococcus laurentii* complex isolates from Brazil

K. Ferreira-Pain,¹ L. Andrade-Silva,¹ D. J. Mora,¹ T. B. Ferreira,¹ F. C. Silva,¹ A. L. Pedrosa,¹ M. S. C. Melhem,² D. M. C. Silva² and M. L. Silva-Vergara¹

¹Triângulo Mineiro Federal University, Internal Medicine, Uberaba, Brazil; ²Adolfo Lutz Institute, Mycology Department, São Paulo, Brazil

Background: The *Cryptococcus* sp. are worldwide distributed and species such as *Cryptococcus laurentii* has been classically considered as saprophytic, despite several human cases of cryptococcosis were already reported. *Cryptococcus laurentii* specie is in fact a complex of



Actualidades en Micología Médica

Compiladores

Luis J. Méndez Tovar
Rubén López Martínez
Francisca Hernández Hernández



Sefirot



ACTUALIDADES EN MICOLOGÍA MÉDICA

Compiladores

Luis J. MÉNDEZ TOVAR

Rubén LÓPEZ MARTÍNEZ

Francisca HERNÁNDEZ HERNÁNDEZ

Editorial Sefirot, S.A. de C.V.

Tel. 53 67 75 21

Fax 53 67 14 44

Primera edición: Sefirot, 2012

Sexta edición: UNAM, 2012

DR© Universidad Nacional Autónoma de México. Ciudad Universitaria, 04510, México, D.F.

DR © Editorial Sefirot, S.A. de C.V., 2012

Av. Tlalnepantla No. 46, Col. Prado Ixtacala, C.P. 54160, Tlalnepantla, Edo. de México

Director editorial: J. Miguel Martínez Cárdenas

Editor: Alberto Téllez Aguilar

Diseño de portada e interiores: Ma. Guadalupe Martínez Mendoza

Corrección de estilo: Ernesto Jáuregui, Abelardo Rojas F.

Formación: Raymundo Hernández Angel

ISBN SEFIROT: 9786077728337

ISBN UNAM: 9786070232794

La presentación, disposición y demás características de esta obra son propiedad de Editorial Sefirot, S.A. de C.V.

Queda prohibida la reproducción o transmisión total o parcial de este libro en cualquier medio sin permiso escrito de la editorial.

Impreso en México • Printed in Mexico



www.editorialsefirot.com

sefirot@editorialsefirot.com

Síguenos en Editorial Sefirot @E_Sefirot

CONTENIDO

<i>Colaboradores</i>	VI	
<i>Prefacio a la sexta edición</i>	<i>IX</i>	
<i>Semblanza</i>	<i>X</i>	
PARTE I		
GENERALIDADES DE HONGOS		1
Capítulo 1		
<i>Generalidades de micología médica</i>	2	
RUBÉN LÓPEZ MARTÍNEZ		
Capítulo 2		
<i>Morfología general de los hongos</i>	4	
FRANCISCA HERNÁNDEZ-HERNÁNDEZ		
Capítulo 3		
<i>Morfología y fisiología de los hongos patógenos</i>	7	
LUIS J. MÉNDEZ TOVAR		
Capítulo 4		
<i>Reproducción asexual en hongos conidiogénesis y esporangiosporogénesis</i>	12	
BLANCA EDITH MILLÁN CHIU		
Capítulo 5		
<i>Reproducción sexual en hongos</i>	16	
ELVA BAZÁN MORA		
Capítulo 6		
<i>Avances en el conocimiento de la diversidad de hongos y los cambios en los esquemas clasificatorios</i>	21	
MARGARITA VILLEGAS RÍOS ITZEL RAMÍREZ LÓPEZ		
Capítulo 7		
<i>Campos de estudio de la micología: el cultivo de hongos comestibles, un ejemplo de micología aplicada y una opción de desarrollo sustentable</i>	25	
GERARDO MATA		
Capítulo 8		
<i>Ecología de los hongos y su impacto en el hombre</i>	32	
SIGFRIDO SIERRA GALVÁN SANDRA CASTRO SANTIUSTE		
PARTE II		
GENERALIDADES DE MICOLOGÍA MÉDICA		35
Capítulo 9		
<i>Mecanismos de patogenicidad en hongos patógenos humanos</i>	36	
CONCHITA TORIELLO		
Capítulo 10		
<i>Inmunología de las micosis</i>	43	
LAURA E. CASTRILLÓN RIVERA ALEJANDRO PALMA RAMOS		
Capítulo 11		
<i>Técnicas de laboratorio para el diagnóstico micológico</i>	51	
CUDBERTO CONTRERAS PÉREZ PATRICIA GUTIÉRREZ GARCÍA CLAUDIA RÍOS ROSAS		
Capítulo 12		
<i>Histopatología de las micosis</i>	55	
GISELA NAVARRETE FRANCO		
PARTE III		
MICOSIS SUPERFICIALES		59
Capítulo 13		
<i>Propedéutica dermatológica</i>	60	
AARÓN VÁZQUEZ HERNÁNDEZ		
Capítulo 14		
<i>Dermatofitos: ecología y morfología</i>	65	
PATRICIA MANZANO-GAYOSO		
Capítulo 15		
<i>Dermatofitosis: epidemiología y cuadros clínicos</i>	73	
VÍCTOR M. TARANGO MARTÍNEZ		
Capítulo 16		
<i>Dermatofitosis: diagnóstico y tratamiento</i>	84	
PATRICIA MANZANO-GAYOSO		

Capítulo 17	Capítulo 29
<i>El género malassezia y patologías asociadas.....</i>	<i>Nocardiosis</i>
FRANCISCA HERNÁNDEZ HERNÁNDEZ	LUCIO VERA CABRERA OLIVERIO WELSH LOZANO
Capítulo 18	Capítulo 30
<i>Pitiriasis versicolor</i>	<i>Actinomycosis</i>
ALICIA LEMINI LÓPEZ	LUIS J. MÉNDEZ TOVAR
Capítulo 19	PARTE V
<i>Piedras y tiña negra</i>	MICOSIS SISTÉMICAS
MARINA ROMERO NAVARRETE	143
Capítulo 20	Capítulo 31
<i>Pseudomicosis superficiales</i>	<i>Características relevantes de histoplasma capsulatum y de la epidemiología molecular de la histoplasmosis</i>
ELSA VÁSQUEZ DEL MERCADO MOCTEZUMA	TAYLOR ML, RODRÍGUEZ-ARELLANAS G RAMÍREZ JA, GONZÁLEZ-GONZÁLEZ AE, SAHAZA JH, VITE-GARÍN T ESTRADA-BÁRCENAS DA
PARTE IV	Capítulo 32
MICOSIS SUBCUTÁNEAS	<i>Histoplasmosis. Clínica, diagnóstico y tratamiento ...</i>
107	RUBÉN LÓPEZ MARTÍNEZ
Capítulo 21	Capítulo 33
<i>Micetoma: etiología y epidemiología</i>	<i>El género coccidioides</i>
FRANCISCA HERNÁNDEZ HERNÁNDEZ	LAURA ROSÍO CASTAÑÓN OLIVARES
Capítulo 22	Capítulo 34
<i>Micetoma: cuadro clínico y diagnóstico diferencial ...</i>	<i>Coccidioidomycosis clínica, diagnóstico y tratamiento .</i>
PATRICIA MANZANO-GAYOSO	RUBÉN LÓPEZ MARTÍNEZ RAFAEL LANIADO-LABORÍN
Capítulo 23	Capítulo 35
<i>Micetoma: diagnóstico de laboratorio</i>	<i>Paracoccidioidomycosis</i>
FRANCISCA HERNÁNDEZ-HERNÁNDEZ	RAMÓN FERNÁNDEZ ROBERTO ARENAS
Capítulo 24	Capítulo 36
<i>Avances en la fisiopatogenia y el tratamiento de los actinomicetomas</i>	<i>Blastomicosis</i>
OLIVERIO WELSH LUCIO VERA-CABRERA MARIO C. SALINAS-CARMONA	GABRIELA MORENO-COUTIÑO
Capítulo 25	PARTE VI
<i>El género sporothrix y epidemiología de la esporotricosis</i>	MICOSIS POR HONGOS OPORTUNISTAS
ALEJANDRA PAULA ESPINOSA TEXIS GERMÁN LARRIBA CALLE	173
Capítulo 26	Capítulo 37
<i>Esporotricosis</i>	<i>El género candida</i>
FRANCISCA HERNÁNDEZ-HERNÁNDEZ	MARÍA DE LOS ÁNGELES MARTÍNEZ RIVERA
Capítulo 27	Capítulo 38
<i>Cromoblastomicosis</i>	<i>Papel del estrés y el ciclo parasexual en la variabilidad genética del patógeno oportunitista candida albicans</i>
VÍCTOR FERNANDO MUÑOZ ESTRADA ANA DANIELA CASTREJÓN PÉREZ	GERMÁN LARRIBA CALLE
Capítulo 28	
<i>Entomofitoromicosis: conidiobolomycosis y basidiobolomycosis</i>	
JORGE MAYORGA VÍCTOR FERNANDO MUÑOZ ESTRADA	

COLABORADORES

Dra. A. Montoya

Centro de Investigaciones en Ciencias Biológicas, Universidad Autónoma de Tlaxcala, San Martín Texmelucan-Tlaxcala, Ixtacuixtla, Tlaxcala.

Dr. A. Ramírez-Terrazo

Facultad de Ciencias, Universidad Nacional Autónoma de México.

A. E. González-González

Laboratorio de Inmunología de Hongos, Departamento de Microbiología y Parasitología, Facultad de Medicina, UNAM.

Dr. Aarón Vázquez Hernández

Servicio de Dermatología y Micología Médica, Hospital de Especialidades, CMN Siglo XXI.

M. en C. Alejandra Paula Espinosa Texis

Centro de Investigaciones en Ciencias Microbiológicas, Instituto de Ciencias Benemérita Universidad Autónoma de Puebla, Edificio 103 "J", Ciudad Universitaria, Puebla, Puebla, México.

A. Montoya A. Ramírez-Terrazo

M. en C. Alejandro Palma Ramos

Departamento de Sistemas Biológicos, Universidad Autónoma Metropolitana Unidad Xochimilco.

M. en C. Alejandro Bonifaz Trujillo

Laboratorio de Micología Médica, Servicio de Dermatología, Hospital General de México, SS.

Dra. Alicia Lemini López

Servicio de Dermatología, Hospital General de Zona N° 8, IMSS.

Dra. Ana Daniela Castrejón Pérez

Departamento de Dermatología y Micología, Centro de Investigación y Docencia en Ciencias de la Salud (CIDOC), Facultad de Medicina, Universidad Autónoma de Sinaloa, Culiacán, Sinaloa, México.

Dra. Blanca Edith Millán Chiu

Laboratorio de Micología Médica, Departamento de Microbiología y Parasitología, Facultad de Medicina, UNAM.

Dra. Carolina Segundo Zaragoza

Facultad de Medicina Veterinaria y Zootecnia, UNAM.

Dra. Cécile-Marie Aliouat

Servicio de Parasitología-Micología, Facultad de Ciencias Farmacéuticas, Universidad de Lille, Francia.

Biól. Claudia Ríos Rosas

Laboratorio de Micología, Instituto de Diagnóstico y Referencia Epidemiológicos SS.

Dra. Conchita Torriello Nájera

Laboratorio de Micología Básica, Departamento de Microbiología, Facultad de Medicina, UNAM.

Q.R.B. Cudberto Contreras Pérez

Laboratorio de Micología, Instituto de Diagnóstico y Referencia Epidemiológicos SS.

Dr. D. A. Estrada-Bárcenas

Laboratorio de Inmunología de Hongos, Departamento de Microbiología y Parasitología, Facultad de Medicina, UNAM.

Dra. Denisse Vázquez González

Laboratorio de Micología Médica
Dermatología, Hospital General de México, SS.

Dr. Eduardo Del-Cas

Servicio de Parasitología-Micología, Facultad de Medicina (Universidad de Lille), Francia.

Dr. El Moukhtar Aliouat

Servicio de Parásitología-Micología, Facultad de Ciencias Farmacéuticas, Universidad de Lille, Francia.

Dra. Elsa M. Vázquez del Mercado

Servicio de Dermatología, Hospital General "Manuel Gea González", SS.

Biól. Elva Bazán Mora

Laboratorio de Micología Médica, Departamento de Microbiología y Parasitología, Facultad de Medicina, UNAM.

Dra. Francisca Hernández Hernández

Laboratorio de Micología Médica, Departamento de Microbiología y Parasitología, Facultad de Medicina, UNAM.

Dra. Gabriela Moreno Coutiño

Servicio de Dermatología, Hospital General "Manuel Gea González", SS.

M. en C. Gabriela Rodríguez Arellanes

Laboratorio de Inmunología de Hongos, Departamento de Microbiología y Parasitología, Facultad de Medicina, UNAM.

Dr. Gastón Guzmán

Investigador Emérito del Instituto de Ecología, Xalapa, Veracruz, México.

Dr. Gerardo Mata

Red Manejo Biotecnológico de Recursos
Instituto de Ecología, A.C., Xalapa, Veracruz, México.

Dr. Germán Larriba Calle

Departamento de Ciencias Biomédicas, Grupo de Investigación RECA. Área Microbiología, Facultad de Ciencias, Universidad de Extremadura, Badajoz, España.

Dra. Gisela Navarrete Franco

Departamento de Hipatopatología, Centro Dermatológico "Dr. La-dislao de la Pascua" SS.

Isabelle Durand-Joly

Servicio de Parasitología-Micología, Facultad de Medicina (Universidad de Lille), France.

Itzel Ramírez López

Área de Micología, Depto. de Biología Comparada, Facultad de Ciencias, UNAM.

J. A. Ramírez

Laboratorio de Inmunología de Hongos, Departamento de Microbiología y Parasitología, Facultad de Medicina, UNAM.

J. H. Sahaza

Laboratorio de Inmunología de Hongos, Departamento de Microbiología y Parasitología, Facultad de Medicina, UNAM.

QFB. Javier Araiza Santibañez

Laboratorio de Micología Médica, Servicio de Dermatología, Hospital General de México, OD.

Biol. Jorge Mayorga

Centro de Referencia en Micología (CEREMI).
Instituto Dermatológico de Jalisco "Dr. José Barba Rubio" Guadalajara, Jal.

Dra. Josefina Carbajosa Martínez

Servicio de Dermatología, Hospital de la Nutrición "Salvador Zubirán" SS.

Dr. Josep Maria Torres Rodríguez

Universitat Autònoma de Barcelona. Unitat d'Al·lèrgia Téknion.
Barcelona.

Dra. Laura Estela Castrillón Rivera

Laboratorio de Inmunobiología, Departamento de Sistemas Biológicos, Universidad Autónoma Metropolitana-Xochimilco.

Dra. Laura Rosio Castañón Olivares

Laboratorio de Micología Médica, Departamento de Microbiología, Facultad de Medicina, UNAM.

PhD. Leonel Mendoza

Biomedical Laboratory Diagnostics, Microbiology and Molecular Genetics, Michigan State University, East Lansing Michigan, USA.

Dr. Lucio Vera Cabrera

Servicio de Dermatología, Hospital Universitario, U.A.N.L., Monterrey, Nuevo León, México.

Dr. Luis J. Méndez Tovar

Laboratorio de Investigación Médica en Dermatología y Micología, Hospital de Especialidades, Centro Médico Nacional Siglo XXI, IMSS.

Dra. Magali Chabé

Servicio de Parasitología-Micología, Facultad de Ciencias Farmacéuticas, Universidad de Lille, France.

Dra. Magda Carvajal Moreno

Departamento de Botánica, Instituto de Biología, UNAM.

Dra. Margarita Villegas Ríos

Área de Micología, Depto. de Biología Comparada, Facultad de Ciencias, UNAM.

Dra. María de los Ángeles Martínez Rivera

Escuela Nacional de Ciencias Biológicas, Instituto Politécnico Nacional.

Dra. María Lucia Taylor Cunha e Mello

Laboratorio de Inmunología de Hongos, Departamento de Microbiología y Parasitología, Facultad de Medicina, UNAM.

Dra. Marina Romero Navarrete

Servicio de Dermatología, Hospital General de Acapulco, SS. México.

Dr. Mario Salinas Carmona

Departamento de Inmunología, Facultad de Medicina, Universidad Autónoma de Nuevo León, Monterrey, Nuevo León, México.

Dr. Oliverio Welsh

Servicio de Dermatología, Hospital Universitario, Universidad Autónoma de Nuevo León, Monterrey, Nuevo León, México.

Patricia Gutiérrez García

Laboratorio de Micología. Instituto de Diagnóstico y Referencia Epidemiológicos SS.

Dra. Patricia Manzano Gayoso

Laboratorio de Micología Médica, Departamento de Microbiología y Parasitología, Facultad de Medicina, UNAM.

Pere Saballs-Redresa

Servei de Medicina Interna i Malalties Infeccioses, Hospital del Mar. Barcelona.

PhD. Rafael Laniado Laborín

MD, MPH, FCCP PMB953, 482-W. Isidro, Blv No2. San Isidro CA, 92173, USA.

Colaboradores**Dr. Ramón Felipe Fernández**

Servicio de Dermatología, Hospital General "Manuel Gea González", SS.

Raquel Vilela

Instituto Superior de Medicina y Dermatología, Belo Horizonte, Brasil.

Roberta L. Motta

Instituto Superior de Medicina y Dermatología, Belo Horizonte, Brasil.

Dr. Roberto Arenas Guzmán

Sección de Micología, Hospital General "Manuel Gea González", SS.

Dr. Roberto Arnulfo Cervantes Olivares

Facultad de Medicina Veterinaria y Zootecnia, UNAM.

Dra. Rocío Orozco Topete

Departamento de Dermatología

Instituto Nacional de Ciencias Médicas y Nutrición "Salvador Zubirán", México.

Dr. Rubén López Benítez

Departamento de Radiodiagnóstico, Clínica Quirúrgica, Universidad de Heidelberg, Alemania.

Dr. Rubén López Martínez

Laboratorio de Micología Médica, Departamento de Microbiología y Parasitología, Facultad de Medicina, UNAM.

Sandra Castro Santisteban

Laboratorio de Taxonomía de Hongos Tremeloides (Heterobasidiomycetes), Laboratorios de Micología, Facultad de Ciencias, UNAM.

Sanfi Grau

Farmacia Hospitalaria del IMAS, Facultat de Medicina, Universitat Autònoma de Barcelona.

Sergio Ayvar Serna

Departamento de Botánica, Instituto de Biología, UNAM.

Dr. Sigfrido Sierra Galván

Lab. de Taxonomía de Hongos Tremeloides (Heterobasidiomycetes), Laboratorios de Micología, Facultad de Ciencias, UNAM.

T. Vite Garín

Laboratorio de Inmunología de Hongos, Departamento de Microbiología y Parasitología, Facultad de Medicina, UNAM.

Dr. Victor Fernando Muñoz Estrada

Departamento de Dermatología y Micología, Centro de Investigación y Docencia en Ciencias de la Salud (CIDOCSS), Facultad de Medicina, Universidad Autónoma de Sinaloa, Culiacán, Sinaloa, México.

Dr. Victor Tarango Martínez

Centro Dermatológico de Occidente, Guadalajara, Jalisco, México.

Dra. Virginia Vanziani Z.

Hospital Asociación Para Evitar la Ceguera en México. "Dr. Luis Sánchez Bulnes".

CARACTERÍSTICAS RELEVANTES DE *Histoplasma capsulatum* Y DE LA EPIDEMIOLOGÍA MOLECULAR DE LA HISTOPLASMOSIS

Taylor MI., Rodríguez-Arellanes G., Ramírez JA., González-González AL., Sahaza JH., Vite -Garin T. y Estrada-Bárcenas DA.

Histoplasma capsulatum: Generalidades

El agente causal de la histoplasmosis, micosis sistémica de gran prevalencia en el continente americano, es el hongo dimórfico *Histoplasma capsulatum*. Este organismo eucariota es heterotálico y tiene los tipos haploides de compatibilidad sexual ("mating types"): (a⁺) o ("major") y (a⁻) o ("minor"). Los tipos a⁺ y a⁻, están representados en el locus MAT1 por dos regiones idiomorfas MAT1-1 y MAT1-2, respectivamente. El estado asexuado o anamorfo de este hongo lo constituye la especie haploide *H. capsulatum*. El estado sexuado o teleomorfo resultante del apareamiento de sus haplotipos sexuales es el ascóomiceto *Ajellomyces capsulatus*. *Histoplasma* y *Ajellomyces* constituyen el mismo hongo holomorfo, término asignado a los hongos con esporulación teleomorfa junto con todos sus estados anamorfos.

Histoplasma capsulatum: Ecología y ciclo de vida

En el ambiente *H. capsulatum* crece favorablemente en guano de murciélagos y aves (factores bióticos) o en alimento balanceado para ganado (gallinazos o pollinazas), debido a que contienen altas concentraciones de nutrientes como nitrógeno y fósforo, además de oligoelementos. Las condiciones físicas como poca luz (que favorece la esporulación), temperaturas óptimas (de ambiente y de suelo) en el rango 25-30°C y humedad relativa >60% sumadas a los factores bióticos, conforman el nicho ecológico ideal para el desarrollo de este microorganismo. En la Figura 1 se esquematiza el ciclo de vida de *H. capsulatum* en la naturaleza.

Taylor *et al.*, en 1994, han aislado el hongo de muestras de guano colectadas de diferentes profundidades y evidencias indirectas, por ensayos de ELISA para detección de anticuerpos en ratones inoculados con sobrenadantes de guano, han demostrado la presencia de *H. capsulatum* en muestras de guano de hasta 22.5 cm de profundidad. Actualmente, se demuestra la presencia de este patógeno en muestras de diferentes naturalezas por métodos moleculares, los cuales resultan ser más rápidos y sensibles que los inmunológicos y más aún que los micológicos.

Se han realizado, por distintos investigadores, estudios sobre la micobiotia asociada al nicho ecológico de *H. capsulatum*. Particularmente en México, Lappe *et al.* 1998 y Ulloa *et al.*, en 2006, han descrito algunas especies de hongos filamentosos como *Acromonium* spp., *Aspergillus terreus*, *A. versicolor*, *Gymnascella citrina*, *Gymnoascus daskaliensis*, *Malbranchea aurantiaca*, *Penicillium* spp., *Aphanoascus fulvescens*, *Chaetomidium fumeti*, *Phoma* sp. y de levaduras como *Candida catenulata*, *C. ciferrii*, *C. famata*, *C. guilliermondii*, *Rhodotorula* spp.

Ácaros micófagos que se alimentan de hongos del género de murciélagos forman parte de una cadena trófica asociada al nicho ecológico de *H. capsulatum* y, posiblemente, desempeñan un papel de dispersión del hongo a través de un mecanismo foráneo, según lo sugerido por Hoffmann en 1998 y demostrado por Estrada-Bárcenas *et al.* en 2010 para *Sancassania sphacergaster* (*S. ca. sphacergaster*) (Astigmata: Acari: Acaridae).

Histoplasma capsulatum: Aspectos morfológicos y bioquímicos

Histoplasma capsulatum en su fase micelial (M) saprobi-geofítica (forma infectiva) posee crecimiento lento (semanas) en cultivos a 25-28°C, donde desarrolla colonias albinas (tipo A) o pigmentadas (tipo B- del inglés brown). Estas últimas tienen un color que varía de pardo claro a oscuro, el cual está adjudicado a la presencia de melanina que se encuentra tanto en la pared de las hifas y condílos como en las células de la fase levaduriforme (L) parasitaria (forma virulenta). Con frecuencia las colonias B cambian al tipo A con la constante resiembra en medios de cultivo (pleomorfismo colonial). En algunas cepas se han descrito un pigmento difusible al medio que varía del rosa al rojo, el cual no se encuentra asociado a las estructuras celulares del hongo. La primera descripción de cepas con pigmento rojo fue hecha por Morris *et al.* en 1986, y correspondió a un aislamiento de suelo de un cañaveral. En México, Taylor *et al.* obtuvieron, en 1999, algunos aislamientos con esta característica poco común, los cuales se lograron de muestras de guano de murciélagos. La presencia de pigmento rojo también se ha observado en aislamientos de *H. capsulatum* en su forma levaduriforme (L).

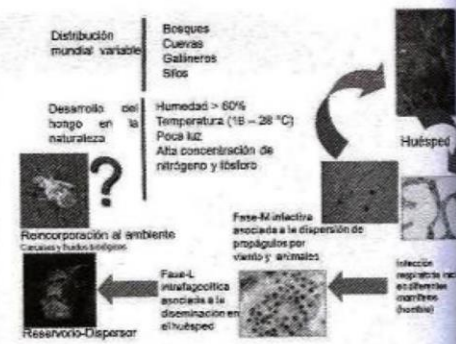


Figura 1. Ciclo de vida de *H. capsulatum*. El esquema muestra las tres morfologías de *H. capsulatum*, fase M y L, así como las condiciones ambientales, físicas y químicas asociadas al desarrollo de cada morfología.

imientos obtenidos de pacientes con el síndrome de inmunodeficiencia adquirida (SIDA) (Taylor ML, com pers.) Sin embargo, la naturaleza química de este pigmento de *H. capsulatum* permanece aún como un hecho inusitado que exige más estudios sobre la variabilidad fenotípica del hongo.

Al examen microscópico de la fase M del hongo se encuentran hifas septadas que miden de 1.0-2.5 mm de diámetro, con dos tipos de conidios solitarios (aleuroconidios): microconidios y macroconidios (estructuras reproductivas asexuales). Los microconidios son redondos, piriformes o en forma de clavas, de 1-4 x 2-6 μm de diámetro y pueden estar fijos (sésiles) o unidos a las hifas por pequeños conidióforos. Los macroconidios típicos de la especie son de paredes gruesas, por lo general redondos de 8-14 μm de diámetro y tienen proyecciones de diferentes tamaños que simulan dedos, razón por la cual son llamados digitiformes. Los macroconidios también son llamados tuberculados y ocasionalmente pueden tener forma de clava; están adheridos a las hifas por conidióforos cortos que con frecuencia forman un ángulo aproximado de 90° con las mismas (Figura 2). Algunas veces se observan aislamientos atípicos con macroconidios lisos sin proyecciones que, con cierta frecuencia, proceden de pacientes con SIDA. La abundancia de macroconidios está asociada, por lo general, a las colonias B y es dependiente del tiempo de cultivo de los aislamientos.

En el estado teleomorfo, el hongo presenta fructificaciones denominadas cleistotecios (estructura diploide), las cuales contienen ascas subesféricas evanescentes donde se realizan dos reducciones meióticas para dar origen a ascosporas haploides (estructuras reproductivas de origen sexual), las cuales son subesféricas y miden de 1.2-1.5 mm de diámetro.

En su fase L, *H. capsulatum* se desarrolla tanto como parásito intracelular de fagocitos profesionales (macrófagos, polimorfonucleares, células dendríticas) y no profesionales (células epiteliales y endoteliales) de huéspedes susceptibles, así como a 37°C en medios de cultivo sintéticos adicionados con suplementos, especialmente glucosa y cisteína. Las colonias de levaduras tienen aspecto cremoso con color variable del beige claro a oscuro, pueden ser adhérentes o no al medio y presentan superficie rugosa (colonias R) o lisa (colonias S), esta última asociada a células avirulentas sin α-(1,3)-glucana en la pared celular. La micromorfología de las levaduras está representada por células ovaladas que varían de 1.3-2 x 2-4 μm de diámetro, uninucleadas y unigemantes con brotamiento de base estrecha.

Debido a que existen similitudes morfológicas y antigenicas de *H. capsulatum* con algunas especies de hongos y otros microorganismos (Tabla 1), es importante diferenciarlo tanto en su fase M en cultivo como en su fase L en tejidos parasitados.

Los dos morfotipos de *H. capsulatum*, poseen los mismos mecanismos de captación de hierro en condiciones de carencia de éste. El hierro es un cofactor esencial para los procesos metabólicos del microorganismo, incluyendo la respiración y la síntesis de ácidos nucleicos, aunque en exceso puede ser tóxico. Durante la infección por *H. capsulatum*, éste capta hierro de las proteínas del huésped transportadoras de este elemento (transferrina, lactoferrina) o de moléculas del huésped que contiene hierro en su estructura química (hemoglobina). Además, *H. capsulatum* desarrolla una actividad reductora de hierro a través de una enzima extracelular (reductasa férrica) y, en un entorno de baja concentración de este oligoelemento, el mecanismo más utilizado por el hongo para la captación de hierro es la producción de sideróforos (derivados del ácido hidroxámico) que tienen la función de quitar y proveer hierro necesario para el crecimiento y sobrevivencia de *H. capsulatum* en el ambiente hostil intracelular, captando iones Fe²⁺ liberados por la modulación del pH intrafagosomal inducida por el patógeno. Por otro lado, el ácido hidroxámico liberado en el medio de cultivo de la fase L de *H. capsulatum* actúa como factor de crecimiento para pequeños inóculos de sus respectivos micelios o levaduras.

No obstante que las características mencionadas se consideran prototípico para este patógeno, se tienen referencias de cepas que presentan cambios fenotípicos de morfología colonial y microscópica, antigenicidad (particularmente relacionada a los antígenos H-asociado a la enfermedad activa y M-revelado durante todo el curso de la histoplasmosis e incluso después de la curación clínica y biológica), virulencia, habilidad para convertirse a la fase L y sensibilidad a la temperatura.

La inhibición de la transición dimórfica M-L por inhibidores de grupos sulfhidrilos produce cepas avirulentas para

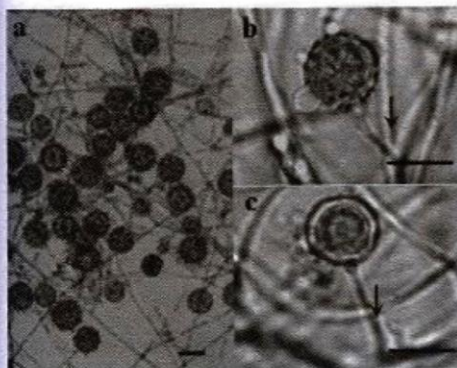


Figura 2. Micromorfología de *H. capsulatum*. a) Abundantes hifas delgadas y macroconidios digitiformes o tuberculados. b) y c) Macroconidios con conidióforos cortos formando ángulos de 90° con sus respectivas hifas de origen (flechas).

Tabla 1. Similitudes morfológicas y antigenicas de *H. Capsulatum* con otras especies de microorganismos.

Morfológicas	Micromorfología colonial	Histopatología
(conidiación de tipo	(fase parasitaria/tejido)	
<i>Chrysosporium</i>	<i>Candida glabrata</i>	
<i>Sepedonium</i>	<i>Blastomyces dermatitidis</i>	
<i>Chrysosporum</i>	(formas pequeñas)	
<i>Renispora</i>	<i>Cryptococcus neoformans</i> (células pequeñas, cápsula pequeña)	
	<i>Penicillium marneffei</i> (conidios intracelulares)	
	<i>Coccidioides immitis</i> (endosporas)	
	<i>Leishmania</i> spp. (amastigotes)	
	<i>Pneumocystis carinii</i> (formas quísticas)	
Antigenicas	Antígeno M	Antígeno no identificado
	<i>Paracoccidioides brasiliensis</i>	<i>Blastomyces dermatitidis</i>
	<i>Sporothrix schenckii</i>	<i>Coccidioides immitis</i>
		<i>Mycobacterium</i> spp.
		<i>Nocardia</i> spp.



el ratón. Por lo general, el tiempo de transición M*L en cultivo varía entre 1-3 semanas. Este proceso está relacionado a estímulos ambientales, como: cambios de temperatura de incubación; tensión de CO₂; potencial redox (grupos-SH); factores nutricionales como la dependencia de aminoácidos azufrados para el crecimiento en fase L. Por la técnica genómica de microarreglos se han identificado en *H. capsulatum* varios genes específicos de fase. Sin embargo, en la práctica, pocos han sido estudiados. Se destacan algunos genes asociados las fases y al dimorfismo de *H. capsulatum*, entre ellos: el de la actina (disminuye su expresión durante la transición M*L); los de α- y β-tubulina (aumentan sus expresiones en fase M); el *CDC2* involucrado en el ciclo celular del hongo (aumenta su expresión en fase L); el *CaM* que codifica para la calmodulina (aumenta su expresión en fase L); los *HSP* que promueven el dimorfismo fúngico a través de la expresión de las proteínas de choque térmico *Hsp60* (ligando de la fracción CD18 de las integrinas de la familia β2), *Hsp70* y *Hsp82* están regulados por el gen *OLE1*, el cual codifica para la desaturasa-Δ9 de ácido graso que modula el estado físico de la membrana celular del hongo al suscitar cambios en la fluididad de ésta, dados por la relación entre la concentración de ácidos grasos saturados y no saturados que influyen en la expresión de los genes *HSP*. Un hallazgo interesante asociado al dimorfismo de *H. capsulatum* y que involucra la activación de genes específicos de fase es la participación del gen *RYP1* (del inglés, Required for Yeast Phase), el cual es requerido para el crecimiento de la fase L a 37°C y para la expresión de varios genes específicos de fase L, algunos de los cuales están relacionados con la virulencia del hongo. Todo indica que *Ryp1* actúa como un regulador transcripcional para el cambio dimórfico de *H. capsulatum*, regulado por temperatura.

Los genes específicos que se expresan únicamente en la fase L (*YPS= Yeast Phase Specific, CBP1= Calcium Binding Protein*) destacan por su importante asociación con la virulencia de la cepa, los *YPS* (*YPS3* e *YPS21:E-9*), de los cuales el *YPS3* codifica una proteína que se localiza en la pared celular de *H. capsulatum* y que a su vez es el ligando para *TLR2* (del inglés, Toll Like Receptor); el *CBP1* codifica para una proteína de unión a calcio que se expresa en condiciones de bajas concentraciones de éste, durante la infección de macrófagos. Finalmente, los genes específicos de fase M denominados *MS* "mold-specific" (*MS8* y *MS88*) están asociados a la formación normal de hifas.

Histoplasma capsulatum: Sistemática clásica y molecular

El género *Histoplasma* con la especie *capsulatum*, comprende tres variedades taxonómicas identificadas por su micromorfología, distribución geográfica, especificidad para el huésped y cuadro clínico:

- *H. c. var. capsulatum - Darling, 1906.*
- *H. c. var. duboisi (Vanbreuseghem, 1957) - Ciferri, 1960.*
- *H. c. var. farciminosum (Rivolta, 1873) - Weeks, Padhye, et Ajello, 1985.*

El análisis de seis genes, *18S rRNA*, *28S rRNA*, *5.8S rRNA*, *EF1a* (factor de elongación-1a), *RPB1* y *RPB2* (subunida-

des de la RNA polimerasa II), sitúa a la especie *H. capsulatum* en el Reino Fungi, Phylum Ascomycota, Clase Eurotiomycetes, Subclase Eurotiomycetidae, Orden Onygenales, Familia Onygenaceae y/o Ajellomycetaceae.

Kasuga *et al.* en 1999 y 2003 sugieren que *H. capsulatum* es un complejo de especies cripticas y proponen una distribución filogeográfica del hongo considerando su clasificación filogenética con base en la secuencia parcial de cuatro genes, *ARF* (factor de ribosilación de ADP), *H-ANTI* (precursor del antigeno H), *OLE1* (desaturasa-Δ9 de ácido graso) y *TUB1* (α-tubulina), se formaron ocho clados (poblaciones genéticas) distintos, de los cuales siete constituyeron especies filogenéticas bien definidas (especiación) (Tabla 2). Entre los 137 aislamientos de *H. capsulatum* estudiados, procedentes de 25 países, se incluyeron las tres variedades taxonómicas del hongo. Posteriormente, Taylor *et al.* en 2005, utilizando los mismos marcadores en 14 aislamientos del hongo obtenidos de murciélagos naturalmente infectados capturados en México y con distintos hábitos migratorios sugieren la existencia de un nuevo clado de *H. capsulatum* asociado al murciélago migratorio *Tadarida brasiliensis mexicana*.

Tabla 2. Clasificación filogenética de *H. Capsulatum*.

Clados	Especies filogenéticas
Norte Americano clase 1	NAm 1
Norte Americano clase 2	NAm 2
Latinoamericano grupo A	LAM A (incluye el clado Eurasiano)
Latinoamericano grupo B	LAM B
Australiano	Australia
Holandés-Indonesio	Holanda-Indonesia
Africano	Africa
Eurasiano	-----

Kasuga *et al.* 2003.

Histoplasma capsulatum: feno y genotipificaciones

Se han utilizado distintos criterios para tipificar *H. capsulatum*, entre los cuales destacan diferencias en los parámetros morfológicas, bioquímicas, fisiológicas, así como en las virulencias, serotipos, quimiotipos, y diversidad genética del hongo.

Las levaduras expresan cinco diferentes serotipos de antígenos de superficie, dentro de los cuales están incluidos los quimiotipos I (colonias S) y II (colonias R) que se relacionan con la presencia de glucanas en la pared celular (Tabla 3). Las levaduras del quimiotipo II presentan más α-(1,3)-glucana en pared, hecho que está relacionado a la virulencia de la cepa, como fue elegantemente demostrado por Rappleby *et al.* en 2004 utilizando RNA de interferencia y por Marion *et al.* en 2006, al estudiar la actividad de la α-(1,4)-amilasa en la síntesis de la α-(1,3)-glucana. Recientemente, se ha propuesto que la α-(1,3)-glucana tiene un efecto sobre la respuesta inmune innata del huésped infectado a través del bloqueo de un receptor b-glucánico, conocido como Dectin-1.

Variantes de las colonias S son capaces de sobrevivir dentro de la línea celular de macrófagos P388D1.D2 y en culti-

Tabla 3. Secuencia de levaduras de *H. capsulatum*.

II 1, 2*
II 1, 4* corresponde a quimiotipo II (colección 8)
III 1, 2, 3* corresponde a quimiotipo I (colección 5)
IV 1, 2, 4*
V 1, 2, 3, 4*

*: 4. Diferentes抗原s de superficie de las levaduras.

vos primarios de células epiteliales de tráquea de hámster (HTE) donde asumen morfologías aberrantes, por ejemplo similar a una calabaza, que fueron llamadas alomórficas (Gr. *Allo* = otra; *morp* = forma) por Eissenberg et al. en 1996.

La pared celular de *H. capsulatum* no sólo proporciona soporte estructural para la célula fúngica pero también participa en la interfase huésped-parásito al exponer moléculas que regulan la biología del hongo ya que algunos de sus componentes pueden actuar contra el estrés ambiental y, en particular, sobre los mecanismos efectores antimicrobianos de huésped. La pared celular de *H. capsulatum* está formada por varios tipos de moléculas químicamente definidas: Carbohidratos (quitinina, a-(1,3)-glucana, b-(1,3)-glucana, galactomananas, mananas, manoproteínas y componentes tipo lectinas); Proteínas varias-Hsp60, Hsp70, antígeno M, antígeno H, H2B (proteína tipo histona 2B), proteína Yps3; Pigmento como melanina; Lipidos-ceramida (glicosilinositol fosforilceramida) y más recientemente ha surgido un gran interés sobre las vesículas extracelulares del hongo, formadas por una bicapa lipídica, que están transitoriamente presente en la pared de *H. capsulatum* con una posible función asociada al tráfico de moléculas y vesículas al exterior de la célula fúngica.

A partir de 1986 se iniciaron los estudios de tipificación molecular del hongo, los cuales sirvieron de apoyo para una clasificación molecular propuesta por Keath et al. en 1992 que aún sigue vigente y que agrupa cepas de *H. capsulatum* de América en seis clases y cuatro subclases. Esta clasificación se fundamenta en el análisis del polimorfismo genético del hongo, determinado por hibridación con sondas de mtDNA y de un fragmento del gen YPS3 (Tabla 4).

Se ha descrito una importante diversidad genética intraespecífica de *H. capsulatum* que revela cambios en su genoma, lo que contribuye a la genotipificación de la especie.

Tabla 4. Clasificación molecular de *H. capsulatum*.

Clases mtDNA	YPS3 (Kb)	subgrupo	aislamiento	origen geográfico
1	7.0, 1.8, 0.9		Downs	Missouri
2	3.2, 2.0		G-217B	Estados Unidos
3	2.4, 1.8		G-186B	Panamá
4	1.8, 0.9		FLS1	Fuerte Panamá
5	12, 2.4	a	589	
5	12, 2.4	b	130	Nueva York (Puerto Rico)
5	12, 2.4	c	140	Nueva York (Puerto Rico)
5	12, 2.4	d	RW	MISSOURI-(América Central)
6	4.2		1718	Panamá

Keath et al. 1992.

Distintas estructuras de poblaciones (clonales y recombinantes) de *H. capsulatum* han sido referidas al utilizar las secuencias parciales de los genes, *ARF*, *H-ANT1*, *OLE1* y *TUB1* (ver Tabla 2). Los aislamientos de *H. capsulatum* del clado LAm A, donde se incluyen los procedentes de México, son los más diversos genéticamente y, posiblemente, asociados a una estructura de población recombinante, mientras que los clados que quedaron confinados en áreas geográficas delimitadas de zonas templadas, presentan menos diversidad genética y tienden a la clonalidad, como es el caso de LAm B y NAm 1 que se consideran grupos monofiléticos.

El análisis de *H. capsulatum* con marcadores bialélicos y, en particular, los multialélicos (microsatélites) que se caracterizan por tener motivos repetitivos hipervariables y ser altamente polimórficos, fue utilizado para distinguir aislados individuales e identificar poblaciones fúngicas de Estados Unidos y de otras procedencias geográficas. En un estudio de Carter et al. realizado, en 2001, con los marcadores microsatélites (GA)_n, (GT)_n y GT(A)_n, se detectaron diferencias en la estructura de población de *H. capsulatum* en un gran número de cepas de Estados Unidos y en escasos ejemplares de Colombia, sugiriendo los autores la separación de amplias poblaciones geográficas del hongo en distintas especies, de acuerdo con el concepto de especie filogenética. Recientemente, Taylor et al. en 2012, analizaron aislamientos de *H. capsulatum* obtenidos de varias especies de murciélagos con el microsatélite (GA)_n y los resultados confirmaron hallazgos previos de que los aislamientos de *T. brasiliensis mexicana* forman un clado independiente, posiblemente asociado a una nueva especie filogenética. Sin embargo, estos hallazgos deben ser corroborados en estudio más amplio utilizando un número mayor de marcadores moleculares.

Histoplasma capsulatum también ha sido agrupado de acuerdo con la secuencia parcial de la subunidad grande del gen 28S rRNA nuclear (región D1/D2). Los grupos establecidos fueron independientes de las tres variedades taxonómicas y se propone que estas variedades deben ser reclasificadas considerando la relación filogenética del hongo.

La secuencia parcial de la subunidad pequeña del gen 18S rRNA nuclear ha evidenciado la cercanía filogenética de *H. capsulatum* con *Coccidioides immitis* y *Renispora flavissima* dentro de la familia Onygenaceae.

En los anteriores, un gran número de trabajos han contribuido al estudio de la diversidad genética de *H. capsulatum* con base en el análisis del DNA genómico. Los perfiles de RFLP y RAPD-PCR, la utilización de sondas específicas y de secuencias génicas, el uso de marcadores microsatélites, así como de las regiones ITS (del inglés "internal transcribed spacer"), han servido de herramientas para estudios taxonómicos, de estructura de la población fúngica, además de estudios epidemiológicos y de distribución geográfica del patógeno.

La diversidad genética de *H. capsulatum* también ha sido estudiada por cariotipificación (particularmente caracterización de electrocariotipos) así como por el polimorfismo cromosomal. Inicialmente, se describió polimorfismo cromosómico en las cepas de *H. capsulatum* más utilizadas como referencia, Downs y G-217B de Estados Unidos y G-186B de Panamá. En la cepa Downs, considerada de baja virulencia, se detectaron siete cromosomas mientras que en las cepas virulentas G-186B y G-



G-217B se encontraron cuatro y tres cromosomas, respectivamente. Con base en los índices de DNA calculados para la Downs y la G-186AS, el estadio haploide de ambas cepas fue sugerido por Carr y Shearer en 1998. Sin embargo, se encontraron copias duplicadas de los genes de *a* y *b* tubulina en la cepa Downs, lo que permitió proponer una reconsideración sobre su ploidía sugiriendo una posible diploidía parcial o una aneuploidía. Recientemente, un estudio más amplio realizado por Canteros et al. en 2005, aplicado a 19 aislamientos clínicos de *H. capsulatum* procedentes de Argentina, México y Guatemala, así como a la cepa de referencia G-186B, mostró una mayor variabilidad en el polimorfismo de los electrocariotipos de este hongo, lográndose la resolución de cinco a siete bandas cromosómicas.

Los grandes enigmas sobre la complejidad genómica de este hongo cuentan ahora con nuevas estrategias. En la actualidad, están en curso dos proyectos para elucidar el genoma de *H. capsulatum*, uno por parte del Broad Institute Fungal Genome (http://www.broadinstitute.org/annotation/genome/histoplasma_capsulatum) donde se procesan las cepas WV24 (pertenecientes al clado NAm 1), así como las cepas H143 y H88 agrupadas en el clado África y la cepa que pertenece al linaje de Panamá (G-186B). Esta última y la cepa G-217B que pertenece al clado NAm 2 son modelo de estudio del proyecto genoma que se realiza en el Genomic Sequencing Center, Washington University, St. Louis, MO, US (http://genome.wustl.edu/genomes/view/histoplasma_capsulatum/). Los datos arrojados por ambos proyectos podrán proveer más información sobre la complejidad genómica de este patógeno. Aunque la genómica de algunas cepas seleccionadas del hongo sean muy útiles, la constante búsqueda y comparación con nuevos aislados o con especies filogenéticas muy cercanas (hermanas), debe ser el marco de referencia para agrupar especímenes de *H. capsulatum*.

Para los estudios de genómica estructural de *H. capsulatum* se puede también recurrir al Centro de Secuenciación del Genoma (<http://genome.wustl.edu/projects/hcapsulatum/index.php>), en Estados Unidos, donde existe información disponible sobre la secuencia y mapeo genómico del hongo.

Histoplasma capsulatum: Colección de cepas

A partir de 1994, el Laboratorio de Inmunología de Hongos del Departamento de Microbiología y Parasitología, Facultad de Medicina, UNAM, inició la creación de una colección de *H. capsulatum*, la cual contiene aislamientos de la naturaleza y de casos clínicos de México, además de cepas de referencia de otros países. La colección puede ser considerada como única por la peculiaridad de albergar el mayor número de especímenes fúngicos obtenidos de murciélagos infectados. Además de contar con un catálogo, se encuentra registrada en la base de datos de la "World Data Centre for Microorganisms" (WDCM) de la "World Federation for Culture Collections" (WFCC) con el número LIH-UNAM_WDCM817, la cual puede ser consultada, por Internet, a través de la página de histoplasmosis (<http://www.histoplas-mex.unam.mx>). La colección de *H. capsulatum* muestra una gran variedad de aislamientos de diferentes fuentes y procedencias geográficas. A la fecha existen 269 aislamientos y/o cepas, 159 de

casos clínicos humanos, 83 de animales naturalmente infectados y 27 de diferentes tipos de guano. Los aislamientos y/o cepas de la colección representan un gran acervo biológico que ha servido de base para múltiples estudios que refieren datos sobre la feno y genotipificación de sus especímenes fúngicos.

Epidemiología de la histoplasmosis en México

La enfermedad ha sido descrita inicialmente en las regiones tropicales y subtropicales del mundo, entre los paralelos 45° N y 35° S; sin embargo, un nuevo registro de un brote autóctono en la latitud 54° N en Alberta, Canadá, sugiere una mayor dispersión del patógeno en la naturaleza. Esto indica que la distribución geográfica de *H. capsulatum* ha sido ampliada y que, posiblemente, está relacionado al mayor alcance en la migración de mamíferos y de aves que actúan como sus dispersores. En particular, destacan los murciélagos, mamíferos voladores que además de dispersores pueden servir como reservorios del patógeno, lo que implica una aclimatación tanto del dispersor como del hongo en nichos ecológicos localizados en áreas geográficas alejadas de los trópicos.

Casos autóctonos han sido referidos en cinco continentes y más de 60 países, con predominio en las Américas. *Histoplasma capsulatum* no es considerado endémico para Europa, sin embargo se ha referido casos aislados autóctonos de la enfermedad en algunos países y en animales silvestres. Las áreas endémicas más importantes, determinadas por la prueba cutánea con el antígeno crudo soluble de *H. capsulatum* denominado histoplasmina, se concentran en Estados Unidos (valles de los ríos Mississippi, Ohio y Missouri), en Centro y Sudamérica. En la última década, se ha adquirido un panorama más preciso sobre diferentes aspectos de la epidemiología de la histoplasmosis, debido a los estudios inmunológicos y moleculares realizados en áreas geográficas representativas de la República Mexicana. Las formas endémica y epidémica de la enfermedad son de amplia distribución en el país, aunque la última es más importante por su alto porcentaje de letalidad. La histoplasmosis infección revelada por la intradermorreacción positiva con la histoplasmina, ha sido referida en la mayoría de los estados mexicanos. Sin embargo, su prevalencia es variable según las zonas geográficas e incluso cambia dentro de una misma entidad federativa, hecho que está relacionado con ciertas actividades laborales asociadas a factores socio-económicos.

En México, *H. capsulatum* se encuentra en lugares especiales que pueden ser definidos como sitios de alto riesgo de infección y que se asocian a la forma epidémica de la enfermedad; en particular, ambientes cerrados como, cuevas, cuevas, minas, bocaminas, túneles, puentes, criptas de iglesias y casas abandonadas donde se acumulan diferentes tipos de guano de murciélagos. El hongo también se encuentra disperso en los denominados sitios de bajo riesgo de infección asociados a la forma endémica de la enfermedad, en general, ambientes abiertos como, patios caseros donde se deposita guano de aves o bajo el follaje de los árboles en parques y paseos públicos. La presencia de propagulos fúngicos en zonas urbanas resulta importante para explicar casos clínicos que no refieren visitas y exposición en sitios de alto

riesgo. Aislamientos de *H. capsulatum* de zonas urbanas en México son menos frecuentes, aunque algunos han sido referidos de gato de murciélagos, como el de una Unidad Habitacional en Culiacán, Sinaloa; de excretas de zanate y golondrina del parque público de Tlalpan, D.F.; de excretas de gallo de pelea en una casa habitación en Guerrero; y de material de compost (fertilizante orgánico) en un hotel en Acapulco, Guerrero.

Los mamíferos silvestres infectados, particularmente los murciélagos, así como diferentes especies de aves no migratorias o migratorias cavernícolas como los guácharos, pueden actuar como agentes biológicos en la distribución del hongo en la naturaleza, en zonas urbanas y rurales. Sin embargo, no hay que olvidar el posible papel de otros organismos que comparten el nicho ecológico de *H. capsulatum* y de agentes mecánicos, como los vientos, que producen corrientes de aire tanto en espacios cerrados como abiertos, moviendo en pequeñas distancias los propagulos fúngicos.

Aunque no se tienen datos que apoyen la infección de aves de parques (zanates, estorninos, palomas) y corrales (gallinazos), la cual podría estar limitada por la elevada temperatura corporal de las aves, éstas pueden desplazar al hongo depositado en sus plumajes a distancias cortas, y son uno de los principales agentes asociados a la infección por *H. capsulatum* en zonas urbanas.

En los últimos años, para estudiar diferentes aspectos epidemiológicos de la histoplasmosis en México se han empleado herramientas moleculares que han permitido proponer patrones moleculares de la distribución geográfica del hongo en el ambiente (filogeografía), así como caracterizar las fuentes de infección de aislamientos de diferentes orígenes en la naturaleza y su relación con brotes epidémicos.

El estudio molecular de brotes epidémicos de histoplasmosis ha contribuido a trazar una nueva historia en la epidemiología moderna de esta enfermedad en el país. Por ejemplo, con base en ensayos inmunológicos y moleculares realizados por un equipo de investigadores mexicanos, se aisló *H. capsulatum* de tierra mezclada con compost, utilizada en jardinerías con plantas ornamentales colocadas en diferentes sitios de un hotel en Acapulco, Guerrero, México, donde ocurrió un brote epidémico muy importante con episodios recurrentes en marzo, mayo y septiembre de 2001. Se han relacionado los aislamientos de este brote con los patrones ecotípicos y filogeográficos del hongo distribuidos en el país, a través de procedimientos moleculares, como: la PCR-anidada de un fragmento del gen que codifica para una proteína co-activadora denominada *Hcp100* única de *H. capsulatum*; el perfil polimórfico del DNA genómico obtenido por RAPD-PCR con doble primer; y el análisis de las secuencias de fragmentos de los genes *H-ANT1* y *OLE1*. En 2012, Fries de León *et al.* han reportado el éxito de un nuevo marcador, SCAR-1281-1283₂₀₀, por su especificidad y alta sensibilidad para detectar *H. capsulatum* en diferentes tipos de muestras ambientales y clínicas de distintas procedencias geográficas.

La referencia de brotes en animales cárnicos o de vida libre refuerza la apreciación de ubicuidad del agente etiológico en la naturaleza. En México, han ocurrido brotes de histoplasmosis en animales mantenidos en cautiverio como, maras o liebres de

la Patagonia (*Dolichotis patagonum*) y leopardos de las nieves (*Uncia uncia*). Hallazgos clínico-patológicos y de laboratorio confirmados por los estudios moleculares (PCR-anidada con el marcador *Hcp100* y RAPD-PCR con doble iniciador) apoyaron el diagnóstico de la enfermedad y la identificación de la fuente de infección. La presencia del patógeno identificado por la PCR-anidada con el marcador *Hcp100*, a partir del DNA extraído de órganos de murciélagos silvestres naturalmente infectados y capturados al azar en diferentes latitudes de la República Mexicana resalta la alta frecuencia de murciélagos portadores de la infección, lo cual posiblemente favorece la circulación del patógeno en el ambiente.

Por lo tanto, los estudios de brotes epidémicos de acuerdo con la información molecular de los aislamientos, no sólo sirven para definir casos clínicos de la enfermedad en un episodio común y asociar fuentes de infección, sino que también permiten inferir el comportamiento, ubicuidad, origen y características peculiares de los aislamientos de *H. capsulatum* que pueden estar siendo transportados de regiones geográficas distantes a través del continente, por algún agente dispersor.

Uso de la diversidad genética con fines epidemiológico

La aparición de las técnicas moleculares ha promovido grandes avances en la epidemiología de las micosis sistémicas.

La determinación de patrones geográficos del polimorfismo del DNA genómico de *H. capsulatum* permitirá trazar un mapa epidemiológico con base en el mayor o menor predominio de ciertos marcadores moleculares del hongo asociados a diferentes áreas geográficas. Datos moleculares actuales sobre la distribución de los marcadores de los tipos de compatibilidad sexual *a⁺* o *a⁻*, representados en el locus *MAT1* por dos regiones idiomórficas *MAT1-1* o *MAT1-2*, respectivamente, han aportado importante información sobre el patrón de distribución de estos marcadores en aislamientos de *H. capsulatum* de Norte y Sudamérica, destacando que en Estados Unidos y México la frecuencia del idiomórfico *MAT1-2* es mayor que la del *MAT1-1*, mientras que en Brasil ocurre lo contrario. Todo indica que el locus *MAT1* puede tener una relación con la virulencia de *H. capsulatum*, ya que codifica para factores de transcripción que regulan la expresión de diferentes genes fúngicos, algunos de los cuales podrían actuar como factores de virulencia. Sin embargo, la asociación de un idiomórfico, en particular, con mayor o menor virulencia de aislamientos de *H. capsulatum* carecen de bases científicas a la luz de los hallazgos moleculares, diversidad genética y dispersión del marcador *MAT1* en diferentes regiones geográficas del continente.

Asimismo, una contribución adicional del análisis del marcador microsatélite (GA)n de varios aislamientos del hongo obtenidos de murciélagos naturalmente infectados y capturados al azar en diferentes regiones de México, Argentina y Brasil, reveló una asociación entre hábitos migratorios y el origen geográfico de la infección; comprometiendo a los murciélagos como el principal dispersor del hongo en la naturaleza.

3. ARTÍCULO POR ENVIAR

Duarte-Escalante, E., **Vite-Garín, T.**, Vargas-Mendoza, C.F., Zancopé-Oliveira, R.M., Rodríguez-Arellanes, G., Ramírez, J.A., Reyes-Montes, M.R. And Taylor, M.L.: Genetic diversity, sequence network, and population structure analyses of *Histoplasma capsulatum* isolated from migratory and non-migratory bats captured in Mexico.

4. ALINEAMIENTOS INDIVIDUALES

arf

88
1111122222222223333333334444444444555555556666666666777
56789012345678901234567890123456789012345678901234567890123456789012
G-217B TGGTTGACAGCAACGATCGTGACCGTGTGTCGAGGCTCGGGAGGAGTTGCAGCGAAT
H144
H146
H147
H148 T.
H149
H150
H151
H152
H153
H155
H157
H158
H159
H160
H161
H162
H163
H164
H165
H166
H167
H176
H178 T.
H179
H185
H187
H189
H192 T.
H194

H-anti

H-anti

77
 111111122222222233333333344444444445555555566666666677777777888888
 34567890123456789012345678901234567890123456789012345678901234567890123456
 G-217B CCCAGATGACGCCTTATGCAAATATTTT-CTAATGCTA-GCCAGCCGATTATGTTCTGCTTCCCCGCCG
 EH-671HC.....GT.....-..C....-
 EH-671PC.....GT.....-..C....-
 EH-672BC.....GT.....-..C....-
 EH-672HC.....GT.....-..C....-
 EH-696PC.....G.....-..C....-.....C.
 154-04C.....G.....-..C....-
 190-03C.....G.....-..C....-
 CEPA 2C.....G.....-..C....-
 CEPA 3C.....G.....-..C....-
 L-100-91C.....G.....-..C....-
 EH-46C.....G.....-..C....-
 EH-53C.....G.....-..C....-
 EH-317C.....G.....-..C....-
 APC.....G.....-..A....-
 GeMC.....G.....-..C....-
 WChC.....G.....-..C....-
 1980-.....-
 H.1.02.WC.....G.....-..C....-
 H.1.04.91C.....G.....-..C....-.....T
 H.1.11.94C.....G.....-..C....-
 H.1.12.96C.....G.....-..C....-
 DOWNSC.....G.....-..C....-
 G-186BC.....G.....-..CT....-
 G-184BC.....G.....-..CT....-
 G-186AC.....G.....-..CT....-
 CA_1C.....G.....-..C....-
 CA_2C.....G.....-.....-
 CO_1C.....G.....-..C....-
 CO_2C.....G.....-..C....-
 CO_3C.....G.....-.....-
 TX_1C.....G.....-.....-
 H11G.....-.....-
 H60C.....G.....-..C....-
 H61C.....G.....-..C....-
 H62C.....G.....-..C....-
 H63C.....G.....-..A....-
 H66C.....G.....T..C....-
 H67C.....G.....-..C....-
 H69C.....G.....-..C....-
 H77G.....-.....-
 H79C.....G.....-..C....-
 H87C.....G.....-..CT..A..
 H97G.....-.....-
 H126C.....G.....-..C....-
 H127C.....G.....-..C....-
 H137C.....G.....-..CT..A..
 H139G.....-.....-
 H140T..C.....G.....-..C....-
 H144C.....G.....-..C....-
 H146C.....G.....-.....-
 H147C.....G.....-..CT..A..
 H148A..C.....G.....-..C....-
 H149C.....G.....-..C....-
 H150A.....C.....G.....-..C....-
 H151C.....G.....-.....-.....T..
 H152A.....C.....G.....-..C....-
 H153G.....C.....G.....-..C....-.....C..
 H155A.....C.....G.....-..C....-
 H157C.....G.....-..C....-
 H158C.....G.....-..C....-
 H159C.....G.....-..C....-
 H160C.....G.....-..C....-
 H161C.....G.....-..C....-
 H162C.....G.....-..C....-
 H163C.....G.....-..C....-
 H164C.....G.....-..C....-
 H165C.....G.....-..C....-

ole1

ole1

	444444444444444
	333444444444455
	789012345678901
G-217B	ACTAAAAATATATCT
EH-450H
EH-521
EH-522
EH-626B
EH-655I
EH-655P
EH-658H
EH-658P
EH-670B
EH-670H
EH-671P
EH-672B
EH-672H
EH-696P	...T.....
154-04
190-03
CEPA 2
CEPA 3
L-100-91
EH-46
EH-53
EH-317
AP
GeM
WCh
H.1.02.W
H.1.04.91
H.1.11.94
H.1.12.96
DOWNS
G-186B
G-184B
G-186A
H11
H60
H61
H62
H63
H66	G.....
H67
H69
H77
H79
H87
H97
H126
H127
H137
H139
H140
H144	..G.....
H146
H147
H148
H149
H150
H151
H152
H153	..T.....
H155
H157
H158
H159
H160
H161
H162
H163

ole1

	44444444444444
	33344444444455
	789012345678901
G-217B	ACTAAAAATATATCT
H164
H165
H166
H167
H176	..G.....
H178
H179
H185
H187
H189
H192
H194

tub1

tub1

8888888888888888888888888888888888
33333333344444444555555556666
0123456789012345678901234567890123
G-217B AACTGTTCTCTCGGCAGCCGACGGATACCTG
EH-696P
154-04
190-03
CEPA 2
CEPA 3
L-100-91
EH-46
EH-53
EH-317
AP
GeM
WCh
1980
H.1.02.W
H.1.04.91
H.1.11.94
H.1.12.96
DOWNSA.....
G-186BT.....
G-184BT.....
G-186AT.....
CA 1A-----
CA 2A-----
CO 1A-----
CO 2A-----
CO 3A-----
TX 1A-----
H11
H60
H61
H62
H63
H66
H67
H69
H77
H79A.....
H87T.....
H97
H126A.....
H127A.....
H137T.....
H139
H140
H144T.....T.....
H146
H147T.....
H148
H149T.....
H150
H151C.....T.....
H152
H153
H155
H157
H158
H159
H160
H161
H162
H163
H164
H165
H166
H167A.....
H176T.....T.....
H178

tub1

(GA)_n

ITS1-5.8S-ITS2

ITS1-5.8S-ITS2

ITS1-5.8S-ITS2